

Metabolic Reprogramming of Cystic Fibrosis Macrophages through the Unfolded Protein Response

Samuel Jose Lara Reyna

Submitted in accordance with the requirements for the degree
of Doctor of Philosophy

The University of Leeds

Faculty of Medicine and Health

January 2020

Intellectual Property and Publication Statement:

The candidate confirms that the work submitted is his own, except where work which has formed part of jointly-authored publications has been included. The contribution of the candidate and the other authors to this work has been explicitly indicated below.

The candidate confirms that appropriate credit has been given within the thesis where reference has been made to the work of others.

Publication: “Metabolic Reprogramming of Cystic Fibrosis Macrophages via the IRE1 α Arm of the Unfolded Protein Response Results in Exacerbated Inflammation”.

Frontiers in Immunology, 02 August 2019

Authors: Samuel Lara-Reyna, Thomas Scambler, Jonathan Holbrook, Chi Wong, Heledd H. Jarosz-Griffiths, Fabio Martinon, Sinisa Savic, Daniel Peckham and Michael F. McDermott

Author Contributions

Methodology, S.L.-R., T.S., F.M., S.S., D.P., M.F.M.; Validation, S.L.-R., T.S., C.W.; Formal Analysis, S.L.-R., T.S., C.W.; Investigation, S.L.-R., T.S., C.W., J.H., H.H.J.-G., S.S., D.P., M.F.M.; Resources, S.L.-R., T.S., S.S., D.P., M.F.M.; Data Curation, S.L.-R., T.S., C.W.; Writing – Original Draft, S.L.-R.; Writing – Review & Editing, S.L.-R., T.S., C.W., J.H., H.H.J.-G., S.S., D.P., M.F.M.; Visualization, S.L.-R., T.S.; Supervision, S.S., D.P., M.F.M.; Funding Acquisition, S.L.-R., T.S., S.S., D.P., M.F.M.

This copy has been supplied on the understanding that it is copyright material and

that no quotation from the thesis may be published without proper

acknowledgement.

©2020 The University of Leeds and Samuel Jose Lara Reyna

This thesis is dedicated to

**The memory of my father, Dr Angel Lara Cordova, who is
my everyday inspiration.**

Acknowledgements

I want to express my deepest and most sincere gratitude to all my doctorate supervisors. Professor Daniel Peckham, who taught me all I know about respiratory disorders, particularly about cystic fibrosis. Professor Peckham's positivity and support always kept me on the right track of this journey. Dr Sinisa Savic's energy and insight taught me the importance of resilience in the laboratory and to have an analytical mind when doing medical research. I must thank Dr Savic as he was always there to support me in every aspect of this ride. Finally, I want to thank Professor Michael McDermott which properly taught all the aspects of academic life. Professor McDermott's lessons were invaluable as he taught me how to be a scientist, writer and an academic. Thank you all, as you were always there to support me in every aspect of my personal and academic life. It was a great privilege and honour to work and study under their guidance. I am incredibly grateful for what they have taught me.

I am incredibly grateful to Dr Chi Wong as he was always there to provide me with his expert word of advice in any issue. Dr Wong always help me with any difficulty during my PhD. I also want to say thanks to Dr Heledd Jarosz-Griffiths, she was always supportive during this research and she was always there when most needed. Also, I would like to say thanks to my friends and research colleagues, Dr Thomas Scambler, Mr Jonathan Holbrook, Dr Shelly Pathak, Mr Tobias Russell, Miss Payal Ganguly, Dr Jorge Jimenez, Mr Georgi Georgiev, Dr Dragos Ilas and Dr Daniel Perez, which make conferences, experiments, coffee breaks, night outs and office time more enjoyable. Thanks to my parents for their love, prayers, caring, advice and sacrifices for educating and preparing me for this scientific career. I am very much thankful to my wife, Ms Ana Lara Urby for her unconditional love, understanding and continuing support to complete this research work, as she was always there for me. Thanks to my son

Samuel Lara Lara, who was born during my research studies and showed me what is pure love. Also, I want to express my thanks to my siblings for their support.

Thanks to all the patients and clinical team, particularly Lindsey Gillgrass and Anne Wood, of the Adult Cystic Fibrosis Unit at St. James's Hospital, Leeds. I also would like to thank all the staff of the Wellcome Trust Brenner Building for their kindness. Thanks to CONACyT for supporting me during my research studies. Finally, my thanks to all the people who have supported me to complete the research work directly or indirectly.

Abstract

Cystic fibrosis (CF) is a life-threatening autosomal genetic disease, which affects approximately 48,204 individuals in Europe and 29,887 in the USA. This condition is caused by mutations in the cystic fibrosis transmembrane conductance regulator (CFTR). In CF, the mutated CFTR, in the case of $\Delta F508$, causes accumulation of misfolded proteins leading to endoplasmic reticulum (ER) stress, with activation of the IRE1 α -XBP1 pathway. This pathway is essential in the regulation of a subset of genes controlling proinflammatory and metabolic responses in immune cells; nevertheless, the metabolic rates of immune cells and the role of this pathway in CF remain elusive. In this study, it was shown that innate immune cells from patients with CF show significantly higher levels of ER stress, particularly in the IRE1 α -XBP1 signalling pathway. Interestingly, ER stress was only present in neutrophils, monocytes and macrophages from patients with CF. Overactivation of the IRE1 α -XBP1 signalling pathway rewires M1 macrophages from patients with CF, and increases macrophages' metabolic rates, with high glycolytic rates and mitochondrial function. The increased activity of the IRE1 α -XBP1 signalling pathway and the increased metabolic rates were associated with excessive production of TNF and IL-6. Specific inhibition of the RNase domain of the IRE1 α arm decreased the excessive glycolytic rates, mitochondrial function and production of inflammatory cytokines. Furthermore, Orkambi, Symkevi and Ivacaftor had an essential impact in changing the metabolic profile of cells with CF mutations. This study shows how innate immune cells from CF patients are affected by ER stress, in particular, M1 macrophages. Moreover, the IRE1 α -XBP1 signalling pathway is essential for the increased metabolic rates seen in

M1 macrophages with CF mutations. Modulation of ER stress might be an exciting option to recover the metabolic fitness of cells with CF mutations.

Table of Contents

Acknowledgements	iv
Abstract	vi
Table of Contents	viii
Abbreviations	xii
Lists of figures	xiv
Lists of tables	xv
Chapter 1 – Introduction	1
1.1 Cystic Fibrosis	1
1.1.1 The history and pathophysiology of cystic fibrosis.....	1
1.1.2 CF Mutations	6
1.1.3 Understanding the current treatments in CF.....	8
1.2 Inflammation in CF	14
1.2.1 Inflammation in human bronchial epithelial cells.....	14
1.2.2 Animal models of CF and inflammation	15
1.2.3 Monocytes, macrophages and neutrophils in CF.....	19
1.3 ER Stress and the Unfolded Protein Response	23
1.3.1 The UPR signalling pathways.....	23
1.3.2 Inflammation and the UPR.....	26
1.3.3 CF and the UPR	29
1.4 Cellular Metabolism	32
1.4.1 Glycolysis and the Krebs cycle	32
1.4.2 Immunometabolism: macrophage metabolism	38
1.5 Hypotheses	42
1.5.1 List of Hypotheses	42
1.5.2 Aims and Objectives	42
Chapter 2 – Methods	44
2.1 Cellular culture	44

2.1.1	Cell Lines.....	44
2.1.2	Isolation and processing of primary immune cells	45
2.1.3	Culture of primary immune cells	47
2.1.4	Macrophage culture and polarisation.....	47
2.2	RNA Isolation and detection	48
2.2.1	RNA isolation and cDNA conversion	48
2.2.2	Real-time PCR (qPCR).....	48
2.2.3	Reverse transcription PCR (RT-PCR)	50
2.3	Cytokine expression	51
2.4	Western blots	52
2.5	Flow cytometry.....	52
2.6	Immunofluorescence microscopy.....	54
2.7	Metabolic experiments	55
2.7.1	Cellular ROS detection	55
2.7.2	Glycolytic and mitochondrial assays (Extracellular Flux Analyzer)	55
2.8	Statistical analysis	57
2.9	Table of resources	58
Chapter 3 – The UPR in Cystic Fibrosis		61
3.1	Introduction	61
3.2	Methods	62
3.2.1	RNA isolation and detection	62
3.2.2	Western blotting.....	62
3.2.3	Flow cytometry	62
3.2.4	Cellular stimulations	63
3.3	Results	64
3.3.1	UPR activation in CF HBEC lines	64
3.3.2	UPR activation in PBMCs from patients with CF	74
3.3.3	No difference in UPR activation in lymphocytes	76
3.3.4	BiP, IRE1 α , ATF4 and CHOP upregulation in neutrophils.....	78
3.3.5	IRE1 α , PERK, ERdj4, ATF4, CHOP and GADD34 upregulation in monocytes	80
3.3.6	The IRE1 α -XBP1 pathway is overactive in CF M1 macrophages.....	83

3.3.7	XBP1s is not induced in CF M2 macrophages	89
3.4	Discussion	90
Chapter 4 – Inflammation and the UPR in Cystic Fibrosis		94
4.1	Introduction	94
4.2	Methods	95
4.2.1	RNA isolation and detection	95
4.2.2	Flow cytometry	95
4.2.3	Cytokine expression	96
4.2.4	Cellular stimulations	96
4.3	Results	97
4.3.1	Upregulation of IL-6 in CF HBECs	97
4.3.2	Expression of TNF and IL-6 in lymphocytes and neutrophils.....	99
4.3.3	Upregulation of TNF in CF monocytes.....	102
4.3.4	Deficient polarisation of M2 Macrophages in patients with CF	105
4.3.5	TNF and IL-6 are overexpressed in M1 Macrophages from CF patients	107
4.3.6	IRE1 α inhibition reduces TNF and IL-6 in CF M1 Macrophages	111
4.4	Discussion	113
Chapter 5 – Metabolism in Cells with CF Mutations and the Effects of IRE1α		
Inhibition		115
5.1	Introduction	115
5.2	Methods	116
5.2.1	Cellular ROS detection in HBECs and M1 macrophages	116
5.2.2	Mitochondrial ROS (mitoSOX) detection	117
5.2.3	Glycolytic and mitochondrial assays	117
5.3	Results	119
5.3.1	Increased ROS and mitochondrial ROS in CF HBECs.....	119
5.3.2	Increased ROS in CF M1 macrophages.....	121
5.3.3	Heightened glycolytic rate and mitochondrial flux in CF monocytes ...	122
5.3.4	Heightened mitochondrial flux and glycolytic rate in CF M1 macrophages	125
5.3.5	IRE1 α inhibition recovers the heightened glycolytic rate and mitochondrial flux.....	128

5.3.6	Ivacaftor reduces OCR levels in CF macrophages with class III mutations	131
5.3.7	Orkambi selectively reduces OCR levels in CF macrophages (Δ F508/ Δ F508)	136
5.3.8	Ivacaftor and Symkevi alter the metabolic profile of HBECs.....	139
5.4	Discussion	145
Chapter 6 – Discussion.....		148
6.1	The UPR exacerbates inflammation in cystic fibrosis	148
6.2	The UPR and the regulation of macrophage metabolism.....	151
6.3	Abnormal metabolic and inflammatory profiles in CF HBECs	155
6.4	CF as an autoinflammatory condition	156
6.5	Conclusion.....	158
6.6	Study limitations	160
6.7	Future Directions	161
Appendix.....		162
References.....		165

Abbreviations

2-DG	2-Deoxy-d-glucose
ASL	Airway surface liquid
ATF4	Activating transcription factor 4
ATF6	Activating transcription factor 6
ATP	Adenosine triphosphate
<i>B. cepacia</i>	<i>Burkholderia cenocepacia</i>
BIP	Binding immunoglobulin protein
BSA	Bovine serum albumin
CF	Cystic fibrosis
CFTR	Cystic fibrosis transmembrane conductor regulator
CHOP	C/EBP homologous protein
Cl ⁻	Chloride ion
COPD	Chronic obstructive pulmonary disorders
DAMP	Danger-associated molecular patterns
ECAR	Extracellular acidification rate
eIF2	Eukaryotic initiation factor 2
ENaC	Epithelial sodium channel
ER	Endoplasmic reticulum
ETC	Electron transport chain
FEV	Forced Expiratory Volume
FBS	Foetal Bovine Serum
GADD34	Growth arrest and DNA damage-inducible protein
GLUT1	glucose transporter 1
GSH	Glutathione
HBEC	Human bronchial epithelial cell
HCO ₃ ⁻	Bicarbonate
HS	Hypertonic saline
Hsp	Heat shock protein
IL	Interleukin
IRE1	Inositol requiring enzyme 1
LPS	Lipopolysaccharide

mROS	Mitochondrial ROS
NAC	N-acetylcysteine
NAD ⁺ /NADH	Nicotinamide adenine dinucleotide
NE	Neutrophil extracellular trap
NF-κB	Nuclear factor-kappaB
NLRP3	NOD-, LRR- and pyrin domain-containing protein 3
NO	Nitric oxide
Nrf2	Nuclear factor erythroid 2-related factor 2
OCR	Oxygen consumption rate
OxPhos	Oxidative Phosphorylation
P/S	Penicillin and streptomycin
PAMP	Pathogen-associated molecular patterns
PBMC	Peripheral blood mononuclear cells
PE	Phycoerythrin
PerCP	Peridinin Chlorophyll Protein Complex
PERK	Double-stranded RNA-activated protein kinase (PKR)-like ER kinase
PKA	Protein kinase A
RIDD	Regulated IRE1-dependent decay
RIPA	Radioimmunoprecipitation assay buffer
ROS	Reactive oxygen species
RPMI	Roswell Park Memorial Institute
<i>S. aureus</i>	<i>Staphylococcus aureus</i>
TLR	Toll-like receptor
Tg	Thapsigargin
Tn	Tunicamycin
TNF	Tumour necrosis factor
UPR	Unfolded protein response
XBP1	X box-binding protein 1
XBP1s	X box-binding protein 1 spliced

Lists of figures

Figure 1 – History and median predicted survival age for patients with CF	2
Figure 2 – Cellular pathophysiology of CF HBECs.....	4
Figure 3 – Organs affected in CF and common manifestations	5
Figure 4 – Prevalence of respiratory pathogens, by age, in respiratory cultures of patients with CF	10
Figure 5 – The UPR signalling pathway	26
Figure 6 – Glycolysis and the Krebs cycle.....	33
Figure 7 – Glycolytic pathway	34
Figure 8 – The Krebs cycle	36
Figure 9 – Electron transport chain	37
Figure 10 – The Krebs cycle in M1 and M2 macrophages	41
Figure 11 – UPR induction time course.....	65
Figure 12 – UPR activation in CF HBECs	66
Figure 13 – Activation the BIP, IRE1 α , ATF6 and PERK.	69
Figure 14 – Activation the XBP1s, XBP1u, eIF2 α , CHOP and GADD34.....	72
Figure 15 – IRE1 α , pIRE1 α , ATF6 and PERK protein expression in HBECs.....	73
Figure 16 – UPR activation in primary PBMCs from patients with CF	74
Figure 17 – ER stress in PBMC stimulated with Tn and Tg.....	75
Figure 18 – UPR gene expression in lymphocytes from patients with CF	76
Figure 19 – ER stress in lymphocytes stimulated with Tn and Tg	77
Figure 20 – UPR gene expression in neutrophils from patients with CF	78
Figure 21 – ER stress in neutrophils stimulated with Tn and Tg	79
Figure 22 – UPR gene expression in monocytes from patients with CF.....	81
Figure 23 – ER stress in monocytes stimulated with Tn and Tg.....	82
Figure 24 – Differentiation process of M1/M2 macrophages	85
Figure 25 – UPR gene expression in M1 macrophages from patients with CF	86
Figure 26 – ER stress in M1 macrophages stimulated with Tn and Tg	87
Figure 27 – XBP1s in M1 macrophages from CF patients	88
Figure 28 – XBP1s is absent in M2 macrophages from CF patients	89
Figure 29 – IL-6 expression in HBECs with CF mutations.....	98
Figure 30 – IRE1 α inhibition reduces IL-6 in HBECs.	98
Figure 31 – TNF and IL-6 expression in lymphocytes.	100
Figure 32 – TNF and IL-6 expression in neutrophils.....	101
Figure 33 – TNF and IL-6 expression in monocytes.....	103
Figure 34 – Apoptosis percentage in human monocytes.....	104
Figure 35 – Reduced polarisation of CF M2 macrophages.	105
Figure 36 – CFTR expression in M2 macrophages.	106
Figure 37 – Upregulation of IL-6 in M1 macrophages.	107
Figure 38 – CFTR expression in M1 macrophages.....	108
Figure 39 – CFTR expression in CF M1 macrophages.....	109
Figure 40 – Upregulation of TNF and IL-6 in CF M1 macrophages.....	110
Figure 41 – IRE1 α inhibition reduces TNF and IL-6 secretion in CF M1 macrophages.	112
Figure 42 – Increased levels of ROS and mROS in CF HBECs.....	120

Figure 43 – Increased levels of ROS in CF M1 macrophages	121
Figure 44 – Increased mitochondrial flux and glycolytic rates in CF monocytes. ...	123
Figure 45 – Glycolytic function	124
Figure 46 – Increased mitochondrial flux and glycolytic rates in CF M1 macrophages.	126
Figure 47 – mRNA expression of metabolic enzymes in M1 macrophages.	127
Figure 48– Mitochondrial function	129
Figure 49 – The IRE1 α -XBP1 pathway regulates metabolism in CF M1 macrophages.	130
Figure 50 – Ivacaftor reduces the increased OCR levels in CF Macrophages.	134
Figure 51 – Orkambi partially reduces the increased OCR levels in CF macrophages.	138
Figure 52 – CFTR modulators decrease the high OCR levels in CF HBECs	142
Figure 53 – No impact of CFTR modulators in the ECAR levels of CF HBECs.....	144
Figure 54 – The IRE1 α -XBP1 signalling pathway of the UPR in CF.	150
Figure 55 – Altered signalling pathways in CF macrophages.....	153

Lists of tables

Table 1 – Classification of the CFTR mutations	8
Table 2 – Patients' information and clinical data.	45
Table 3 – Primer sequences	49
Table 4 – Seahorse Calculations	56
Table 5 – Table of resources.....	60

Chapter 1 – Introduction

1.1 Cystic Fibrosis

1.1.1 The history and pathophysiology of cystic fibrosis

Cystic fibrosis (CF) is the most common life-limiting autosomal recessive genetic disorder, with a prevalence of one in 2,500 in the UK, and approximately with one in 25 individuals being carriers of the gene causing CF. While CF has been present in humans for more than a millennium, the disease was first mentioned in the medical literature around the middle ages, and it was associated with the presence of salty skin and damage to the pancreas in early child mortality [1]. It was not until 1938 when Dr Dorothy H Andersen first described the disease in autopsies of children who died by malnutrition, where it was referred to as “cystic fibrosis of the pancreas” [2]. The chromosomal location of the CF gene was discovered in 1985 at position q31.2 on the long arm of chromosome 7 [3]. Later in 1989, the CF gene was fully mapped and identified by Lap-Chee Tsui, John R. Riordan (Hospital for Sick Children, Toronto) and Francis S. Collins (University of Michigan). The gene was named the cystic fibrosis transmembrane conductance regulator (CFTR) (Figure 1) [4, 5]. The CFTR is a cellular membrane protein composed of 1,480 amino acids, that is part of the ATP-binding cassette (ABC) transporter family of membrane proteins, which main function is to transport ions through the cellular membrane [6].

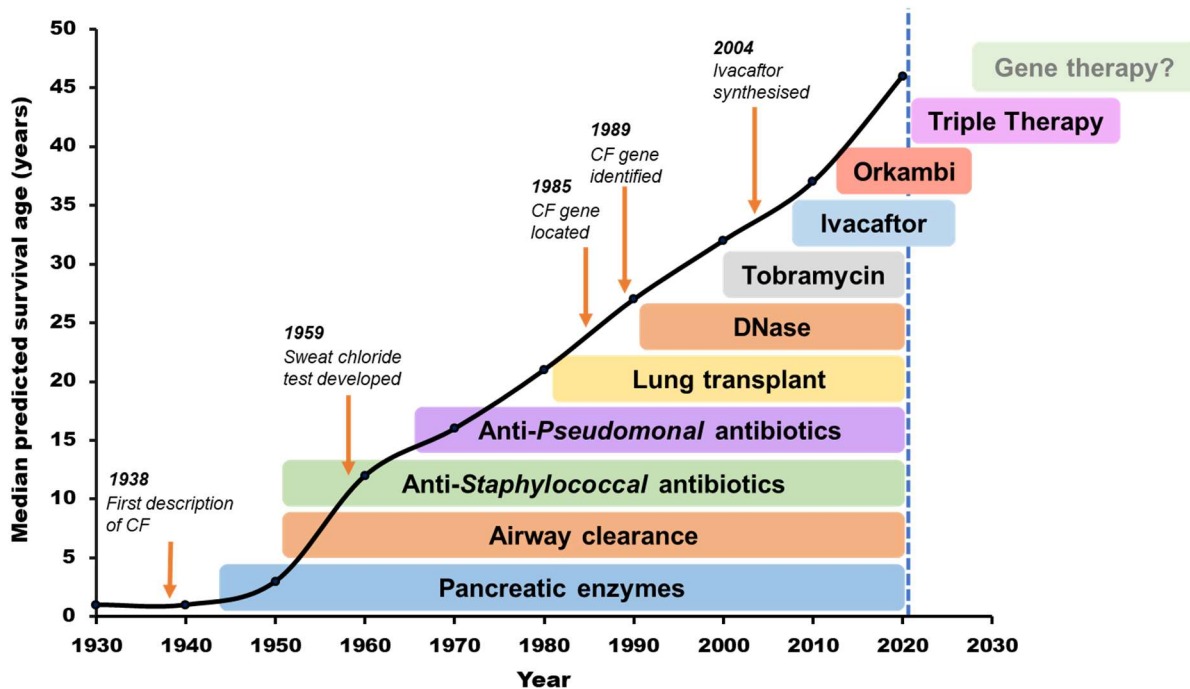


Figure 1 – History and median predicted survival age for patients with CF

The median predicted survival age of patients with CF from 1930 to 2020 is shown by the black line. All primary treatments in CF are shown below the curve. The orange arrows show significant checkpoint discoveries. Data were taken from the CF foundation patient registry, 2017 Annual Data Report and from the UK CF patient registry, 2018 annual data report.

Most human epithelial cells express the CFTR, including cells present in the respiratory, digestive, and urogenital tracts, which are mostly epithelial and secretory cells, expressing the CFTR and, consequently, the most affected by CFTR mutations. Although it was believed that the CFTR was not present or functional in any other types of cells, there is now evidence to suggest that the opposite is the case. Studies have shown CFTR expression in different cells of the peripheral and central nervous system [7-11], cardiac cells [12, 13], red blood cells [14] and cells of the innate and adaptive immune systems [15-19]. In the case of epithelial and secretory cells, CFTR mutations result in abnormal chloride (Cl^-), bicarbonate (HCO_3^-), and sodium (Na^+) transport, in addition to the intracellular accumulation of misfolded proteins, in the case

of class II mutations [20, 21]. Patients with CF present frequent respiratory complications, resulting from (ASL) airway surface liquid dehydration derived from the abnormal ion channel function present in bronchial epithelial cells. Opportunistic pathogens exacerbate these recurrent pulmonary complications, the most common being *Pseudomonas aeruginosa* (*P. aeruginosa*), *Staphylococcus aureus* (*S. aureus*), *Haemophilus influenza* (*H. influenza*) and *Burkholderia cenocepacia* (*B. cenocepacia*); these opportunistic pathogens promote an inflammatory process in the lung mainly caused by overwhelming secretion of pro-inflammatory cytokines, such as TNF, IL-1 β , IL-6, IL-8 and IL-18 [22, 23]. The chronicity of these pulmonary infections underlines and dominates the clinical picture of patients with CF and, if not treated adequately, these can lead to further complications, by reducing pulmonary function and causing lung tissue destruction. A summary of the cellular pathophysiology seen in human bronchial epithelial cells (HBECs) with different CF mutations is summarised in Figure 2. The different classes of mutations, based on their cellular phenotype, will be discussed in the next section.

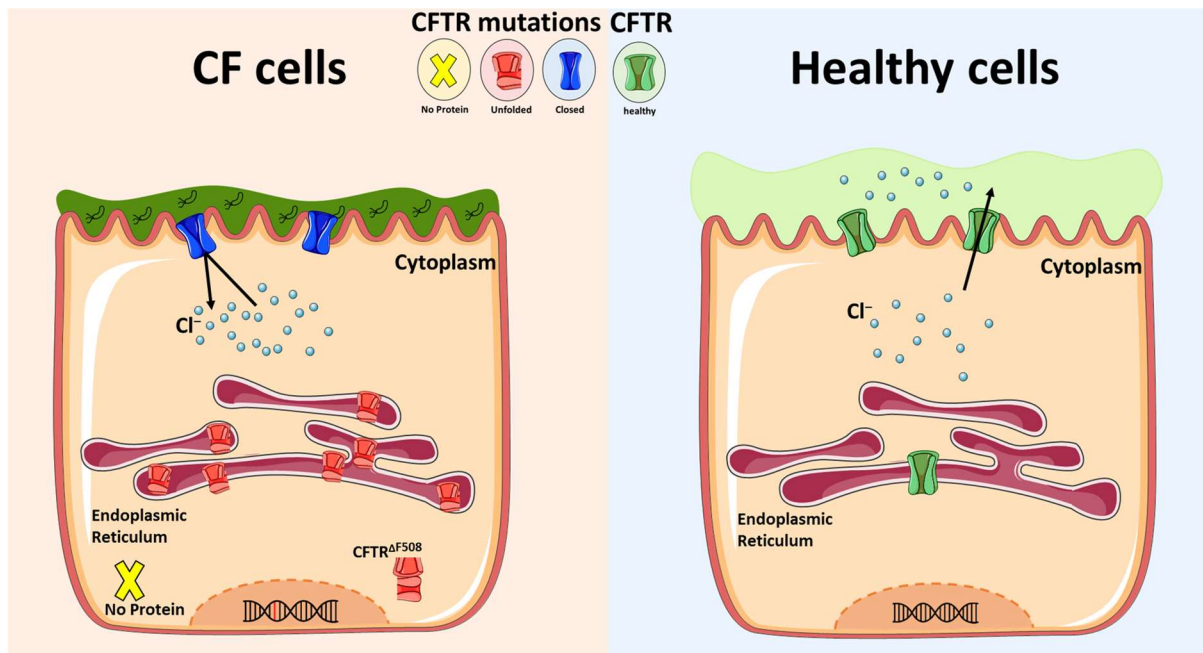


Figure 2 – Cellular pathophysiology of CF HBECS

In healthy HBECS the CFTR is typically produced and transported to the apical membrane, where it transports Cl⁻ ions into the ASL. HBECS with CF mutations lack a proper flux of Cl⁻ ions and this results in dehydration of the mucus layer, favouring bacterial infections. Different types of mutations lead to different types of CFTRs being produced. Refer to **Table 1** for the classification of CF mutations.

Pancreatic insufficiency (PI) is another complication of CF, affecting around 85% of patients with this genetic disorder [24]. The clinical manifestations of PI usually are present soon after birth; however, some patients develop these complications later in life [24]. Furthermore, early PI has been reported in patients with class I, II, III and VI mutations, commonly presenting with PI at birth [25]. It has been recently identified that pancreatic destruction starts *in utero*, and it has also been debated whether small molecule therapy will provide an adequate therapeutic option during pregnancy [26-28]. Malnutrition is another complication of CF and patients typically struggle to gain weight, suffering a decline in both body mass index (BMI) and pulmonary function, due to the combination of pancreatic insufficiency and the hypermetabolic state of their cells [29, 30]. Arthritis is another complication that some patients with CF develop

throughout their lives. It is estimated that the prevalence of CF-associated arthritis (CFA) affects 1 in 10 patients with CF. [31]. In conclusion, CF is a multi-organ disorder, severely affecting the quality of life of patients who suffer from it, and which may lead to dramatic changes in their routine daily activities (Figure 3).

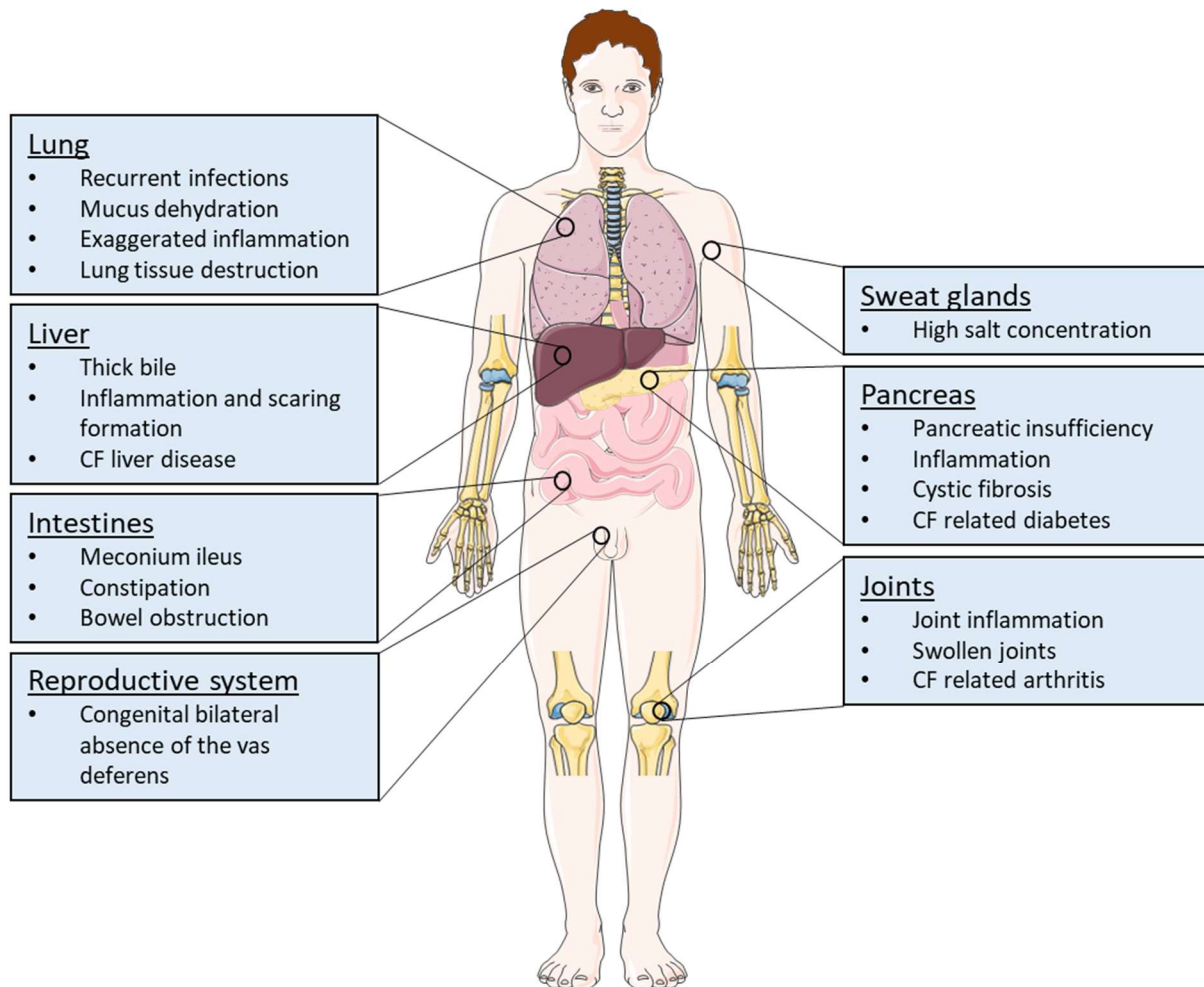


Figure 3 – Organs affected in CF and common manifestations

CF is a multi-organic disorder affecting several organs, with the most prominent being the lung, liver, intestines, pancreas, reproductive system and joints. One feature in common is that all the affected organs show inflammation.

1.1.2 CF Mutations

As mentioned previously, CF is a recessive genetic disorder meaning that people who suffer from this condition carry two copies of the mutated *CFTR* gene. The most common CF mutation, referred to as the $\Delta F508$ mutation, involves the deletion of three nucleotides in position 508, which results in the loss of the amino acid phenylalanine [4]. The $\Delta F508$ mutation is the most common alteration in European patients with CF, with more than 80% carrying at least one copy of the class II mutation and with the $\Delta F508$ being the most frequent mutation, this produces an abnormal CFTR channel, which is improperly folded and retained within the ER [32, 33]. More than 1900 different mutations have been identified in the *CFTR* gene at this point, with most of them causing CF [32]. CFTR mutations are classified into seven classes according to the specific characteristics of the CFTR protein or the messenger RNA (mRNA). Class I mutations include nonsense, frameshift and splice mutations, such as W1282X, which result in an unstable truncated mRNA, that is usually quickly degraded [34]. Class II mutations encompass mostly missense and amino acid deletion mutations, leading to a misfolded CFTR protein, followed by defective trafficking of the product. The $\Delta F508$ mutation is the most representative alteration of the class II spectrum, and it is also the most common CF mutation producing an abnormal CFTR channel, which is improperly folded and retained within the ER (**Figure 2**) [32, 33]. The class III mutations category includes the G551D, S549R and G1349D mutations, all of which are associated with a fully expressed membrane protein, but with defective channel regulation, thereby impeding normal ion trafficking through the cellular membrane [34]. An estimated 5% of patients with CF are carriers of at least one copy of the G551D mutation, which is the most common mutation in the class III spectrum. Moreover, patients with class III mutations strongly respond to

ivacaftor (VX-770), which is a small molecule that functions as a CFTR potentiator or channel opener, restoring CFTR functionality [34]. Class IV mutations are similar to class III mutations, in essence, as the CFTR is fully expressed and reaches the cellular membrane; however, there is a reduction in the channel conductance, in class IV mutations, rather than impaired gating, as described within class III mutations [34]. Class V mutations are characterised by insufficient production of CFTR protein, thereby reducing the ion flux, not because of defective cellular transcription or translation, but rather because of insufficient amount of protein being produced, frequently due to promoter or splicing site abnormalities [35]. In class VI mutations, there is decreased stability of the CFTR channel, leading to a reduction of the protein product. Class VI mutations can also cause activation of internalisation signalling pathways, resulting in decreased CFTR protein in the membrane and reduced surface expression [36]. Finally, class VII mutations were recently proposed, branching off from the class I category, with the same result as class I mutations, with no protein production, but with the unique characteristic of the lack of mRNA [37, 38]. A summary of the different CFTR classes is presented in

Table 1 and includes the most common examples of each of the seven different classes. Patients with CF frequently present with a heterogeneous combination of different classes of CF mutations, with the $\Delta F508$ mutation being by far the most common mutation encountered. It is reasonable to hypothesise that the different class mutations will have different molecular and pathophysiological mechanisms, with the same outcome in terms of channel conductance, but with different and unique aspects regarding other signalling pathways, such as cellular stress, inflammation, metabolism and autophagy.

Class type mutations							
WT CFTR	I	II	III	IV	V	VI	VII
CFTR defect	No protein	Trafficking block	Impaired gating	Altered conductance	Less protein	Unstable	No mRNA
Example	W1282X G542X 621+1G->T	ΔF508 N1303K I507del	G551D S549N G1349D	R117H D1152H R347P	A455E 2789+5G->A 3849+10kbC->T	G1412X R553X Q1412X	CFTRdele2,3 1717-1G->A
Treatments	None at present	VX-809, VX-770, VX-661, VX-445	VX-770	VX-770	CFTR Correctors (for A455E)	VX-445	None at present

Table 1 – Classification of the CFTR mutations

1.1.3 Understanding the current treatments in CF

Since the identification of CF, treatments have mainly been focused on managing the consequences of the disease, rather than the actual cause. In CF, the chronic infections and unresolved inflammation cause the production of a thick, dry and viscous mucus which predisposes to bacterial colonisation of the lung parenchyma [39]. In the clinic, mucolytic agents are currently being used to remove the thick mucus layer formed in the lumen of the lungs; in addition, because this mucus is characterised by high a concentration of DNA, special attention has been given to treating this complication of CF [39]. These increased DNA levels are mainly derived from abnormal neutrophilic infiltrations in the lungs, followed by an exaggerated inflammatory response, with increased levels of neutrophil extracellular traps (NETs) [40]. The formation NETs has been referred as an alternative mechanism by which neutrophils can get rid of bacteria, which will be explained in more detail in section

1.2.3, entitled “Monocytes, macrophages and neutrophils in CF” [41, 42]. The increased amounts of free DNA, which originate from NETs in patients with CF, have been associated with a decline in lung function [43-45]. Dornase alfa is a purified recombinant human deoxyribonuclease (DNase), which enzymatically hydrolyses the DNA present in the mucus of these patients, clearing the obstructed airways and helping to restore normal pulmonary function [46]. Another common mucolytic that has been used in the last decade, not only in CF but also in chronic obstructive pulmonary disease (COPD), is N-acetylcysteine (NAC) [47]. While treatment with NAC is safe in patients with CF, some controversies exist relating to NAC efficacy in the clinic [48-50]. Hypertonic saline (HS) is a cheap, safe, effective and commonly used additional therapy in CF, which helps mucociliary clearance by rehydration of the mucus present in the airway surfaces. HS is efficient in reducing the number of pulmonary exacerbations, by 56% compared to the control group, when used in combination with intravenous (IV) antibiotics [51]. Mannitol is another compound which helps in the restoration of a normal airway liquid surface. Mannitol is a sugar alcohol which helps in the clearance of airway mucus by changing the osmotic gradient, leading to rehydration of the airway surface [47]. Correct intervention with mannitol aids in the recovery of FEV₁% and in the reduction of pulmonary exacerbations in patients with CF [52, 53].

Antibiotics are commonly used in the clinic to treat patients with CF, in different types of situations, depending on the cohort of patients being treated and the pathogens which could potentially, be present during the infection. Antibiotics are mainly used in the eradication of early infections and to control chronic bacterial infections; however, they are also often used to control pulmonary exacerbations and prophylactically to prevent infections developing in patients with CF. The lung microbiome constitutes an

essential aspect in the pathogenesis of CF [47]. For instance, during the early ages of this disease, the most frequent pathogen cultured from the lungs of young children is *S. aureus*, which represents the most prevalent pathogenic bacteria in paediatric cohorts [54, 55]. Interestingly, the composition of the lung microbiome changes during the lifetime of patients with CF. After the age of 10, colonisation with *P. aeruginosa* progressively increases until it is the primary pathogen present in the lungs of these patients, while the prevalence of *S. aureus* is reduced in the adult cohort (Figure 4) [54, 56].

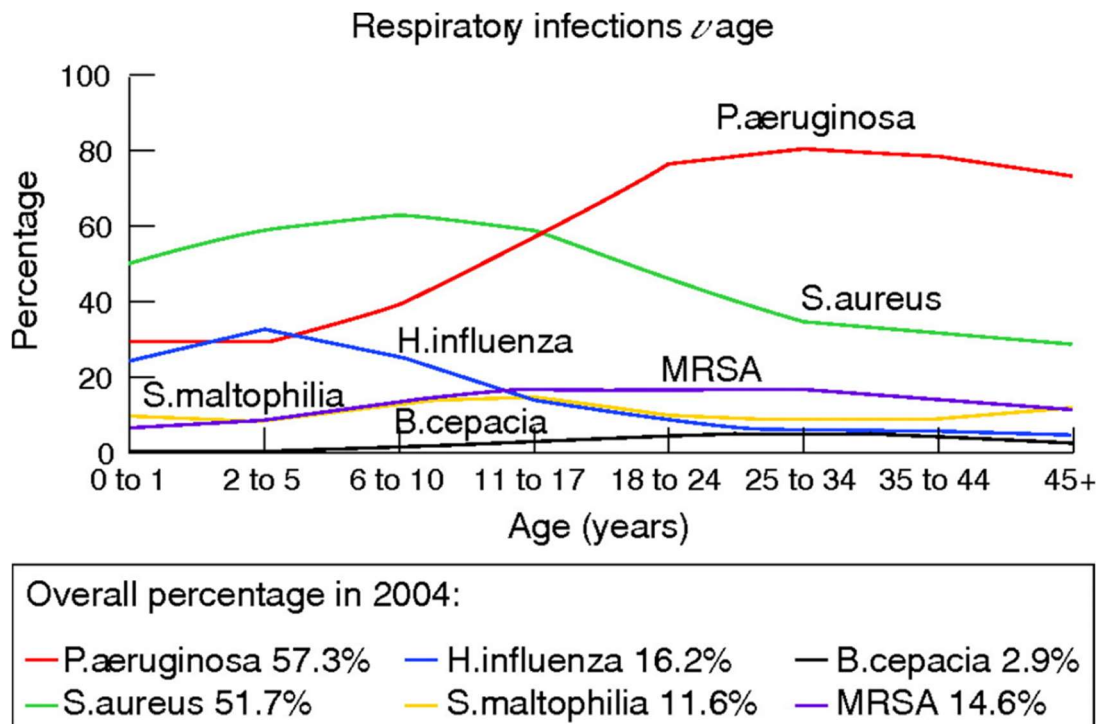


Figure 4 – Prevalence of respiratory pathogens, by age, in respiratory cultures of patients with CF

Data from Cystic Fibrosis Foundation Patient Registry, 2004 annual data report to the centre directors [56] © Cystic Fibrosis Foundation, 2005.

P. aeruginosa is the most common pathogen found in adults with CF, with an estimated 80% of the patients being infected with this pathogen, which is generally associated with clinical complications [54]. While antibiotics have helped in the

treatment of CF, antimicrobial resistance has become a severe problem in the treatment of CF. Antimicrobial resistance needs to be taken very seriously in CF because it is creating a significant challenge in the eradication of pathogens during respiratory infections [57].

Inflammation, which will be explained in detail in section 1.2, represents a significant challenge in CF, and, while not completely understood, there are studies which help to shed light on the mechanisms behind this problem [30, 58, 59]. Non-steroidal anti-inflammatory drugs (NSAIDs) are commonly used in CF, to treat the symptoms related to the inflammation, and, when necessary, corticosteroids are used to control the excessive inflammation presented by patients with CF [47]. Macrolides are efficient in controlling the inflammation in patients with CF, in particular, azithromycin, which is regularly used in the clinic [60, 61]. Patients treated with azithromycin, over a six months period, showed reduced incidence of the *S. aureus* pathogen, as well as a significant reduction in pulmonary exacerbations [62]; however, it has been shown that some pathogens in patients with CF, such as *P. aeruginosa*, can acquire resistance to macrolides, which will represent an even more serious challenge in the future [63].

While all the treatments mentioned previously were focused towards ameliorating the consequences of the disease, rather than fixing the actual root of the problem, which is the mutated CFTR, several novel small-molecule therapies are currently available for the treatment of CF. In January 2012 ivacaftor (VX-770), developed by Vertex pharmaceuticals, under the trade name of Kalydeco, was the first small molecule therapy approved by the FDA for patients with CF. Ivacaftor is a CFTR potentiator or channel opener, restoring the CFTR functionality and improving the abnormal ion flux [64]. Ivacaftor is an effective therapy for patients with class III

mutations, initially restricted only to patients with G551D mutations but most recently shown to be efficient in other mutations, such as non-Gly551Asp and R117H class IV mutations [65-67]. Several studies have shown that ivacaftor significantly restores predicted FEV₁% by more than 10%, decreases sweat chloride and increases weight/BMI, in patients with CF with at least one G551D mutation [67]. A combination drug under the brand name of Orkambi, composed of lumacaftor (VX-809) and ivacaftor (VX-770), a channel corrector and potentiator respectively, has been used to treat patients with two copies of the Δ F508 mutation, with some controversial results [68, 69]. While the FDA approves Orkambi and it is licenced for its use in the UK, the National Institute for Health and Care Excellence (NICE), initially rejected its use, due to cost-inefficient results and the lack of long-term data; however, after negotiations with the pharmaceutical company Vertex, it is now available in the UK. While some clinical trials have shown a modest but still significant improvement of the predicted FEV₁%, which ranged from 4 to 6.7%, and a reduction in pulmonary exacerbations by ~35%, there was no significant reduction in sweat chloride nor an increase in the weight/BMI ratio [70, 71]. One of the most significant problems with Orkambi is the prevalence of adverse effects in patients treated with this drug combination [72]. In a retrospective cohort study, 39.7% of patients who started treatment with Orkambi reported adverse effects related to the drug [73]. In another study, it was reported that 51% of the subjects, under the double therapy, suffered respiratory adverse effects, and 30% of the participants discontinued the treatment [74]. Tezacaftor, a new channel corrector, is now used in combination with ivacaftor for the treatment of patients homozygous for the Δ F508 mutation. The combination of tezacaftor and ivacaftor has shown to be efficacious in the treatment of patients with CF, showing similar results than its predecessor Orkambi but without a significant increase in the adverse effects

shown by Orkambi [72]. The most recent addition of VX-445, a channel corrector, in combination with tezacaftor and ivacaftor, which is referred as triple combination therapy, significantly increased the predicted FEV₁% by 13.8% in patients with a single copy of the Δ F508 mutation [75-77]. Impressively, Δ F508 homozygous patients incorporating VX-445 to their tezacaftor and ivacaftor regimen showed a significant 11% increase in their predicted FEV₁%, and both groups reported a reduction in sweat chloride [75, 76]. Several other compounds are under development for the treatment of CF, which are being developed by the pharmaceutical companies Vertex, Proteostasis Therapeutics and Galapagos [78]. A timeline of the CF drugs developed can be seen in Figure 1.

Finally, it is important to mention the recent development of gene therapy as a potential cure for CF. Initial investigations have demonstrated that lentiviral vector delivery might be a suitable option to “cure” CF, or at least to offer a cure for some of the lung complications [79]. Another promising future “cure” for CF, with potentially less off-target effects than lentiviruses, are genomically guided therapies or gene editing, with the use of powerful tools, such as CRISPR-Cas9, which potentially represent a complete correction of the mutated CFTR [80]. It is fascinating how gene editing might develop into a powerful correction therapy or “cure” in the near future.

1.2 Inflammation in CF

1.2.1 Inflammation in human bronchial epithelial cells

Inflammation is a severe complication in CF and management of this problem is a crucial factor in achieving an excellent clinical prognosis. The immune system is the principal regulator of the inflammatory response, and several cells of the innate immune system are intrinsically affected by CF mutations [30, 59]. While lung inflammation in CF remains unclear, it is known that bronchial epithelial cells play an essential role in the abnormal inflammatory response seen in patients with CF. It has been shown that HBECs, affected by CF mutations, have an abnormal inflammatory response [81]. CF HBECs, stimulated by the pro-inflammatory cytokines, TNF and IL-1 β , produce significantly higher amounts of IL-6 and IL-8 compared to wild type (WT) and CF corrected HBECs [82]. A similar response was observed in a different study, when CF cells were challenged with *P. aeruginosa* producing significantly higher quantities of IL-8, IL-6 and GM-CSF [83]. These observations are consistent with the clinical complications observed in patients with CF, which show raised levels of IL-8 and IL-6 during bacterial infections [22, 23]. Similar findings were observed in BECs obtained from children with CF <5 year old, where significantly higher amounts of IL-8 mRNA were detected in CF infants compared with control infants [84]. While several limitations exist in all studies mentioned earlier, they consistently show an exaggerated inflammatory response. The CFTR can be chemically inhibited by the CFTR_{inh}-172, and this potent inhibitor has been able to mimic the abnormal inflammatory response seen in CF [85]. HBECs exposed to CFTR_{inh}-172, for more than 72, hours showed a significant increase in IL-8 under basal conditions and increased activity in NF- κ B after TNF and IL-1 β stimulation [85]. Another vital player

during the inflammatory response is reactive oxygen species (ROS), which play a significant role in the clearance of bacteria and are also capable of influencing the inflammatory response [86]. Oxidative stress has been shown to be increased in HBECs with CF mutations and it has been associated with an increased number of apoptotic cells and high levels of IL-8 and IL-6 [86, 87]. Furthermore, the chronic inflammatory environment present in the lungs of patients with CF can trigger an expansion of ER Ca^{2+} stores, directly contributing to the exaggerated inflammatory response [88, 89]. It would be of interest to investigate the interaction between bronchial epithelial and immune cells to discern whether these interactions contribute to the unresolved chronic inflammation seen in patients with CF.

1.2.2 Animal models of CF and inflammation

The excessive inflammation present in patients with CF has been replicated in several animal models helping us to understand the underlying mechanisms behind this abnormal inflammation and its relation to CFTR mutations. Animal models are fundamental strategies to achieve a better understanding in the pathophysiology of diseases. There is an extensive repertoire of different animal models with a CF like-disease such as, mouse, rat, sheep, pig, ferret and zebrafish which, to a certain extent, resembles the complications seen in CF [90].

The first CF animal model created was a mouse, and it was generated soon after the identification of the *CFTR* gene. Today, there are more than 14 different CF mouse models which resemble some of the aspects seen in CF [90]. While mice models provide us with new insights for a better understanding of CF, certainly these models present certain limitations in the study of CF, as some models have shown an

alternative conductance of Cl⁻ which compensates the lack of CFTR functionality in some organs [91]. This study described an alternative conductance of Cl⁻ that was only detected in lung and pancreatic epithelial cells, which displayed a moderate disease severity while being completely absent in the intestinal tract, where the severity of the disease was more pronounced [91]. Later, it was found that this alternative conductance of Cl⁻ was undoubtedly due to the mixed genetic background of the mice and, indeed, the model was improved by creating an inbred congenic CFTR-knockout mouse [92]. This new CF mouse model presented spontaneous and progressive lung disease, including defective mucociliary transport, idiopathic pulmonary fibrosis, enhanced immune cell infiltrations and severe inflammation. Interestingly, this CF mouse model developed a chronic inflammatory disease in the absence of pathogenic organisms and, also, mice were more susceptible to *P aeruginosa* infections compared to the WT control mice [92-95]. Consistent with the levels of pro-inflammatory cytokines seen in patients with CF, CF mice also presented increase levels of several pro-inflammatory cytokines including TNF, IL-1 β , IL-6 and IL-8 [94, 96]. The cells that are found mainly in the lung of CF mice are macrophages and neutrophils, which are discussed in the next section and, indeed, contribute to the high degree of inflammation seen in CF [96]. The abnormal inflammation seen in CFTR-knockout mice is not restricted to the respiratory and intestinal tract, as it has been reported chronic inflammation and infiltration of immune cells in the liver and pancreas of these CF mice, causing damage and destruction of the tissue [95]. Another alternative and interesting CF mice model is the β -ENaC model, which develops a similar lung phenotype shown by patients with CF [97]. This model was created by overexpressing the β subunit of the epithelial Na⁺ channel (ENaC), which

is overactive in CF, and has as a consequence increased Na⁺ transport mimicking the CF phenotype [97, 98].

The controversies presented by CF mouse models led to the development of a CF pig model, as these animals share some anatomical and morphological features seen in humans [99]. The first pig model was a CFTR-Knockout, CFTR^{-/-}, created by homologous recombination in primary fibroblast followed by somatic cell nuclear transfection [99]. New-born CFTR^{-/-} piglets present intestinal and pancreatic abnormalities similar to those seen in humans, with inflammation and infiltration of immune cells into the affected tissues [99]. Furthermore, at birth these piglets did not present any abnormality in airway epithelial cells or mucosal glands, at first sight; however, these animals rapidly developed a severe lung infection and inflammation with a more severe phenotype when compared to humans [90, 99, 100]. When CFTR^{-/-} piglets were challenged to *S aureus*, the most common pathogen present in children with CF, piglets with CFTR mutations failed to eradicate this bacterial infection causing chronic infection and inflammation with further destruction of lung tissue [100]. The first CF mouse model reported a residual CFTR conductance, and the later CFTR^{ΔF508/ΔF508} pig model also reported this residual function with about 6% of WT function [101]. New-born CFTR^{-/-} piglets usually present gastrointestinal abnormalities including, pancreatic destruction, bowel obstruction and early biliary cirrhosis, and while lungs appeared to be healthy after birth, this organ also develops a rapid inflammation which evolves into a severe lung disease [101]. Similar to pigs, ferrets with CFTR mutations also develop spontaneous lung inflammation, pancreatic and gastrointestinal abnormalities within the first weeks after being born, showing increased levels of IL-8 and TNF [102, 103]. One study demonstrated that new-born CF ferrets were unable to eradicate *P aeruginosa* infections compared to their WT

counterparts; also, they showed a deficient innate immune system and pulmonary hyper-inflammation [104]. It was recently demonstrated that ferrets homozygous $CFTR^{G551D/G551D}$ could be rescued by administration of ivacaftor, ivacaftor, in utero and after birth [105]. administration of ivacaftor in utero in $CFTR^{G551D/G551D}$ ferrets corrects the abnormal formation of the vas deferens and epididymis, augments growth and partially recovers the normal pancreatic function [105]. Postnatal administration of ivacaftor improves lung function and helps in the reduction of bacterial infections, and withdrawal of the treatment leads to the development of CF lung disease [105]. The CF sheep model also corroborates certain features present in the other models of CF, with the most common being pancreatic destruction, gastrointestinal abnormalities, absence of the vas deferens, and obstruction of the epididymis; however, an abnormal lung phenotype was not correlated with mutations in the *CFTR* gene in this model [106]. A feature of this, and other models of CF, is the early infiltration of immune cells followed by an abnormal inflammatory process with eventual damage and destruction of the pancreatic tissue [90, 106]. Pancreatic destruction is another common characteristic seen in CF, which has been replicated in a CF zebrafish model. In this unique model of CF, $CFTR^{-/-}$ zebrafish larvae frequently presented higher numbers of neutrophilic infiltration in the pancreas with further damage to the organ [107]. In a similar study, it was found that macrophages are crucial for the development of the pathogenic bacteria *B cepacia*, as this pathogen was unable to proliferate in zebrafish depleted of macrophages [108]. It is interesting how different models of CF coincide in similar phenotypic abnormalities which are also present in humans, making these models a valuable tool to investigate the origin of his disease and to test new drug compounds for the treatment and potential cure of this disease.

1.2.3 Monocytes, macrophages and neutrophils in CF

As seen in the previous sections, inflammation is a common feature in CF. While epithelial cells play an important role in the pathogenesis of inflammation, certainly immune cells orchestrate the initiation and the restoration of the inflammatory response. The immune system is subdivided into two branches, known as the adaptive and the innate immune system, the former composed mainly by T, B and natural killer (NK) cells and the latter by basophils, eosinophils, neutrophils, monocytes and macrophages [109]. While both branches of the immune system are fundamental parts for the clearance of any infection, today there has not been a direct relationship between CFTR mutations and abnormal activity of the adaptive immune system. Adaptive immune cells are crucial in the eradication of any infection and, in fact, a subpopulation of T cells, Th17, are largely found in the submucosa layer of the lung of patients with CF [110]. A correlation between Th17 cells and neutrophil counts in these patients, suggesting that it might be the abnormal amount of neutrophils what is causing the Th17 cells to be recruited to the site of the infection [110]. It is uncertain whether the cells of the adaptive immune system are affected by CF mutations, and further research is encouraged to explore this alternative.

In the case of the innate immune system, there is abundant evidence suggesting a direct correlation between CFTR mutations and an intrinsic defect in monocytes, macrophages and neutrophils [18, 19, 30, 59, 108, 111-114]. Monocytes are phagocytic cells that originate from the bone marrow with the capacity to be differentiated into macrophages and dendritic cells, which are professional antigen-presenting cells (APC). Some reports demonstrate that monocytes and macrophages, from CF children, present downregulation of the surface markers CD14 and HLA-DR with deficient phagocytosis [115]; however, these findings have been challenged by

other reports showing that there is no difference in monocyte subpopulations [18, 116]. Expression of the surface markers M-CSF, TLR4, IL-4R α , IL-13R α 1, TIMP-1 and Cox-2, were shown to be upregulated in CF monocytes, demonstrating that CFTR mutations intrinsically affect monocytes from patients with CF [18]. Interestingly TLR4 has been reported to be consistently upregulated in both monocytes and macrophages from patients with CF and it was not related to pulmonary infections [17, 18, 117]. In another study, IL-8 was shown to be upregulated in CF monocytes after an LPS challenge, and this IL-8 overexpression was not associated with TLR4 overexpression but, rather, to an alternation in MAPK signalling [118]. The importance of CFTR expression in myeloid cells was demonstrated in a conditional KO mice model, where only myeloid-derived cells suffer from the lack of CFTR [119]. Normally, these conditional myeloid CFTR KO mice did not show any differences compared to WT mice; however, when these mice were challenged to bacterial pathogens in the lung, these mice displayed a significantly higher inflammatory response and decreased survival rate compared to WT mice [119].

When monocytes are recruited to the site of infection or inflammation, these myeloid cells can be differentiated into classically activated macrophages, pro-inflammatory (M1), or alternatively activated macrophages, anti-inflammatory (M2) [120]. As monocytes differentiate toward macrophages, their ER is expanded, and their size becomes expanded, providing these unique cells with a greater capacity to promote inflammation and phagocytosis. Other types of macrophages also exist, known as tissue-resident macrophages. While monocytes derived macrophages originate from the bone marrow, tissue-resident macrophages are derived either from the yolk sac or foetal liver and reside in specific tissues with unique characteristics [121, 122]. Not only have different types of tissue-resident macrophages been

characterised, but different subtypes of monocyte-derived macrophages, such as M2a, M2b, M2c and M2d, have also been described in the literature [123, 124]. In CF, alveolar macrophages are partially responsible for the high degree of airway inflammation and it is known that patients with CF present a large number of macrophages in the lung, with high concentrations of neutrophils as well [113, 125]. Increased expression of the pro-inflammatory cytokines IL-1 β and CCL-2 was reported in alveolar macrophages from CF mice stimulated with the TLR4 agonist LPS, while the expression of IL-10 was decreased in these mice [126]. Interestingly, azithromycin efficiently reduced the exaggerated inflammatory response decreasing the high levels of TNF, IL-1 β and CCL-2 in M1 macrophages [126]. Furthermore, this study reported that both M1 and M2 macrophage polarisation was significantly increased in alveolar and peritoneal macrophages from CFTR $\Delta F508/\Delta F508$ mice [126]. Although, both M1 and M2 macrophages are increased in CF mice, the opposite was reported in human macrophages with no difference in the polarisation of M1 and a significant decrease in the polarisation of M2 [19, 30]. A different study reported a significant upregulation of M2 macrophage polarisation in patients with CF at baseline, meaning that they pushed monocytes to macrophages right after the blood isolation, and downregulation of M1 macrophages 48 hours after the polarising stimulus [111]. The discrepancies of these studies might originate in the different surface markers used for macrophage characterisation, the method for macrophage polarisation and, ultimately, in the isolation method for these monocytes. Certainly, monocytes and macrophages harbouring CFTR mutations present with intrinsic abnormalities affecting their cellular functions and contributing towards an abnormal inflammatory response.

Neutrophils are also important players in the pathogenesis of CF and these multinucleated cells are reported to be increased in the lung of patients with CF [22].

It was recently reported that delayed apoptosis of CF neutrophils increased NET formation in the lungs of patients with CF, helping to explain that certain characteristics of CF neutrophils are not entirely related to inflammation, but rather to an intrinsic cellular defect mainly associated with CFTR mutations [59]. Furthermore, the stimulation of macrophages with NETs induced the production of TNF and IL-8, and both cytokines were significantly higher in CF macrophages compared to HC volunteers [59]. In the clinic, the levels of TNF and IL-8 have shown a positive correlation with disease progression and it is known that the high levels of these cytokines can induce the infiltration of neutrophils in the lung [127, 128].

Inflammation is certainly a problem in CF and the underlying cause of this abnormal process is not solely due to a single factor but, rather, to a combination of different environmental and intrinsic defects present in cells with CFTR mutations. For that reason, it is critical to understand the underlying impact of CFTR mutations in different immune cells and their interaction with other cells.

1.3 ER Stress and the Unfolded Protein Response

1.3.1 The UPR signalling pathways

The unfolded protein response (UPR) is a conserved and unique cellular mechanism, which is present in mammalian and yeast cells [129]. The UPR is activated under cellular stress, with endoplasmic reticulum (ER) stress being one of the principal activators of this unique mechanism [129, 130]. The UPR can be activated when either unfolded or misfolded proteins are detected, causing activation of three classes of ER-resident proteins, referred to as inositol requiring enzyme 1 (IRE1), double-stranded RNA-activated protein kinase (PKR)-like ER kinase (PERK), and activating transcription factor 6 (ATF6) [129]. It is essential to mention that UPR activation can be induced by several other stimuli such as, oxidative stress, starvation, inflammatory cytokines and pathogens, making the UPR a complex signalling pathway [131-134]. Another player, in the regulation of these three UPR ER-resident proteins, is the heat shock protein binding immunoglobulin protein (BiP), also known as HSPA5. With the accumulation of misfolded proteins in the lumen of the ER, BiP, which is generally bound to IRE1, PERK and ATF6, is dissociated from these proteins and sequestered by the misfolded proteins, with subsequent activation of the UPR signalling pathway [129]. The three primary arms of the UPR work in concert to re-establish normal cellular function decreasing cellular stress, and when this is not possible, to induce cellular apoptosis.

The most characterised arm of the UPR is IRE1 a dual ER transmembrane protein, with both kinase and RNase activity, that is found in two isoforms, IRE1 α and IRE1 β , with IRE1 α being the most common isoform. The oligomerisation of IRE1 α causes phosphorylation of its kinase subunit, with subsequent activation of its RNase

domain favouring the degradation of specific RNAs in a process known as regulated IRE1-dependent decay (RIDD) [130, 135]. This particular process is known to interact with more than 120 different RNAs, causing the degradation of these transcripts or, in particular cases, the modification of them [135]. The mRNA of a transcription factor known as X box-binding protein 1 (XBP1) can be directly affected by the RNase domain of IRE1 α and, when active, it causes a translational frameshift removing a 26 nucleotide intron producing a shorter isoform referred to as XBP1 spliced (XBP1s) [136, 137]. XBP1s is a potent pro-survival transcription factor involved in several cellular regulatory mechanisms including metabolism, inflammation and autophagy, dynamically regulating other ER stress-responsive genes [138-141].

The next arm of the UPR is ATF6, which is found in two different isoforms ATF6 α and ATF6 β with some evidence demonstrating that ATF6 β is a negative regulator of ATF6 α [129, 142]. After detecting cellular stress, ATF6 is moved to the Golgi apparatus where it is proteolytically cleaved releasing a cytoplasmic fragment that is further translocated into the nucleus directly upregulating XBP1, CHOP and several chaperone proteins [129, 142].

The last arm of the UPR is PERK, which has been identified for its kinase activity but lacking the unique RNase domain present in IRE1. In a similar manner to IRE1, removal of BiP from the luminal domain of PERK induces protein dimerisation followed by auto-phosphorylation and eventual activation of the ER transmembrane protein [129, 143]. PERK activation is followed by a complex and dynamic pathway that regulates protein synthesis via eukaryotic initiation factor 2 (eIF2 α) [144]. When PERK is activated, it causes phosphorylation of eIF2 α which, in turn, halt protein synthesis helping to reduce the ER protein load to reduce cellular stress [143, 144]

eventually. Paradoxically, the activation of eIF2 α also induces the production of activation transcription factor 4 (ATF4), a potent transcription factor which is involved in the regulation of genes related to metabolism, autophagy and cellular oxidation [144]. Importantly, when cells are exposed to chronic ER stress, ATF4 induces the expression of C/EBP homologous protein (CHOP), and accumulation of CHOP has been associated with apoptosis [145, 146]. Activation of eIF2 α is negatively regulated by growth arrest and DNA damage-inducible protein (GADD34). Induction and activation of GADD34 can be achieved by CHOP and ATF4, functioning as a phosphatase of eIF2 α , thereby restoring protein synthesis to its normal state and downregulating PERK activation [129, 147]. Furthermore, there is some evidence suggesting that PERK can regulate the oxidative response through activation of nuclear factor erythroid 2-related factor 2 (Nrf2), which is known to be a strong regulator of the antioxidant response [148, 149]. The UPR signalling pathway has been summarised in the next diagram (Figure 5). The UPR is versatile and complex signalling pathway and it has been demonstrated to strongly regulate the inflammatory response as it will be explained in the next section.

Unfolded Protein Response (UPR)

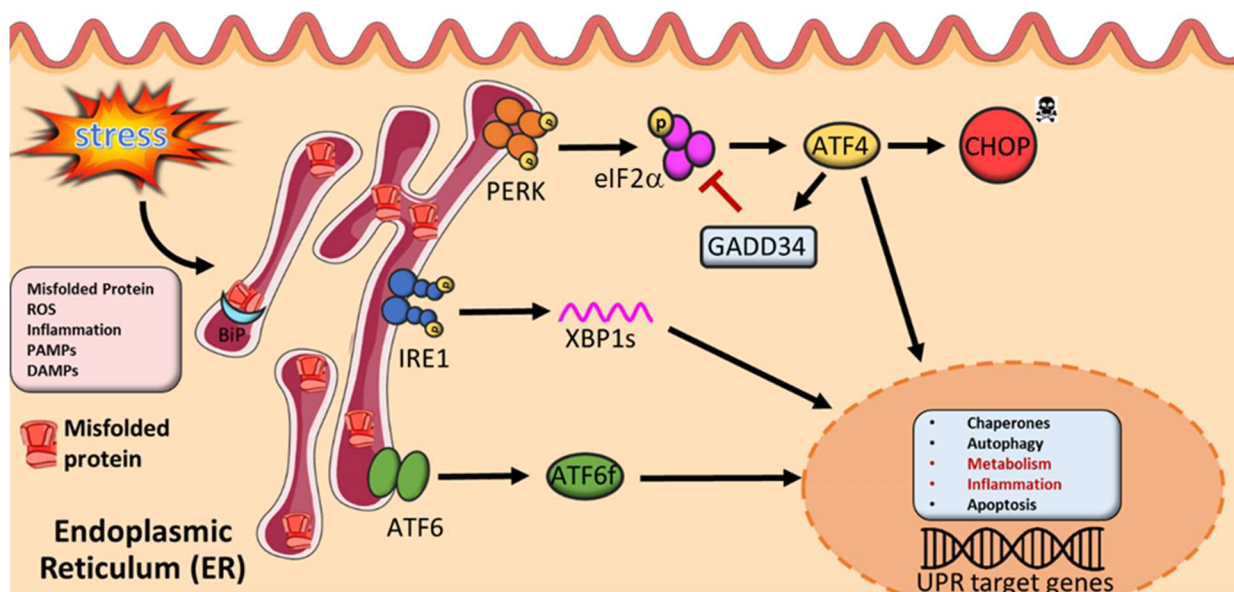


Figure 5 – The UPR signalling pathway

BiP detects unfolded protein within the ER, activating ATF6, IRE1, and PERK. ATF6 activation leads to the production of ATF6f, which upregulates UPR target genes. IRE1 is auto-phosphorylated, inducing mRNA degradation through RIDD. The RNase domain of IRE1 induces the unconventional splicing of the transcript XBP1 and produces XBP1s. PERK activation induces phosphorylation of eIF2 α selectively upregulating ATF4 inducing UPR target genes, including GADD34 and CHOP.

1.3.2 Inflammation and the UPR

Inflammation is one of the main consequences of bacterial infections, tissue damage, autoimmunity or autoinflammation. Autoinflammation can be described as a self-directed inflammation with a direct influence of the local tissue environment followed by activation of the innate immune system, causing tissue damage and cellular death [150]. Autoinflammation can also be induced by intrinsic cellular insults, normally caused by genetic mutations, generating a low-grade chronic inflammation responsible in priming and, eventually, exacerbating the inflammatory response [30, 151, 152]. This low-grade chronic inflammation can be caused by the accumulation of

misfolded proteins in the ER, hence activating the UPR. It has been shown that the IRE1 α arm of the UPR regulates the transcription of several pro-inflammatory cytokines, such as TNF, IL-1 β , IL-6 and IFN- β [151, 153, 154]. It is known that activation of TLR4 and TLR2 can induce the activation of the IRE1 α -XBP1 signalling pathway inducing the transcription of the pro-inflammatory cytokines TNF and IL-6 (Figure 5) [133, 151]. Furthermore, XBP1s is indeed recruited to the promoter region of TNF and IL-6 inducing transcriptional activation of these two cytokines [151].

Similarly, ATF4 was shown to interact with IL-6 binding region, promoting upregulation of IL-6 in macrophages [155]. Activation of main signalling pathways necessary for the production of pro-inflammatory cytokines, such as NF- κ B, can work in synergy with the IRE1 α -XBP1 signalling pathway inducing an exaggerated inflammatory response [30, 133, 151]. The UPR has been shown to induce cellular stress and inflammation in several immune-related disorders, particularly in autoinflammatory disorders [156]. The autoinflammatory condition tumour necrosis factor receptor-associated periodic syndrome (TRAPS), is a genetic disorder mainly characterised by recurrent periodic fevers and uncontrolled episodes of inflammation [157]. TRAPS is characterised by intracellular accumulation of tumour necrosis factor receptor 1 (TNFR1), causing ER stress followed by activation of the UPR [158, 159]. Cells with TRAPS mutations showed significantly higher levels of XBP1s, PERK and ROS, showing an exaggerated response to LPS with further secretion of TNF, IL-6 and IL-1 β [158, 159]. IL-1 β is an important inflammatory cytokine which is normally elevated in patients suffering from autoinflammatory conditions. This cytokine is mainly regulated by the NLR Family Pyrin Domain Containing 3 (NLRP3). The NLRP3 is a conserved innate immune mechanism created to detect pathogen-associated

molecular patterns (PAMPs) and danger-associated molecular patterns (DAMPs), ultimately activating the pro-inflammatory cytokines IL-1 β and IL-18 [160].

ER stress and the UPR signalling pathway have been directly involved in the activation of the NLRP3 inflammasome with further production of IL-1 β [161-163]. The NLRP3 responds to ER stress and induces the production of IL-1 β independently of IRE1 and XBP1 [161]. In another study, it was shown that TXNIP, a protein-coding gene induced by IRE1 α , is an important inducer of IL-1 β and ROS and, silencing of TXNIP led to reduction of IL-1 β with a further reduction of inflammation [163, 164]. Furthermore, caspase-2 and BID were shown to be fundamental in the classical activation of the inflammasome and the secretion of IL-1 β [163]. A recent study indicates that the RNase activity of IRE1 α is an important player in the assembly of the NLRP3 and its eventual activation [154]. This study shows that inhibition of IRE1 α RNase domain diminishes NLRP3 activity, reducing caspase-1 activation and IL-1 β [154]. While the production of IL-1 β is directly affected by inhibition of IRE1 α certainly IL-18 is not, suggesting that the NLRP3 is a complex mechanism that can be influenced by more than one signalling pathway. ER stress, followed by UPR activation, has been detected in synovial fibroblast and PBMCs from patients with rheumatoid arthritis (RA) [133]. Macrophages and neutrophils from myeloid-conditional IRE1 α ^{-/-} mice showed a reduction of pro-inflammatory cytokines with amelioration in the clinical disease score after inducing arthritis, compared to WT mice [165]. Furthermore, inhibition of IRE1 α RNase domain with 4 μ 8C, in the same mice, showed a reduction in the inflammation after inducing arthritis [165]. GSK-3 β can also induce IL-1 β through IRE1 α activation but independent of XBP1 [166]. Moreover, inhibition of GSK-3 β selectively downregulated IL-1 β gene expression, while inhibition

of IRE1 α with STF083010 only inhibited TNF production without any effect in IL-1 β [166].

Cigarette smoke can also stimulate multiple signalling pathways in airway epithelial cells generating ROS, ER stress and activation of the UPR [167, 168]. Several UPR related proteins including BIP, calreticulin, ATF4 and NRF2, were upregulated in smokers compared to non-smokers [168]. In a different study, it was demonstrated that ATF6 mediates the regulation of the pro-inflammatory cytokines TNF and IL-6 during ischemia-reperfusion [169]. Liver macrophages exposed to ischemia showed induction of ER stress with an emphasis in ATF6 upregulation. Modulation of ER stress during this ischemia-reperfusion model by ATF6 siRNA, decreased the level of inflammation in the liver, protecting the organ from ischemia-reperfusion injury [169]. The UPR plays an important role in the regulation of the inflammatory response; therefore, a better understanding of this signalling pathway is encouraged.

1.3.3 CF and the UPR

ER stress and the UPR are essential players in the pathogenesis of different diseases as shown in the previous sections. Some reports show an abnormal UPR activation in cells with CF mutations [170]. In CF there is an abnormal mucus formation which favours the colonisation of bacterial pathogens in the lung. Furthermore, when airway epithelial cells are exposed to supernatants from this mucus material from patients with CF, the ER becomes enlarged with an increased capacity to sequester Ca²⁺ [88]. This ER expansion is an innate immune response to chronic infections and inflammation, which is regulated by several ions including Ca²⁺ [88]. This ER

enlargement may potentially induce cellular stress and activation of the UPR. After exposure to the supernatant from the mucus material, CF HBECs were shown to be hyperinflammatory with higher levels of IL-8 production compared to non-CF cells [89]. This hyperinflammatory response was mediated by an increased Ca^{2+} flux a result from an enlarged ER in these epithelial cells [89]. In a different study, the ER expansion and the increased Ca^{2+} flux in HBECs were associated with increased levels of XBP1. Isolated HBECs from patients with CF, with inflamed or infected lungs, showed an increased expression in XBP1s [171]. This finding was corroborated in mouse models and cell lines, showing the importance of XBP1s in the enlargement of the ER and production of IL-8 [171].

Atypical activation of the UPR was reported in CF with an upregulation of the IRE1 α -XBP1 pathway and a lack of induction of PERK-eIF2 α [172]. In this study, it was shown that XBP1u and XBP1s were both upregulated in immortalised CF HBECs, CF lung tissue and PBMCs, while the PERK-eIF2 α pathway was downregulated only in the CF HBECs [172]. Furthermore, MAPK p38 is overactive in CF HBECs inducing the production of IL-6, which can be reduced by inhibiting p38 MAPK with SB203580 [172]. In a different study, TNF and IL-6 were significantly upregulated in alveolar macrophages from patients with CF under basal conditions and after LPS stimulation [113]. The overexpression of XBP1s was correlated with the exaggerated inflammatory response, as inhibition of XBP1s with the inhibitor 4 μ 8C reduced cytokine production ameliorating the inflammatory response [113]. Interestingly XBP1-KO in the monocytic-like cell line THP-1, completely abrogated the production of TNF at both the mRNA and cytokine level, even after LPS stimulation, while IL-6 was significantly downregulated [113]. XBP1 plays an essential role in the pathogenesis of CF, modulating inflammatory pathways in this genetic disorder. One study

demonstrated that overexpression of Δ F508-CFTR in human airway cells is associated with the amount of XBP1s produced by the cells [173]. In this study, the authors overexpressed different levels of Δ F508-CFTR in the Calu3 cell line. While only the cell line with the highest expression of Δ F508-CFTR showed a significantly higher amount of XBP1s under basal conditions, all the cells expressing Δ F508-CFTR showed increased XBP1s production after induction of UPR activation with tunicamycin [173]. This finding supports the idea that undetected low-grade chronic ER stress could prime the cells towards an exaggerated response after a second challenge. ATF6 is activated in cells harbouring CFTR mutations [174]. Δ F508-CFTR expressing cells showed an increase in BiP and activation of ATF6, demonstrated by ATF6 fragmentation [174]; however, in a different study, this finding was challenged showing that ATF6 is downregulated in CF cell lines and bronchial brushings from patients with CF compared to HC controls [175]. The authors also demonstrated that overexpression of miRNA-221 in CF cells downregulates ATF6 expression [175]. While the UPR plays an essential role in CF, more research is needed to elucidate the consequences of its activation.

1.4 Cellular Metabolism

1.4.1 Glycolysis and the Krebs cycle

While this section will cover the significant aspects of glycolysis and Krebs cycle, by no means will cover every single aspect of cellular metabolism as this topic can be overwhelming and extensive. Metabolism is the process of converting food into energy, better known as adenosine triphosphate (ATP), by a series of complicated biochemical reactions [176]. The three primary sources of energy for mammalian cells are known to be carbohydrates, proteins and fatty acids, which are broken down by a series of different enzymes with the final goal of producing ATP [176]. While fatty acid and protein metabolism, also known as β oxidation and protein catabolism, are regulated by different molecules, they both produce at the end pyruvate that under normal circumstances enters the Krebs cycle producing 36 molecules of ATP by every two molecules of pyruvate [176]. To avoid confusion while reading this topic, it would be easier to digest all these pathways by showing a simple diagram with all metabolic pathways together, before getting into the full glycolytic pathway and the Krebs cycle (Figure 6).

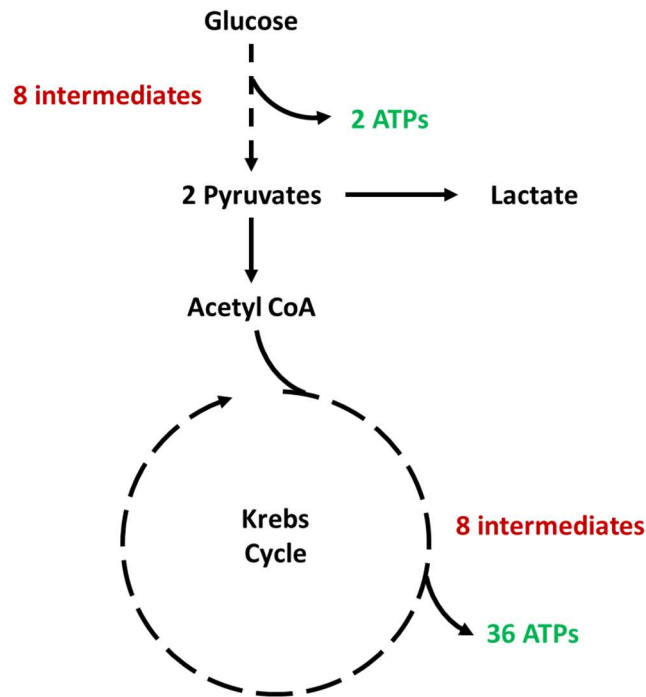


Figure 6 – Glycolysis and the Krebs cycle

The production of energy in most mammalian cells starts through the glycolytic pathway converting glucose into two molecules of pyruvate, producing 2 ATPs. Pyruvate is converted into Acetyl CoA within the mitochondrial space and enters the Krebs cycle in the form of citrate producing 36 ATPs.

Glycolysis is the process of breaking down glucose to convert it into pyruvate, and this reaction does not require oxygen directly. In glycolysis, glucose is transported inside the cell, and it is converted into glucose-6-phosphate, which then is committed to undergo glycolysis resulting into the production of two molecules of pyruvate and ATP for every molecule of glucose [176]. Glycolysis can be carried out under anaerobic conditions until the point of pyruvate conversion. Under anaerobic conditions, pyruvate is transformed to lactate by lactate dehydrogenase producing ATP from the glycolytic pathway and replenishing the system quickly, although to the cost of producing lactic acid [176]. On the other hand, when O_2 is present pyruvate is transported to the mitochondria converted to acetyl-CoA and entered into the citric acid cycle, also known as the Krebs cycle [177]. It is essential to mention that the

opposite reaction, the conversion of non-carbohydrates substrates to glucose, can also be carried out by mammalian cells in a process known as gluconeogenesis [178]. Gluconeogenesis is an important mechanism to store energy and maintain normal blood glucose levels when required, and this process mainly takes place within liver cells [178]. Some enzymes within the glycolytic pathway will be discussed later; therefore, the full pathway can be reviewed in Figure 7.

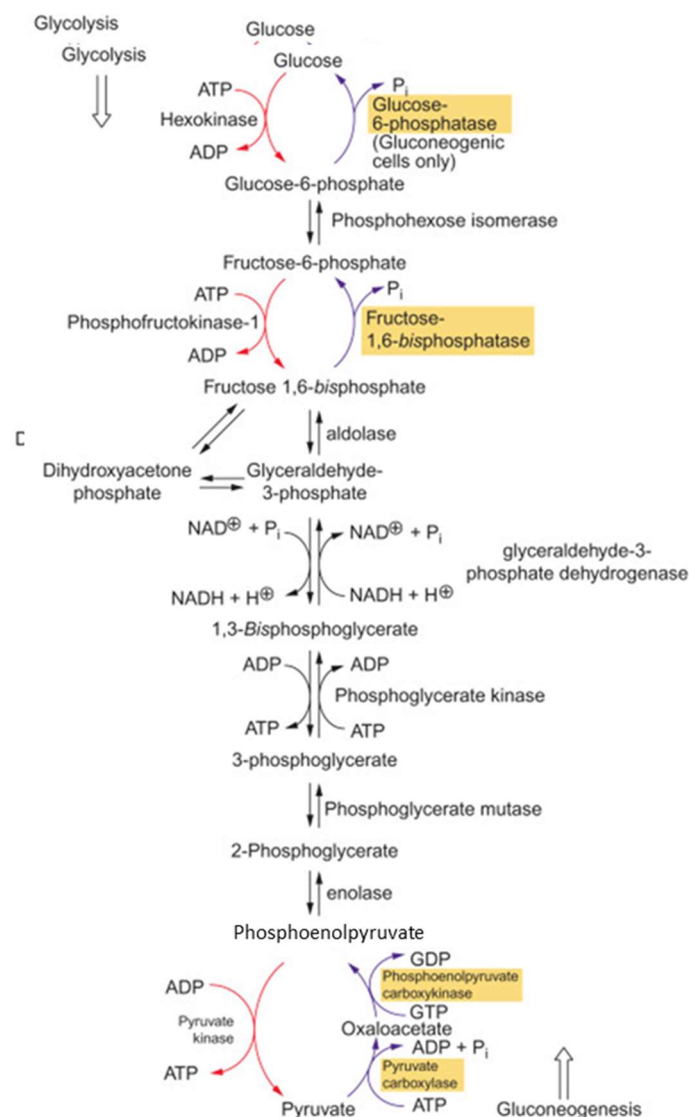


Figure 7 – Glycolytic pathway

The diagram shows the main glycolytic pathway with intermediates and enzymes. The red arrows indicate an irreversible reaction, in most of the cells, while the blue arrows indicate steps involved in gluconeogenesis. Image adapted from, Human biochemistry chapter 8, figure 8.5 [178].

While the Krebs cycle is the process of converting acetyl-CoA into ATP through a series of biochemical reactions, it is not the Krebs cycle which produces the ATP, but the electron transport chain (ETC). During the Krebs cycle, a molecule known as nicotinamide adenine dinucleotide (NAD^+) is converted to its reduced form, NADH. The ETC oxidises NADH by a series of mitochondrial transmembrane protein complexes producing NAD^+ within the inner of the mitochondria and transferring protons (H^+) to the intermembrane mitochondrial space [176]. This process creates an electrochemical H^+ gradient that favours the synthesis of ATP, from ADP, by a proton pump under the name of ATP synthase. In summary, one molecule of glucose is converted into two pyruvates within the cell. Moreover, under aerobic conditions pyruvate is converted to acetyl-CoA entering the Krebs cycle producing NADH, and also FADH, which is oxidised by the ETC producing ATP from the electrochemical gradient generated by this process [177]. An overview of the full Krebs cycle can be reviewed in Figure 8 and a simplification of the ETC in Figure 9.

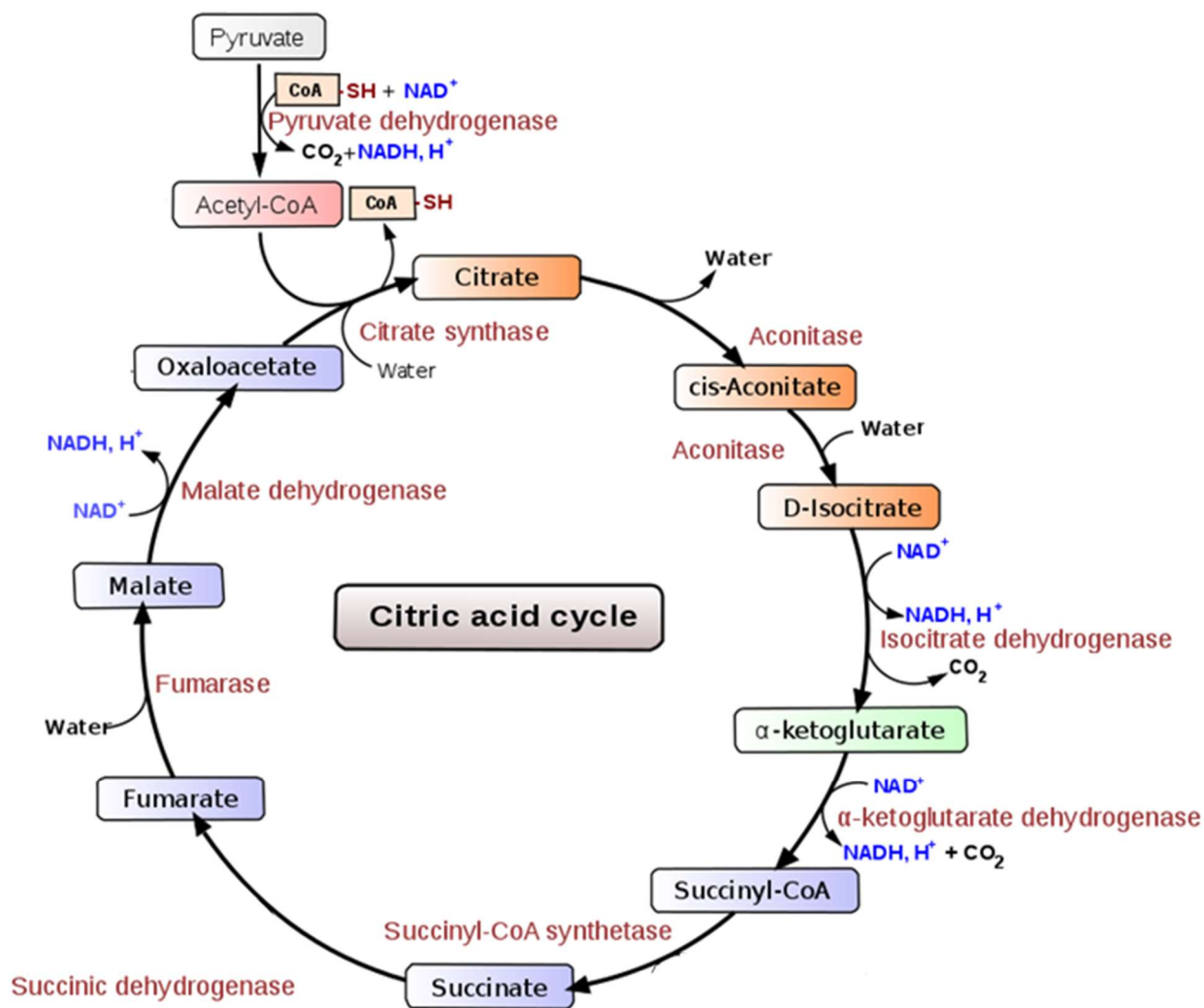


Figure 8 – The Krebs cycle

The diagram shows the Krebs cycle, citric acid cycle, with all the intermediates and enzymes. During the Krebs cycle citrate is converted to oxaloacetate by a series of enzymatic reactions and H₂O, CO₂ and NADH/FADH₂ are produced. This process is carried out inside the mitochondrial space. Image adapted from Narayane, WikiUserPedia, YassineMrabet, TotoBaggins -<http://biocyc.org/META/NEW-IMAGE?type=PATHWAY&object=TCA>

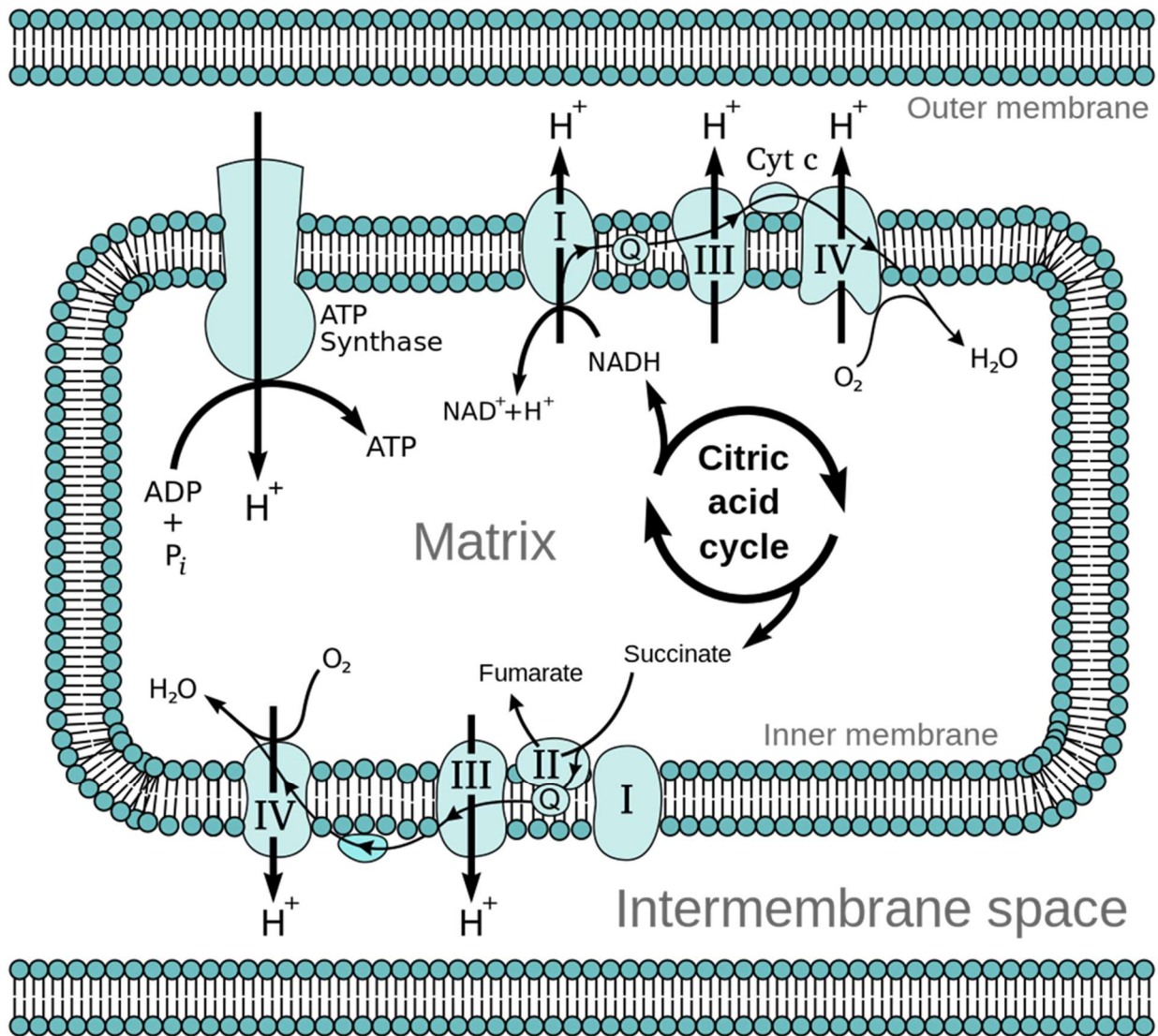


Figure 9 – Electron transport chain

The ETC is the process of converting NADH/FADH₂ into ATP by mitochondrial complexes I, II, III and IV. During these processes, a proton gradient is produced in mitochondrial intermembrane space creating the conditions for ATP production by the ATP synthase pump. Oxygen is the final electron acceptor in the ETC, and without it, the ETC and Krebs cycle stop favouring glycolysis. Image source: Fvasconcellos 22:35, 9 September 2007 (UTC) - Vector version of w:Image:Etc4.png by Tim Vickers, content unchanged., Public Domain.

Finally, it is important to mention that under certain circumstances, the cells favour the glycolytic pathway and lactic acid formation even under aerobic conditions. This phenomenon was first described in cancer cells by Otto Heinrich Warburg, and he referred to this process as the Warburg effect [179]. Interestingly, specific immune cells, when activated, display a similar metabolic behaviour like the one seen in cancer cells, favouring the quick production of ATP via glycolysis and lactic acid formation, which is going to be discussed in the next section [180-182]. Indeed, genetic mutations that affect critical proteins of these metabolic pathways can generate metabolic disorders which are known to have an impact on human health.

1.4.2 Immunometabolism: macrophage metabolism

Immunometabolism has been a hot topic in the field of immunology over the past decade. While this topic was undoubtedly introduced more than 40 years ago, today new technological advances allow us to explore this field with better detail [183]. One of the first articles published in macrophage metabolism was in 1986, describing the high enzymatic activity of hexokinase during glycolysis, but a low glucose utilisation on resting or non-activated macrophages [184]. Later it was found that macrophages have a rapid glucose consumption via the glucose transporter 1 (GLUT1) when stimulated with LPS, contributing to the systemic hypoglycemia seen during endotoxemia [185]. Glycolysis is indeed the pathway of preference of activated M1 macrophages and T cells, providing these cells with a rapid energy source needed for the circumstances encountered [183]. While glycolysis is crucial in the activation of the pro-inflammatory M1 macrophages, it is not the same for their counterpart anti-inflammatory M2 macrophages. Activated M2 macrophages prefer the production of ATP through the Krebs cycle and oxidative phosphorylation [186]. Usually, during the

resolution of the inflammatory response the normal oxygen levels are restored within the tissue and cytokines, such as IL-4 and IL-13, are secreted favouring oxidative phosphorylation and the polarisation of M2 macrophages [187, 188]. In the case of M1 macrophages hypoxia, bacterial components, PAMPs, DAMPs, ROS and other danger signals, induce macrophage activation upregulating glycolysis promoting the inflammatory response [187, 188]. It has been shown that during hypoxia, the transcription factor HIF1 α , alongside with succinate, is upregulated in macrophages favouring the production of IL-1 β [189, 190]. In a different study, it was shown that accumulation of ROS within macrophages induce the transcription of TXNIP favouring the production of IL-1 β [191]. Interestingly, when the hexokinase inhibitor 2-deoxyglucose (2-DG) was administered to macrophages, before activation, the inflammatory response was significantly reduced [192-194]. 2-DG certainly reduces the inflammatory response; however, it was recently shown that 2-DG treatment decreases the amount of M2 macrophage polarisation, inhibiting the expression of some of the most common markers of M2 polarisation, such as Arg, Ym-1, and CD206 [195]. Heightened glycolysis has also been shown in LPS-activated dendritic cells (DC), activated NK, effector T and B cells [183]. Macrophages which are activated via LPS/IFN γ , TLR-2, TLR-3, TLR-4 and TLR-9 showed higher activity of ubiquitous phosphofructokinase-2 (uPFK2), rather than the liver-PFK2, increasing the glycolytic flux [196]. The first enzyme in the glycolytic pathway, hexokinase 1, is a critical regulator of the NLRP3 inflammasome, interacting with the NLRP3 complex within the mitochondrial space, resulting in its activation and realising IL-1 β [197].

While glycolysis is indeed an essential player in the inflammatory response the Krebs cycle and the ETC are also crucial players in immune cell activation. For instance, in memory T cells, the pathway of preference is the Krebs cycle and the

ETC, this is mainly due to their quiescent activity [198]. The Krebs cycle is a central regulator of macrophage polarisation and behaviour. While in M2 macrophages there is a fully functional Krebs cycle followed by the production of ATP by the ETC, in M1 macrophages there is a disruption of the citric acid cycle with the accumulation of citrate and succinate (Figure 10) [186]. The accumulation of citrate favours the fatty acid synthesis pathway, allowing these phagocytic cells to be able to engulf bacterial pathogens with the formation of cellular membrane [183]. Citrate accumulation also induces the production of itaconate a potent newly described antimicrobial and anti-inflammatory metabolite, alongside the formation of nitric oxide (Figure 10) [199-201]. The other part of the Krebs cycle that is disrupted is the conversion of succinate to fumarate. In fact, it has been suggested that itaconate prevents succinate dehydrogenase from regulating succinate and IL-1 β production (**Figure 10**) [201]. Another study demonstrated that itaconate mainly induces its potent anti-inflammatory effects via NRF2 activation and further inhibition of IL-1 β [199]. Certainly, itaconate is a potent anti-inflammatory metabolite; however, its mechanism of action remains to be fully deciphered. Immune cells differ widely and require unique types of metabolism depending on their function. It is crucial to understand how these metabolic pathways are affected at the molecular level during disease and what are the consequences of these disruptions, not only in macrophages but in other immune cells as well.

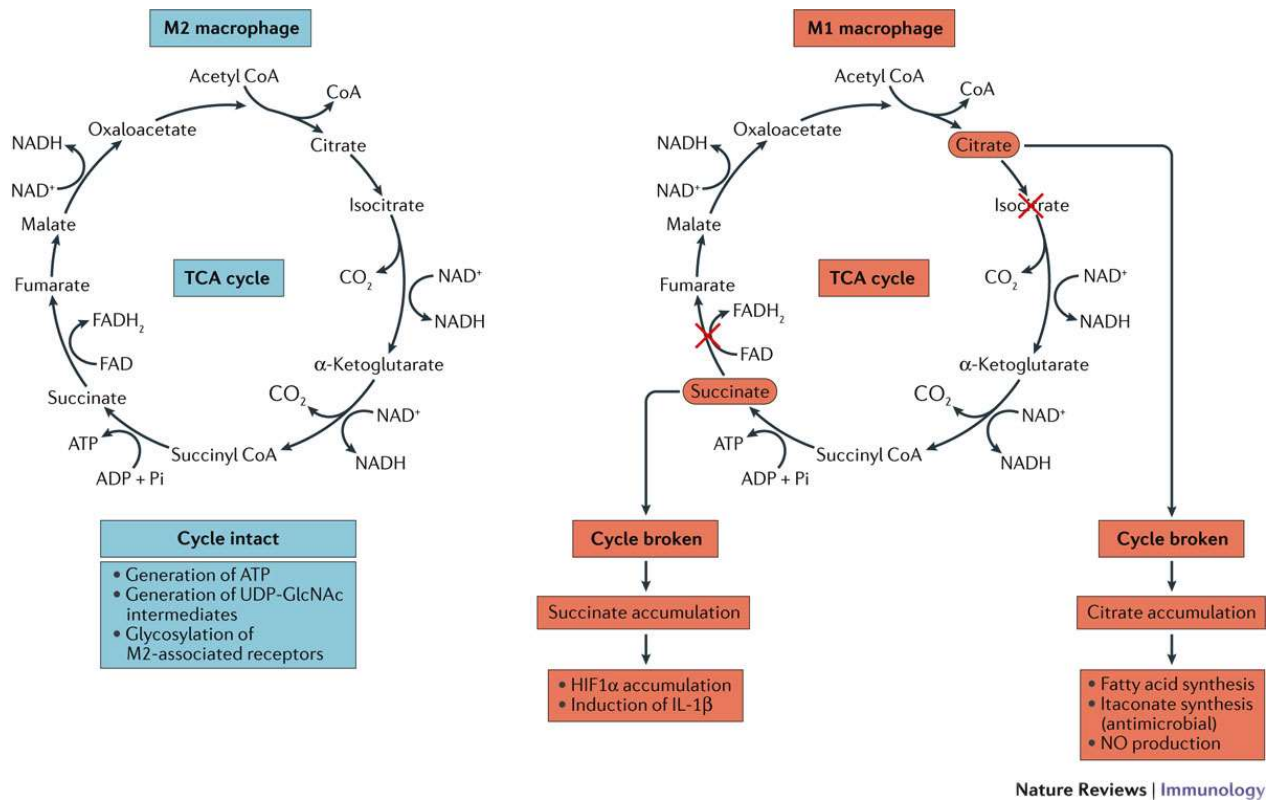


Figure 10 – The Krebs cycle in M1 and M2 macrophages

M2 macrophages display a fully functional Krebs cycle with the efficient production of ATP. When activated, with LPS/IFN γ , M1 macrophages undergo metabolic reprogramming favouring glycolysis and breaking the Krebs cycle. Citrate and succinate are accumulated having as a bio-products, respectively itaconate and IL-1 β . Reprinted by permission from Springer Nature: (Nature Reviews Immunology) [183] Copyright Clearance Centre RightsLink® 2019.

1.5 Hypotheses

1.5.1 List of Hypotheses

Hypothesis 1: Atypical activation of the UPR, existing in HBECs, is CFTR genotype-dependent.

Hypothesis 2: Activation of the UPR is only present in specific subsets of immune cells.

Hypothesis 3: Cells with CFTR mutations present an abnormal metabolic state associated with UPR activation.

Hypothesis 4: That the abnormal metabolic state and UPR activation seen in CF is related to the exaggerated inflammatory responses.

1.5.2 Aims and Objectives

Hypothesis 1:

1 – To establish whether UPR activation is different in HBECs bearing various CFTR mutations.

2 – To investigate whether this UPR activation leads to an exaggerated inflammatory response in different HBECs with various CFTR mutations.

3 – To investigate whether CF HBECs respond similarly after stimulations with bacterial components and UPR inducers.

Hypothesis 2:

1 – To investigate whether the UPR activation is specific for individual immune cells or all CFTR mutated cells are affected by ER stress.

2 – To investigate whether the exaggerated inflammatory response seen in CF immune cells is UPR dependent.

3 – To investigate how immune cells affected by ER stress respond to stimulations with bacterial components and ER stressors.

Hypothesis 3:

1 – To investigate whether the innate immune cells affected by ER stress display an abnormal metabolic state.

2 – To investigate the mitochondrial function and glycolytic flux of monocytes and M1 macrophages bearing CFTR mutations

3 – To investigate whether this abnormal hypermetabolic state is associated with the UPR activation seen in CF cells.

Hypothesis 4:

1 – To establish whether the abnormal metabolic state and the UPR activation seen in CF macrophages are associated with the exaggerated inflammation

2 – Investigate the impact of IRE1 α in the abnormal metabolic state seen in CF macrophages.

3 – To investigate how CF small molecule therapies impact in macrophage metabolism.

Chapter 2 – Methods

2.1 Cellular culture

2.1.1 Cell Lines

A full table of resources is provided at the end of this chapter with all the details of the chemicals, reagents, cell lines and software used during this research **Table 5**. Four different HBEC lines were used during this research. The control cell line BEAS2-B^{WT/WT} and three CF cell lines with different CFTR mutations, CuFi-1^{ΔF508/ΔF508}, CuFi-4^{G551D/ΔF508} and IB3-1^{ΔF508/W1282X} were obtained from ATCC, all the details regarding these cell lines are deposited in their web page. HBEC lines were grown on Cell+ surface plates or flasks (Sarstedt) under sterile conditions in a category two tissue culture hood. BEAS-2B and IB3-1 cells were cultured in LHC basal medium (Thermo Fisher Scientific) supplemented with 10% FBS, 50 U/ml penicillin and 50 μg/ml streptomycin (1%P/S). CuFi-1 and CuFi-4 were cultured in LHC-9 medium (Thermo Fisher Scientific), as described by the manufacturer. Cell lines were expanded initially in T75, and T175 positively charged flasks (Sarstedt) in an incubator at 37°C and 5% CO₂, 95% air atmosphere. Cells were left to grow until 80-90% confluency was reached, and then washed once with Dulbecco's phosphate-buffered saline (DPBS) without calcium and magnesium (Gibco). After washing, cells were detached using 1X (0.05%) Trypsin-EDTA (Thermo Fisher Scientific) for no longer than 15 min in the incubator. After the cells were detached, trypsin was neutralised with the corresponding media and cells were centrifuged at 300 g for 5 min. After centrifugation, the supernatant was carefully removed to avoid disturbing the cell pellet, and cells were resuspended in the corresponding media. Cells were counted

and seeded into six-well positively charged plates (Sarstedt) at 1×10^6 cells per well in 1ml of media and left overnight to allow cells to adhere to the plate.

2.1.2 Isolation and processing of primary immune cells

All work involving human samples from patients with CF or HC volunteers was approved by the Health Research Authority, research ethics committee reference 17/YH/0084. Patients diagnosed with CF were recruited from the adult cystic fibrosis unit at St. James's University Hospital, Leeds. All patients had disease-causing CFTR mutations and clinical features consistent with the diagnosis of CF. Patients who were post-lung transplant, suffering from clinical exacerbations, on CFTR modulators or clinically not stable were excluded from this study unless otherwise stated. Informed written consent was obtained from all participants at the time of the sample collection. Age and sex-matched healthy controls were recruited from the St. James's University Hospital premises, Leeds, UK.

	CF (n = 62)	HC (n = 37)
Age range (years)	19-50 (32)	21-44 (29)
Male (%)	54.84%	48.65%
CFTR genotype		
ΔF508 / ΔF508	88.71%	N/A
ΔF508 / 621+1 (G>T)	1.61%	N/A
ΔF508 / G551D	1.61%	N/A
W1282X / W1282X	1.61%	N/A
ΔF508del / c.1521_1523delCTT	4.84%	N/A
3484C>T (p.Arg1162X) / R1162X	1.61%	N/A
BMI (mean)	23.1	N/A
FEV ₁ (%)	45.9%	N/A

Table 2 – Patients' information and clinical data.

Blood samples were collected in EDTA pre-coated tubes (Greiner-bio-one) and processed the same day of collection. PBMCs were isolated from whole blood using a standard density gradient centrifugation method. Blood was mixed with an equal volume of DPBS without Ca^{2+} and Mg^{2+} containing 2% FBS, referred from now on as DPBS separation buffer, and mixed by pipetting up and down. Then 37ml of the homogenous mixture was carefully layered onto 15ml of Lymphoprep (Stem Cell) and centrifuged at 1200g for 20 min at full speed and without brakes. The white buffy layer was carefully removed and washed twice in DPBS separation buffer by centrifuging, the first time at 300g for 5 min full speed with full brake, and the second time 180g for 10 min full speed without breaks, to remove platelets. Finally, PBMCs were counted and resuspended in RPMI medium (Merck) containing 10% FBS, 2 mM L-glutamine, 50 U/mL penicillin and 50 $\mu\text{g}/\text{mL}$ streptomycin, referred from now on as complete RPMI medium.

Isolation of specific subsets of immune cells was done as follows. Isolation of human lymphocytes was carried out directly from blood using the EasySep Direct Human Total Lymphocyte Isolation Kit (Stem Cell) following the manufacturer's instructions. Primary neutrophils were isolated directly from blood using the EasySep Direct Human Neutrophil Isolation Kit (Stem Cell) following the manufacturer's instructions. Monocytes were isolated the same day after collection of the PBMCs using the Pan Monocyte Isolation Kit, human (Miltenyi Biotec), following all the manufacturer's instructions. All cells were cultured in complete RPMI medium (Merck) and kept in a humidified incubator at 37°C, 5% CO_2 .

2.1.3 Culture of primary immune cells

After isolation, described in the previous section, PBMCs, lymphocytes, neutrophils, monocytes and macrophages were cultured in complete RPMI medium (Merck). PBMCs and lymphocytes were seeded at 2×10^6 cell/ml, plated in 6 well plates and stimulated the day after. Neutrophils were seeded at 3×10^6 cell/ml, plated in 6 well plates and stimulated the same day. Monocytes were seeded at 1×10^6 cell/ml, plated in 6 well plates and stimulated the next day. All cells were cultured in complete RPMI medium (Merck) and kept in a humidified incubator at 37°C, 5% CO₂.

2.1.4 Macrophage culture and polarisation

After monocytes were counted and plated as described before, the next protocol for macrophage differentiation and polarisation was performed. Initially, monocytes were cultured in complete RPMI medium (Merck) supplemented with either 20 ng/mL human GM-CSF (Pepro Tech), for M1 differentiation, or 20 ng/mL human M-CSF (Pepro Tech), for M2 differentiation. Monocytes were incubated for six days adding half of the initial media, without removing the initial media, with their respective factors on day 3. On day six M0 macrophages were activated with either 100 ng/mL human IFN- γ (Pepro Tech) and 50 ng/mL LPS, for M1 macrophage polarisation, or 20 ng/mL IL-13 (Pepro Tech) and 20 ng/mL IL-4 (Pepro Tech), for M2 macrophage polarisation, and incubated for further 24 h.

2.2 RNA Isolation and detection

2.2.1 RNA isolation and cDNA conversion

Total RNA isolation was performed using TRIzol reagent and the Phasemaker Tubes (Thermo Fisher Scientific) according to the manufacturer's protocol. Briefly, after stimulation and removal of the supernatants, 1 ml of TRIzol reagent was added to the cells, and the mixture was homogenised by pipetting up and down several times. Samples were stored at -80°C until extraction. RNA extraction was performed following the manufacturer's instructions incorporating the Phasemaker Tubes (Thermo Fisher Scientific) to avoid DNA contamination. After the extraction, the RNA quality and quantity were further determined by 260/280 and 260/230 ratios using a NanoDrop spectrophotometer, and only samples with 260/280 ratios above 1.75 and 260/230 ratios above 1.90 were used. RNA was converted to cDNA using no more than 1 mg of the sample with the High-Capacity cDNA Reverse Transcription Kit (Thermo Fisher Scientific). cDNA was stored at -20°C until used to run qPCR.

2.2.2 Real-time PCR (qPCR)

Gene expression was quantified by qPCR in the QuantStudio 7 Flex Real-Time PCR System (Applied Biosystems) using Power SYBR Green PCR Master Mix (Thermo Fisher Scientific) or TaqMan Universal PCR Master Mix (Thermo Fisher Scientific) in 384 well plates done in triplicates or duplicates. Custom-synthesized oligonucleotide primers (Integrated DNA Technologies), designed with the online Primer-Blast designing tool or pre-designed TaqMan oligonucleotide primers, were used to quantify mRNA. All designed primers were used at concentrations of 300nM. Sequences used can be found in **Table 3**. Relative mRNA expression was calculated

using the $\Delta\Delta C_t$ method with HPRT and PPIA as the housekeeping genes to normalise other mRNAs. A total of 15ng of cDNA was used in each reaction. All primer sequences showed specific amplification of only one product, based on melt curves, and no primer-dimer amplification. All values used were between 10 to 33 cycles.

Gene Target	Forward Sequence (5'->3')	Reverse Sequence (5'->3')
<i>BiP</i>	GAACGTCTGATTGGCGATGC	TCAACCACCTTGAACGGCAA
<i>IRE1α</i>	TAGTCAGTTCTGCGTCCGCT	TTCCAAAAATCCCGAGGCCG
<i>PERK</i>	GCGCGGAAAGTTTGCTCAAT	GAGCTCCCAAGAAGGCAAGG
<i>ATF6</i>	ATGAAGTTGTGTCAGAGAACC	CTCTTTAGCAGAAAATCCTAG
<i>XBP1s</i>	CTGAGTCCGCAGCAGGTG	AGTTGTCCAGAATGCCCAACA
<i>XBP1u</i>	TCCGCAGCACTCAGACTACG	AGTTGTCCAGAATGCCCAACA
<i>ERdj4</i>	GTCGGAGGGTGCAGGATATTAG	GCGCTCTGATGCCGATTTTG
<i>CHOP</i>	GGAACCTGAGGAGAGAGTGTT	GTCCCGAAGGAGAAAGGCAA
<i>GADD34</i>	CTGGCTGGTGGAAAGCAGTAA	TATGGGGGATTGCCAGAGGA
<i>ATF4</i>	GCCAAGGGGGAAGCGATTTA	CTACGCTTTCCCGATCCCAG
<i>IL-6</i>	CCAGCTATGAACTCCTTCTC	GCTTGTTCTCACATCTCTC
<i>TNF</i>	CACCACTTCGAAACCTGGGA	TGTAGGCCCCAGTGAGTTCT
<i>HPRT</i>	GGAAAGAATGTCTTGATTGTGGAAG	GGATTATACTGCCTGACCAAGGAA
<i>PPIA</i>	ACGTGGTATAAAAGGGGCGG	CTGCAAACAGCTCAAAGGAGAC
<i>PDK4</i>	Assay ID: Hs01037712_m1	
<i>PFKB1</i>	Assay ID: Hs00997227_m1	
<i>HK2</i>	Assay ID: Hs00606086_m1	
<i>ESRRA</i>	Assay ID: Hs00607062_gH	
<i>PPARA</i>	Assay ID: Hs00947536_m1	
<i>UCP3</i>	Assay ID: Hs01106052_m1	
<i>HPRT</i>	Assay ID: Hs02800695_m1	

Table 3 – Primer sequences

2.2.3 Reverse transcription PCR (RT-PCR)

XBP1 mRNA splicing was also detected by reverse transcription (RT)-PCR using the following set of primers: Forward 5'-CTGAAGAGGAGGCGGAAGC-3' and reverse 5'-AATACCGCCAGAATCCATGG-3', which recognise both the XBP1s and XBP1u mRNA. The reaction was performed using the OneTaq Hot Start DNA Polymerase kit (New England Biolabs) using the Routine PCR protocol described by the manufacturer. The PCR thermal cycling profile was: 1 cycle at 94°C for 5 min, 35 cycles at 94°C for 30s/55°C for 30s/72°C for 1min, one cycle at 72°C for 10 min. The transcripts were then identified on a 3.5% agarose gel using ultra-pure agarose and TBS buffer, and visualised against a 100bp ladder on the BioRad Gel Doc. Gels were run at 120V for 1-2 hours.

2.3 Cytokine expression

Cytokines levels from cell cultured media were detected by the IL-6, TNF, and IL-10 ELISAs kits listed in the table of reagents, following the manufacturer's recommendations. Supernatants were collected from stimulated cells and stored at -80°C until required. Briefly, ELISA plates were coated with 100 µl cytokine capture antibody in PBS overnight at 4°C. Plates were washed four times with PBST (PBS containing 0.5% Tween 20) and the wells blocked in 300 µl assay buffer (0.5% BSA, 0.1% Tween 20 in PBS) by incubating for one h. Then, plates were washed twice with PBST and 100 µl of sera/culture supernatants, together with appropriate standards, were added to wells in duplicates. 50 µl of detection antibody was added to all wells and incubated for two h. After incubation, the plates were washed five times with PBST and 100 µl of tetramethylbenzidine (TMB) substrate solution (Sigma) was added to all wells and incubated for 30 min. The reaction was stopped by adding 100 µl of 1.8 N H₂SO₄ and absorbance measured at 450 nm and reference at 620 nm. All incubation steps were done at room temperature with continual shaking at 700 rpm.

2.4 Western blots

After stimulation cells were washed with DPBS and then lysed using radioimmunoprecipitation assay (RIPA) buffer (10 mM Tris-Cl, 1 mM EDTA, 1% Triton X-100, 0.1% sodium deoxycholate, 0.1% SDS and 140 mM NaCl), containing 10% (w/v) protease and phosphatase inhibitor cocktail (Roche and Sigma). The samples were then homogenised by pipetting up and down several times and stored at -80°C. Then, samples were centrifuged at 14,000 g for 10 min and the supernatant transferred to another Eppendorf tube for further quantification using bicinchoninic acid assay (BCA). Proteins were resolved by SDS-PAGE using 10% polyacrylamide gels at 100 V for 1 hour and transferred to immobilon polyvinylidene difluoride (PVDF) membrane (Bio-Rad) for 1 hour. Following electrotransfer in transfer buffer (25 mM Tris, 192 mM glycine, and pH 8.3, 20% methanol) at 100 V for one h, the membranes were blocked for one h in blocking solution (PBS containing 0.1% Tween 20 and 5% (w/v) non-fat milk). After four washes in PBST (PBS with 0.5% Tween 20), primary antibodies were incubated with PVDF membrane overnight at 4°C. The membrane was washed three times with PBST, and secondary antibody HRP-linked antibody was added and incubated for one h with constant rocking at room temperature. The membrane was washed five times with PBST and 3 ml of ECL detection system (Merck) were added to the membrane for 1 min, before being imaged with the ChemiDoc Imaging System (Bio-Rad).

2.5 Flow cytometry

The CytoFLEX-S (Beckman Coulter) was used for the detection of (PE) IRE1 α , (PerCP) pIRE1 α , (AF647) ATF6 α and (AF488) PERK in the HBEC lines. For the characterisation of M1/M2 macrophages the surface and intracellular markers, referenced in the Inflammation and the UPR in Cystic Fibrosis section, were used and analysed in the BD Bioscience FACS Calibur. Compensation was done by fluorescence minus one (FMO) for all the antibodies and using the isotype controls to identify non-specific binding. During sample acquisition, 20,000-30,000 events were captured per sample, consistent with each experiment. The pIRE1 α (GeneTex) and its Rabbit IgG isotype control (GeneTex) antibodies were conjugated using the LYNX Rapid PerCP Antibody Conjugation Kit (Bio-Rad), as per the manufacture's recommendations. Brilliant stain buffer (BSB) was used as the final resuspension buffer for running the samples. Human IgG (Merck I2511) and Mouse serum (M5905) were used to 'Fc Block' the cells when mentioned.

2.6 Immunofluorescence microscopy

Cells were visualised by Immunofluorescence (IF) using the CFTR monoclonal antibody (Cell Signaling) and an isotype control. The next protocol was followed: monocytes were differentiated into M1, or M2 macrophages in eight well millicel EZ microscope slides (Merck), following the protocol described before. Cells were fixed for 20 min in 4% paraformaldehyde at room temperature, washed 3X with PBS and, when indicated, permeabilised for 15 min either with 0.2% Triton X-100 solution or Saponin in PBS (3% BSA). Cells were washed 3X with PBS, then the primary antibody was added (CFTR 1:800) or the isotype control (1:800) and incubated overnight at 4°C. Cells then were washed 3X with PBS and incubated for two h at room temperature with the secondary antibody (Anti-rabbit IgG CS 1:1000). To stain the actin filaments phalloidin dye (Insight Biotechnology) was included with the secondary antibody at final concentration of 40 U/ml. Cells were washed 3X with PBS, and a drop of ProLong diamond anti-fade with DAPI (Thermo Fisher) was added to each slide and covered. The slides were left for 24 h at room temperature in the dark. Cells were visualised using the confocal laser scanning microscope - Nikon A1R and all images were taken using the same parameters during sample acquisition. Excitation lasers used 405nm, 457-514nm, 561nm and 642nm. Fluorescent emission was captured at the wavelength recommended by the manufacturer of each antibody. Images were produced using the Nikon NIS Elements Analysis software. Images were acquired on a Leica TCS SP confocal microscope with a

2.7 Metabolic experiments

2.7.1 Cellular ROS detection

ROS were measured by using the Cellular ROS Assay Kit (Abcam) as described by the manufacturer. Fluorescence was detected with excitation at 485 nm and emission at 535 nm using the Cytation 5 Imaging Plate Reader (BioTek).

2.7.2 Glycolytic and mitochondrial assays (Extracellular Flux Analyzer)

All the metabolic parameters were calculated as shown in Table 4. Normally 3–5 technical replicates per sample were examined. Immediately after the metabolic analysis, cells were fixed for 10 min in methanol/acetone (4:1), and cell number of each well was determined by nuclear DNA staining with DAPI (BD Biosciences), ECAR and OCR values were normalised accordingly.

Parameter	Equation
Glycolysis	(maximum rate measurement after glucose stimulation) – (rate measurement before glucose stimulation)
Glycolytic capacity	(maximum rate measurement after glucose stimulation) – (maximum rate measurement after oligomycin stimulation)
Glycolytic reserve	(maximum rate measurement after oligomycin stimulation) – (rate measurement before oligomycin stimulation)
Basal respiration	(measurement before oligomycin stimulation) – (rate measurement after rotenone/antimycin A stimulation)
Proton leak	(minimum rate measurement after oligomycin stimulation) – (minimum measurement after rotenone/antimycin A stimulation)
Maximal respiration	(maximum rate measurement after FCCP stimulation)– (minimum rate measurement after rotenone/antimycin A stimulation)
Reserve respiratory capacity	(maximal respiration) – (basal respiration)
ATP production	(basal respiration) – (minimum rate measurement after oligomycin stimulation)

Table 4 – Seahorse Calculations

2.8 Statistical analysis

No statistical tests were used to predetermine sample size. All statistical analyses were performed using GraphPad Prism v7. Data are presented as mean \pm SEM. P-values of $P < 0.05$ were considered to be statistically significant. Statistical significance was determined using Two-way ANOVA, Dunnett's test with Bonferroni-Dunn correction when comparing between different cell lines. Paired Student's t-test was used when comparing drug responses within the same cell line, * $p < 0.05$, ** $p < 0.01$, *** $p < 0.001$. Statistical comparisons were performed by unpaired independent Student's t-test, * $p < 0.05$, ** $p < 0.01$, *** $p < 0.001$ when comparing between groups. Mann-Whitney non-parametric test was used to compare the medians between groups, * $p < 0.05$, ** $p < 0.01$, *** $p < 0.001$.

2.9 Table of resources

REAGENT or RESOURCES	SOURCE	IDENTIFIER
Antibodies		
IRE1 alpha (phospho Ser724)	GeneTex	Cat# GTX63722; RRID: N/A
Rabbit IgG isotype control	GeneTex	Cat# GTX35035; RRID: N/A
IRE1 α Antibody (B-12) PE	Santa Cruz	Cat# sc-390960-PE; RRID: N/A
Normal mouse IgG1 PE (Isotype)	Santa Cruz	Cat# sc-2866; RRID: AB_737219
ATF-6 α Antibody (F-7) AF647	Santa Cruz	Cat# sc-166659- AF488; RRID: AB_2058901
Normal mouse IgG1 Alexa Fluor 647	Santa Cruz	Cat# sc-24636; RRID: AB_737215
PERK Antibody (B-5) AF488	Santa Cruz	Cat# sc-377400; RRID:AB_2762850
Normal mouse IgG1 Alexa Fluor 488	Santa Cruz	Cat# sc-3890; RRID: AB_737214
V500 Mouse Anti-Human CD14	BD Biosciences	Cat# 561391; RRID: AB_10611856
Anti-HLA-DR PerCP	BD Biosciences	Cat# 347402; RRID: N/A
FITC Mouse Anti-Human CD206	BD Biosciences	Cat# 551135; RRID: AB_394065
PE Rat Anti-Human IL-10	BD Biosciences	Cat# ; RRID: AB_397227
APC Mouse Anti-Human CD274	BD Biosciences	Cat# 563741; RRID: AB_2738399
PE-Cy7 Mouse Anti-Human CD86	BD Biosciences	Cat# 561128; RRID: AB_10563077
BV421 Mouse Anti-Human TNF	BD Biosciences	Cat# 562783; RRID: AB_2737790
Purified anti-XBP-1s Antibody	BioLegend	Cat# 619501; RRID: AB_315907
HPRT Antibody (FL-218)	Santa Cruz	Cat# sc-20975; RRID: N/A
Goat anti-Rabbit IgG (H+L) Poly-HRP Secondary Antibody	Thermo Fisher Scientific	Cat# 32260; RRID: AB_1965959
CFTR (D6W6L) Rabbit mAb	Cell Signaling Technology	Cat# 78335; RRID:AB_2799913
Anti-rabbit IgG (H+L), F(ab') ₂ Fragment (Alexa Fluor 488 Conjugate)	Cell Signaling Technology	Cat# 4412; RRID:AB_1904025
Biological Samples		
Human Blood Samples	St James's University Hospital	Health Research Authority REC reference 17/YH/0084
Chemicals, Peptides, and Recombinant Proteins		
Lymphoprep	StemCell Technologies	Cat# 07861
EasySep Direct Human Total Lymphocyte Isolation Kit	StemCell Technologies	Cat# 19655
EasySep Direct Human Neutrophil Isolation Kit	StemCell Technologies	Cat# 19666
Pan Monocyte Isolation Kit, human	Miltenyi Biotec	Cat# 130-096-537
Recombinant Human GM-CSF	Pepro Tech	Cat# 300-03
Recombinant Human M-CSF	Pepro Tech	Cat# 300-25
Recombinant Human IFN- γ	Pepro Tech	Cat# 300-02
Recombinant Human IL-13	Pepro Tech	Cat# 200-13
Recombinant Human IL-4	Pepro Tech	Cat# 200-04
LPS	InvivoGen	Cat# tlrl-3pelps
4 μ 8c	Merck	Cat# 412512
MKC-3946	Cayman Chemical	Cat# 19152
PowerUp SYBR Green Master Mix	Thermo Fisher Scientific	Cat# A25780
TaqMan Universal PCR Master Mix	Thermo Fisher Scientific	Cat# 4304437

TRIzol Reagent and Phasemaker Tubes Complete System	Thermo Fisher Scientific	Cat# A33251
Thapsigargin	Merck	Cat# T9033
Tunicamycin	Cell Signaling Technologies	Cat# 12819S
PhosSTOP	Merck	Cat# 4906845001
Pierce Protease Inhibitor Mini Tablets	Thermo Fisher Scientific	Cat# A32955
Immobilon Western Chemiluminescent HRP Substrate	Merck	Cat# WBKLS0500
DPBS, no calcium, no magnesium	Thermo Fisher Scientific	Cat# 14190144
Trypsin-EDTA (0.5%), no phenol red	Thermo Fisher Scientific	Cat# 15400054
StemPro Accutase Cell Dissociation Reagent	Thermo Fisher Scientific	Cat# A1110501
ProLong Diamond Antifade Mountant with DAPI	Thermo Fisher Scientific	Cat# P36966
Phalloidin, CF555, 50u	Insight Biotechnology	Cat# 00040-T
Critical Commercial Assays		
High-Capacity cDNA Reverse Transcription Kit	Thermo Fisher Scientific	Cat# 4368814
ELISA IL-6 Human	Thermo Fisher Scientific	Cat# CHC1263
ELISA TNF alpha Human	Thermo Fisher Scientific	Cat# CHC1753
ELISA IL-10 Human	Thermo Fisher Scientific	Cat# CHC1323
LYNX Rapid PerCP Antibody Conjugation Kit	Bio-Rad	Cat# LNK072PERCP
Fixation/Permeabilization Solution Kit	BD Biosciences	Cat# 554714
Glycolysis Stress Test Kit	Agilent Technologies	Cat# 103020-100
Pierce BCA Protein Assay Kit	Thermo Fisher Scientific	Cat# 23225
VACUETTE EDTA pre-coated tubes	Greiner-bio-one	Cat# 455036
OneTaq Hot Start DNA Polymerase	New England Biolabs	Cat# M0481
UltraPure Agarose	Thermo Fisher Scientific	Cat# 16500100
DCFDA / H2DCFDA - Cellular ROS Assay Kit	Abcam	Cat# ab113851
MitoSOX Red Mitochondrial Superoxide Indicator, for live-cell imaging	Thermo Fisher Scientific	Cat# M36008
Dead Cell Apoptosis Kit with Annexin V Alexa Fluor(tm) 488 & Propidium Iodide (PI)	Thermo Fisher Scientific	Cat# 10652071
Experimental Models: Cell Lines		
BEAS-2B cell line	ATCC	ATCC CRL-9609
CuFi-1 cell line	ATCC	ATCC CRL-4013
CuFi-4 cell line	ATCC	ATCC CRL-4015
IB3-1 cell line	ATCC	ATCC CRL-2777
Oligonucleotides		
Primer Sequences See Table 3	Integrated DNA Technologies	N/A
Software and Algorithms		
GraphPad Prism7	Graphpad software	N/A
CytExpert Software	Beckman Coulter	N/A

Flow Jo Vx0.7	FlowJo, LLC	N/A
Agilent Seahorse Wave	Agilent Technologies	N/A

Table 5 – Table of resources

Chapter 3 – The UPR in Cystic Fibrosis

3.1 Introduction

The UPR plays a vital role in the regulation of cellular homeostasis. CFTR abnormalities, present in patients with CF, disrupt the cellular balance by favouring inflammation [113, 172]. While atypical activation of the UPR in CF has already been shown [172], this current study was done to compare the IB3-1^{ΔF508/W1282X} and C38 (IB3-1 transfected with CFTR by an adeno-associated viral vector) cell lines [172]. The C38 cell line represents the corrected version of the CF IB3-1 cells; however, the C38 cells still produce the mutated $\Delta F508$ CFTR, with potential implications in cellular stress and UPR activation [172]. For this reason, it is essential to examine UPR activation using a range of other CF HBECs with different type class mutations. Furthermore, it is of great interest to explore whether the type of class mutation present in CF HBECs may be associated with different degrees of UPR activation. Certainly, UPR activation exists in alveolar macrophages from patients with CF; however, this finding has never been shown in other immune cells [113]. Although one study has demonstrated XBP1s upregulation in PBMCs from patients with CF, this UPR activation might be due to proportional differences in immune cells, as PBMCs are a mixed population of different immune cells [172]. Based on this, we wanted to expand this finding by isolating different subsets of immune cells, to fully explore UPR activation in individual clusters of immune cells. Furthermore, alveolar macrophages, also known as tissue-resident macrophages, have a different origin from monocyte-derived macrophages, as the latter are originated from the bone marrow [188]. We

also wanted to explore whether this XBP1s irregularity was still present in different subsets of macrophages.

3.2 Methods

3.2.1 RNA isolation and detection

The following cell numbers were used for RNA extraction; 1×10^6 HBECs, 2×10^6 PBMCs, 1×10^6 monocytes, 2×10^6 lymphocytes, 3×10^6 neutrophils and 1×10^6 macrophages. All the RNA processing and detection were done as described in the methods section.

3.2.2 Western blotting

Primary antibodies used, purified anti-XBP-1s Antibody (BioLegend) at 1/250 dilution, HPRT Antibody (Santa Cruz) at 1/500 dilution. The secondary antibody used, Goat anti-Rabbit IgG (H+L) Poly-HRP Secondary Antibody (Thermo Fisher Scientific), was diluted at 1/5000 in PBST. The complete protein detection process through Western blotting was done as described in the methods section.

3.2.3 Flow cytometry

For the detection of IRE1 α , pIRE1 α , PERK and ATF6 in the HBECs the next steps were followed; the intracellular expression of IRE1 α , pIRE1 α , PERK and ATF6 was studied by flow cytometry analysis in the CF HBECs. Corresponding isotype controls for all the antibodies were used. Cells were cultured and detached, as previously mentioned in the methods section. Then, cells were centrifuged at 300g for 5 min, washed with PBS, and fixed (4% paraformaldehyde) and permeabilised (BD

Cytofix/Cytoperm) for 15min, as recommended by the manufacturer. Cells were washed and resuspended in BSB with Human IgG (Merck I2511) and Mouse serum (M5905) to 'Fc Block' the cells for 10min. After non-specific binding was reduced by blocking the cells, the conjugated specific antibodies IRE1 α (GeneTex), pIRE1 α (Santa Cruz), PERK (Santa Cruz) and ATF6 (Santa Cruz), or their isotype controls, Rabbit IgG (GeneTex), Normal mouse IgG1 (Santa Cruz), were added to the cells at a concentration of 5 to 10 μ L/10⁶ cells, as recommended by each manufacturer. Cells were incubated with the antibodies, for 30 minutes on ice in the dark and 30,000 events were captured per sample. Cells were acquired into a CytoFLEX flow cytometer (Beckman Coulter). Any other flow cytometry process was done as described in the methods section.

3.2.4 Cellular stimulations

HBECs, PBMCs, lymphocytes, and monocytes were left unstimulated or stimulated with LPS (10ng/ml), Tn (5 μ g/ml) and Tg (300 nM) for 4 hours. Neutrophils were stimulated with LPS (10ng/ml), Tn (2 μ g/ml) and Tg (150 nM). Macrophages were cultured and activated, as mentioned in the methods section and stimulated with LPS (100ng/ml).

3.3 Results

3.3.1 UPR activation in CF HBEC lines

First, UPR activation was analysed in the BEAS-2B^{WT/WT}, CuFi-1^{ΔF508/ΔF508}, CuFi-4^{G551D/ΔF508} and IB3-1^{ΔF508/W1282X} cell lines. The induction of the UPR was assessed by doing a time-course experiment, using the UPR inducer tunicamycin (Tn) for 2, 4 and 8 h in the BEAS-2B cell line. As expected, *IRE1α*, *PERK*, *XBP1s*, *ATF4*, *CHOP* and *BiP* were upregulated upon stimulation with Tn, and the expression of the transcripts reached a significant fold change after 4 h of stimulation (**Figure 11**). Then, we compared the expression of *BIP*, *IRE1α*, *ATF6*, *PERK*, *XBP1s*, *XBP1u*, *eIF2α*, *ATF4*, *CHOP* and *GADD34* in the CF cell lines at basal conditions. In the CuFi-1 cell line, all the transcripts were significantly upregulated, when compared to the WT control (**Figure 12**). We observed that only *BIP*, *XBP1s*, *eIF2α* and *CHOP* were significantly upregulated in the heterozygous CuFi-4 cell line (**Figure 12**). Surprisingly, in IB3-1 cell line, we detected a downregulation of *IRE1α* and *XBP1s* transcripts, suggesting that UPR activation is dependent on the type of class mutation present in the CF cells (**Figure 12**). While *IL-6* was significantly upregulated in all CF cell lines, this particular aspect will be discussed in section 4.3.1, entitled “Upregulation of inflammatory cytokines in CF HBECs”.

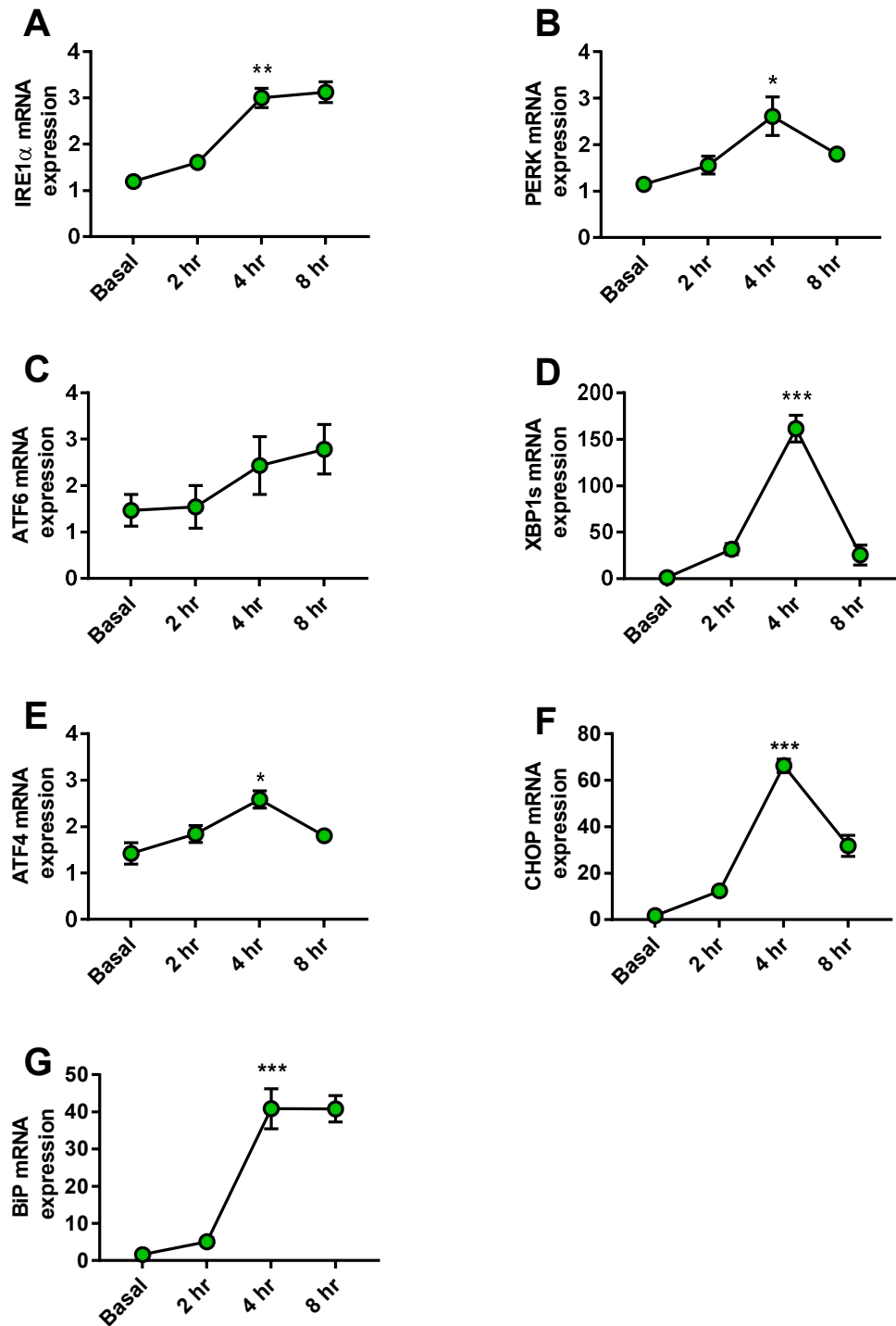


Figure 11 – UPR induction time course.

UPR activation was induced using Tn for 2, 4 and 8 hours in the BEAS-2B cell line. *IRE1 α* , *PERK*, *ATF6*, *XBP1s*, *ATF4*, *CHOP* and *BiP* expression were analysed by qPCR. mRNA expression is represented by fold change, compared to the mean basal expression of each gene. After the time course experiment was completed, cells were lysed, and RNA extracted, as described in the methods section. Paired Student's t-test *p < 0.05, **p < 0.01, ***p < 0.001. n = 3 biological replicates.

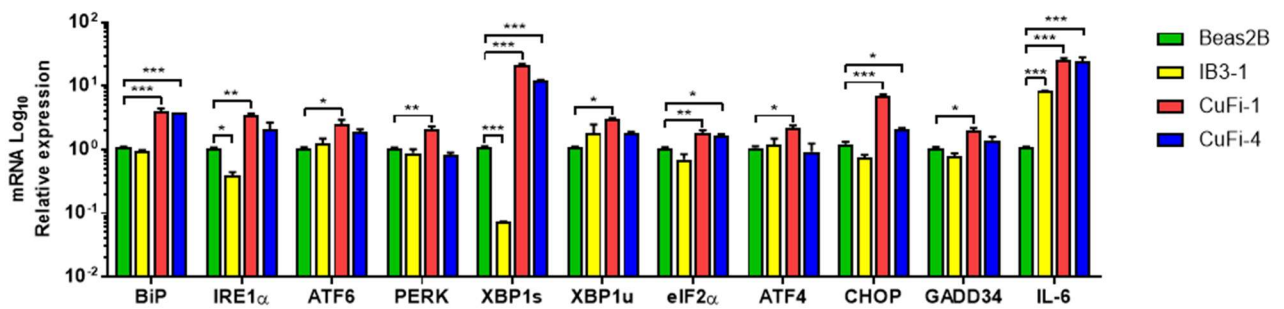
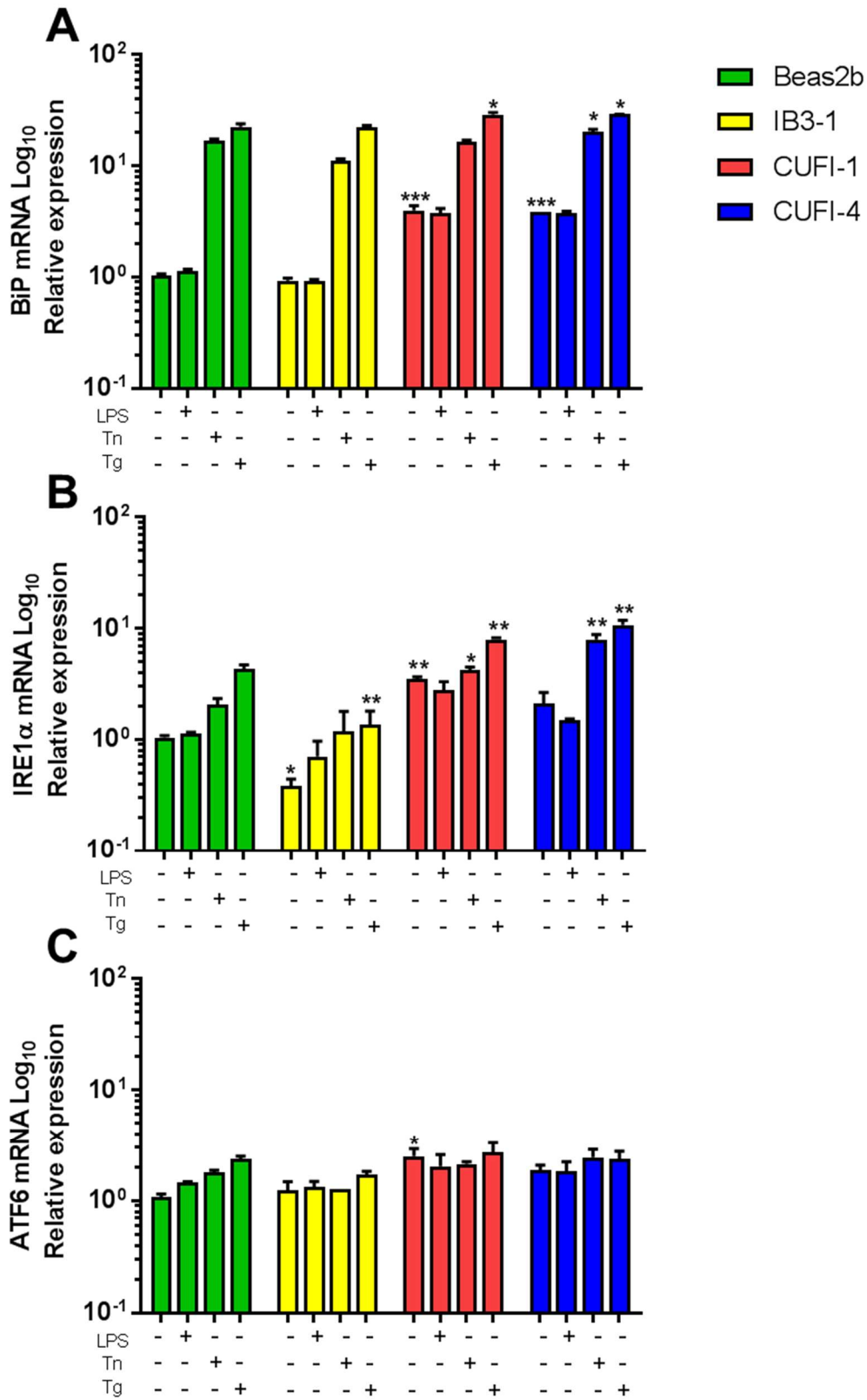


Figure 12 – UPR activation in CF HBECS

UPR activation was measured in the BEAS-2B, IB3-1, CuFi-1, and CuFi-4 cell lines. The mRNA expression of *BIP*, *IRE1 α* , *ATF6*, *PERK*, *XBP1s*, *XBP1u*, *eIF2 α* , *ATF4*, *CHOP*, *GADD34* and *IL-6* was analysed by qPCR. Relative mRNA expression was calculated using the $\Delta\Delta C_t$ method with HPRT and PPIA as the housekeeping genes. Statistical significance was determined using Two-way ANOVA, Dunnett's test * $p < 0.05$, ** $p < 0.01$, *** $p < 0.001$. $n = 4$ biological replicates for all cell lines. Part of these data has been previously published [30].

Next, we investigated the response of the CF cell lines when challenged to LPS, Tn and thapsigargin (Tg), the latter being a stronger UPR inducer. LPS stimulation did not induce a significant response in *BIP*, *IRE1 α* , *ATF6* nor *PERK* transcripts in any of the cell lines (**Figure 13**); however, there were some interesting findings regarding Tn and Tg stimulations. Both drugs, Tn and Tg, induced the upregulation of *BIP* in all cell lines (**Figure 13A**). When stimulated with Tn and Tg, the CF CuFi-1 and CuFi-4 cells lines lost statistical significance when compared to the WT control BEAS-2B ($P < 0.5$) (**Figure 13A**). The expression of *IRE1 α* in the CuFi-1 cell line was still significant when compared to the WT control after stimulation with Tn and Tg, *PERK* expression was only significant after Tg stimulation, and *ATF6* expression was not significant after stimulation with any of the drugs (**Figure 13B-D**). Interestingly, while the CF CuFi-4 cell line was not significantly different to the WT control cell line, under basal

conditions, the CuFi-4 cell line reached a significantly high level of expression of the IRE1 α transcript after stimulation with the drugs. (**Figure 13B-D**).



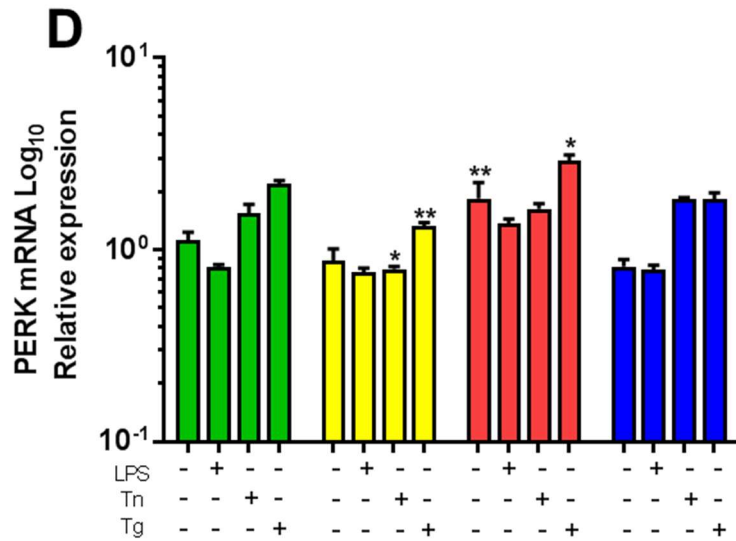
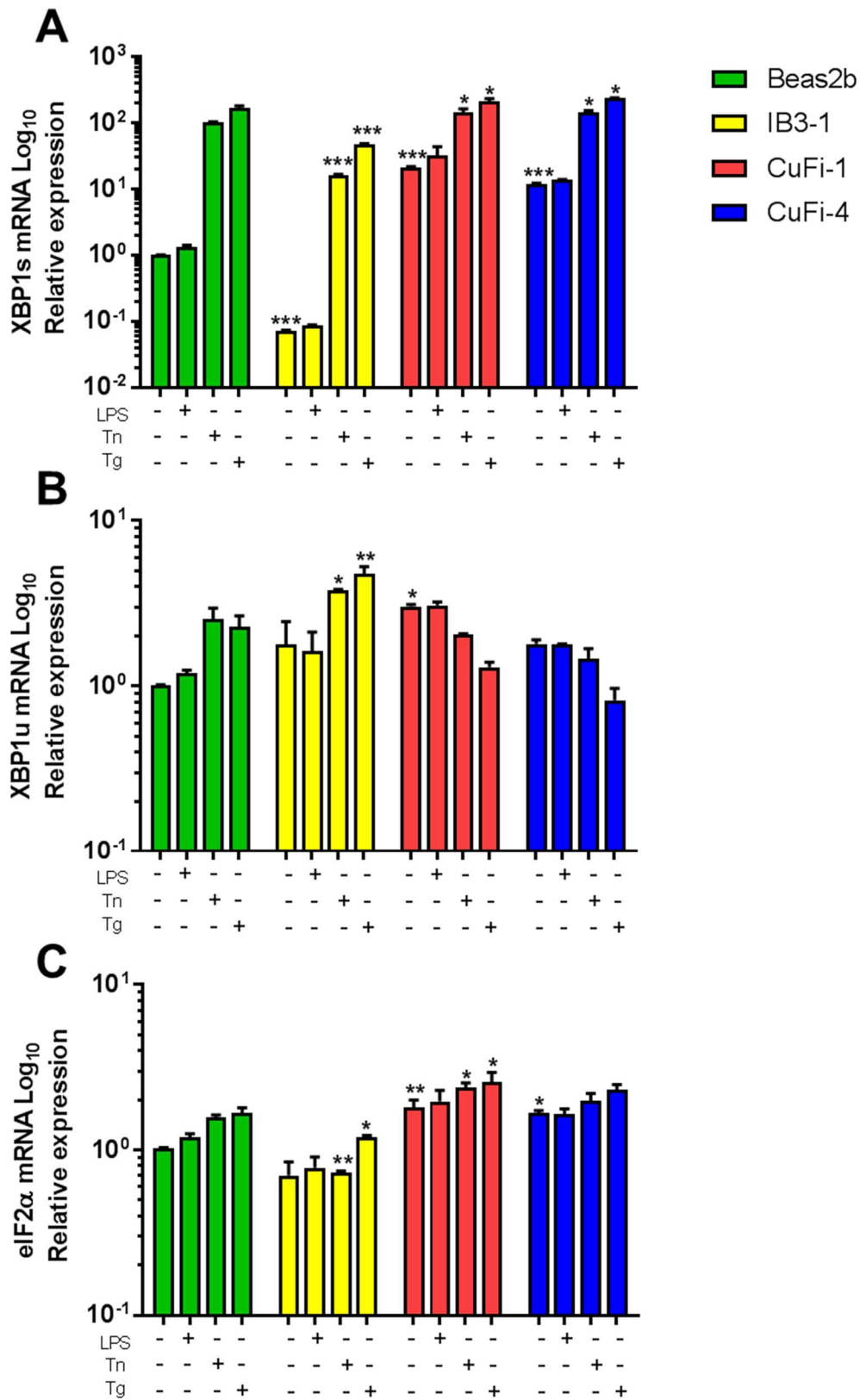


Figure 13 – Activation the BIP, IRE1 α , ATF6 and PERK.

UPR activation was measured in the BEAS-2B, IB3-1, CuFi-1, and CuFi-4 cell lines after stimulation with LPS (100ng/ml), Tn (5 μ g/ml) and Tg (300 nM) for 4 hours. The mRNA expression of *BIP*, *IRE1 α* , *ATF6*, and *PERK* was analysed by qPCR. Relative mRNA expression was calculated using the $\Delta\Delta$ Ct method with HPRT and PPIA as the housekeeping genes. All the comparisons were made versus the BEAS-2B cell line comparing each stimulation accordingly. Statistical significance was determined using unpaired independent student's t-test, for each of the stimulations. *p < 0.05, **p < 0.01, ***p < 0.001. n=4 biological replicates for all cell lines.

The IB3-1 cell line displayed no difference in the expression of ATF6 nor BiP. Surprisingly, the IB3-1 cells showed a downregulation of IRE1 α under basal conditions and after Tg stimulation (**Figure 13B-D**). Finally, while the expression levels of PERK were not different under basal conditions, both levels were significantly downregulated after stimulation with Tn and Tg (**Figure 13B-D**). We then explored *XBP1s*, *XBP1u*, *eIF2 α* , *CHOP* and *GADD34* expression, all of them being downstream of the UPR signalling pathway (**Figure 14**). *XBP1s* was strongly upregulated under basal conditions in the CuFi-1 and CuFi-4 cell lines and downregulated in the IB3-1 cell lines (**Figure 14A**). When the cells were stimulated with Tn and Tg they all strongly

upregulated *XBP1s* (**Figure 14A**). This finding suggests that the amount of ER stress that can be induced in a cell is limited, and the higher amounts of ER stress, already present on the CF cell lines, cannot be further increased. While the amount of *XBP1s* was significantly lower in the IB3-1 cell lines, *XBP1u* was upregulated after stimulation with Tn and Tg (**Figure 14B**). Moreover, in the CuFi-1 and CuFi-4 cell lines, *XBP1u* was downregulated upon addition of Tn and Tg (**Figure 14B**). The same observation as that seen with *XBP1s*, was noted in *eIF2 α* and *CHOP* transcripts, with a degree of significance ($P < 0.05$) being lost after stimulation with both drugs (**Figure 14C and D**). The compound heterozygous IB3-1 cell line revealed downregulation of *eIF2 α* after stimulation with Tn and Tg, and downregulation of *GADD34* only after Tg stimulation (**Figure 14C and E**). The two CuFi-1 and CuFi-4 cell lines showed significantly higher levels of *GADD34*, after Tg stimulation, when compared to the WT control (**Figure 14E**). Finally, we evaluated the expression of *IRE1 α* , *pIRE1 α* , *ATF6* and *PERK* proteins in all HBEC lines. As shown previously higher levels of mRNA expression of *IRE1 α* and *XBP1s* were consistently seen in the CuFi-1 and CuFi-4 cell lines. Furthermore both, *IRE1 α* and *pIRE1 α* were upregulated in the CF cell lines when compared to the BEAS-2B cells (**Figure 15A, B and E**). In addition, *ATF6* and *PERK* expression were also both upregulated in the CuFi-1 and CuFi-4 cell lines (**Figure 15C-E**). No significant differences were detected in the IB3-1 cell line when compared with the WT cell line.



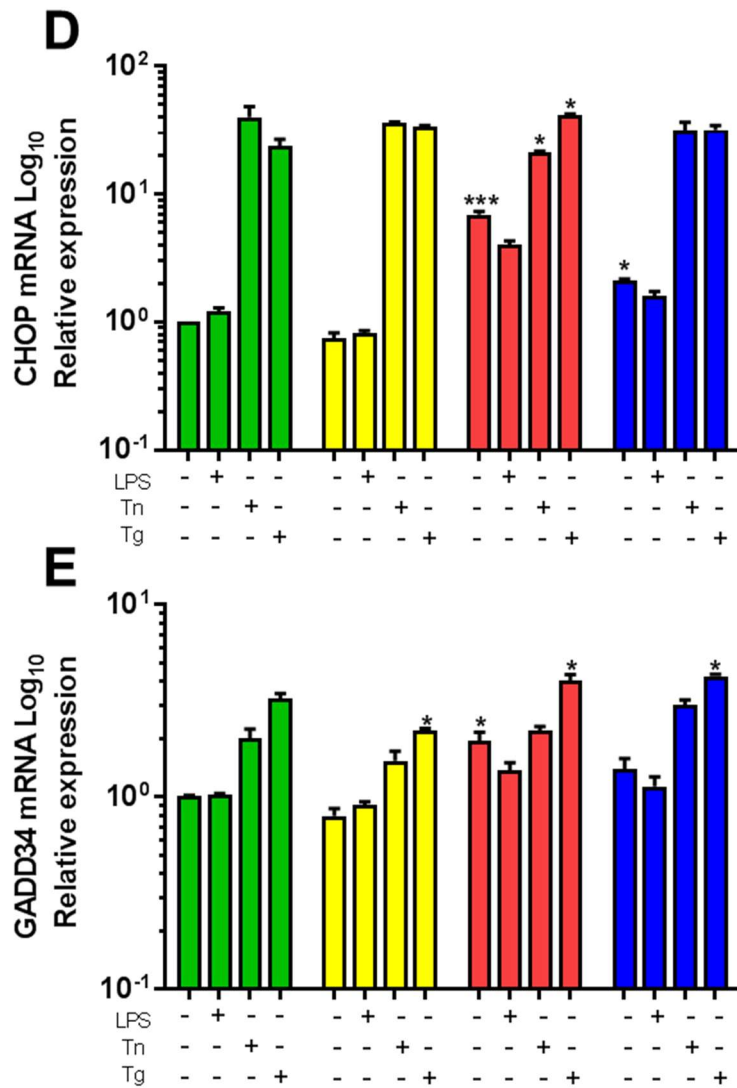


Figure 14 – Activation the XBP1s, XBP1u, eIF2 α , CHOP and GADD34.

UPR activation was measured in the BEAS-2B, IB3-1, CuFi-1, and CuFi-4 cell lines after stimulation with LPS (100ng/ml), Tn (5 μ g/ml) and Tg (300 nM) for 4 hours. The mRNA expression of *XBP1s*, *XBP1u*, *eIF2 α* , *CHOP* and *GADD34* was analysed by qPCR. Relative mRNA expression was calculated using the $\Delta\Delta$ Ct method with HPRT and PPIA as the housekeeping genes. All the comparisons were made versus the BEAS-2B cell line, comparing each stimulation accordingly. Statistical significance was determined by using unpaired independent Student's t-test for each of the stimulations. *p < 0.05, **p < 0.01, ***p < 0.001. n=4 biological replicates for all cell lines.

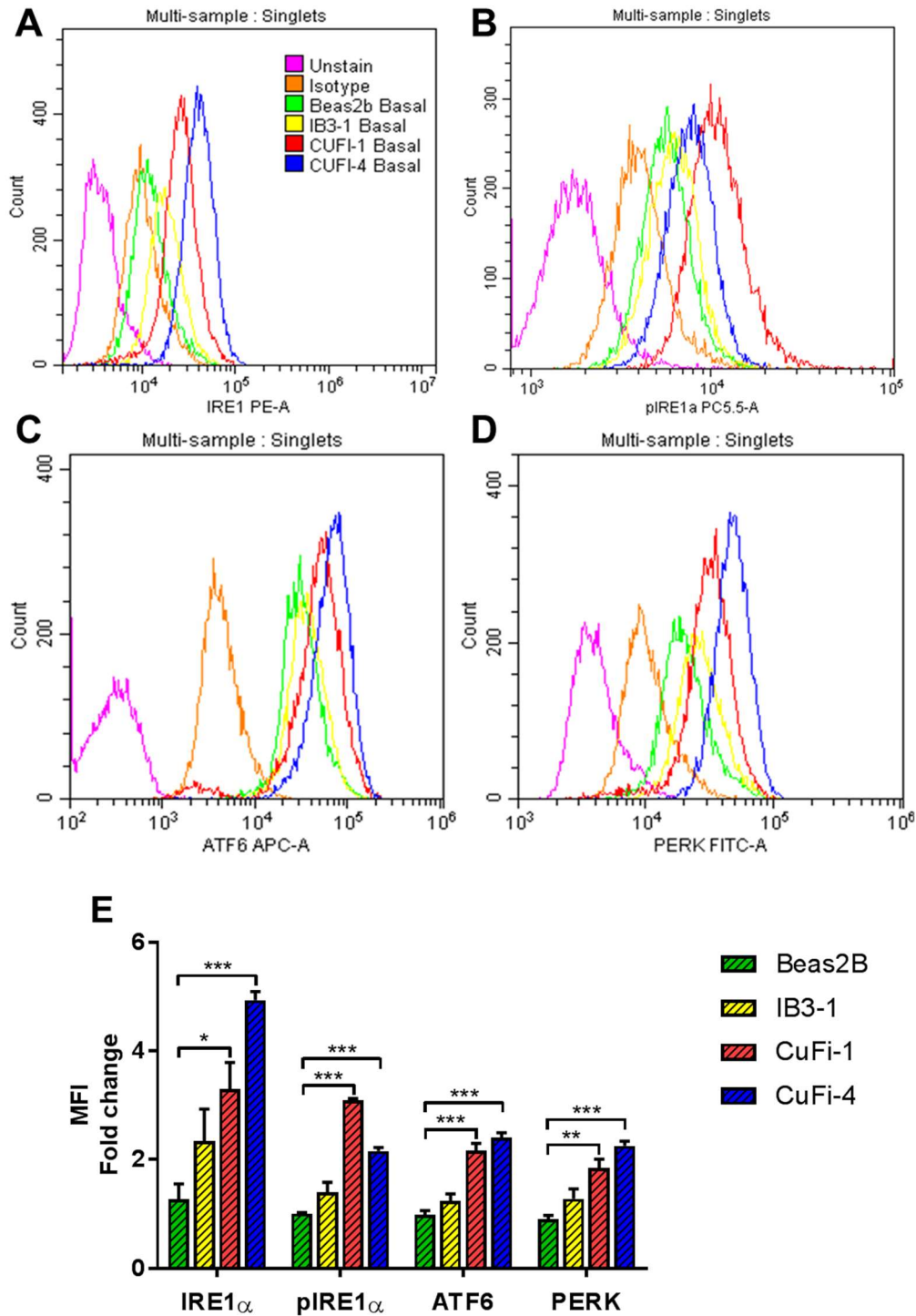


Figure 15 – IRE1 α , pIRE1 α , ATF6 and PERK protein expression in HBECs

Single cells were gated and then used to measure the mean fluorescent intensity (MFI) of each cell line, by flow cytometry; IRE1 α (A), pIRE1 α (B), ATF6 (C) and PERK (D) were measured in the HBECs. The fluorophore measured are shown in the respective panels and also in the methods section. The MFI is represented in panel (E). All antibodies were normalised with their respective isotype controls in each cell line. Statistical significance was determined using unpaired independent Student's t-test. *p < 0.05, **p < 0.01, ***p < 0.001. n=4 biological replicates for all cell lines.

3.3.2 UPR activation in PBMCs from patients with CF

After finding that CF HBECs displayed a unique UPR activation, mainly involving the IRE1 α -XBP1 pathway, we analysed UPR activation in primary PBMCs from patients with CF at basal conditions, after LPS challenge and under ER stress conditions induced by both, Tn and Tg. Under basal conditions, *IRE1 α* and *GADD34* were significantly upregulated in PBMCs from CF patients, while *IL-6* was downregulated (**Figure 16**). Interestingly, stimulation with LPS induced a significant upregulation in *BiP*, *IRE1 α* , *XBP1s*, *ERdj4*, *ATF4*, *GADD34*, *TNF*, and *IL-6* transcripts of PBMCs from CF patients when compared to those from HC volunteers (**Figure 16**). Furthermore, we found similar findings after ER stress induction by Tn with *BiP* and *IRE1 α* significantly upregulated and after stimulation with Tg with significantly higher expression in *PERK* and *XBP1s* (**Figure 17**).

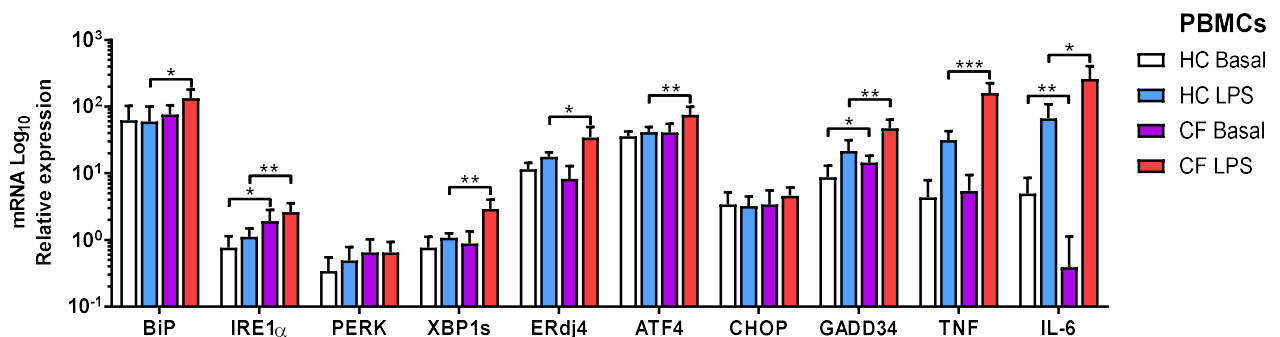


Figure 16 – UPR activation in primary PBMCs from patients with CF

mRNA relative expression of ER stress and UPR markers BiP, IRE1 α , PERK, XBP1s, ERdj4, ATF4, CHOP, GADD34, TNF, and IL-6 were measured in PBMCs from HC volunteers (n=8) and patients with CF (n=14) at basal conditions and stimulated with LPS (10 ng/ml) for 4 h. All n values represent biologically independent samples. Statistical comparisons were performed by unpaired independent Student's t-test, *p < 0.05, **p < 0.01, ***p < 0.001; ND, not detected. These data have been published by the author [30].

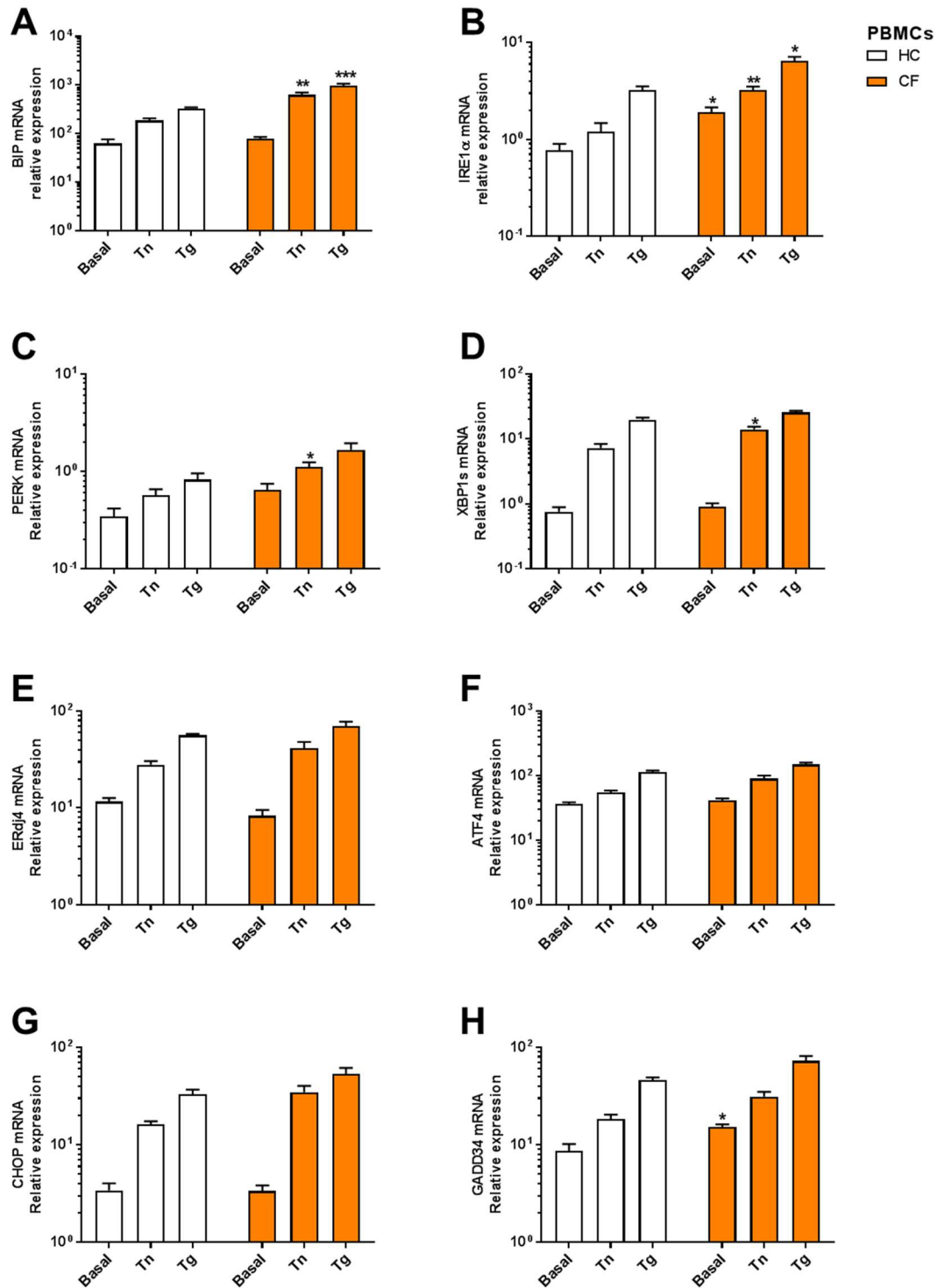


Figure 17 – ER stress in PBMC stimulated with Tn and Tg

UPR activation was measured in primary PBMCs from HC individuals (n=8) and patients with CF (n=14) at basal conditions, stimulated with Tn (5 μg/ml), or Tg (300nM) for 4 hours. (A-H). *BiP*, *IRE1α*, *PERK*, *XBP1s*, *ERdj4*, *ATF4*, *CHOP* and *GADD34* were measured by qPCR. Statistical comparisons were performed by unpaired independent Student's t-test. *p < 0.05, **p < 0.01, and ***p < 0.001. These data have been published by the author [30]

3.3.3 No difference in UPR activation in lymphocytes

PBMCs are composed of a mixed population of different immune cells. Therefore, any differences found within PBMCs in the patients' samples could be due to the heterogeneous composition of PBMCs. To identify ER stress abnormalities in immune cells from patients with CF, I isolated different subsets of immune cells. Isolation of lymphocytes, neutrophils and monocytes, with further differentiation of monocytes to monocyte-derived macrophages was performed in this research project. Lymphocytes from CF patients did not show any significant differences in any of the transcripts measured, either at basal conditions or after LPS stimulation (**Figure 18**). The same was observed after stimulation with Tn and Tg (**Figure 19**).

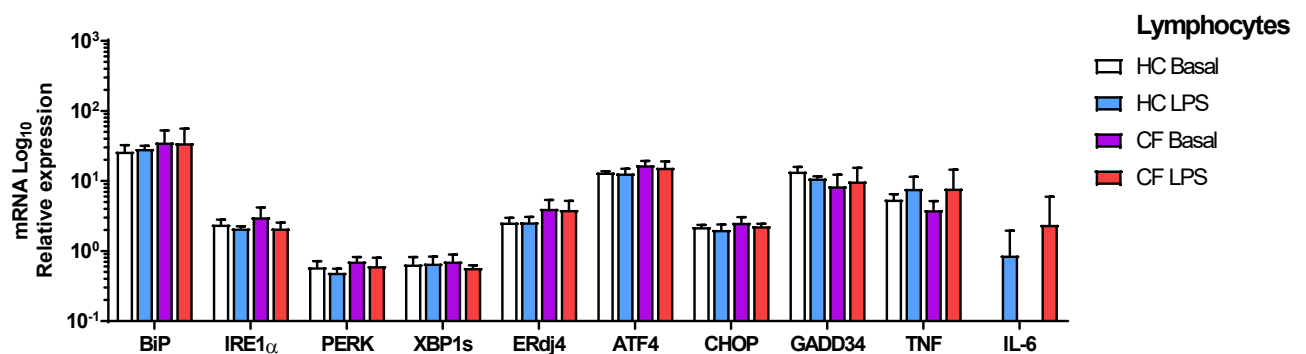


Figure 18 – UPR gene expression in lymphocytes from patients with CF

mRNA relative expression of ER stress and UPR markers *BiP*, *IRE1 α* , *PERK*, *XBP1s*, *ERdj4*, *ATF4*, *CHOP*, *GADD34*, *TNF*, and *IL-6* were measured in lymphocytes from HC volunteers (n=6) and patients with CF (n=6) at basal conditions and stimulated with LPS (10 ng/ml) for 4 h. All n values represent biologically independent samples. Statistical comparisons were performed by unpaired independent Student's t-test, *p < 0.05, **p < 0.01, ***p < 0.001; ND, not detected. These data have been published by the author [30].

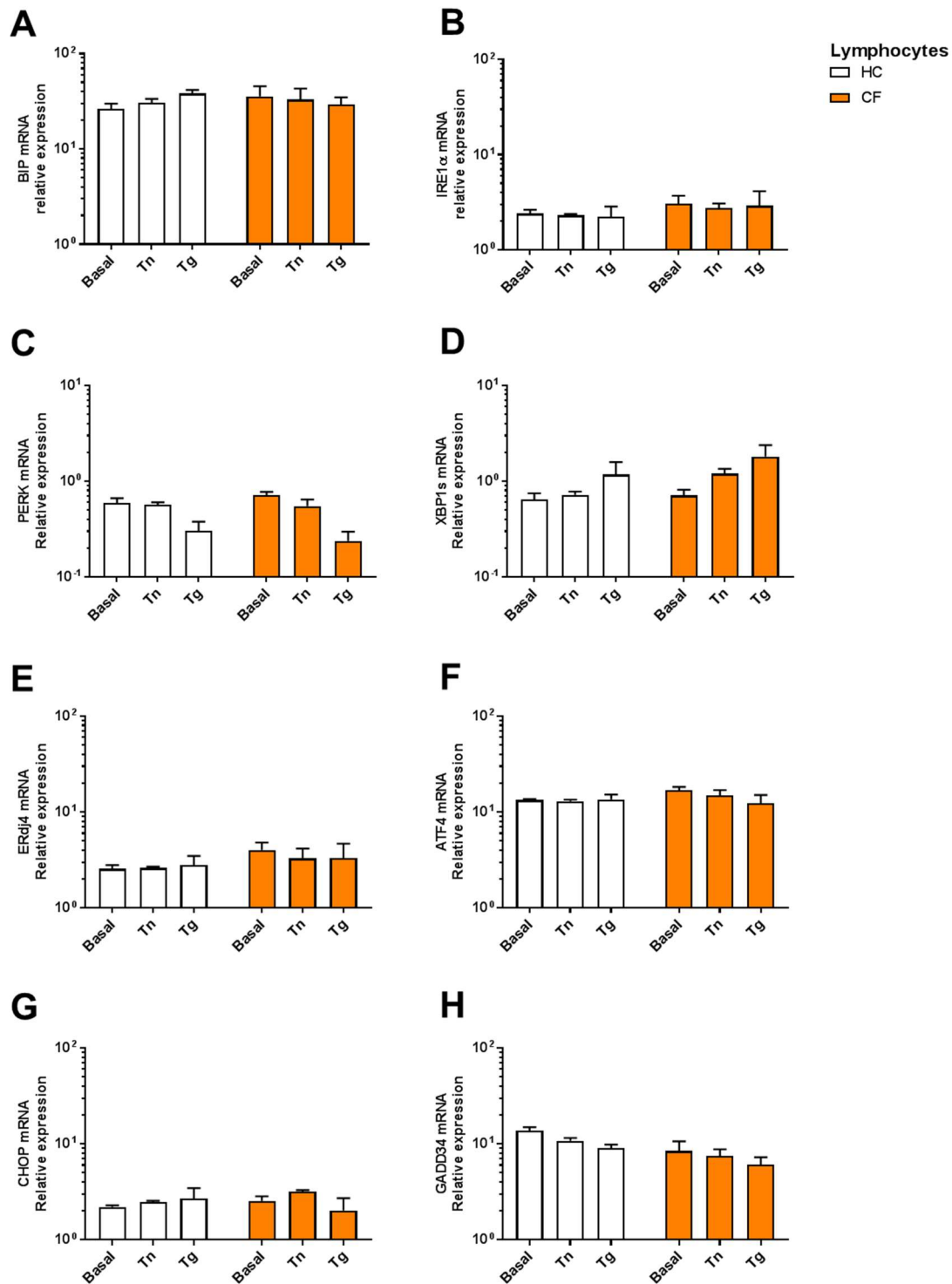


Figure 19 – ER stress in lymphocytes stimulated with Tn and Tg

UPR activation was measured in primary lymphocytes from HC individuals (n=6) and patients with CF (n=6) at basal conditions, stimulated with Tn (5 μ g/ml), or Tg (300nM) for 4 hours. (A-H). *BiP*, *IRE1 α* , *PERK*, *XBP1s*, *ERdj4*, *ATF4*, *CHOP* and *GADD34* were measured by qPCR. Statistical comparisons were performed by unpaired independent Student's t-test. *p < 0.05, **p < 0.01, and ***p < 0.001.

3.3.4 BiP, IRE1 α , ATF4 and CHOP upregulation in neutrophils

After evaluation of ER stress in lymphocytes, we then analysed the same markers in neutrophils from the same patients with CF. Neutrophils carrying CFTR mutations presented upregulation of several ER stress markers. These multinucleated cells showed raised levels of *BiP*, *IRE1 α* , *ATF4*, and *CHOP* at basal conditions, where only *BiP* and *CHOP* were significantly upregulated after stimulation with LPS (**Figure 20**). Stimulations of these cells with 5 μ g/ml of Tn or 300nM of Tg drastically reduced the survival rate of the cells. Therefore, adjusted concentrations of the drugs were administrated to these cells. Neutrophils from CF patients still demonstrated heightened levels of *BiP*, *IRE1 α* , *ATF4*, and *CHOP* following the administration of the drugs, with the only exception being *ATF4*, which was not significantly altered post Tg stimulation (**Figure 21**).

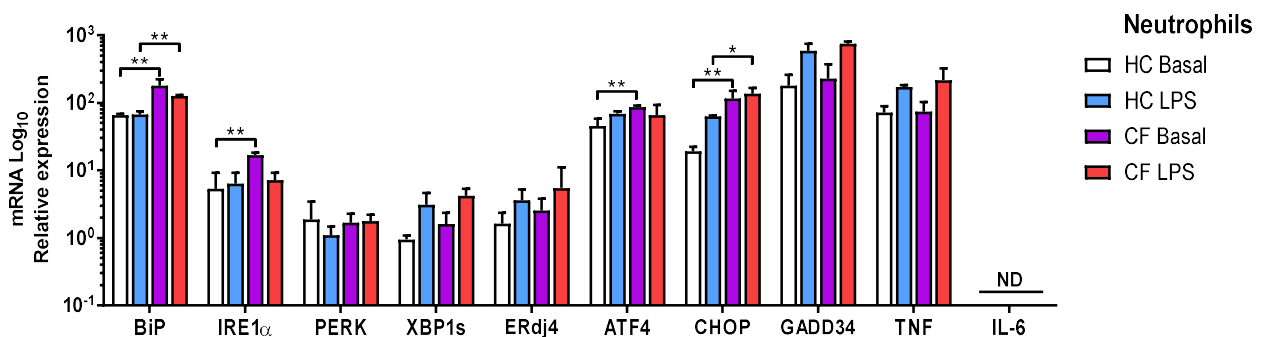


Figure 20 – UPR gene expression in neutrophils from patients with CF

mRNA relative expression of ER stress and UPR markers *BiP*, *IRE1 α* , *PERK*, *XBP1s*, *ERdj4*, *ATF4*, *CHOP*, *GADD34*, *TNF*, and *IL-6* were measured in neutrophils from HC volunteers (n=6) and patients with CF (n=6) at basal conditions and stimulated with LPS (10 ng/ml) for 4 h. All n values represent biologically independent samples. Statistical comparisons were performed by unpaired independent Student's t-test, *p < 0.05, **p < 0.01, ***p < 0.001; ND, not detected. These data have been published by the author [30].

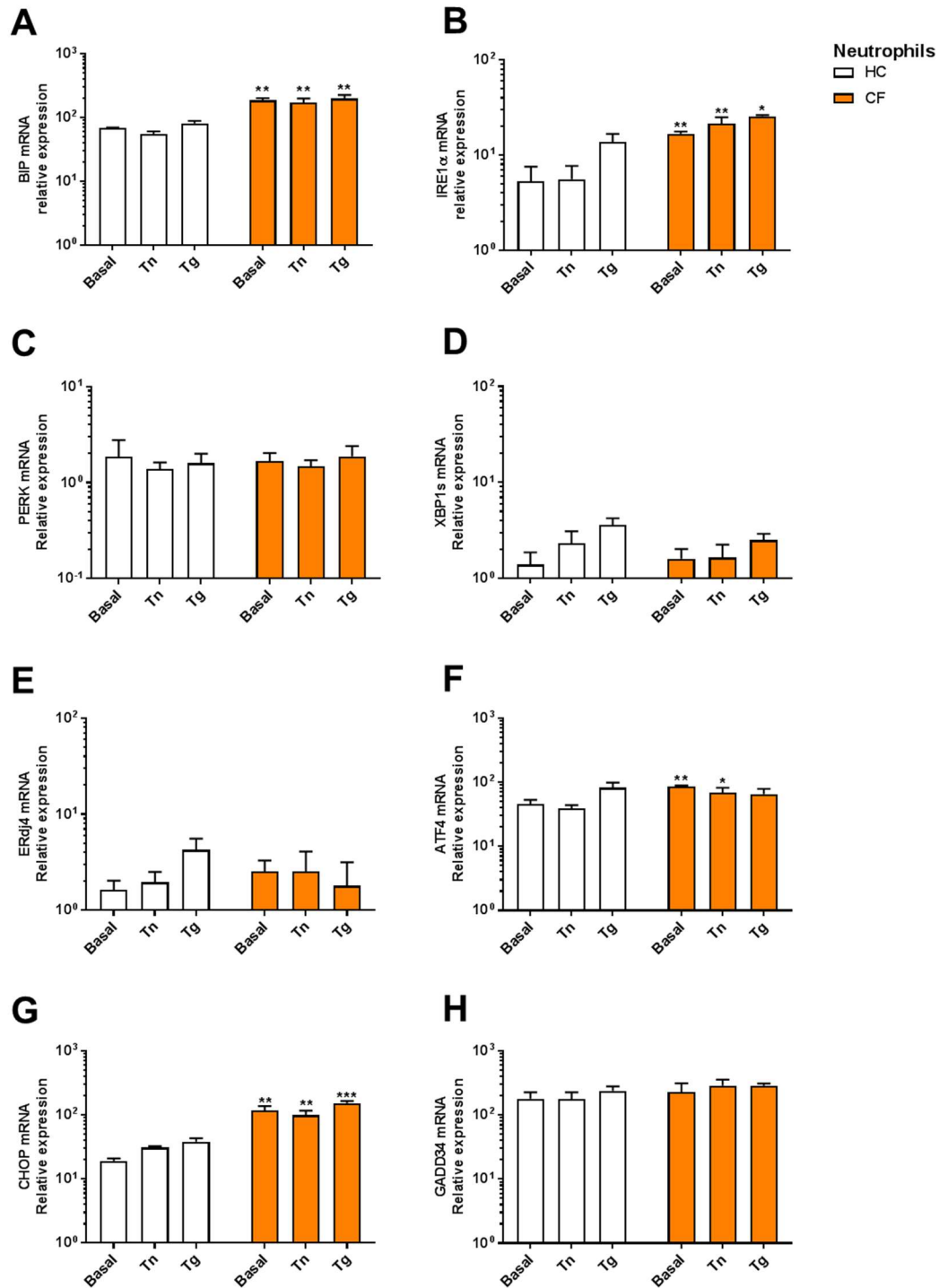


Figure 21 – ER stress in neutrophils stimulated with Tn and Tg

UPR activation was measured in primary neutrophils from HC individuals (n=6) and patients with CF (n=6) at basal conditions, stimulated with Tn (2 μ g/ml), or Tg (150nM) for 4 hours. (A-H). *BiP*, *IRE1 α* , *PERK*, *XBP1s*, *ERdj4*, *ATF4*, *CHOP* and *GADD34* were measured by qPCR. Statistical comparisons were performed by unpaired independent Student's t-test. *p < 0.05, **p < 0.01, and ***p < 0.001.

3.3.5 IRE1 α , PERK, ERdj4, ATF4, CHOP and GADD34 upregulation in monocytes

Human monocytes were studied to assess whether UPR perturbations existed within these phagocytic cells. Monocytes from patients with CF exhibited higher levels of *IRE1 α* and *ATF4* under basal conditions, similar to those seen in neutrophils (**Figure 22**). When monocytes were stimulated with LPS, more significant differences were revealed with regard to the expression of *IRE1 α* , *PERK*, *ERdj4*, *CHOP*, *GADD34* and *TNF* (**Figure 22**). These findings suggest that cells of myeloid origin, carrying CFTR mutations, exhibit similar perturbations at the transcriptional level, with *IRE1 α* being the most predominantly affected. Next, monocytes were stimulated with the UPR inducers, Tn and Tg, as previously described. After stimulation with Tn, *IRE1 α* , *ATF4*, *CHOP* and *XBP1s* transcripts were significantly upregulated in the CF monocytes (**Figure 23**). Furthermore, cells stimulated with Tg only showed a significant upregulation of *IRE1 α* and *ATF4*, when compared to the HC cells (**Figure 23**). All these findings support the idea of abnormal regulation of the UPR signalling pathways in myeloid cells with CFTR mutations.

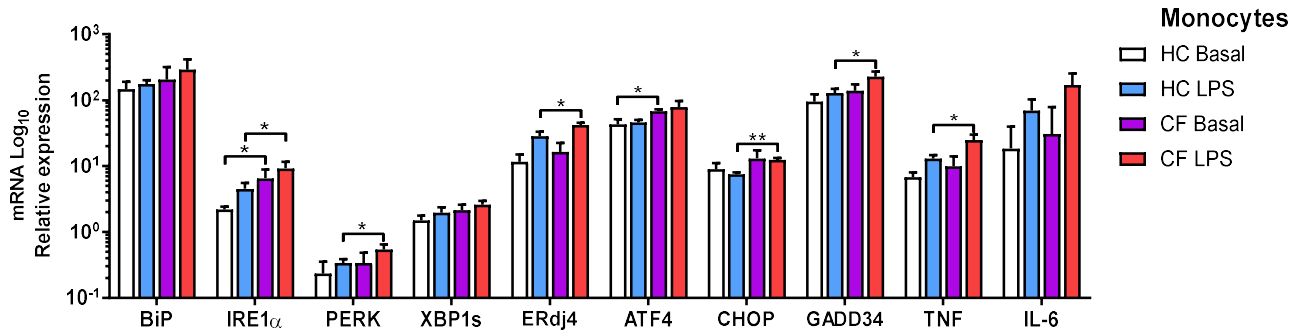


Figure 22 – UPR gene expression in monocytes from patients with CF

mRNA relative expression of ER stress and UPR markers *BiP*, *IRE1 α* , *PERK*, *XBP1s*, *ERdj4*, *ATF4*, *CHOP*, *GADD34*, *TNF*, and *IL-6* were measured in monocytes from HC volunteers (n=6) and patients with CF (n=6) at basal conditions and stimulated with LPS (10 ng/ml) for 4 h. All n values represent biologically independent samples. Statistical comparisons were performed by unpaired independent Student's t-test, *p < 0.05, **p < 0.01, ***p < 0.001; ND, not detected. These data have been published by the author [30].

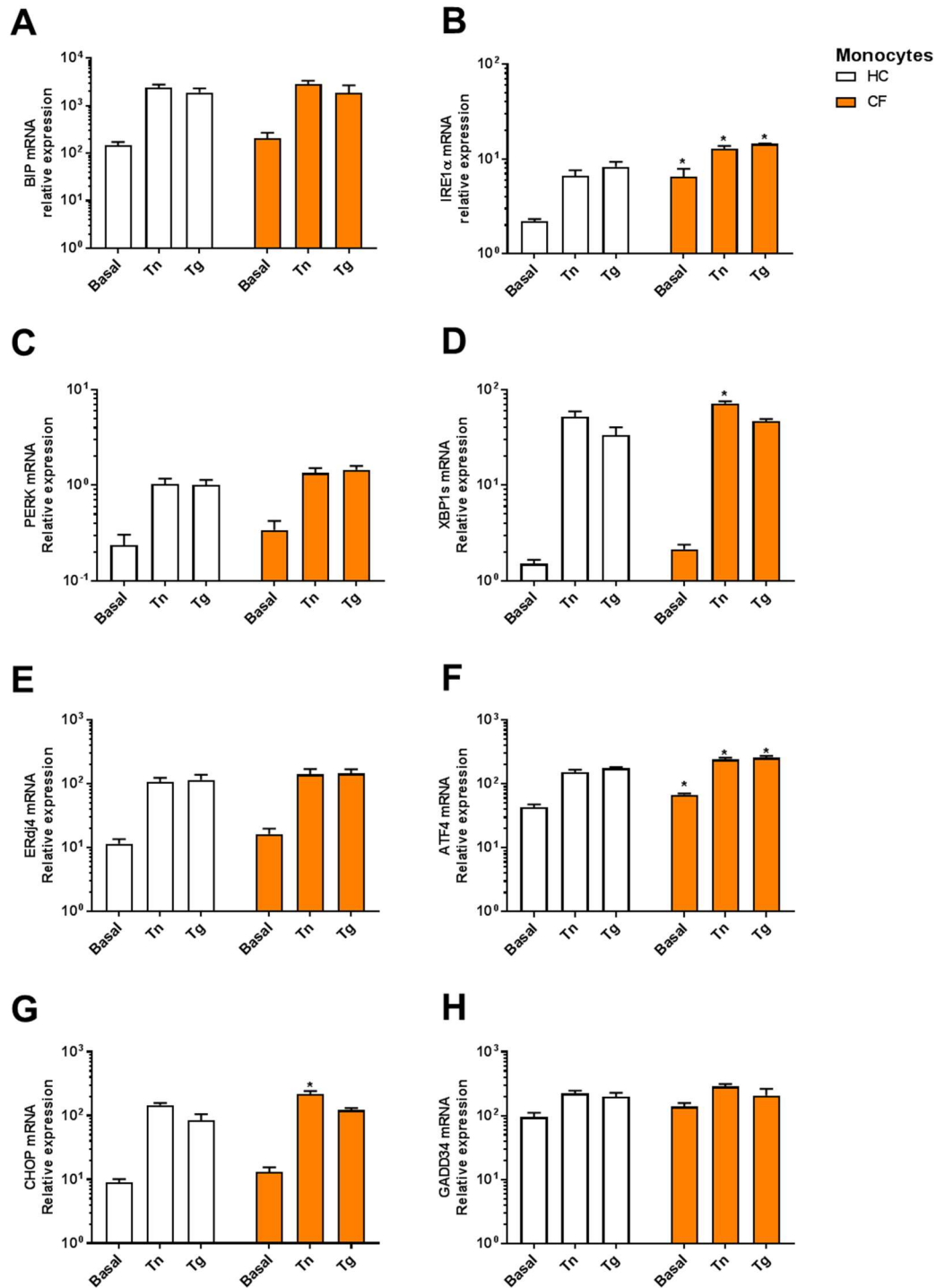


Figure 23 – ER stress in monocytes stimulated with Tn and Tg

UPR activation was measured in primary monocytes from HC individuals (n=6) and patients with CF (n=6) at basal conditions, stimulated with Tn (5 μg/ml), or Tg (300nM) for 4 hours. (A-H). *BiP*, *IRE1α*, *PERK*, *XBP1s*, *ERdj4*, *ATF4*, *CHOP* and *GADD34* were measured by qPCR. Statistical comparisons were performed by unpaired independent Student's t-test. *p < 0.05, **p < 0.01, and ***p < 0.001.

3.3.6 The IRE1 α -XBP1 pathway is overactive in CF M1 macrophages

Monocytes are the natural precursors of macrophages when derived from blood; therefore, we differentiated blood monocytes into macrophages, then, macrophages were polarised into M1 or M2 like-phenotype using LPS/IFN γ and IL-4/IL-13, respectively, and characterised by flow cytometry as described in the methods section and in **Figure 24**. While the polarisation ratios will be discussed later, we did not find any significant difference in the proportion of polarised M1 macrophages in patients with CF; however, the inflammatory profile of M1 macrophages was significantly increased when compared to HC macrophages.

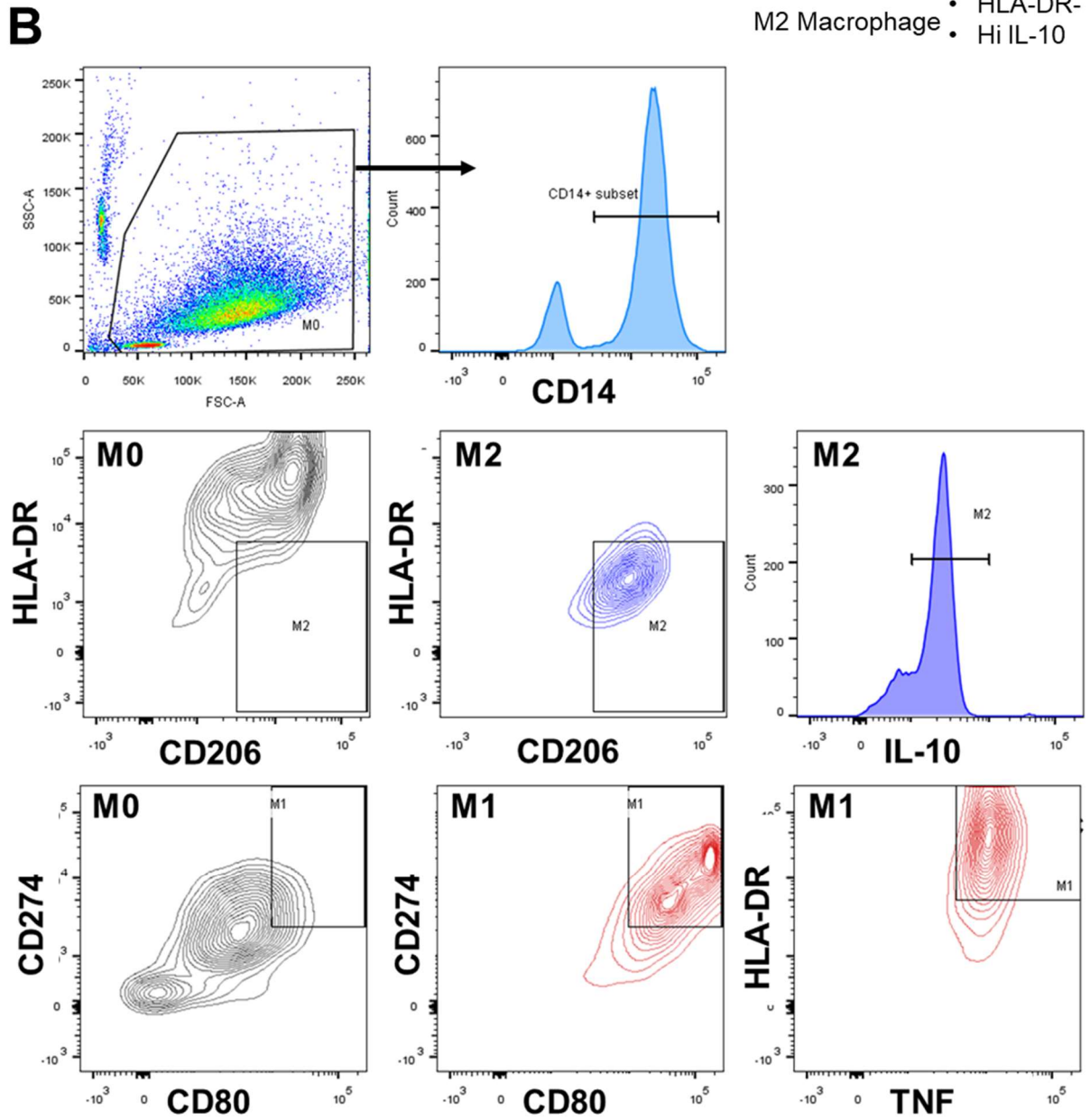
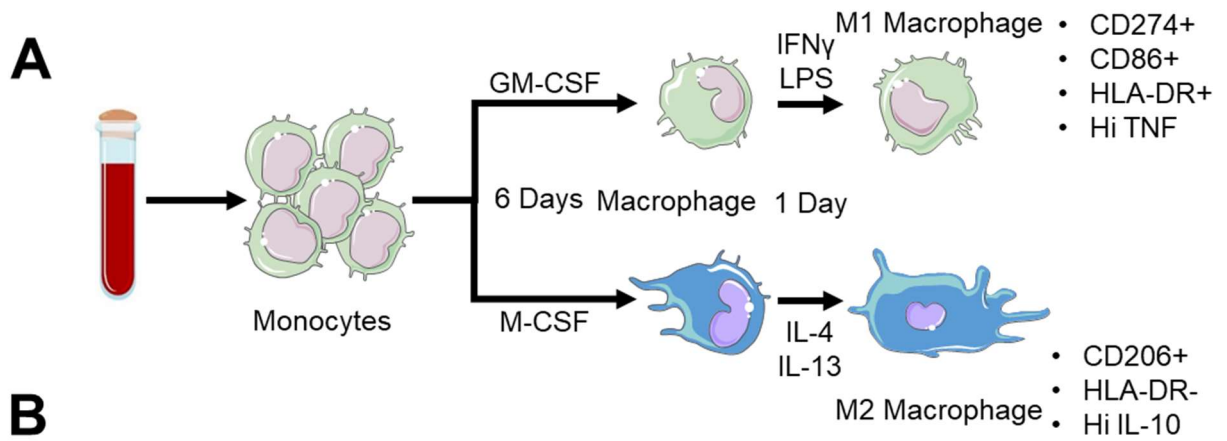


Figure 24 – Differentiation process of M1/M2 macrophages

Human blood monocytes were grown into macrophages, for 6 days, with GM-CSF 20 ng/ml or M-CSF 20 ng/ml. M1 macrophages were activated by stimulating the cells with 100 ng/ml human IFN γ , and 50 ng/ml LPS. M2 macrophages were activated by stimulating cells with 20 ng/ml IL-13 and 20 ng/ml IL-4 (A). Macrophages were characterized as M1-type (markers- CD14+, HLA-DR+, CD274+, CD86+ TNFHI) or M2-type (markers- CD14+, HLA-DR-, CD206+ and IL-10HI) as described in the methods (B). This figure has been published by the author [30].

Therefore, it was hypothesised that the abnormal inflammatory profile seen in CF M1 macrophages could be explained by intrinsic cellular defects caused by the CFTR mutations, which are also seen in the monocytes. Consequently, we analysed UPR activation in fully-activated M1 macrophages under basal conditions, meaning that M1 macrophages were activated for 24 h with LPS/IFN γ , followed by a second challenge with LPS when mentioned. Under basal conditions, a significant upregulation of *BIP*, *XBP1s*, *ERdj4*, *TNF* and *IL-6* transcripts was observed (**Figure 25**), while, after LPS stimulation we detected high levels of *BIP*, *XBP1s*, *TNF* and *IL-6*, with downregulation of *PERK* (**Figure 25**). As already performed with the other immune cells, M1 macrophages were also stimulated with Tn and Tg to assess differences in cell response under stress conditions. The amount of *BIP*, *XBP1s* and *GADD34* transcripts were significantly elevated after both stimulations, while only *ATF4* transcription levels were upregulated post Tg stimulation (**Figure 26**).

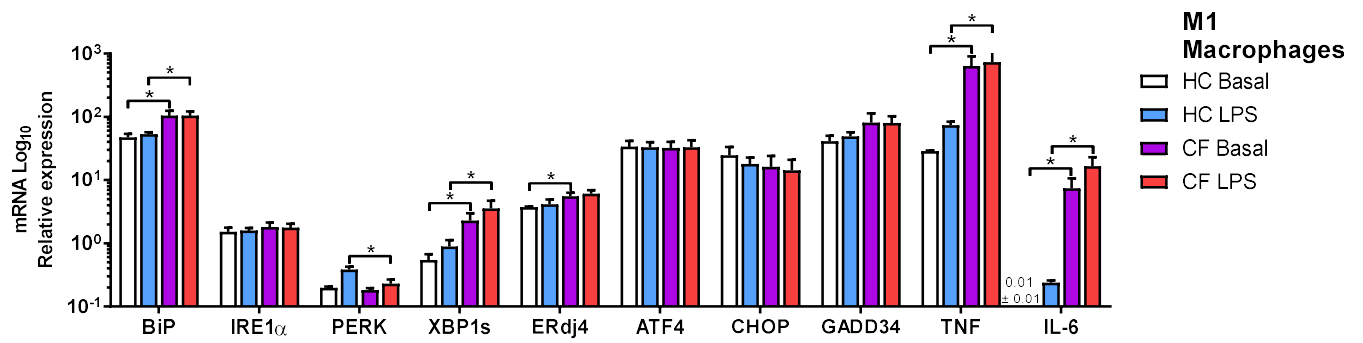


Figure 25 – UPR gene expression in M1 macrophages from patients with CF

mRNA relative expression of ER stress and UPR markers *BiP*, *IRE1 α* , *PERK*, *XBP1s*, *ERdj4*, *ATF4*, *CHOP*, *GADD34*, *TNF*, and *IL-6* were measured in M1 macrophages from HC volunteers (n=9) and patients with CF (n=9) at basal conditions and stimulated with LPS (100 ng/ml) for 4 h. All n values represent biologically independent samples. Statistical comparisons were performed by unpaired independent Student's t-test, *p < 0.05, **p < 0.01, ***p < 0.001; ND, not detected. These data have been published by the author [30].

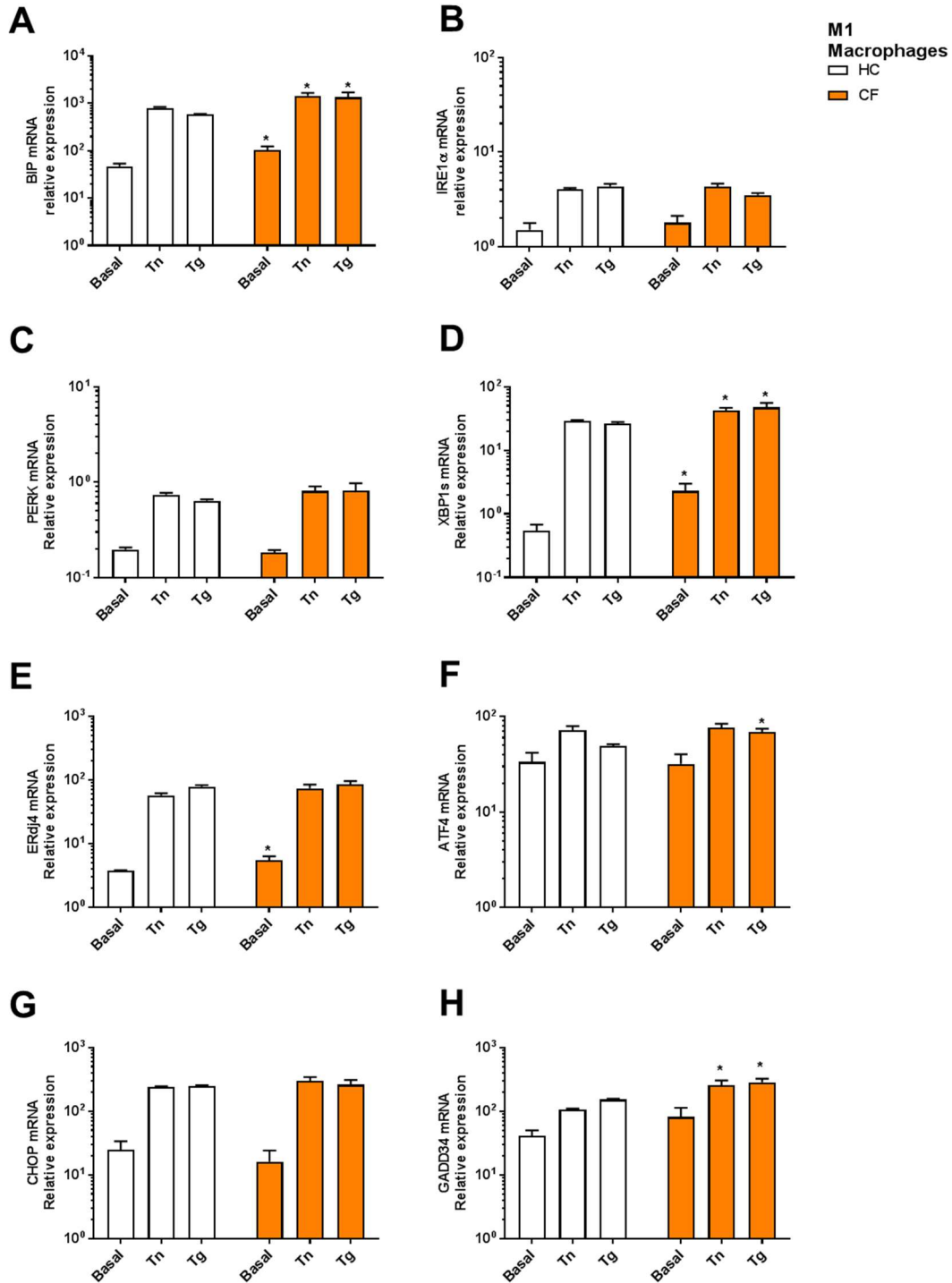


Figure 26 – ER stress in M1 macrophages stimulated with Tn and Tg

UPR activation was measured in M1 macrophages from HC individuals (n=9) and patients with CF (n=9) at basal conditions, stimulated with Tn (5 μ g/ml), or Tg (300nM) for 4 hours. (A-H). *BiP*, *IRE1 α* , *PERK*, *XBP1s*, *ERdj4*, *ATF4*, *CHOP* and *GADD34* were measured by qPCR. Statistical comparisons were performed by unpaired independent Student's t-test. *p < 0.05, **p < 0.01, and ***p < 0.001.

The elevated levels of XBP1s were confirmed by running a conventional RT-PCR gel, which revealed the presence of XBP1s in the majority of the CF M1 macrophage samples (**Figure 27A**). Next, we measured the protein levels of XBP1s in CF M1 macrophages. Levels of XBP1s were also significantly higher in M1 macrophages from CF patients, compared to the HC (**Figure 27B and C**). These findings suggest that the IRE1 α -XBP1s signalling pathway is abnormally upregulated in M1 macrophages from CF patients.

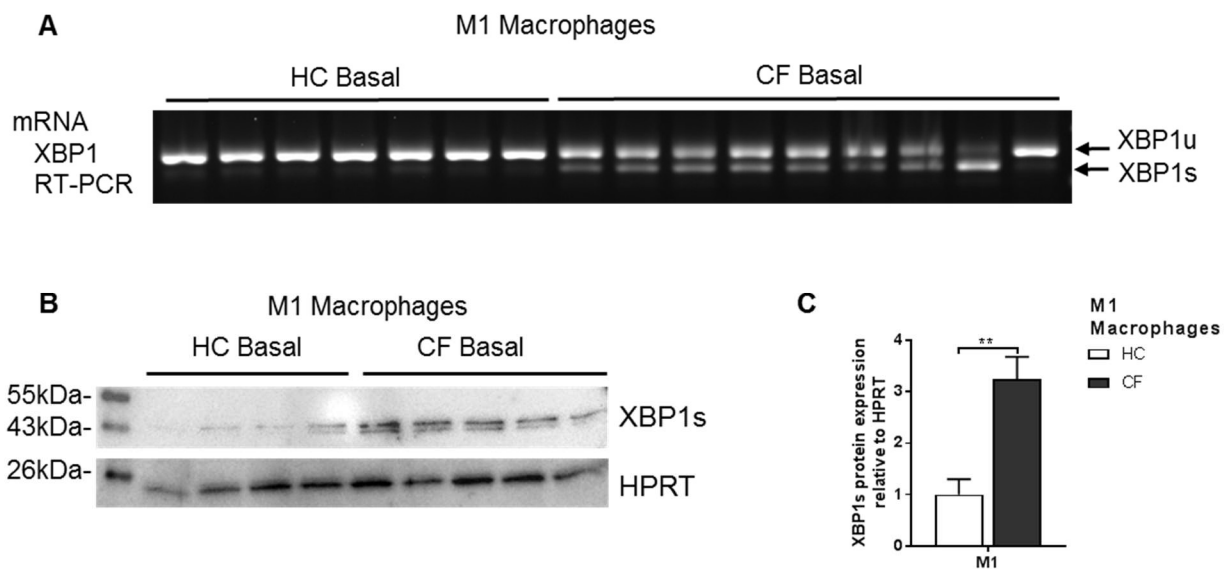


Figure 27 – XBP1s in M1 macrophages from CF patients

(A) XBP1s was measured by RT-PCR in M1 macrophages from HC volunteers (n=7) and patients with CF (n=9). (B and C) XBP1s protein levels were measured in M1 macrophages from HC individuals (n=4) and patients with CF (n=5) by Western blotting. Cell lysates were immunoblotted for XBP1s and HPRT (B), XBP1s was normalized to HPRT, and the ratios were compared to the levels of HC (C). Statistical comparisons were performed unpaired independent Student's t-test, *p < 0.05, **p < 0.01, ***p < 0.001 (C). Part of this figure was produced by Mr Johnathan Holbrook and published by the author [30].

3.3.7 XBP1s is not induced in CF M2 macrophages

While XBP1s was commonly upregulated after LPS stimulation in macrophages, we also quantified XBP1s at the protein level in M2 macrophages from CF patients [151]. It was found that XBP1s was not present in fully activated M2 macrophages (**Figure 28**). This finding demonstrates that XBP1s overexpression is only present in M1 macrophages from patients with CF.

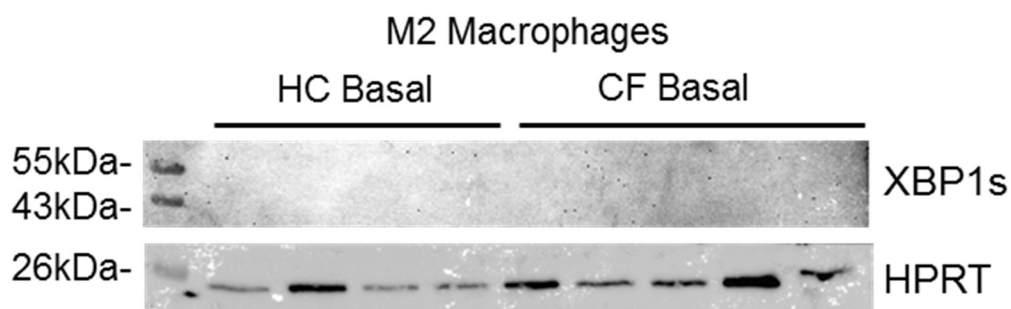


Figure 28 – XBP1s is absent in M2 macrophages from CF patients

XBP1s protein levels were measured in M2 macrophages from HC individuals (n=4) and patients with CF (n=5) by Western blotting. Cell lysates were immunoblotted for XBP1s and HPRT. Statistical comparisons were performed unpaired independent Student's t-test, *p < 0.05, **p < 0.01, ***p < 0.001. This figure was produced with the help of Mr Johnathan Holbrook and published by the author [30].

3.4 Discussion

Clear evidence of abnormal UPR activation was found in cells with CFTR mutations. Interestingly, these abnormalities were only found in innate immune cells. It has been previously shown that activation of the UPR decreases CFTR expression [202]. Therefore, this UPR activation may be contributing to the reduced level of CFTR expression seen in cells with CF mutations. Furthermore, chronic UPR activation can induce the production of several pro-inflammatory cytokines, such as IL-1 β , IL-6 and TNF, and this will be discussed in the next chapter [151]. The CF HBECs CuFi-1, Δ F508/ Δ F508, and CuFi-4, Δ F508/G551D, showed significant upregulation of several markers of ER stress, with the IRE1 α -XBP1 pathway being the most consistent. Remarkably, the CuFi-1 cell line revealed upregulation in all the ER stress markers studied here, while the CuFi-4 cell line only presented increased levels of *BIP*, *XBP1s*, *eIF2 α* and *CHOP*. These findings suggest that the amount of ER stress present in the CF cell lines may be specifically associated with particular genotypes. Surprisingly, the IB3-1 cell line, carrying a class type I mutation, showed decreased levels of *PERK* and *IRE1 α* , with no change in any other marker, as opposed as those findings described by Blohmke *et al.* [172], where the authors found raised levels of *XBP1s*. The discrepancies found in here could be due to differences between the cell lines, as these come from different individuals or the culturing conditions. In fact, to validate these findings, a collaboration has been established with Professor Martinon, to create a BEAS-2B cell line Δ F508 homozygous for the CFTR and BEAS-2B CFTR-KO, by using CRISPR/Cas9. These cell lines will provide us with direct answers about whether the mutated Δ F508 CFTR is directly associated with the activation of the UPR.

Considering that the CuFi-1 cell line carries two copies of the CFTR, with $\Delta F508$ mutations then, in theory, this could be the cell line with more misfolded protein, and thus more ER stress. Indeed, it was confirmed that, under basal conditions, CuFi-1 cells showed significantly higher expression of *BiP*, *IRE1 α* , *PERK*, and *ATF6*, suggesting that this cell line is under chronic ER stress. These findings are in line with the observations that CuFi-4 cells still show UPR activation (**Figure 12**), but to a lesser than the CuFi-1. It is essential to mention that the IB3-1 cell line also carries one CFTR- $\Delta F508$ allele, implying that ER stress is hypothetically present, mainly caused by misfolded protein accumulation; however, this was not the case and the absence of ER stress in the IB3-1 cells could be due to degradation of the CFTR- $\Delta F508$ in a similar manner to the CFTR-W1282X, where total CFTR degradation results in no misfolded protein accumulation. Another possibility is that different class mutations are regulated in a different manner with similar consequences.

When UPR activation in PBMCs from CF patients was investigated, no significant differences were observed in *XBP1s* expression under basal conditions, as described by Blohmke *et al.* [172]; nevertheless, we observed a significant increase in *XBP1s* after stimulation with LPS and Tn in PBMCs from patients with CF. This difference could be due to the choice of technique used in the isolation of the PBMCs, the media used for culturing the cells, or the timing for RNA collection. While I believe that there is chronic UPR activation in individual immune cells harbouring CFTR mutations, this ER stress is low-grade in nature. Under basal conditions, we detected a consistent upregulation of *IRE1 α* in PBMCs, neutrophils and monocytes, suggesting that this particular pathway is the most affected in innate immune cells with CFTR mutations. Moreover, most of these differences were still maintained after LPS, Tn and Tg stimulations. Besides *IRE1 α* , monocytes showed significant upregulation of ATF4

under basal conditions, with upregulation of *PERK*, *ERdj4*, *CHOP* and *GADD34* after LPS stimulation. These findings suggest that, upon induction of cellular stress through LPS, the low-grade ER stress become significantly evident. Despite the fact that *XBP1s* levels were not significantly different in CF monocytes, under basal conditions, we observed a significant upregulation of this transcript after stimulating the cells with Tn. This finding, aligned with other publications showing that *XBP1s* is overexpressed in alveolar macrophages from patients with CF [113], lead us to investigate ER stress in monocyte-derived macrophages. It is essential to mention that the activation of lymphocytes with LPS is not ideal in this experimental system, as, for instance, T cells require direct cell-to-cell contact with antigen presenting cells to become fully activated; however, we still wanted to include these experiments to compare basal ER stress and to investigate whether there were any differences after stimulation with LPS and any *XBP1s*, due to some papers reporting the existence of some signalling in lymphocytes after TLR4 stimulation [203-205].

When monocytes reach the site of infection or inflammation, and as soon as they are stimulated with granulocyte-macrophage colony-stimulating factor (GM-CSF) or macrophage colony-stimulating factor (M-CSF), they differentiate into monocyte-derived macrophages [206, 207]. When monocytes are being differentiated on the road to become macrophages, their cellular size is enlarged, and this process provides these cells with a more exceptional ability to promote inflammation and phagocytosis. When we differentiated macrophages and polarised into a M1-like phenotype, they showed a consistent upregulation in *XBP1s*. M1 macrophages from CF patients showed significantly increased levels in *XBP1s*, *BIP*, *TNF* and *IL-6*, under basal conditions and after a second LPS challenge. The *XBP1s* transcript levels were confirmed by Western blotting showing a persistent upregulation in *XBP1s* in the M1

macrophages from CF patients. In contrast, M2 macrophages activated with IL-4/IL-13 did not show any difference in XBP1s protein expression. Altogether, these findings suggest that the IRE1 α -XBP1 signalling pathway is overactive in M1 macrophages from CF patients with potential implications in inflammation.

Chapter 4 – Inflammation and the UPR in Cystic Fibrosis

4.1 Introduction

Inflammation is a major component in the pathogenesis of CF, and, as described before, it can be induced via the UPR signalling pathway. The lung is a complex microenvironment and, in CF, this environment is altered, thereby favouring bacterial colonisation. As already demonstrated, an atypical UPR activation exists in CF and it is CFTR dependent, in the case of HBECs, and also cell-specific, as in the case of innate immune cells. Our results are in line with other reports, showing that CF alveolar macrophages have increased levels of XBP1s along with heightened production of TNF and IL-6, as will be described later in this chapter [113].

Stimulation of CF HBECs and PBMCs, from CF patients, with the TLR5 ligand, flagellin, results in increased levels of IL-6 release without PERK/eIF2 α induction [172]. In a different study, in non-CF HBECs, exposure to *P. aeruginosa* conditioned medium induced the expression of XBP1s, CHOP, BiP, and GADD34 [208]. This indicates that the UPR signalling pathway is an important innate cellular mechanism in HBECs that helps in the induction of the inflammatory response. Furthermore, the UPR plays a significant role in the regulation of inflammation in immune cells, as described before [151]. Therefore, based on our evidence that HBECs and innate immune cells showed an atypical UPR activation, with consistent upregulation of IRE1 α , we investigated the consequences of this upregulation involving two important pro-inflammatory cytokines increased in CF, TNF and IL-6.

4.2 Methods

4.2.1 RNA isolation and detection

All the RNA processing and detection were performed, as described in the methods section. The following cell numbers were used for RNA extraction; 1×10^6 HBECs, 2×10^6 PBMCs, 1×10^6 monocytes, 2×10^6 lymphocytes, 3×10^6 neutrophils and 1×10^6 macrophages.

4.2.2 Flow cytometry

For the characterisation of M1 and M2 macrophages, the following protocol was used. Negatively selected monocytes, as described in the main methods, were cultured in complete RPMI medium (Merck) to generate either M1 or M2 macrophages (**Figure 24**). For M1/M2 macrophage characterization using flow cytometry, monocytes were seeded at a density of 1×10^6 cell/ml and were cultured in tissue culture-treated 6 well plates, then stimulated and activated with their respective factors. On day 7 cells were washed twice with DPBS without Ca^{2+} and Mg^{2+} and detached, using DPBS with EDTA 10 mM for M2 macrophages, or Accutase (ThermoFisher) for M1 macrophages. Cells were washed twice with DPBS (2% FBS) and resuspended in BSB, with human and mouse serum for 30 min on ice. Cells were stained with the surface markers for M1-type (CD14+, HLA-DR+, CD274+ and CD86+) and M2-type (CD14+, HLA-DR-, and CD206+) for 30 min on ice. Finally, cells were washed, fixed (4% paraformaldehyde) and permeabilised (BD Cytofix/Cytoperm) for 20 min, as recommended by the manufacturer. The intracellular markers, IL-10 and TNF, were then added for a further 15 min. After the final wash, the cells were resuspended in BSB in FACS collection tubes. All antibodies used are listed in detail

in the table of reagents (**Table 5**). All other flow cytometry procedures were done as described in the main methods section.

4.2.3 Cytokine expression

Cytokine levels from cell cultured media were detected by the IL-6, TNF, and IL-10 ELISAs kits, listed in the table of reagents, following the manufacturer's recommendations and as described in the methods section. All supernatants were collected after each cellular stimulation and stored at -80°C until required.

4.2.4 Cellular stimulations

HBECs, PBMCs, lymphocytes, and monocytes were left unstimulated or stimulated with LPS (10ng/ml), Tn (5µg/ml) and Tg (300 nM) for 4 hours. Neutrophils were stimulated with LPS (10ng/ml), Tn (2µg/ml) and Tg (150 nM). Macrophages were cultured and activated, as mentioned in the main methods section, and stimulated with LPS (100ng/ml). When used, the IRE1 inhibitors 4µ8c (50 µM) and MKC-3946 (10 µM) were administrated 30 min before any activation.

4.3 Results

4.3.1 Upregulation of IL-6 in CF HBECs

As seen in the previous chapter, the UPR signalling pathway is upregulated in CF HBECs, particularly in the CuFi-1 cell line. Therefore, the consequences of this UPR activation regarding the production of IL-6, which is upregulated by the IRE1 α /XBP1 signalling pathway were explored [151]. As seen before, under basal conditions, CF HBECs showed significantly higher levels of *IL-6* (**Figure 29**). Stimulation of HBECs with the UPR inducer Tn resulted in a reduction of *IL-6* expression in the BEAS-2B and the IB3-1 cell lines, and an increase in the CuFi-1 and CuFi-4 cell lines when compared to the basal state of each cell line (**Figure 29**). In contrast, stimulation with Tg led to an increased expression of *IL-6* in all cells, with a significant increase in the CuFi-1 and CuFi-4 CF cell lines, when compared to the WT control (**Figure 29**). mRNA expression of the pro-inflammatory cytokine *IL-1B* was also measured in all the HBECs, and preliminary results suggest that this cytokine is upregulated under basal condition in the CF HBEC lines [209]. The production of IL-6 has been associated with the transcription factor XBP1s [151, 152]; therefore, it was investigated whether the IRE1 inhibitor, 4 μ 8c, would reduce the expression of IL-6. Pre-treatment of the CuFi-1 and BEAS-2B cell lines with the IRE1 inhibitor abolished the expression and the secretion of IL-6 (**Figure 30**). These inhibitory effects were still seen after LPS and Tg stimulation in both HBEC lines (**Figure 30**). In summary, the elevated IL-6 expression, seen in CF HBECs, can be blocked by inhibition of the IRE1 α /XBP1 signalling pathway.

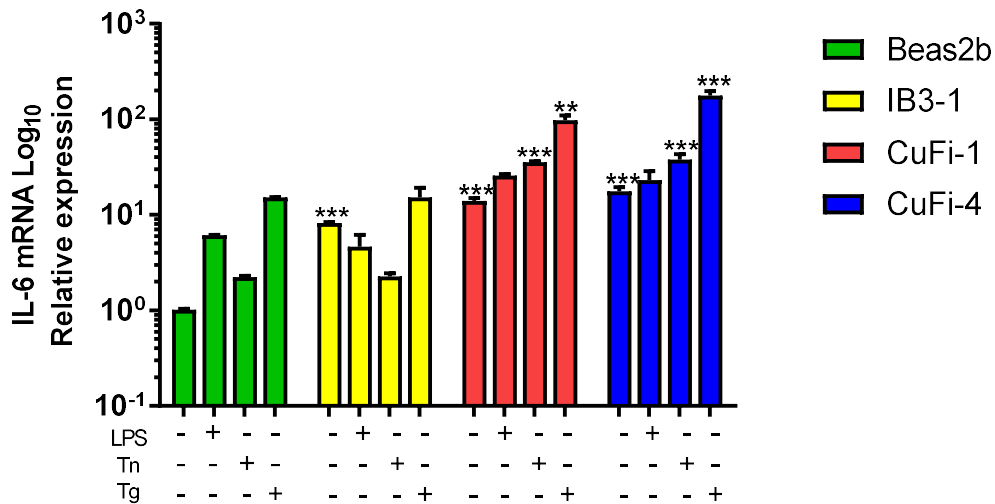


Figure 29 – IL-6 expression in HBECs with CF mutations

IL-6 expression was measured in the BEAS-2B, IB3-1, CuFi-1, and CuFi-4 cell lines after stimulation with LPS (100 ng/ml), Tn (5 μg/ml) and Tg (300 nM) for 4 hours. mRNA expression was analysed by qPCR. All comparisons were made versus the BEAS-2B cell line, comparing each stimulation accordingly. Statistical significance was determined using unpaired independent Student's t-test for each of the stimulations. *p < 0.05, **p < 0.01, ***p < 0.001. n=4 biological replicates for all cell lines.

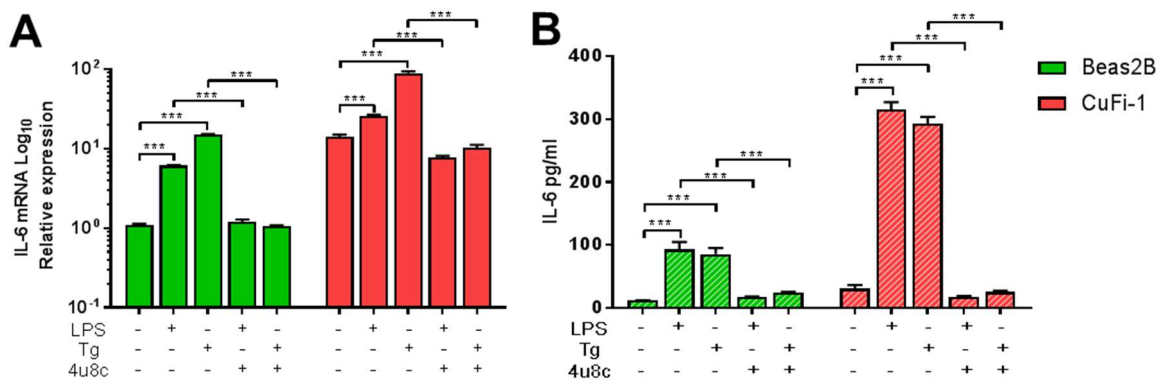


Figure 30 – IRE1α inhibition reduces IL-6 in HBECs.

IL-6 expression and production were measured in response to LPS (100 ng/ml) and Tg (300 nM) for 4 h measuring *IL-6* mRNA (A) and IL-6 cytokine levels (B); when referred, the IRE1α inhibitor, 4μ8c (50 μM), was used 30 min before each stimulation. All data are presented as mean ± SEM and mRNA data represented by logarithmic scale base 10. Statistical significance was determined by using paired Student's t-test. *p < 0.05, **p < 0.01, ***p < 0.001. n=4 biological replicates for all cell lines. These data have been published by the author [30].

4.3.2 Expression of TNF and IL-6 in lymphocytes and neutrophils

Expression of TNF and IL-6 is not a standard characteristic of lymphocytes; however, we wanted to investigate the mRNA levels of these two cytokines under basal conditions and after LPS, Tn and Tg stimulations. While activation of lymphocytes with LPS is not ideal, for the reasons indicated before, I still wanted to evaluate whether there was any response to this stimulation. Lymphocytes showed a modest induction of TNF and a substantial IL-6 mRNA induction after LPS stimulation, with no significant differences between groups (**Figure 31A**). Lymphocytes treated with Tn and Tg displayed a modest but significant reduction in the expression of *TNF*, correspondingly (**Figure 31B**). The levels of expression of IL-6 was not detectable under basal conditions; nevertheless, upon stimulation with Tn and Tg, an increase in IL-6 mRNA was observed in these cells, with no significant differences observed between the two groups (**Figure 31C**).

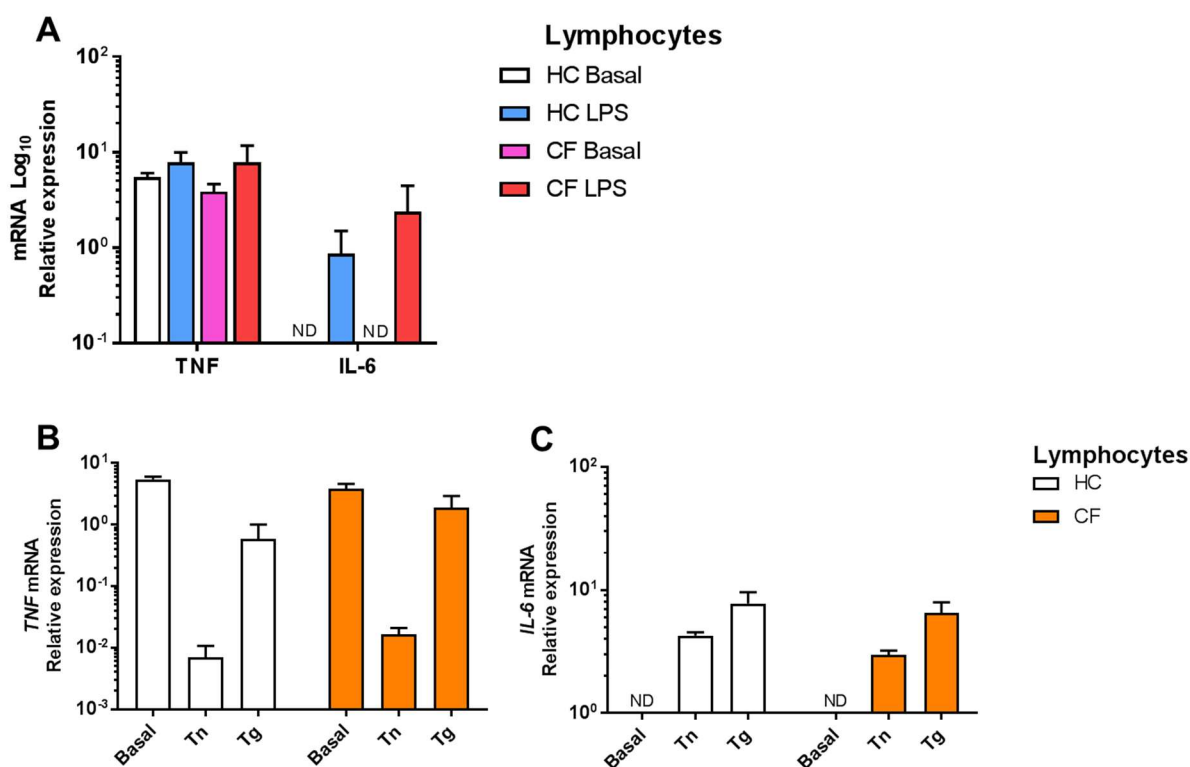


Figure 31 – TNF and IL-6 expression in lymphocytes.

TNF and *IL-6* expression were measured in response to LPS (10 ng/ml) (A), after Tn (5 μ g/ml) and Tg (300 nM) (B and C) for 4 h in lymphocytes from HC (n=6) and patients with CF (n=6). All data are presented as mean \pm SEM and mRNA data represented by logarithmic scale base 10. Statistical comparisons were performed by unpaired independent Student's t-test. * $p < 0.05$, ** $p < 0.01$, and *** $p < 0.001$. ND (not detected).

Next, TNF and IL-6 expression was evaluated in neutrophils. No significant differences were observed in these multinucleated cells, either at basal conditions or after LPS activation (**Figure 32A**). increased levels of *TNF* mRNA were induced by LPS stimulation; however, we did not detect IL-6 expression in these cells (**Figure 32A**). Stimulation of the cells with Tn or Tg induced a modest change in the levels of *TNF* (**Figure 32B**). Altogether, no differences were found in TNF or IL-6 expression between the HC and CF group in either lymphocytes or in neutrophils.

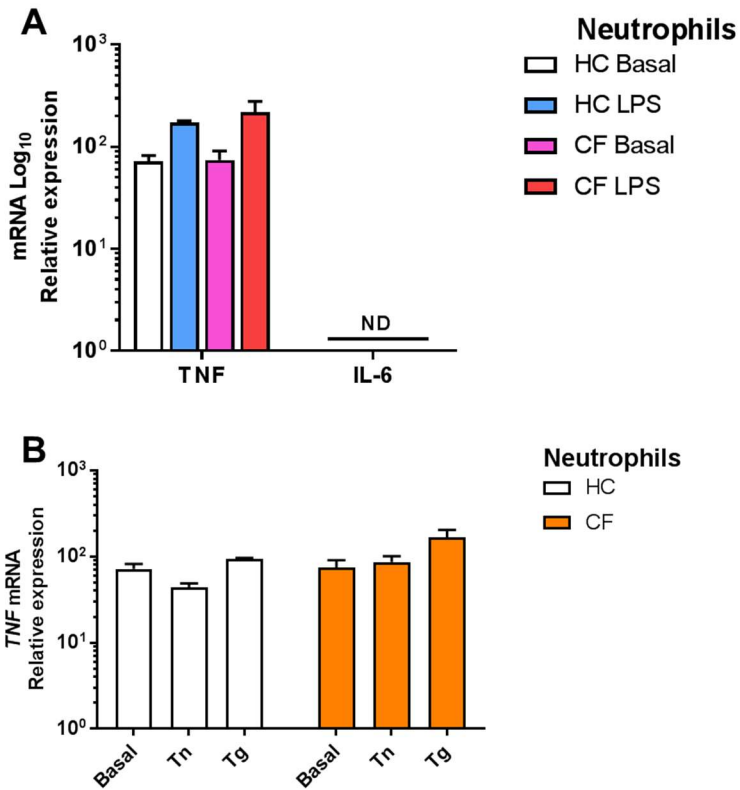


Figure 32 – TNF and IL-6 expression in neutrophils.

TNF and IL-6 expression were measured in response to LPS (10 ng/ml) (A), after Tn (2 μ g/ml) and Tg (150 nM) (B) for 4 h in neutrophils from HC (n=6) and patients with CF (n=6). All data are presented as mean \pm SEM and mRNA data represented by logarithmic scale base 10. Statistical comparisons were performed by unpaired independent Student's t-test. *p < 0.05, **p < 0.01, and ***p < 0.001. ND (not detected).

4.3.3 Upregulation of TNF in CF monocytes

Monocytes are important inducers of the inflammatory response, and when required, these cells can differentiate into macrophages, to control inflammation in a more efficient manner. Monocytes stimulated with LPS showed induction of both inflammatory cytokines, *TNF* and *IL-6* (**Figure 33A**). There were no significant differences under basal conditions when the two groups were compared; however, on addition of LPS, there was a significant upregulation of *TNF* in the CF monocytes (**Figure 33A**). When monocytes were stimulated with Tn and Tg, no significant differences were observed in these cells (**Figure 33B and C**). Then to confirm that our observations were not related to cellular death, we assessed cellular viability by using Annexin V and propidium iodide (PI). Under basal conditions, we observed ~50% of intact cells with less than 5% of late apoptotic cells (**Figure 34A**). Culture of the monocytes with the UPR inducer Tg for 4 h, induced early apoptosis in ~90% of the monocytes, with no significant differences in late apoptosis (**Figure 34B**). When comparing HC and patients with CF, we observed that upon stimulation of monocytes from the CF patients with LPS, Tn and Tg, there was a gradual decrease in the percentage of intact cells (**Figure 34C**). These data suggest that monocytes with CFTR mutations are more sensitive to cellular stress. Moreover, the significant difference observed in the production of the pro-inflammatory cytokine, TNF, might be due to the increased number of early apoptotic cells in the CF monocytes.

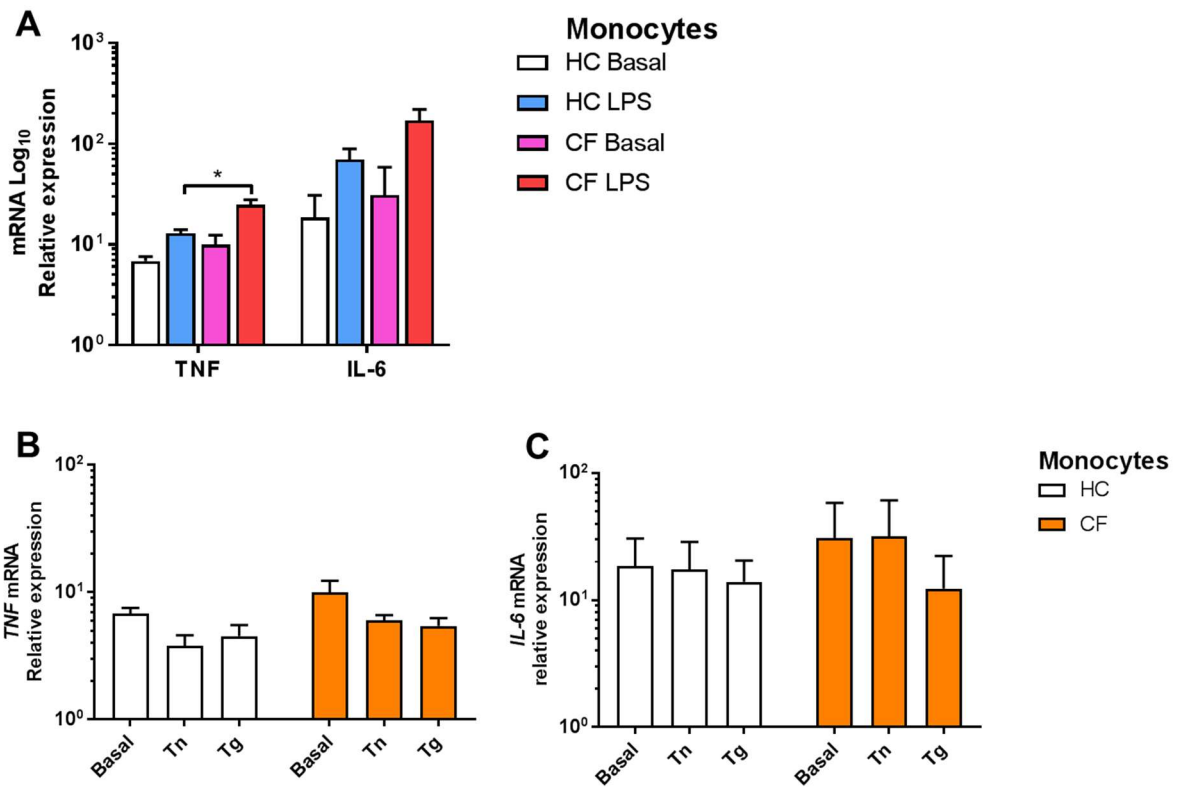


Figure 33 – TNF and IL-6 expression in monocytes.

TNF and *IL-6* expression were measured in response to LPS (10 ng/ml) (A), after Tn (5 μ g/ml) and Tg (300 nM) (B and C) for 4 h in monocytes from HC (n=6) and patients with CF (n=6). All data are presented as mean \pm SEM and mRNA data represented by logarithmic scale base 10. Statistical comparisons were performed by unpaired independent Student's t-test. *p < 0.05, **p < 0.01, and ***p < 0.001.

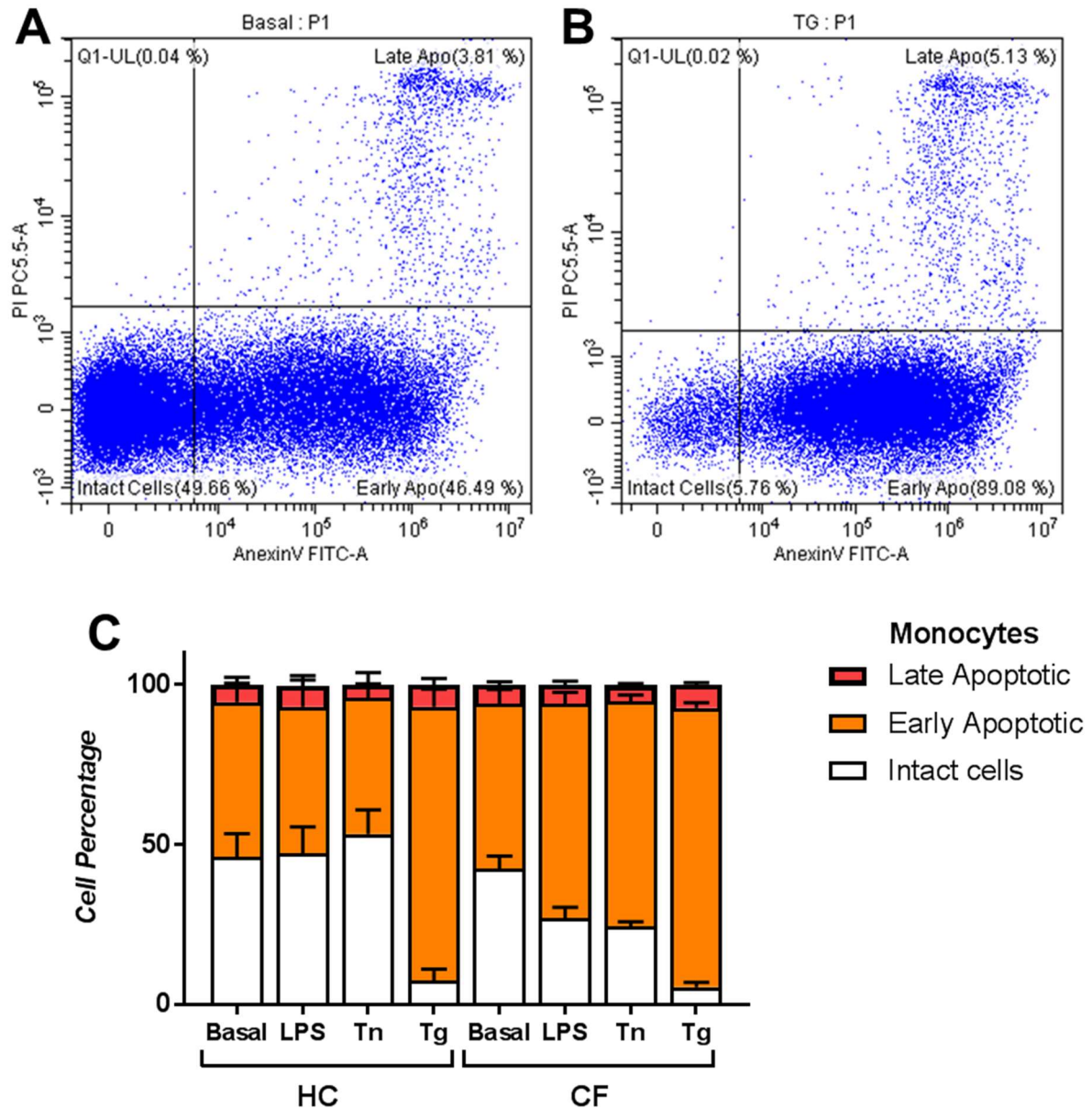


Figure 34 – Apoptosis percentage in human monocytes.

Cell viability was measured using annexin V and propidium iodide (PI). Intact cells, early and late apoptosis were measured in HC and CF monocytes. Cells were either left untouched or stimulated with LPS (10 ng/ml), Tn (5 μ g/ml) or Tg (300 nM) (B and C) for 4 h. HC (n=2) and CF (n=4). All data are presented as mean \pm SEM and

4.3.4 Deficient polarisation of M2 Macrophages in patients with CF

In the previous chapter, we observed that M1 macrophages, from patients with CF, displayed significantly higher levels of XBP1s, while M2 macrophages did not show any differences in expression of this transcription factor (**Figure 27****Figure 28**). Therefore, using the same differentiation protocol, we differentiated monocytes to macrophages and polarised them into a M1 or M2 phenotype (**Figure 24**). We characterised the macrophages phenotypes based on the surface markers (CD14+, HLA-DR+, CD274+ and CD86+) for M1 and (CD14+, HLA-DR-, and CD206+) for M2 (**Figure 24**). After polarisation of M2 macrophages from CF patients and HC, we observed a significantly lower amount of M2 macrophages in patients with CF, with reduced levels of the anti-inflammatory cytokine, IL-10 (**Figure 35**).

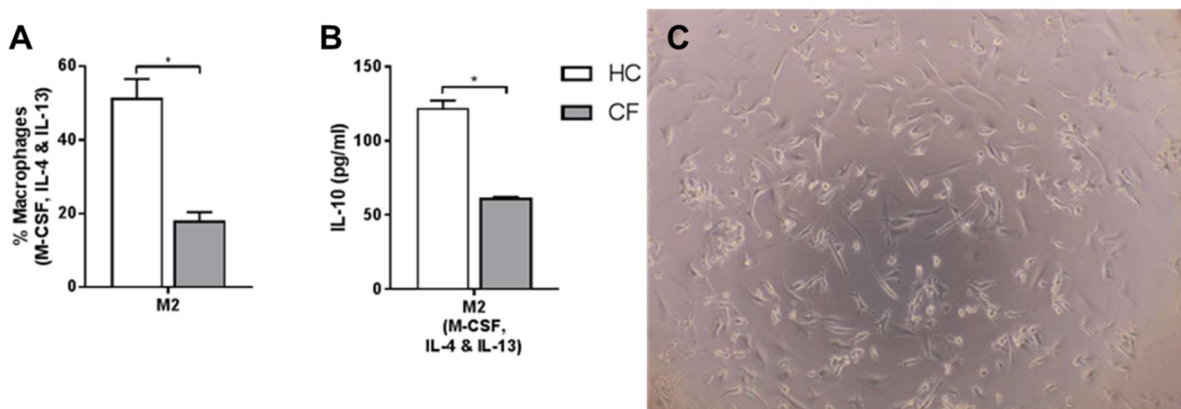


Figure 35 – Reduced polarisation of CF M2 macrophages.

(A) Polarised M2 macrophages (M-CSF, IL-4, and IL-13) from HC volunteers (n=7) and patients with CF (n=7) are presented as percentage M2 of total macrophages measured by flow cytometry. (B) IL-10 cytokine levels from M2 polarised macrophages measured by ELISA. (C) Phenotypic picture of M2 macrophages by light microscopy (20X). All data are presented as mean \pm SEM. Statistical comparisons were performed by Mann-Whitney non-parametric test, *p < 0.05, **p < 0.01, ***p < 0.001. Part of this figure was produced by Dr Thomas Scambler, and published by the author [30].

To confirm that the CFTR is expressed in M2 macrophages, we performed a simple immunofluorescent (IF) staining of the CFTR and analysed the cells by confocal microscopy (**Figure 36**). We found that the CFTR is expressed in M2 macrophages. The CFTR transmembrane protein was detected in both non-permeabilised and cells permeabilised with Triton X-100 and saponin (**Figure 36**). Permeabilised cells showed a higher degree of staining when compared to non-permeabilised cells (**Figure 36**).

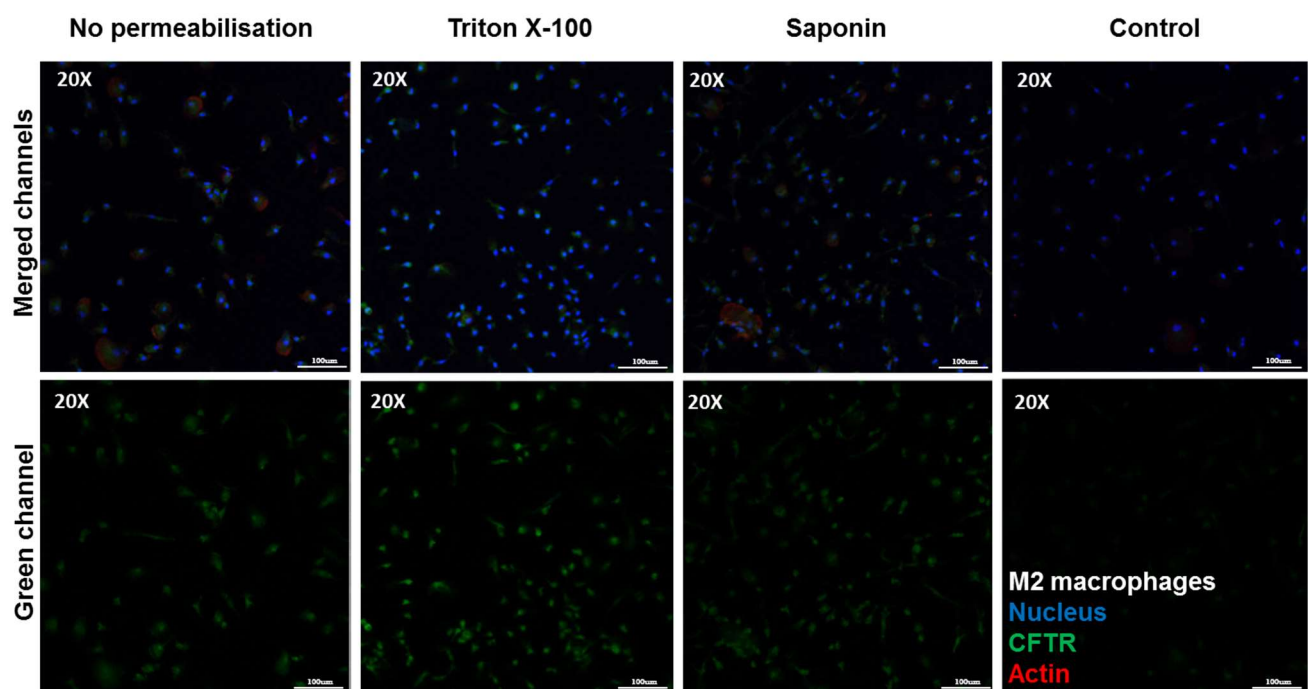


Figure 36 – CFTR expression in M2 macrophages.

CFTR expression was analysed by IF in HC M2 macrophages. All images were taken using the same parameters. Cells were left either, unpermeabilised, permeabilised with Triton X-100 or saponin. Control images show cells incubated with a CFTR isotype control antibody. The nucleus was stained with DAPI (blue), the CFTR (green) with a specific antibody and actin filaments with phalloidin staining dye (red) (bar=100 µm).

4.3.5 TNF and IL-6 are overexpressed in M1 Macrophages from CF patients

As reported in the previous section, the proportion of M2 macrophages was diminished in patients with CF. Phenotypically, M2 macrophages show an enlarged shaped (**Figure 35C**), while M1 macrophages acquire a rounded conformation (**Figure 37C**). In the case of M1 macrophages, we did not observe any significant differences in the proportion of these pro-inflammatory cells (**Figure 37A**); however, the amount of IL-6 secreted by these phagocytic cells was significantly increased in the patients with CF (**Figure 37B**). In the same manner as with the M2 macrophages, IF of the M1 macrophages was performed to confirm that the CFTR was expressed in these myeloid cells. It was confirmed that the CFTR is expressed in the classically activated macrophages, with a higher degree of staining on permeabilised cells compared to non-permeabilised (**Figure 38**).

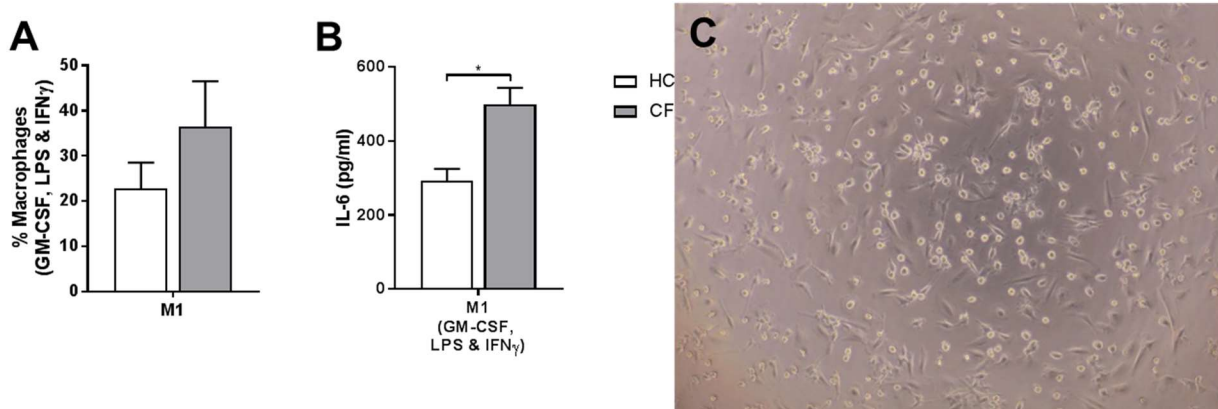


Figure 37 – Upregulation of IL-6 in M1 macrophages.

(A) Polarised M1 macrophages (GM-CSF, LPS and IFN γ) from HC volunteers (n=7) and patients with CF (n=7) are presented as percentage M1 of total macrophages measured by flow cytometry. (B) IL-6 cytokine levels from M1 polarised macrophages measured by ELISA. (C) Phenotypic picture of M1 macrophages by light microscopy (20X). All data are presented as mean \pm SEM. Statistical comparisons were performed by Mann-Whitney non-parametric test, *p < 0.05, **p < 0.01, ***p < 0.001. Part of this figure was produced by Dr Thomas Scambler and published by the author [30].

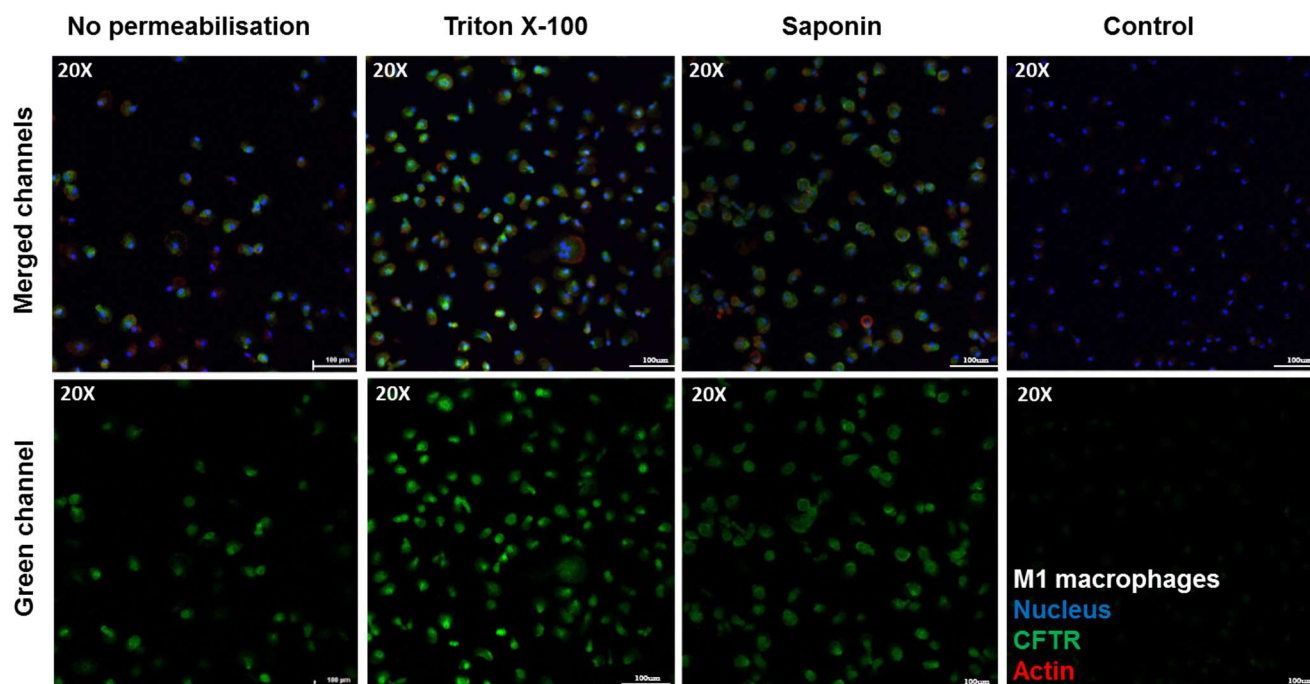


Figure 38 – CFTR expression in M1 macrophages.

CFTR expression was analysed by IF in HC M1 macrophages. All images were taken using the same parameters. Cells were left either, unpermeabilised, permeabilised with Triton X-100 or saponin. Control images were incubated with a CFTR isotype control antibody. The nucleus was stained with DAPI (blue), the CFTR (green) with a specific antibody and actin filaments with phalloidin staining dye (red) (bar=100 µm).

After confirming CFTR expression in human macrophages, we investigated whether the CFTR was also expressed in M1 macrophages from patients with CF. We observed CFTR expression in M1 macrophages from patients with CF, which was comparable to the HC macrophages (**Figure 39**). Finally, we investigated *TNF* and *IL-6* expression in M1 macrophages from both groups. *TNF* and *IL-6* expression were significantly increased in M1 macrophages, from patients with CF after 24h of activation, and subsequently after a second challenge with LPS (**Figure 40A**). In the same manner, the levels these two pro-inflammatory cytokines were still significantly increased after stimulation with Tn and Tg (**Figure 40B and C**).

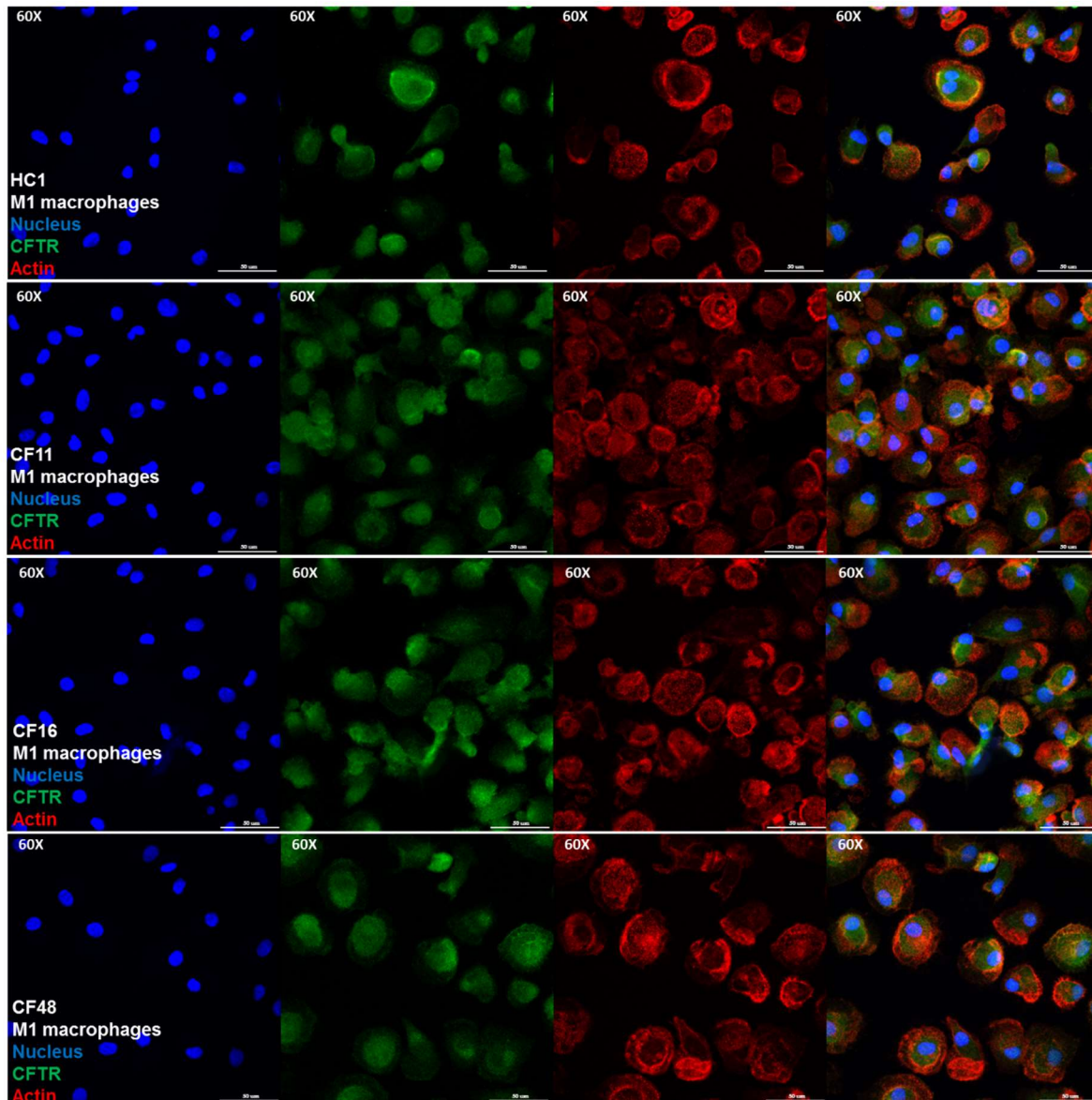


Figure 39 – CFTR expression in CF M1 macrophages.

CFTR expression was analysed by IF in M1 macrophages. All images were taken using the same parameters. HC (n=1) or CF (n=3) M1 macrophages were left either, unpermeabilised, permeabilised with Triton X-100 or saponin. Control images were incubated with a CFTR isotype control antibody. The nucleus was stained with DAPI (blue), the CFTR (green) with a specific antibody and actin filaments with phalloidin staining dye (red) (bar=50 µm).

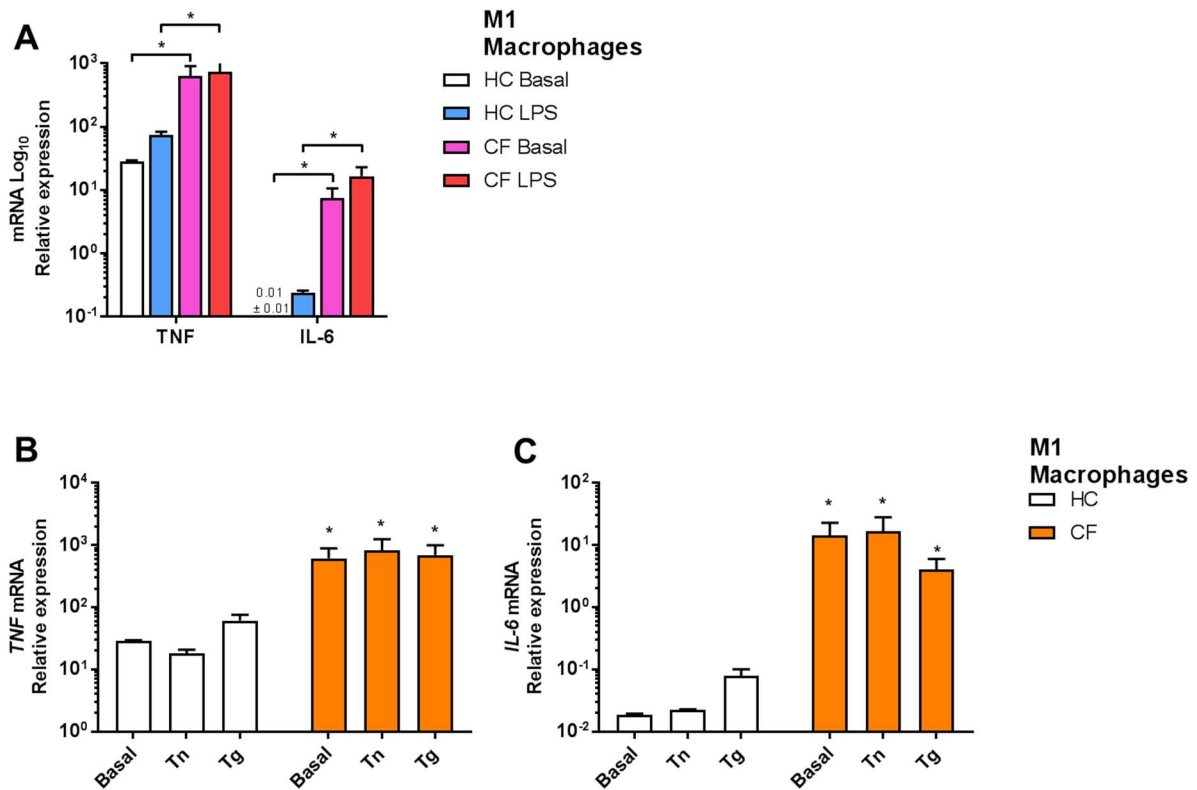


Figure 40 – Upregulation of TNF and IL-6 in CF M1 macrophages.

TNF and *IL-6* expression were measured in response to LPS (100 ng/ml) (A), after Tn (5 μ g/ml) and Tg (300 nM) (B and C) for 4 h in M1 macrophages from HC (n=9) and patients with CF (n=9). All data are presented as mean \pm SEM and mRNA data represented by logarithmic scale base 10. Statistical comparisons were performed by unpaired independent Student's t-test. * $p < 0.05$, ** $p < 0.01$, and *** $p < 0.001$. Some of these data have been published by the author [30].

4.3.6 IRE1 α inhibition reduces TNF and IL-6 in CF M1 Macrophages

M1 macrophages from patients with CF were not proportionally different from the macrophages from HC volunteers; however, the levels of TNF and IL-6 were still significantly higher in the former group (**Figure 37**). High levels of XBP1s have been observed in other disorders, such as TRAPS and RA, in association with an increased expression of pro-inflammatory cytokines, as mentioned above. Therefore, we used two different IRE1 α inhibitors to test this hypothesis in the M1 macrophages. Inhibition of the RNase domain of IRE1 α with 4 μ 8c and MKC-3946 did not affect the polarisation ratios of M1 macrophages in either the HC or in the CF group (**Figure 41A**). To confirm that the two inhibitors reduced the inflammation produced by the M1 macrophages, we measured IL-6 and TNF at the transcriptional and protein level. As seen before, the 4 μ 8c and MKC-3946 inhibitors showed their strong suppressive effects on *XBP1s* (**Figure 41B**). Inhibition of the IRE1 α -XBP1 pathway led to a reduction of *IL-6*, but not TNF in M1 macrophages from patients with CF (**Figure 41B**). Similarly, as observed with the transcription levels, the two inhibitors significantly reduced the higher levels of IL-6 produced by M1 macrophages from patients with CF (**Figure 41C**). While TNF was not reduced at the transcriptional level, both inhibitors displayed a significant effect at reducing the cytokine levels of TNF (**Figure 41D**). Altogether, these results validate that the IRE1 α -XBP1 pathway is associated with the higher expression of TNF and IL-6 in M1 macrophages from patients with CF.

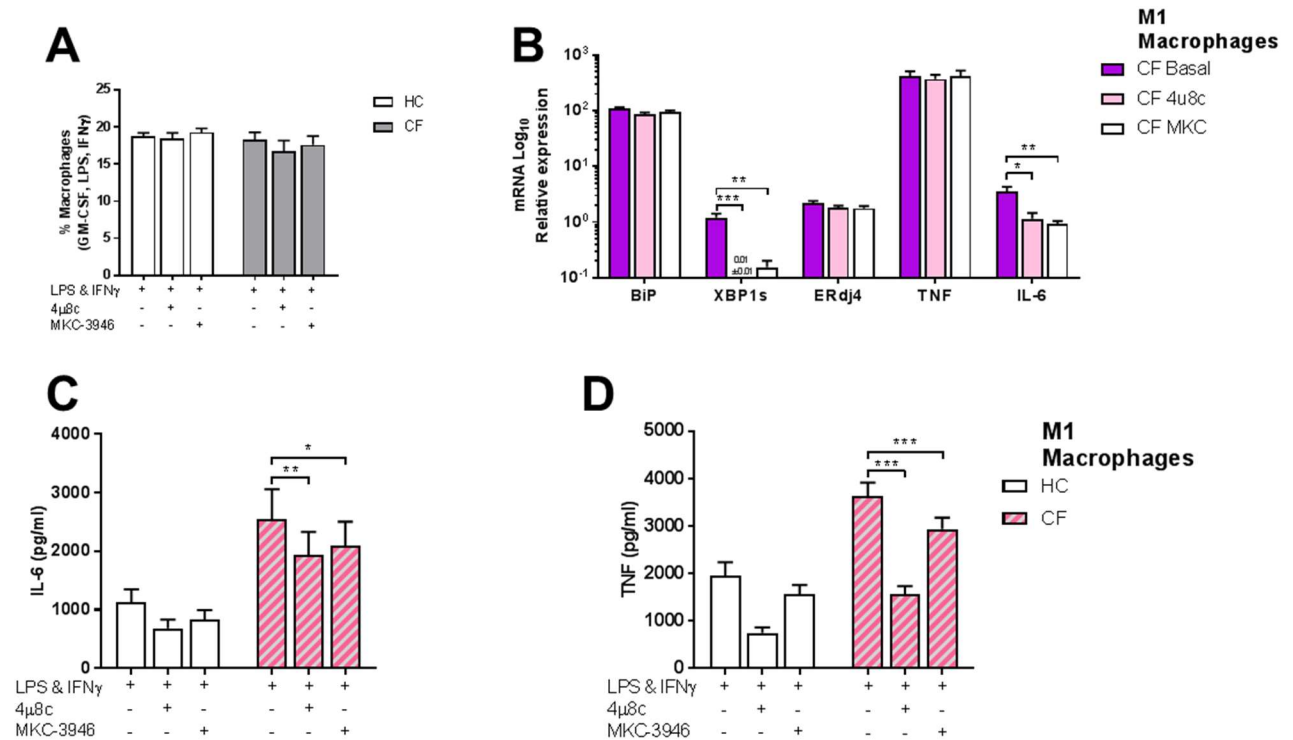


Figure 41 – IRE1 α inhibition reduces TNF and IL-6 secretion in CF M1 macrophages.

The IRE1 inhibitors 4 μ 8c (50 μ M) and MKC-3946 (10 μ M) were used 30 min before M1 macrophages activation. (A) Polarised M1 macrophages from HC volunteers (n=9) and patients with CF (n=9) are presented as percentage M1 of total macrophages measured by flow cytometry. (B) *BiP*, *XBP1s*, *ERdj4*, *TNF*, and *IL-6* mRNA relative expression were quantified in M1 macrophages from HC volunteers (n=6) and patients with CF (n=6). (C and D) IL-6 and TNF cytokine levels in M1 macrophages measured by ELISA, HC volunteers (n=6) and patients with CF (n=6). All data are presented as mean \pm SEM. Data in panel B are represented by logarithmic scale base 10. Statistical comparisons were performed by paired Student's t-test, *p < 0.05, **p < 0.01, ***p < 0.001. These data have been published by the author [30].

4.4 Discussion

Inflammation is a natural physiological process elicited by several cells in the human body. The main goal of the inflammatory response is to recruit other types of cells to the site of inflammation, mostly immune cells, in order to recover the tissue homeostasis. We have demonstrated that the proportion of the anti-inflammatory macrophages, M2, in patients with CF is lower when compared to HC volunteers. While the proportion of M1 macrophages was not affected, the amount of IL-6 and TNF was certainly increased in patients with CF. These imbalances in the proportion of macrophages and the excessive amounts of inflammatory cytokines produced, help to explain the chronic and excessive inflammation seen in patients with CF. This abnormal response is not only seen in M1 macrophages with CFTR mutations, but also in CF HBECs. While the basal levels of *IL-6* mRNA were significantly increased in all CF HBECs, stimulation of these cells with LPS, Tn and Tg showed varying results, regarding the IB3-1 cell line. Stimulation of the IB3-1 cell line with LPS did not induce the upregulation in *IL-6*. Tn reduced the amount of *IL-6* transcription, not only in the IB3-1 cell line but also in the WT control cell line. Tg showed a consistent increasing effect on all HBECs. The CuFi-1 and CuFi-4 CF cell lines showed consistently higher levels of IL-6 when compared to the WT cell line. Furthermore, the higher levels of IL-6 were reduced by the addition of the IRE1 α inhibitor, in both the WT and the CuFi-1 cell lines. These findings suggest that the increased activity of IRE1 α led to increased levels of IL-6 which can be reduced by inhibition of IRE1 α . While no significant differences were recorded neither in lymphocytes nor in neutrophils, this is understandable, as these cells are not notable producers of these two cytokines. Monocytes from patients with CF showed increased levels of TNF after

LPS stimulation, while the levels of IL-6 were not affected. Culture of these cells with either Tn or Tg did not elicit a significant response, regarding these two pro-inflammatory cytokines. As already mentioned, the polarisation ratios were not different in patients with CF, regarding M1 macrophages; however, the excessive amounts of TNF and IL-6 were reduced by blocking the RNase domain of IRE1 α . The reduction in these two pro-inflammatory cytokines were associated with a reduction in *XBP1s*, with no difference in the polarisation ratios of the M1 macrophages. These findings suggest that an overactive IRE1 α -XBP1 pathway is responsible for the excessive amount of TNF and IL-6 produced by M1 macrophage in patients with CF. The abnormal levels of pro-inflammatory cytokines may be responsible for the lung damage and the decreased respiratory capacity observed in patients with CF. Moreover, this may help to explain the pancreatic inflammation seen in patients with CF-related diabetes. While certain discrepancies exist in whether the CFTR is expressed by immune cells, we observed CFTR expression in both M1 and M2 macrophages. The degree of CFTR staining was increased after permeabilisation of the macrophages. These differences could be due to increased contact of the CFTR specific antibody with the transmembrane channel, or due to the expression of the CFTR in cellular organelles. In summary, it was demonstrated that the levels of TNF and IL-6 were significantly increased, mainly in M1 macrophages from patients with CF. Furthermore, the excessive levels of these two pro-inflammatory cytokines were driven by an overactive IRE1 α -XBP1 pathway.

Chapter 5 – Metabolism in Cells with CF Mutations and the Effects of IRE1 α Inhibition

5.1 Introduction

Metabolism plays a vital role during different cellular processes, and it is crucial during cellular differentiation and activation, particularly in immune cells [183]. In fact, the UPR has been linked with immunometabolism and dysregulation of the UPR has been reported to be in a number of different diseases [30, 140, 210]. Furthermore, the IRE1 α -XBP1 pathway of the UPR has been shown to be involved in the regulation of metabolic pathways involving immune cells [140]. Since XBP1s has been shown to be significantly upregulated in M1 macrophages from patients with CF, we hypothesised that these increased levels of XBP1s might play an essential role in the regulation of metabolism in these pro-inflammatory cells. Moreover, based on some preliminary data, generated by our group, showing increased levels of extracellular acidification rate (ECAR) and oxygen consumption rate (OCR) in monocytes, expansion these findings was sought by investigating immunometabolism in monocyte and macrophage from patients with CF. Frequently, patients with CF receive a high caloric diet to compensate for the lack of nutrients, mostly due to malabsorption in the gut. Malabsorption is both a consequence of pancreatic dysfunction and small intestinal pathology in CF, which leads to malnutrition and weight loss. It was investigated whether monocytes and macrophages showed alterations and abnormalities in metabolism, which could be associated with the increased energy demands in patients with CFTR mutations.

5.2 Methods

5.2.1 Cellular ROS detection in HBECs and M1 macrophages

For detection of ROS in the HBEC lines, the following steps were followed; BEAS-2B and CuFi-1 cells were detached from the flasks, as previously described in the main methods section, washed 2 times with DBPS and seeded into 96 well plates, with a clear flat bottom and black sides, at a concentration of 2.5×10^4 cells per well and left overnight to allow the attachment of the cells. The next day, cells were washed once with the buffer provided and stained using 25 μ l of DCFDA, diluted in the buffer provided, and left for 45 min in the incubator at 37°C. After the incubation period, cells were washed once with the washing buffer and stimulated for 4 h in the incubator. Levels of ROS were measured after the stimulation, as described in the main methods section. A total of 3 to 4 technical replicates were used per stimulation.

The same protocol used for M1 macrophages as for the cell lines, with the following modifications. M0 macrophages were grown for 6 days, as per the M1 macrophage protocol, described above. Before activation, macrophages were detached from the wells and seeded into 96 well plates with a clear flat bottom and black sides at a concentration of 3.0×10^4 cells per well and activated with LPS/IFN γ for 24 h. The next day, cells were washed once with the buffer provided and stained using 25 μ l of DCFDA, diluted in the buffer provided, and left for 45 min in the incubator at 37°C. After the incubation period, cells were washed once with the washing buffer and stimulated for 4 h in the incubator. The detection of ROS was measured as described before after the stimulation. A total of 3 to 4 technical replicates were used per stimulation.

5.2.2 Mitochondrial ROS (mitoSOX) detection

Mitochondrial ROS (mROS) were detected using MitoSOX, following the manufacturer's recommendation. Briefly, 13 μ l of sterile DMSO was incorporated into one vial of MitoSOX (to make 5 mM MitoSOX solution), and dissolved into DPBS 1/1000 to a final concentration of 5 μ M MitoSOX reagent working solution. Then HBECs were detached, counted and transferred into FACS tubes at 0.5×10^6 cells per tube. Cells were stimulated with 50ng of LPS for 4 h, then the media was removed, and the cells were washed with PBS. 5 μ M MitoSOX reagent working solution was added into the tubes, 500 μ l of the mix, and incubate at 37°C for 10 minutes. Then the cells were washed 2 times with DPBS supplemented with 2% FBS. Finally, the cells were resuspended in BSB and run the cells through the flow cytometer.

5.2.3 Glycolytic and mitochondrial assays

The glycolytic assays were done using the following protocol, as previously published [30]. Negatively isolated monocytes were seeded into a density of 1.0×10^5 in XF96 cell-culture microplates previously coated with CellTak (Corning), according to the manufacturer's instructions, and wait for 1 h for cellular adherence. Immediately after, the levels of ECAR and OCR were measured on an XFe96 Extracellular Flux Analyzer (Agilent). For the experiments involving M1 macrophages, cells were grown as described in the M1/M2 macrophage polarization section; on day 6, the cells were detached, using Accutase (Thermo Fisher Scientific), and seeded at a density of 3.0×10^4 in XF96 cell-culture microplates. The inhibitory effects of 4 μ 8c 50 μ M (Merck) and MKC-3946 10 μ M (Cayman Chemical) were examined by pre-treating macrophages 30 min before the addition of LPS and IFN γ , and then the cells were cultured for a further 24 h in complete RPMI medium for full activation. After activation, the

supernatants were collected for cytokine detection, the cells were washed twice and media changed to Agilent Seahorse XF base medium containing 10 mM Glucose (only for the Mito Stress Kit), 2 mM L-glutamine, 1 mM sodium pyruvate, and 1 mM HEPES. ECAR and OCR measurements were analysed on an XFe96 Extracellular Flux Analyzer (Agilent). Once basal ECAR and OCR measurements were obtained, ECAR changes in response to glucose (10 mM) were recorded, oligomycin (1 μ M), 2-Deoxy-D-glucose (2-DG, 50 mM), following the instructions outlined in the XF Cell Glycolysis Stress Test Kit (Agilent), or stimulated with oligomycin (1 μ M), FCCP (1 μ M), and rotenone/antimycin A (0.5 μ M) following the instructions stated in the XF Cell Mito Stress Test Kit (Agilent).

5.3 Results

5.3.1 Increased ROS and mitochondrial ROS in CF HBECs

HBECs with CF mutations showed an altered inflammatory profile, with activation of the UPR and high levels of XBP1s being observed. The UPR is a complex mechanism that can be activated in response to several stimuli [129, 211, 212]. ROS are naturally formed during oxygen metabolism, producing superoxide (O_2^-), which is normally the first step in the formation of other types of ROS [213]. When active, the UPR has been shown to induce the formation of ROS, and this interplay is associated with the production of inflammatory cytokines [152, 214, 215]. This link between UPR and ROS formation made us speculate that cells with CFTR mutations have increased levels of ROS, with potential implications for the inflammatory response. Under basal conditions, the CuFi-1 cell line showed increased levels of ROS when compared to the WT HBEC line (**Figure 42A**). These heightened levels produced by the CF cell line were further significantly increased upon stimulation with LPS and Tg (**Figure 42A**). Incubation of the CuFi-1 cell line with the natural antioxidant glutathione (GSH), led to a significant reduction in the levels of ROS (**Figure 42A**). Moreover, not only the levels of ROS were altered in the CuFi-1 cell line, but also the basal levels of mitochondrial ROS (mROS) were significantly increased (**Figure 42B**). In summary, we confirmed that the levels of ROS and mROS were elevated in cells with CFTR mutations. Furthermore, these increased levels of ROS and mROS may be associated with the high levels of pro-inflammatory cytokines and XBP1s production by these cells.

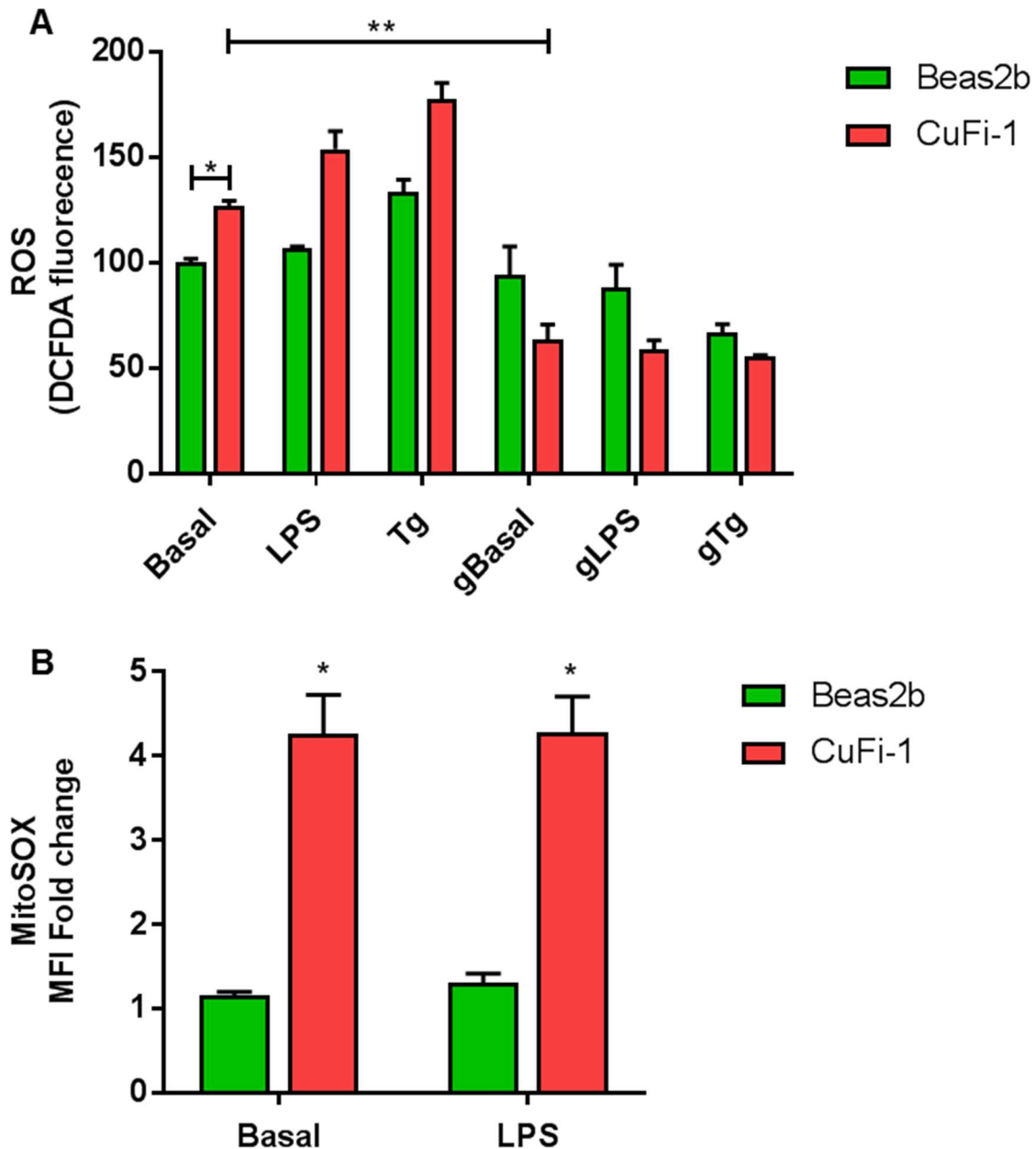


Figure 42 – Increased levels of ROS and mROS in CF HBECs

The levels of ROS and mROS were measured in the two HBECs, BEAS-2B (WT) and CuFi-1 ($\Delta F508/\Delta F508$). The levels of ROS were measured under basal condition or upon stimulation of LPS (100 ng/ml) and Tg (300 nM) for 4 h. When mentioned, the antioxidant glutathione (GSH) was included in the culture media at a concentration of 5mM. gBasal, gLPS and gTg represent conditions where 5 mM glutathione was present in the culture media. All data are presented as mean \pm SEM. Statistical significance was determined by using unpaired or paired Student's t-test. * $p < 0.05$, ** $p < 0.01$, *** $p < 0.001$. $n=4$ biological replicates for all cell lines.

5.3.2 Increased ROS in CF M1 macrophages

The increased levels of ROS and mROS in the CF HBECs led us to investigate whether macrophages from CF patients showed an increased production of ROS. As previously shown, M1 macrophages from CF patients showed significantly higher levels of IL-6 and TNF that were associated with the higher expression of XBP1s. The amount of ROS that were formed in the M1 macrophages from CF patients was significantly higher when compared to HC volunteers (**Figure 43**); however, upon stimulation with LPS, the significantly higher levels of ROS observed in the CF M1 macrophages were lost (**Figure 43**).

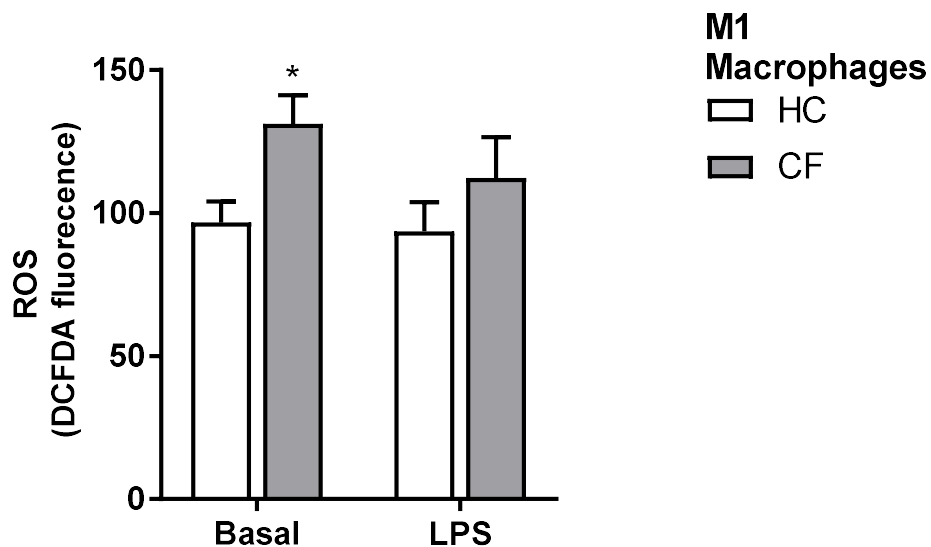


Figure 43 – Increased levels of ROS in CF M1 macrophages

The levels of ROS were measured in fully polarised M1 macrophages from HC volunteers (n=5) and patients with CF (n=5). The levels of ROS were measured under basal condition or upon stimulation of LPS (100 ng/ml). All data are presented as mean \pm SEM. Statistical significance was determined by using unpaired Student's t-test. *p < 0.05, **p < 0.01, ***p < 0.001.

5.3.3 Heightened glycolytic rate and mitochondrial flux in CF monocytes

Next, we investigated metabolism in monocytes and macrophages from HC volunteers and patients with CF, by using the Seahorse XFe96 Analyzer. Through the utilisation of this instrument, we can assess the glycolytic rates by measuring the ECAR, and the mitochondrial flux by measuring OCR. Under basal conditions, monocytes from CF patients presented higher levels of ECAR when compared to the HC volunteers, with no significant difference in OCR (**Figure 44A and B**). CF monocytes, stimulated with LPS, showed significantly higher levels of both ECAR and OCR (**Figure 44A and B**). These findings suggest that monocytes with CFTR mutations utilise oxygen more rapidly only when exposed to a bacterial challenge. The process of converting glucose to pyruvate, better known as glycolysis, can be measured by the addition of glucose to the medium culture (**Figure 45**). Furthermore, the glycolytic capacity of the cells can also be measured by the addition of oligomycin, which effectively stops oxidative phosphorylation (OxPhos) and switches metabolism towards glycolysis. Similarly, the glycolytic reserve of the monocytes can be measured by the addition of 2-deoxy-glucose (2-DG), a glucose analogue that inhibits glycolysis (**Figure 45**). While the ECAR basal levels were significantly higher in the CF monocytes, glycolysis was not shown to be altered (**Figure 44C and D**); conversely, the glycolytic capacity and reserve of the monocytes from CF patients were significantly higher (**Figure 44C and D**). Altogether, monocytes from CF patients have an altered glycolytic function with higher ECAR levels and increased glycolytic capacity and reserve.

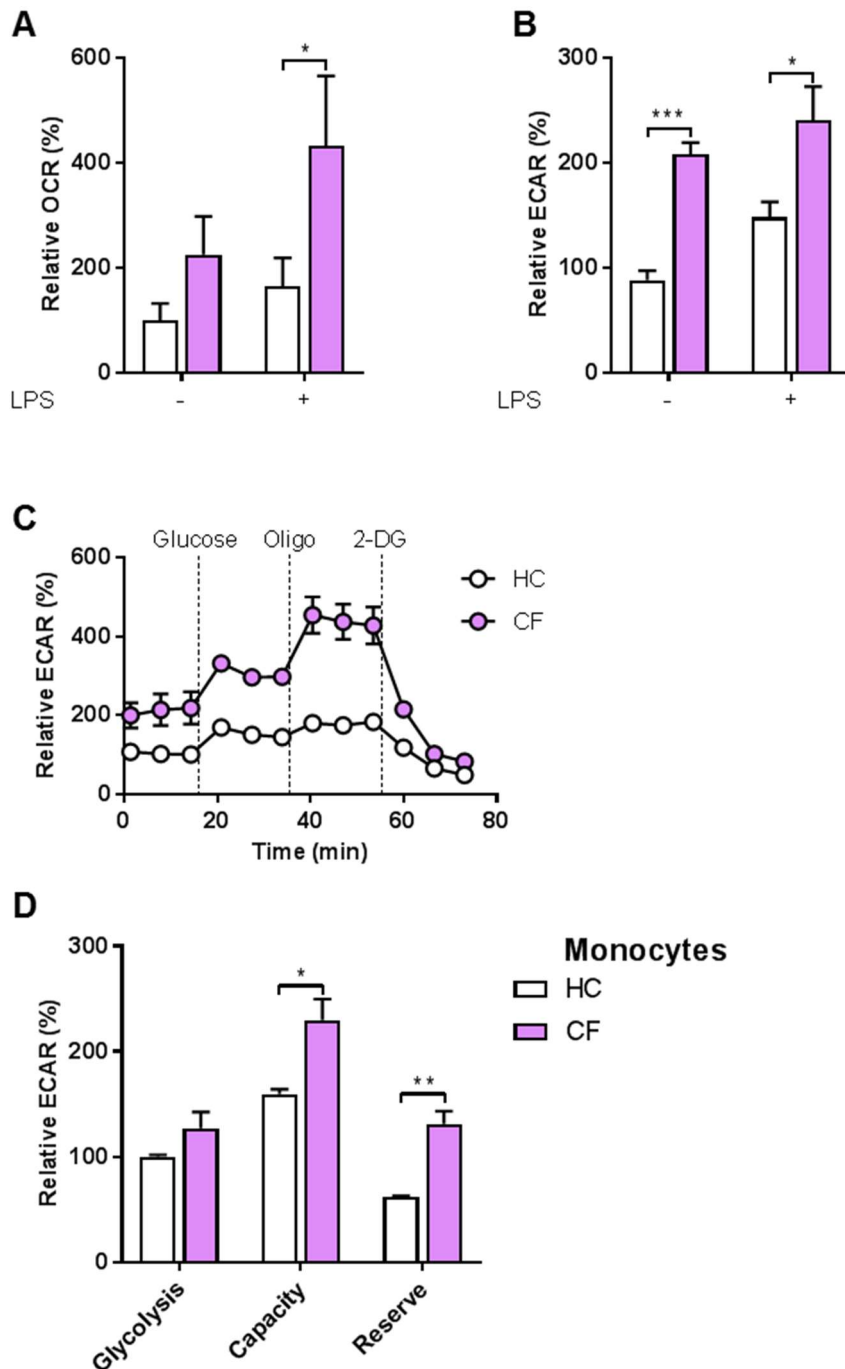


Figure 44 – Increased mitochondrial flux and glycolytic rates in CF monocytes.

ECAR and OCR of monocytes stimulated with glucose (10 mM), oligomycin (1 μ M), and 2-Deoxy-D-glucose (2-DG, 50 mM). (A–D) Measurement of relative OCR (A) or ECAR (B) in monocytes from HC volunteers (n=7) and patients with CF (n=7) under basal conditions and stimulated with LPS (10 ng/ml) for 4 h. The Levels of glycolysis, glycolytic capacity and reserve were measured (C and D). Glycolysis, glycolytic capacity, and reserve were calculated as described in the methods. All data is presented as mean \pm SEM. Statistical comparisons were performed by unpaired Student's t-test, *p < 0.05, **p < 0.01, ***p < 0.001. These data have been published by the author [30].

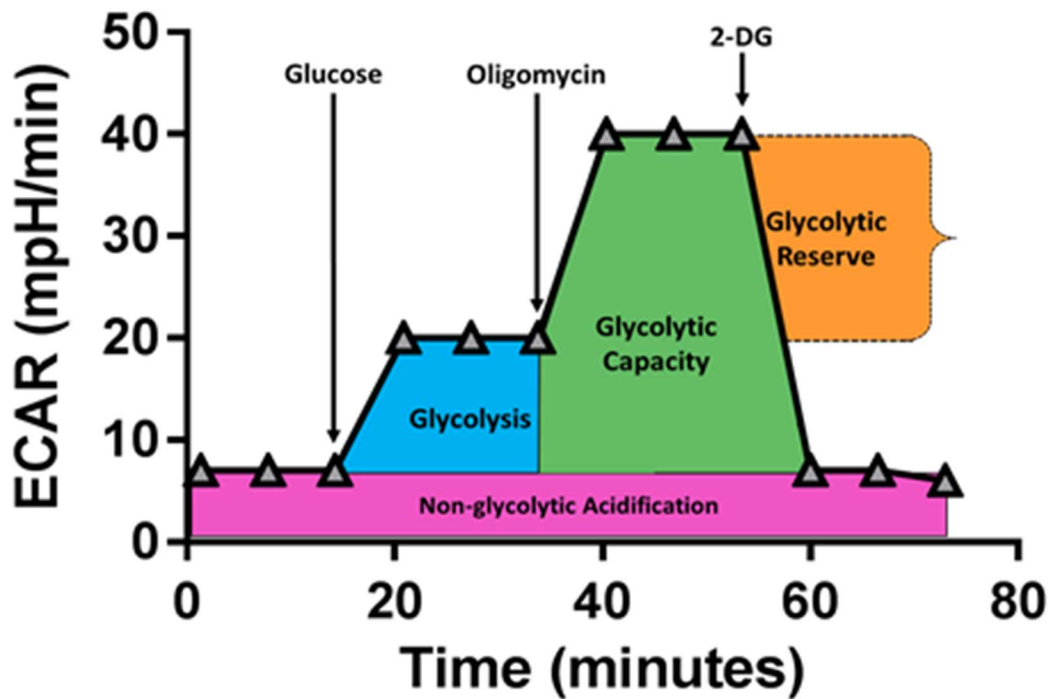


Figure 45 – Glycolytic function

The measurement of Glycolysis, glycolytic capacity and reserve were measured as follow: sequential application of glucose (Glu) oligomycin (Oligo) and 2-deoxy-glucose (2-DG) were carried to dissect basal ECAR, glycolysis, glycolytic capacity, and glycolytic reserve.

5.3.4 Heightened mitochondrial flux and glycolytic rate in CF M1 macrophages

After finding that monocytes with CFTR mutations had altered ECAR and OCR, we sought to investigate the metabolic profile of M1 macrophages, as these cells are metabolically more active. CF M1 macrophages showed increased levels of ECAR and OCR as compared to the HC M1 macrophages (**Figure 46A and B**). Differently than monocytes, M1 macrophages from CF patients showed these raised ECAR and OCR levels before and after polarisation of the cells with LPS/IFN γ (**Figure 46A and B**). The sequential stimulation of the macrophages with glucose, oligomycin and 2-DG, revealed an increased glycolytic capacity and reserve in the M1 macrophages from patients with CF, as also seen in the CF monocytes (**Figure 46C and D**). Interestingly, glycolysis was not shown to be altered. Following on from these findings, we analysed the mRNA expression of some important metabolic enzymes involved in glycolysis and mitochondrial function; hexokinase 2 (HK2), pyruvate dehydrogenase kinase 4 (PDK4), 6-phosphofructo-2-kinase/fructose-2,6-biphosphatase (PFKFB1), oestrogen-related receptor alpha 1 (ESRRA), peroxisome proliferator-activated receptor alpha (PPARA), and uncoupling protein 3 (UCP3). The expression of *PDK4*, *PFKFB1*, *ESRRA* and *UCP3* were not shown to be altered in the M1 macrophages (**Figure 47**); however, the mRNA levels of *HK2* and *PPARA* were shown to be significantly downregulated in the CF M1 macrophages, compared to the HC (**Figure 47**). These findings suggest that the metabolic profile of M1 macrophages with CFTR mutations is altered, showing high ECAR and OCR with no change in glycolysis, but with a significant increase in the glycolytic capacity and reserve.

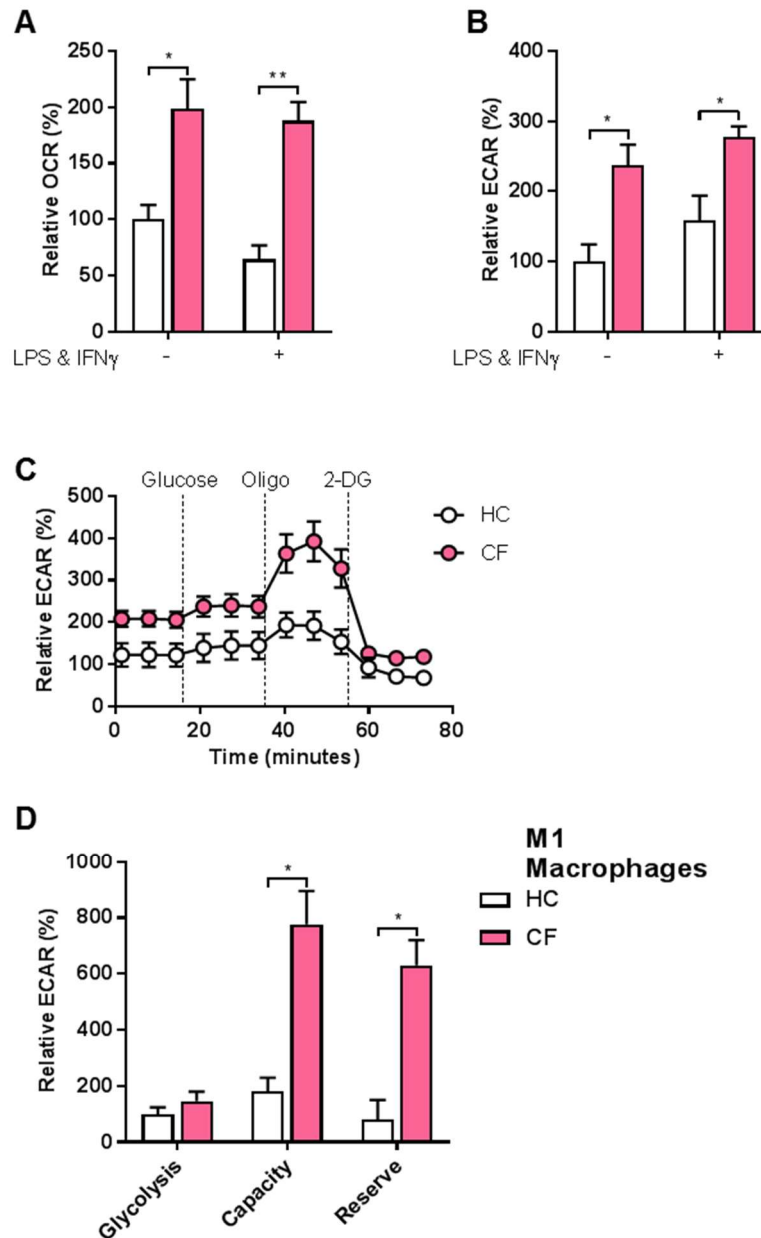


Figure 46 – Increased mitochondrial flux and glycolytic rates in CF M1 macrophages.

ECAR and OCR of M1 macrophages stimulated with glucose (10 mM), oligomycin (1 μ M), and 2-Deoxy-D-glucose (2-DG, 50 mM). (A–D) Measurement of relative OCR (A) or ECAR (B) in M1 macrophages from HC volunteers (n=7) and patients with CF (n=7) under basal conditions and stimulated with LPS/IFN γ . The Levels of glycolysis, glycolytic capacity and reserve were measured (C, D). Glycolysis, glycolytic capacity, and reserve were calculated as described in the methods. All data are presented as mean \pm SEM. Statistical comparisons were performed by unpaired Student's t-test, *p < 0.05, **p < 0.01, ***p < 0.001. These data have been published by the author [30].

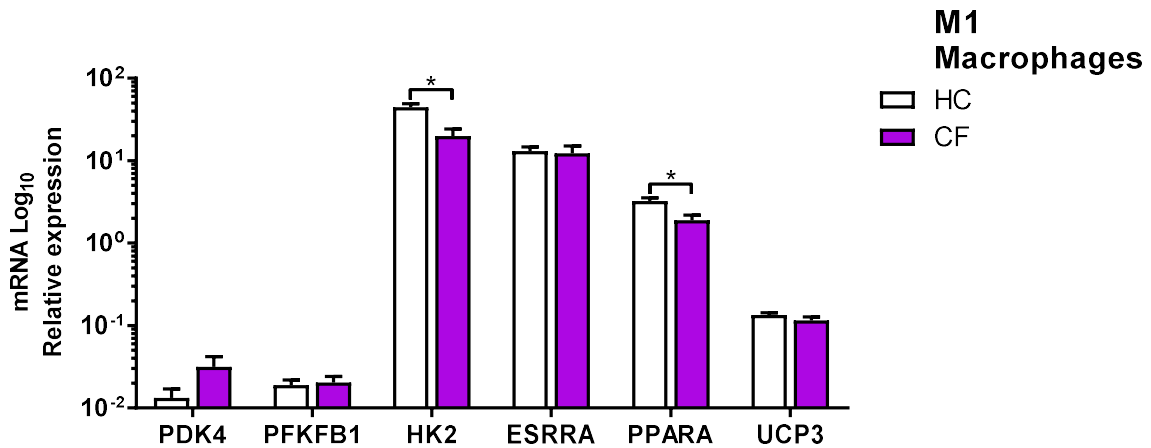


Figure 47 – mRNA expression of metabolic enzymes in M1 macrophages.

The relative mRNA expression of *PDK4*, *PFKB1*, *HK2*, *ESRRA*, *PPARA*, and *UCP3* were measured in M1 macrophages from HC volunteers (n=5) and patients with CF (n=5). All data are presented as mean ± SEM and mRNA data represented by logarithmic scale base 10. Statistical comparisons were performed by unpaired independent Student's t-test. *p < 0.05, **p < 0.01, and ***p < 0.001. These data have been published by the author [30].

5.3.5 IRE1 α inhibition recovers the heightened glycolytic rate and mitochondrial flux

Glycolysis is the first obligated pathway to convert glucose into pyruvate. Followed by this process, pyruvate enters the Krebs cycle to be converted into ATP within the electron transport chain. As shown before, both the ECAR and OCR were elevated in M1 macrophages from CF patients; therefore, it was sought to evaluate mitochondrial flux, including the maximal respiration, reserve respiratory capacity and ATP production in M1 macrophages. These parameters can be evaluated by the sequential addition of oligomycin, carbonyl cyanide-4-phenylhydrazone (FCCP) and rotenone/antimycin A (**Figure 48**). The ECAR and OCR levels were significantly elevated in the M1 macrophages from CF patients (**Figure 49A-C**). Furthermore, while not significantly different, the maximal respiration and reserve respiratory capacity of CF M1 macrophages were elevated (**Figure 49D**). In contrast, the ATP production was shown to be significantly higher in the M1 macrophages from CF patients, when compared to HC volunteers (**Figure 49D**). As XBP1s was shown to be significantly elevated in the CF M1 macrophages, we next evaluated whether inhibition of IRE1 α , with 4 μ 8c and MKC-3946, would have an impact in the raised ECAR and OCR levels. Inhibition of the IRE1 α -XBP1 signalling pathway significantly decreased the heightened ECAR and OCR levels seen in the M1 macrophages from patients with CF (**Figure 49A and B**). Furthermore, both inhibitors significantly reduced the heightened basal respiration, maximal respiration, reserve respiratory capacity and ATP production in the CF M1 macrophages to a level which was comparable to the HC M1 macrophages (**Figure 49D**). In summary, inhibition of the IRE1 α -XBP1 signalling pathway decreases the hyper-metabolic state seen in M1 macrophages from patients with CF.

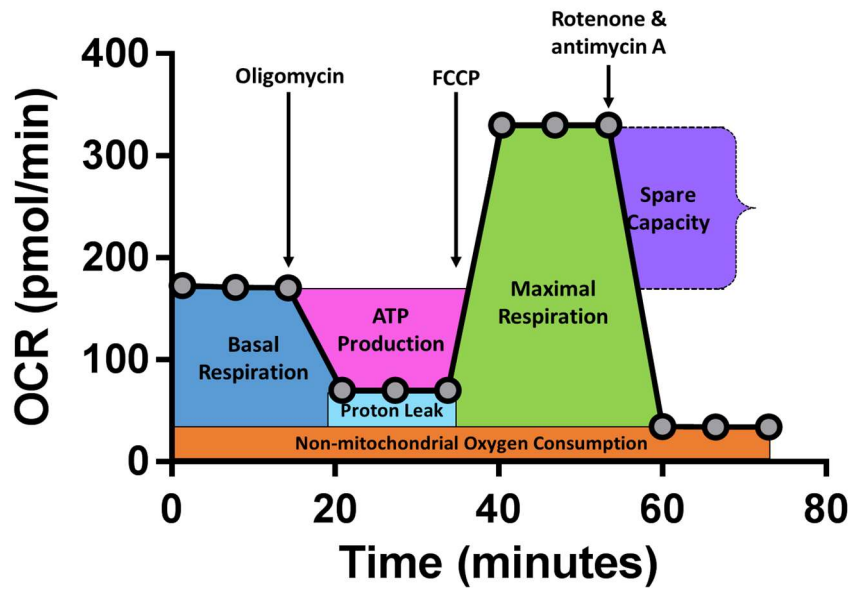


Figure 48– Mitochondrial function

The measurement of basal respiration, ATP production, proton leak, maximal respiration and spare respiratory capacity were measured as follows: sequential addition of oligomycin (Oligo), carbonyl cyanide-4-phenylhydrazone (FCCP) and rotenone/antimycin A were carried to dissect the parameters previously mentioned.

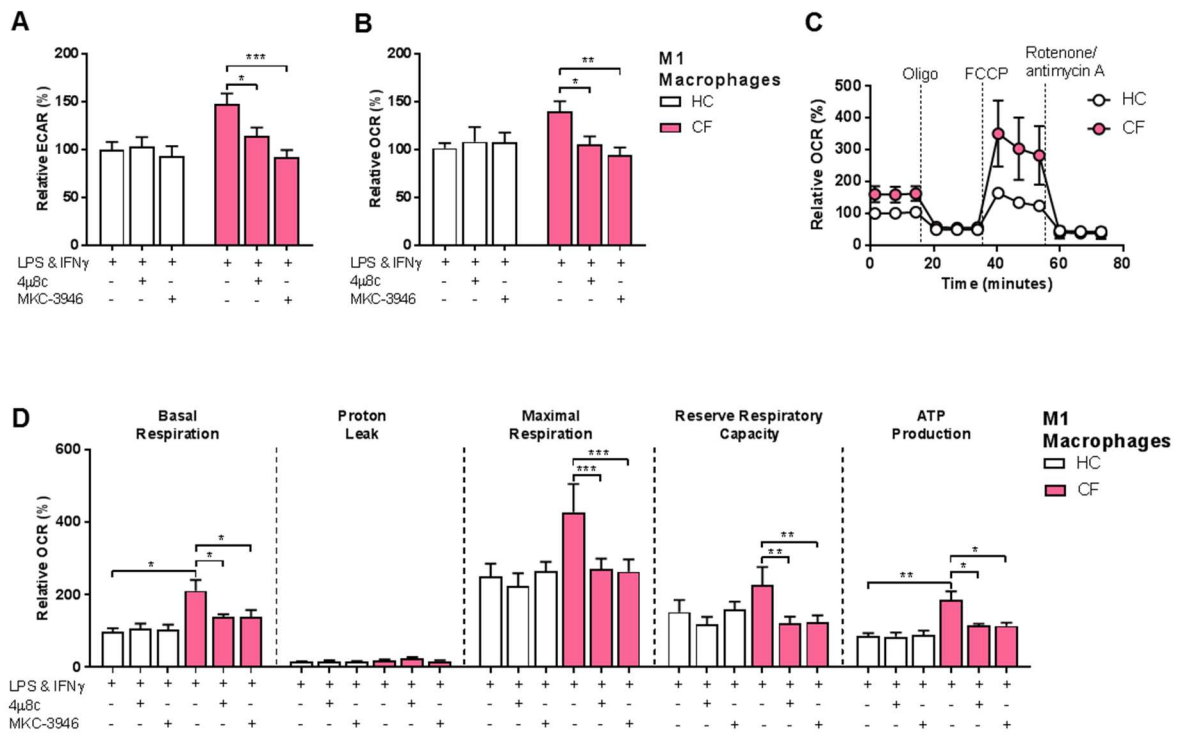


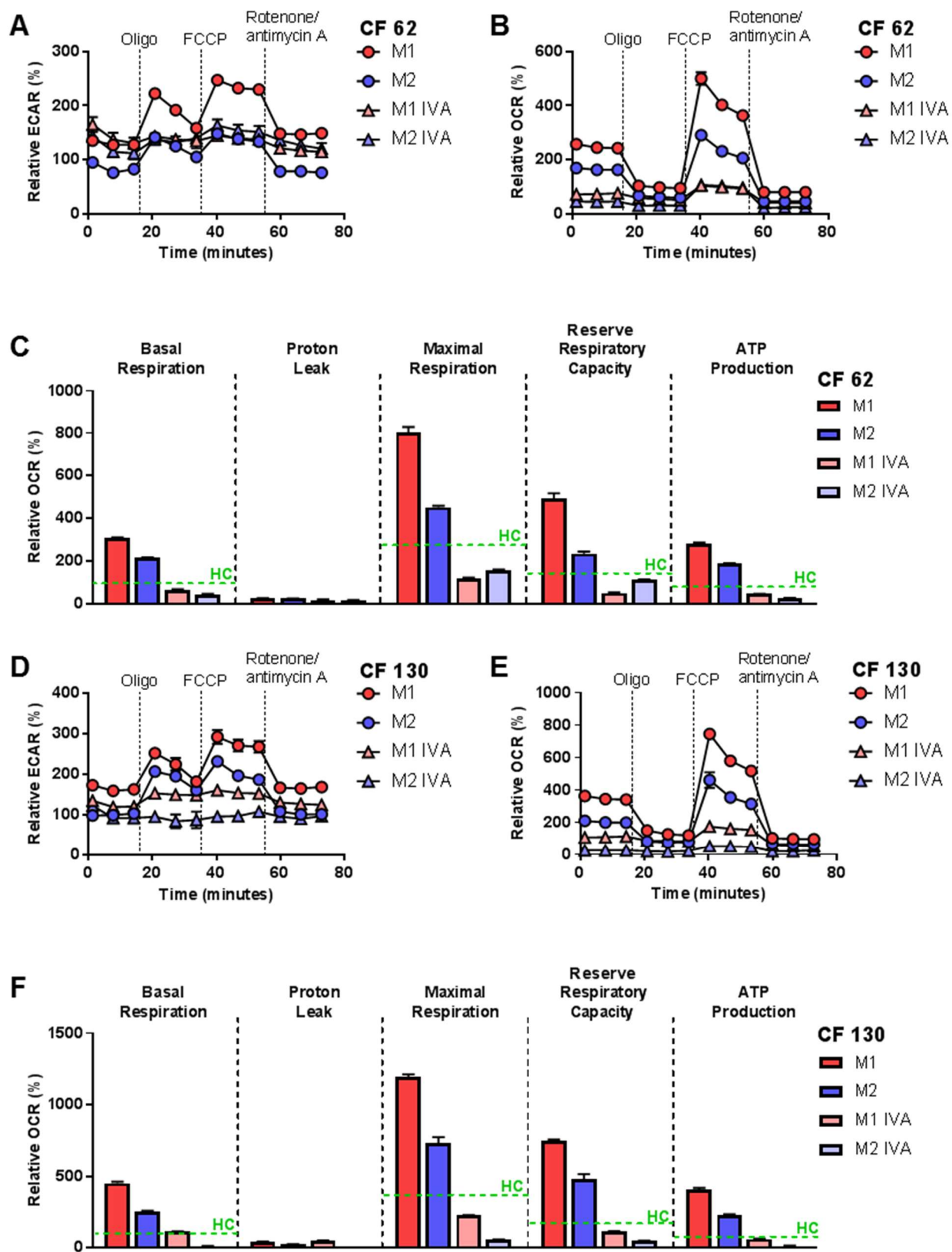
Figure 49 – The IRE1 α -XBP1 pathway regulates metabolism in CF M1 macrophages.

(A-C) ECAR and OCR levels were measured in M1 macrophages from HC volunteers (n=9) and patients with CF (n=9). Cells were stimulated with oligomycin (1 μ M), FCCP (1 μ M), and rotenone/antimycin A (0.5 μ M). When mentioned, the IRE1 α inhibitors 4 μ 8c (50 μ M) and MKC-3946 (10 μ M) were administered 30 min before M1 macrophages polarisation. (C and D) Basal respiration, proton leak, maximal respiration, reserve capacity, and ATP production. All the values were calculated as described in the methods. All data are presented as mean \pm SEM. Statistical comparisons were performed by paired or unpaired Student's t-test, *p < 0.05, **p < 0.01, ***p < 0.001. These data have been published by the author [30].

5.3.6 Ivacaftor reduces OCR levels in CF macrophages with class III mutations

Ivacaftor is regularly used in the clinic to treat patients with CF, with at least one copy of the class III mutation, the most common being G551D mutation. Ivacaftor has been shown to be effective in reducing sweat chloride levels and increasing the %FEV in this cohort of patients [216]. More recently, it has been shown that levels of the pro-inflammatory cytokines, IL-1 β and IL-18, are increased in patients with CF [209, 217]. Furthermore, we have recent evidence to demonstrate that patients with CF, Δ F508/ Δ F508, treated with Orkambi for an initial time course of 3 months showed a significant reduction in the levels of IL-18 but not IL-1 β (In press); whereas, patients receiving tezacaftor and ivacaftor treatment showed a significant reduction in the levels of both cytokines, IL-1 β and IL-18 (In press). Taking into consideration all these data and the fact that M1 macrophages from patients with CF were shown to be hyper-metabolic and inflammatory, it was then examined whether Ivacaftor reduced the increased OCR levels present in macrophages with CFTR mutations. CF M1 macrophages, with at least one copy of the G551D mutation, were treated with Ivacaftor every 48 hours, for the time course of the macrophage differentiation process, described in the main methods section. All M1 macrophages treated with Ivacaftor showed a reduction in OCR levels at, basal respiration, maximal respiration, reserve respiratory capacity and ATP production (**Figure 50**). The reduction in the OCR levels observed in the CF M1 macrophages treated with Ivacaftor was comparable to the levels shown by the HC M1 macrophages (**Figure 50**). We also observed that M2 macrophages were metabolically less active when compared to M1 macrophages. CF M2 macrophages treated with Ivacaftor showed a similar reduction in OCR levels, as seen in the M1 macrophages (**Figure 50**). Overall, these data

suggest that Ivacaftor has a significant impact on the metabolic state of CF macrophages.



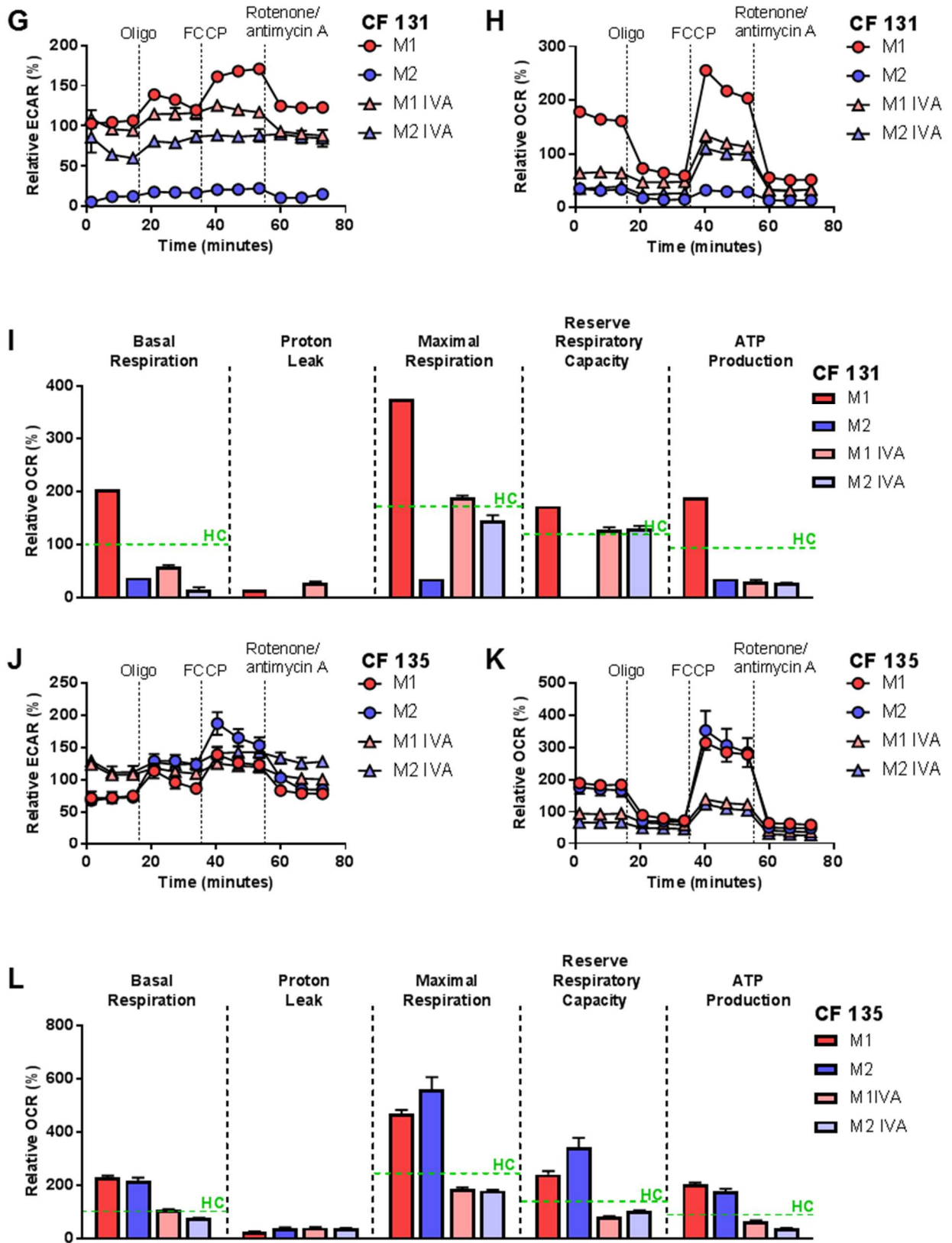
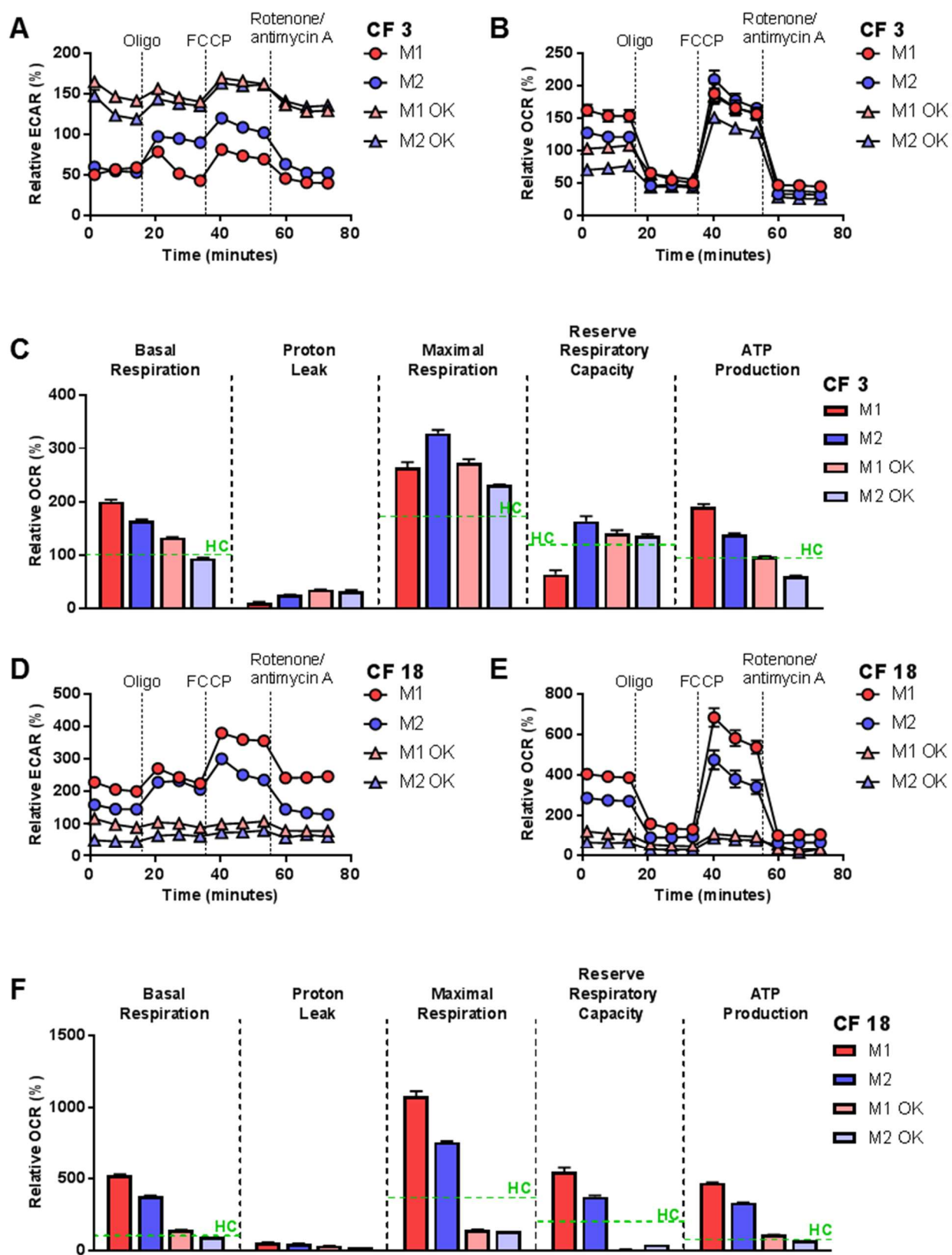


Figure 50 – Ivacaftor reduces the increased OCR levels in CF Macrophages.

(A-L) ECAR and OCR levels were measured in M1 and M2 macrophages from patients with CF (n=4). Cells were stimulated with oligomycin (1 μ M), FCCP (1 μ M), and rotenone/antimycin A (0.5 μ M). Macrophages were differentiated, as previously mentioned, and treated Ivacaftor (2.5 μ M) (IVA) when referred. (C, F, I and L) Basal respiration, proton leak, maximal respiration, reserve capacity, and ATP production were all measured. The green dotted line represents the average basal respiration, maximal respiration, reserve capacity, and ATP production in HC M1 macrophages (HC=9). All the values were calculated, as described in the methods. All data are presented as mean \pm SEM.

5.3.7 Orkambi selectively reduces OCR levels in CF macrophages ($\Delta F508/\Delta F508$)

While Orkambi is regularly used in the clinic in the US, this pharmaceutical compound, at the beginning, was only prescribed under compassionate treatment in the UK, due to its cost-inefficient results. Patients with CF, homozygous $\Delta F508/\Delta F508$, treated with Orkambi, showed an increase in the %FEV1, ranging from 2.6-4.0% [70]. Orkambi has been recently fully approved in the UK. It is still not well understood why some patients with CF strongly respond when treated with Orkambi, while other patients do not respond in a similar manner. We hypothesised that Orkambi, as seen with Ivacaftor, may have a similar effect in the regulation of metabolism in macrophages from patients with CF, mainly $\Delta F508/\Delta F508$. Treatment of CF M1 and M2 macrophages with Orkambi showed a degree of variability in OCR levels measured, among the patients with CF (**Figure 51**). Basal respiration and maximal respiration were reduced in macrophages from two of the patients with CF, while these levels were unaffected in two other patients (**Figure 51C, F, I and L**). The levels of reserve respiratory capacity were reduced in two of the patients with CF while unaffected in the other two patients; however, the variability of these levels was below the average of the HC macrophages in one of the patients (**Figure 51C, F, I and L**). Interestingly, ATP production was reduced in M1 and M2 macrophages from three of the patients with CF, while it was increased in the M1 macrophages from patient CF31 (**Figure 51C, F, I and L**). While treatment of CF macrophages with Ivacaftor showed a consistent reduction in the mitochondrial parameters evaluated here, culturing CF macrophages with Orkambi produced a selective reduction in some of the OCR levels represented in this study.



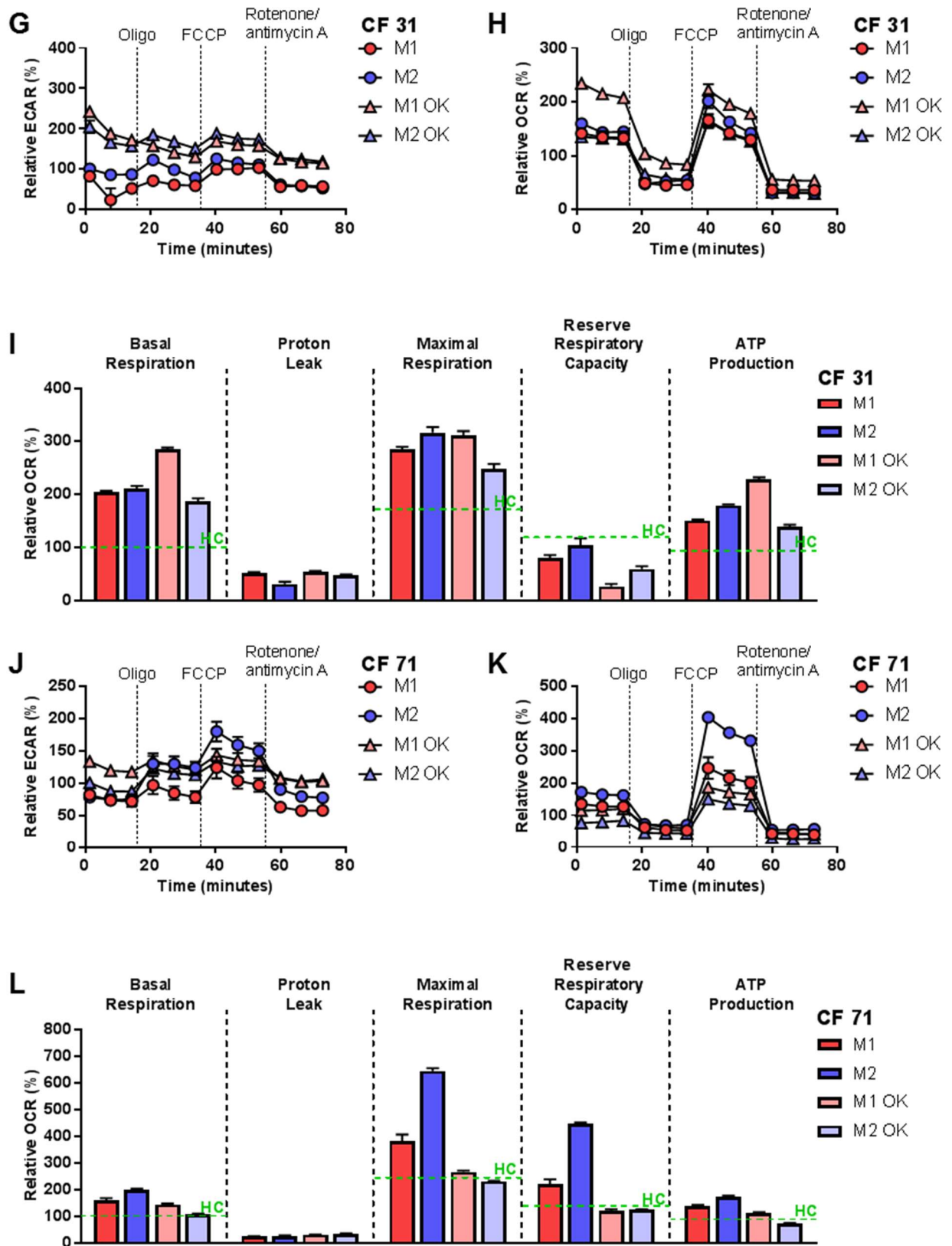


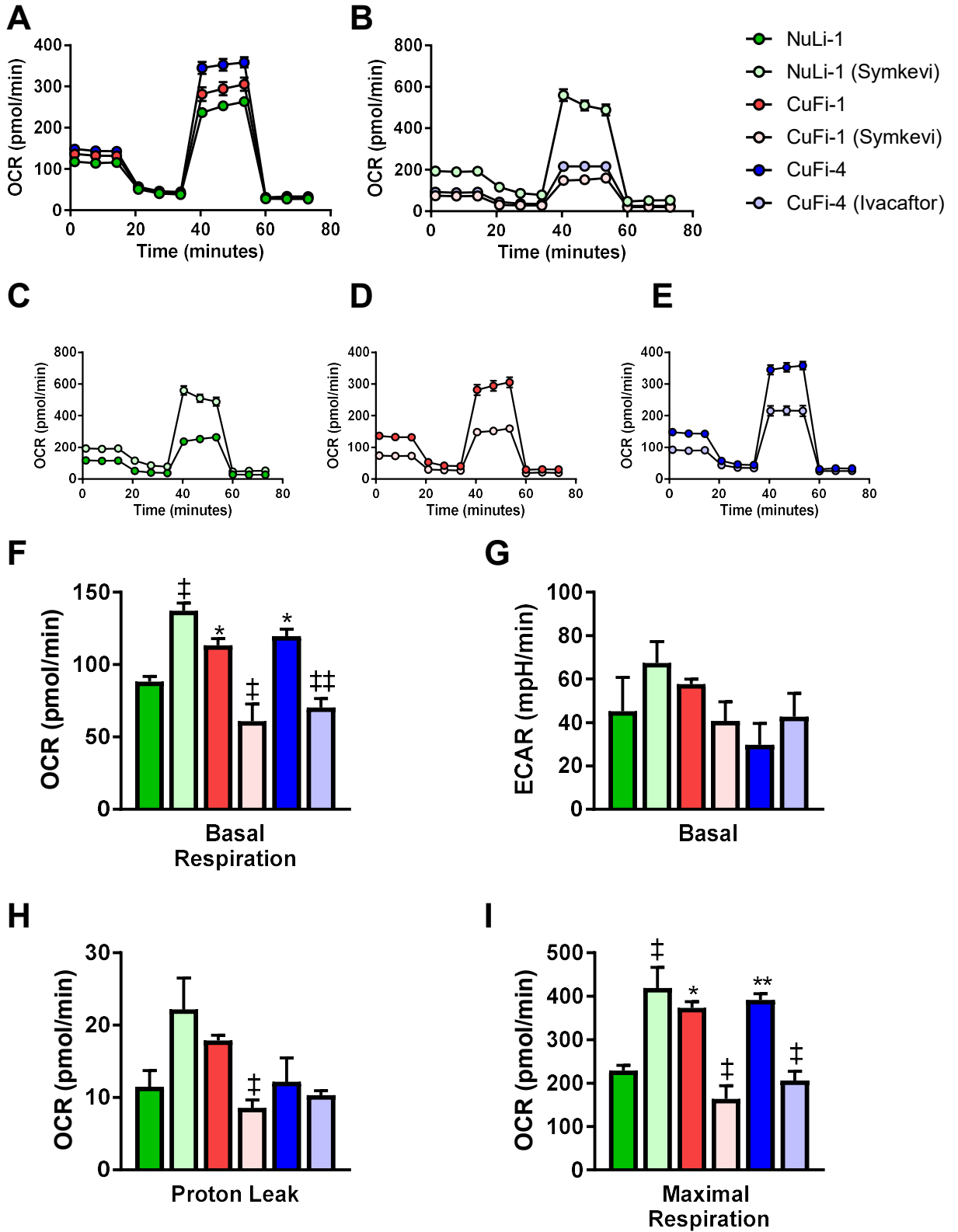
Figure 51 – Orkambi partially reduces the increased OCR levels in CF macrophages.

(A-L) ECAR and OCR levels were measured in M1 and M2 macrophages from patients with CF (n=4). Cells were stimulated with oligomycin (1 μ M), FCCP (1 μ M), and rotenone/antimycin A (0.5 μ M). Macrophages were differentiated, as previously mentioned, and treated with Orkambi (Ivacaftor (2.5 μ M) and Lumacaftor (2.5 μ M)) (OK) when referred. (C, F, I and L) Basal respiration, proton leak, maximal respiration, reserve capacity, and ATP production were all measured. The green dotted line represents the average basal respiration, maximal respiration, reserve capacity, and ATP production in HC M1 macrophages (HC=9). All the values were calculated as described in the methods. All data are presented as mean \pm SEM.

5.3.8 Ivacaftor and Symkevi alter the metabolic profile of HBECs

Symkevi is the successor of Orkambi, replacing Lumacaftor with Tezacaftor. As it was seen in the previous sections, Orkambi and Ivacaftor partially reduced the increased metabolic rates in M1 and M2 macrophages from CF patients. First, it was hypothesised that HBECs with CFTR mutations would show increased metabolic rates as shown by the macrophages, and second, that the CFTR modulators would be able to decrease these increased levels. HBECs with CFTR mutations showed significantly increased levels of OCRs under basal conditions when compared to the WT control (**Figure 52A**). As seen with the macrophages, Symkevi and Ivacaftor reduced the OCRs of the CF HBECs, CuFi-1 and CuFi-4, respectively (**Figure 52B-E**); however, when WT HBECs were cultured in the presence of Symkevi, the OCRs were elevated (**Figure 52C**). CF HBECs showed significantly increased levels of basal respiration, maximal respiration, ATP production and spare respiratory capacity when compared to the WT CFTR cell line (**Figure 52F-L**). These increased metabolic parameters were reduced by the CFTR modulators Symkevi and Ivacaftor (**Figure 52F-L**); however, these parameters were increased by Symkevi in the WT HBEC line (**Figure 52F-L**). No significant differences were detected in ECARs under basal conditions when comparing the HBECs (**Figure 52G**). Then the glycolytic capacity of the cells was tested by using a series of injections containing, glucose, oligomycin and 2-DG, as

shown before. HBECs with CFTR mutations showed no differences in the ECAR levels under basal conditions; however, after injection of glucose, CF HBECs showed non-significant lower ECAR levels when compared to the WT cell line (**Figure 53A**). Interestingly the CFTR modulators did not significantly change the ECAR parameters of CF HBEC lines, but Symkevi showed a pronounced effect in increasing the ECAR levels in the WT HBEC line (**Figure 53C-J**). Consistently, the OCR levels of cells with CFTR mutations were significantly increased and were decreased by the administration of the CFTR modulators Symkevi and Ivacaftor, accordingly (**Figure 53G**).



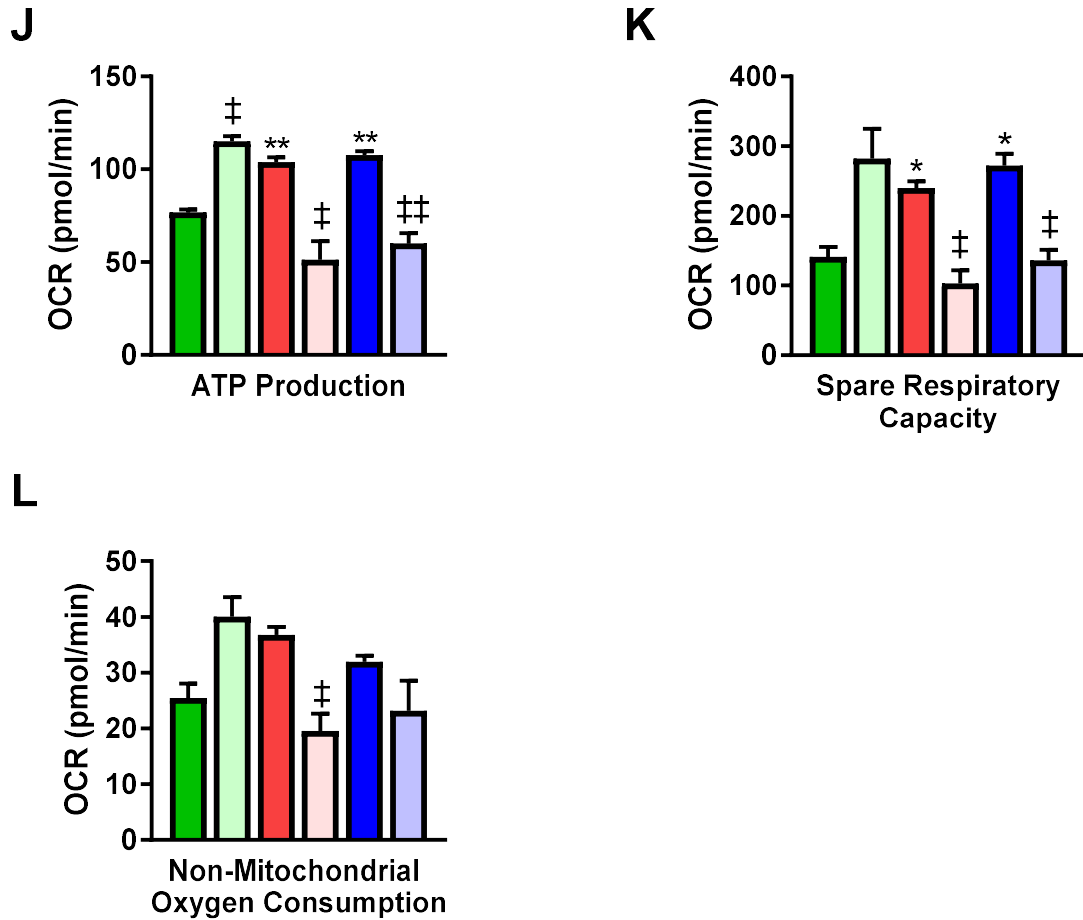
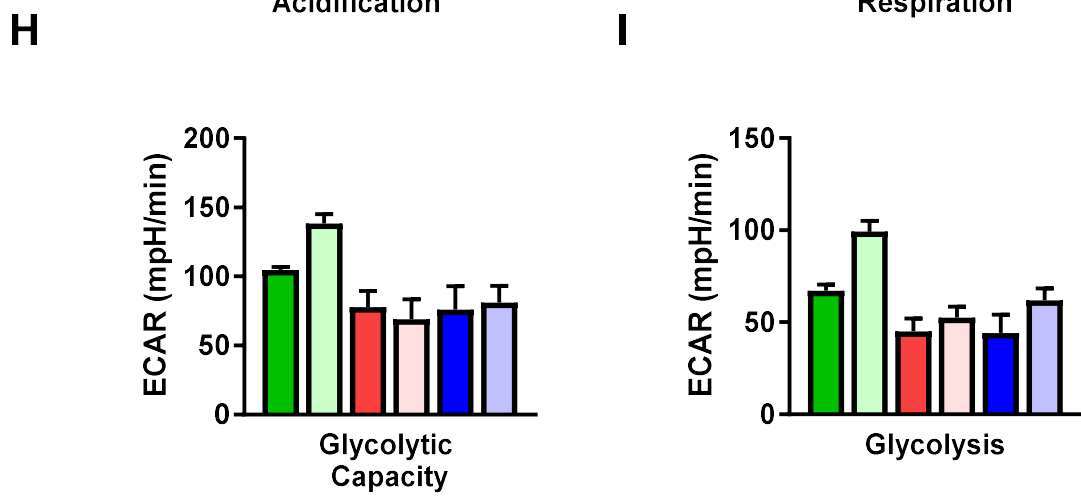
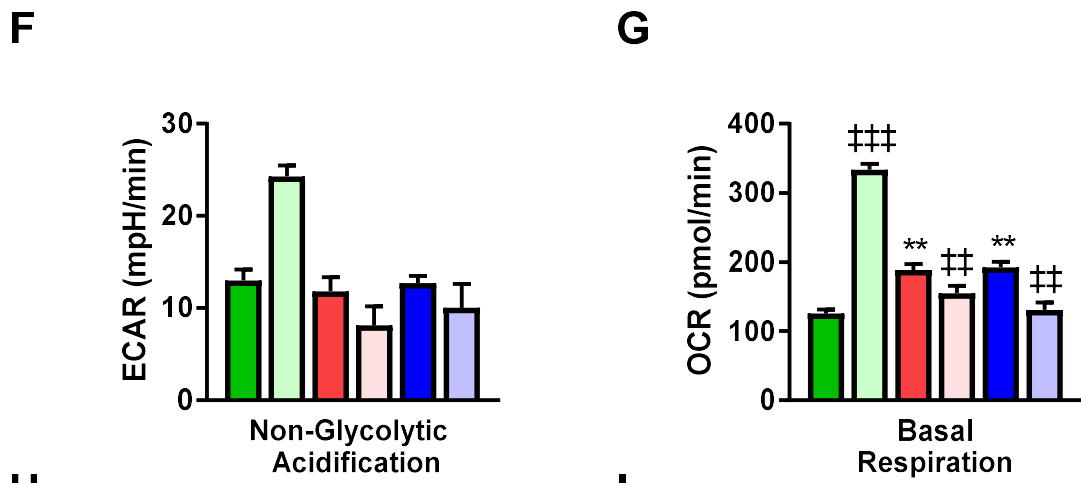
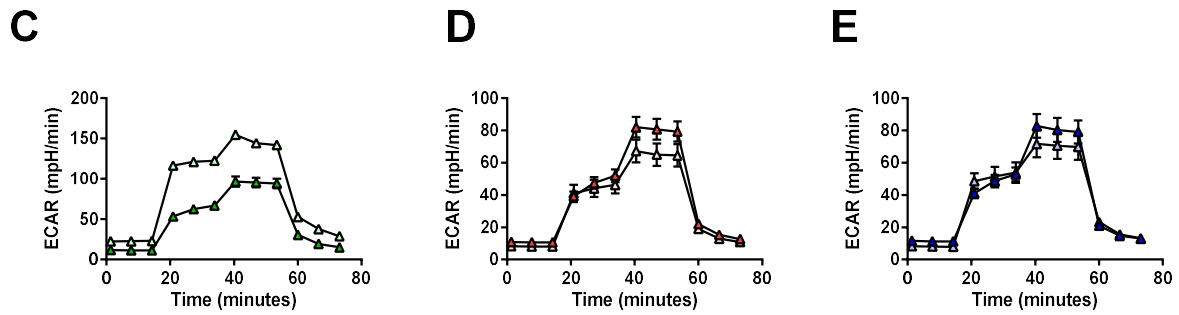
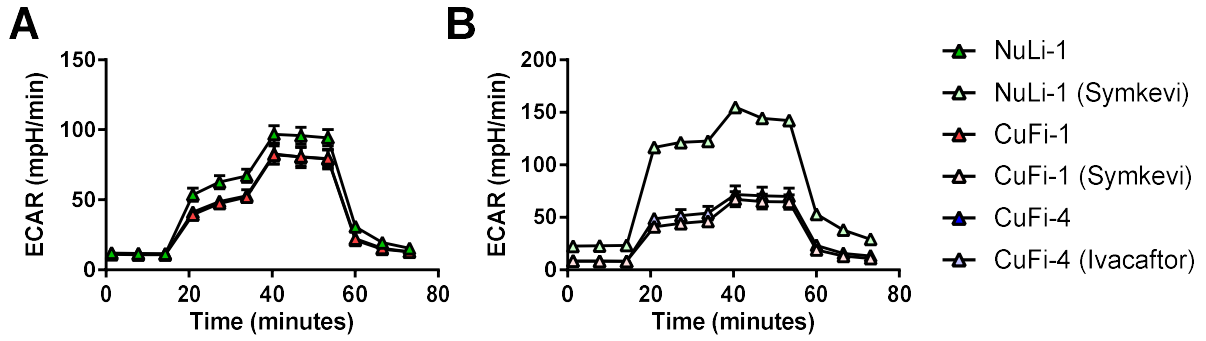


Figure 52 – CFTR modulators decrease the high OCR levels in CF HBECS

(A-L) ECAR and OCR levels were measured in the HBECS NuLi-1 (WT), CuFi-1 ($\Delta F508/\Delta F508$) and CuFi-4 ($\Delta F508/G551D$). Cells were stimulated with oligomycin (1 μM), FCCP (1 μM), and rotenone/antimycin A (0.5 μM). Cells were cultured under basal condition and in the presence of Symkevi, Ivacaftor (2.5 μM) and Tezacaftor (2.5 μM), or Ivacaftor alone. Basal respiration, basal ECAR, proton leak, maximal respiration, ATP production, spare respiratory capacity, and non-mitochondrial oxygen consumption were all measured. These graphs show three independent experiments with four technical replicates in each experiment for each cell line and each condition. All values were calculated as described in the methods. All data are presented as mean \pm SEM. (*) Show comparison with the NuLi-1 cell line, (‡) show paired comparison between untreated and treated cells. Statistical comparisons were performed by unpaired or paired Student's t-test, * $p < 0.05$, ** $p < 0.01$, *** $p < 0.001$.



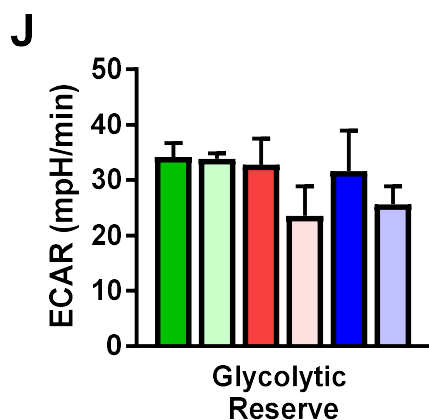


Figure 53 – No impact of CFTR modulators in the ECAR levels of CF HBECs

(A-J) ECAR and OCR levels were measured in the HBECs NuLi-1 (WT), CuFi-1 ($\Delta F508/\Delta F508$) and CuFi-4 ($\Delta F508/G551D$). Cells were stimulated with glucose, oligomycin, and 2-DG. Cells were cultured under basal condition and in the presence of Symkevi, Ivacaftor (2.5 μM) and Tezacaftor (2.5 μM), or Ivacaftor alone. Non-glycolytic acidification, basal respiration, glycolytic capacity, glycolysis and glycolytic reserve were all measured. These graphs show three independent experiments with four technical replicates in each experiment for each cell line and each condition. All values were calculated as described in the methods. All data are presented as mean \pm SEM. (*) Show comparison with the NuLi-1 cell line, (\ddagger) show paired comparison between untreated and treated cells. Statistical comparisons were performed by unpaired or paired Student's t-test, * $p < 0.05$, ** $p < 0.01$, *** $p < 0.001$.

5.4 Discussion

CFTR mutations that are present in innate immune cells from patients with CF have shown to be detrimental to cellular function. We have shown a unique signature of ER stress genes that are disrupted in innate immune cells from patients with CF. These signalling pathways affect the normal innate immune cellular functions, exaggerating the inflammatory response with an associated hypermetabolic state. The CuFi-1 cell line showed increased levels of ROS and mROS when compared to the WT control. We also found elevated ROS levels in M1 macrophages from patients with CF, suggesting that these innate immune cells have a disruption in their cellular machinery that regulates the function of these molecules. Further investigation into the glycolytic pathways employed by these innate immune cells, revealed that monocytes and M1 macrophages from patients with CF have a disruption in their ECAR and OCR levels. When challenged by bacterial components, monocytes and macrophages showed heightened levels of ECAR and OCR levels, as opposed to the ratios shown by HC monocytes and M1 macrophages. Intriguingly, when we calculated glycolysis in both cells, we did not find any significant changes; nevertheless, the glycolytic capacity and reserve in these innate immune cells was significantly increased ($p < 0.05$). The glycolytic capacity is defined as the maximum rate of conversion of glucose to pyruvate/lactate that a cell can achieve. Converting glucose to pyruvate/lactate is carried out by several enzymes within the cytosolic space, but this rapid and inefficient method of generating ATP. The glycolytic reserve indicates the ability of the cell to acutely respond to an energetic demand, for instance, during bacterial challenges. The increased levels in the glycolytic capacity and reserve, as found in the CF monocytes and macrophages, indicate that these cells

respond in an exaggerated manner to bacterial challenges. These findings suggest that the CFTR mutations encountered in these myeloid cells may be associated with this exaggerated metabolic response. Considering that circulating monocytes from CF patients may be activated and acquire a short innate immune memory or “epigenetic memory”, as described by some studies [218-220], this could help to explain the increased glycolytic capacity and reserve levels observed; however, we consider that on top of this hypothetical epigenetic memory in these cells, the CFTR mutations found in innate immune cells may be associated with the increased metabolic rates. Our previous results have shown that M1 macrophages from CF patients have increased activity in the IRE1 α -XBP1 signalling pathway, with associated increased levels of inflammation and mitochondrial flux. By inhibiting the RNase domain of the IRE1 α arm of the UPR, we demonstrated that the hyper-metabolic levels, shown by CF M1 macrophages, are linked to the ER stress found in these cells. Furthermore, while decreasing the hyper-metabolic state in these cells, the two IRE1 α inhibitors also reduced the levels of TNF and IL-6 in the CF M1 macrophages. These findings suggest that the CFTR mutations, in these M1 macrophages, lead to increased levels of cellular stress with further increased cellular metabolism.

Ivacaftor and Orkambi, the most efficient drugs licenced to be administered to patients with CF have shown different outcomes in the clinic, with the former drug being significantly efficient in treating a subset of patients with CF, and the latter showing only a modest efficacy in some of the patients. Orkambi will be eventually replaced by its successor, the triple therapy combination Trikafta, which has shown improved efficacy in patients Δ F508 homozygous, to the level of patients carrying class III mutations taking Ivacaftor alone [75, 77]. Addition of Ivacaftor to the culture media, where the macrophages from patients with class III mutations were being

differentiated, reduced the increased mitochondrial flux observed in these cells, whereas Orkambi only partially reduced these increased metabolic ratios in two of the patients who were homozygous for the $\Delta F508$ mutation.

Chapter 6 – Discussion

6.1 The UPR exacerbates inflammation in cystic fibrosis

The UPR is an essential cellular mechanism that eukaryotic cells have evolved to detect several pathogenic and stress insults by using the three ER transmembrane proteins, ATF6, IRE1, and PERK, which allow cells to recover the equilibrium by restoring ER homeostasis. These complex mechanistic pathways have been frequently reported to regulate the protein load in neurological disorders [221-223]. For instance, in Alzheimer's and Parkinson's disease, the protein aggregation within the neurons is known to cause ER stress and activate the UPR [224, 225]. Thus, it has been hypothesised that UPR activation in these two neurological conditions leads to the progression of these disorders, causing neuronal damage with eventual tissue destruction [224]. It would be interesting to investigate whether this UPR activation is associated with the production of pro-inflammatory cytokines in the brain and whether this process can be inhibited by using specific drug compounds. In fact, one hallmark of neuroinflammation in patients with Alzheimer's and Parkinson's disease, is the presence of TNF, IL-1 β and IL-6 in the brain, cerebrospinal fluid and serum of these patients [226, 227]. The presence of these cytokines could, potentially, be associated with the UPR activation seen in these patients.

In the case of CF, the chronic activation of the IRE1 α -XBP1 signalling pathway may be fundamental in disease progression, in association with the increased neutrophilic infiltration normally seen in the lungs of patients with CF. TNF, IL-1 β and IL-6 are potent pro-inflammatory cytokines that regulate the inflammatory response by activating monocytes and macrophages. Moreover, TNF and IL-1 β enhance the

production of IL-8, which induces lung neutrophilic infiltration [228]. A recent study demonstrated that the levels of IL-1 β in the BAL and sputum of patients with CF was directly correlated with the %FEV1 [217]. It would be interesting to explore whether this chronic UPR activation is linked to the production of IL-1 β in CF. It was demonstrated that the raised levels of XBP1s are associated with the hyperinflammatory response seen in patients with CF. It is worth mentioning, that chronic activation of the IRE1 α -XBP1 signalling pathway was only seen in the M1, but not M2 macrophages, suggesting that this process only affects pro-inflammatory macrophages. Moreover, the abnormal hyper-inflammatory state of the macrophages was observed after activation with LPS and IFN γ , suggesting that the UPR may act as an enhancer of the inflammatory response when activated. The ionic imbalance produced by the CFTR abnormalities, alongside the accumulation of the misfolded proteins, associated with Δ F508 homozygosity, could induce a perpetual chronic low-grade inflammation in CF macrophages, directing these phagocytic cells towards a hyper-inflammatory phenotype, which is mainly driven by XBP1s. This chronic low-grade inflammation can be also exacerbated by other PAMPs and DAMPs, such as TNF, IL-6, LPS and ROS, as shown in other disorders, such as RA and TRAPS (**Figure 54**) [133, 152]. These mechanisms are potentially crucial for the progression of CF, as macrophages are primarily involved in the regulation of the inflammatory response.

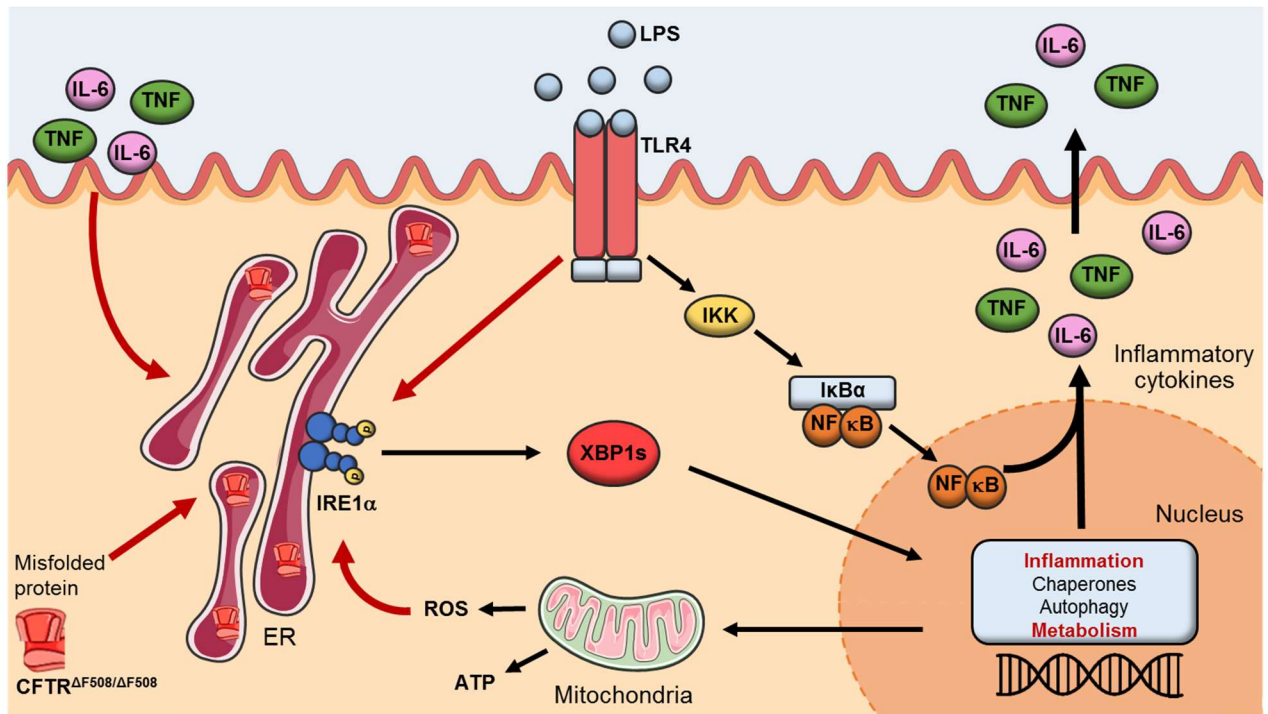


Figure 54 – The IRE1a-XBP1 signalling pathway of the UPR in CF.

In CF macrophages activation of the IRE1 α -XBP1 signalling pathway induces the XBP1s, which in turn activates the transcription of several genes involved in inflammation, protein folding, autophagy and metabolism. CFTR malfunctioning and accumulation of misfolded protein induces a low-grade chronic ER stress, leading to a hyperinflammatory and –metabolic phenotype. The activation of TLR4, through bacterial competes, leads to a further increase in the levels of XBP1s exacerbating the inflammatory response.

6.2 The UPR and the regulation of macrophage metabolism.

Immunometabolism has proven to be an essential mechanism to consider during macrophage differentiation and activation, and a better understanding of the different metabolic pathways encountered in these cells is therefore encouraged. Recent discoveries have shown that the UPR is an important regulator of cellular metabolism [229, 230]. While the UPR positively regulates metabolic pathways in several eukaryotic cells, this process also regulates glucose, lipid and mitochondrial metabolism in different immune cells [140, 210, 231, 232]. In this study, it was demonstrated that monocytes and M1 macrophages from CF patients show increased metabolic rates. The increased glycolytic rates and mitochondrial flux levels observed in the CF M1 macrophages were associated with increased levels of XBP1s. It was confirmed that inhibition of the RNase domain of the IRE1 α arm of the UPR leads to a reduction in the glycolytic rate and mitochondrial flux in CF M1 macrophages, which was comparable to the levels of the HC macrophages. Furthermore, while reducing the increased metabolic levels in CF M1 macrophages, inhibition of IRE1 α also lead to the reduction of TNF and IL-6 pro-inflammatory cytokines. These findings suggest that CFTR mutations in human macrophages lead to activation of the IRE1 α -XBP1 signalling pathway, which in turns regulates the metabolic profile of these cells. As the activity of IRE1 α remains increased in these CF M1 macrophages, the rates of some metabolic parameters remained also increased, such as the glycolytic capacity and reserve, basal cellular respiration and ATP production. These findings support the idea that macrophage metabolic regulation, through the UPR, might be a possible therapeutic option for patients with CF. Modulation of the metabolic pathways in human cells could be an alternative option to treat inflammatory diseases. In fact,

recent discoveries have identified the metabolite itaconate as a potent anti-inflammatory molecule in macrophages, acting through Nrf2, which is capable of reducing the inflammation in vivo [199]. This study demonstrated that a derivate of this metabolite, 4-octyl itaconate (OI), protected mice against LPS induced lethality and reduced the levels of TNF and IL-1 β secretion [199]. While OI can reduce the inflammatory response via Nrf2, IRE1 α inhibitors may be used for the same proposes when inflammation and metabolic profiles are raised in certain diseases. Although these compounds can serve as potent anti-inflammatory drugs, it is essential to consider their side effects when administered in vivo, as Nrf2 and IRE1 α are critical mechanistic pathways that regulate cellular homeostasis. A summary of various dysregulated pathways in M1 macrophages is shown in **Figure 55**.

Recent studies have shown that the UPR can influence macrophage polarisation [210, 233]. In one study, conditional ablation of IRE1 α in mouse myeloid cells increased the proportion of M2 macrophage polarisation [210]; however, in this study, it was not observed any change in macrophage polarisation when the two IRE1 α inhibitors were administered before macrophage polarisation. These discrepancies may be due to the differences in species, or due to the short exposure of the two drugs in macrophages. It would be interesting to investigate further whether the UPR regulates human macrophage polarisation in health and disease.

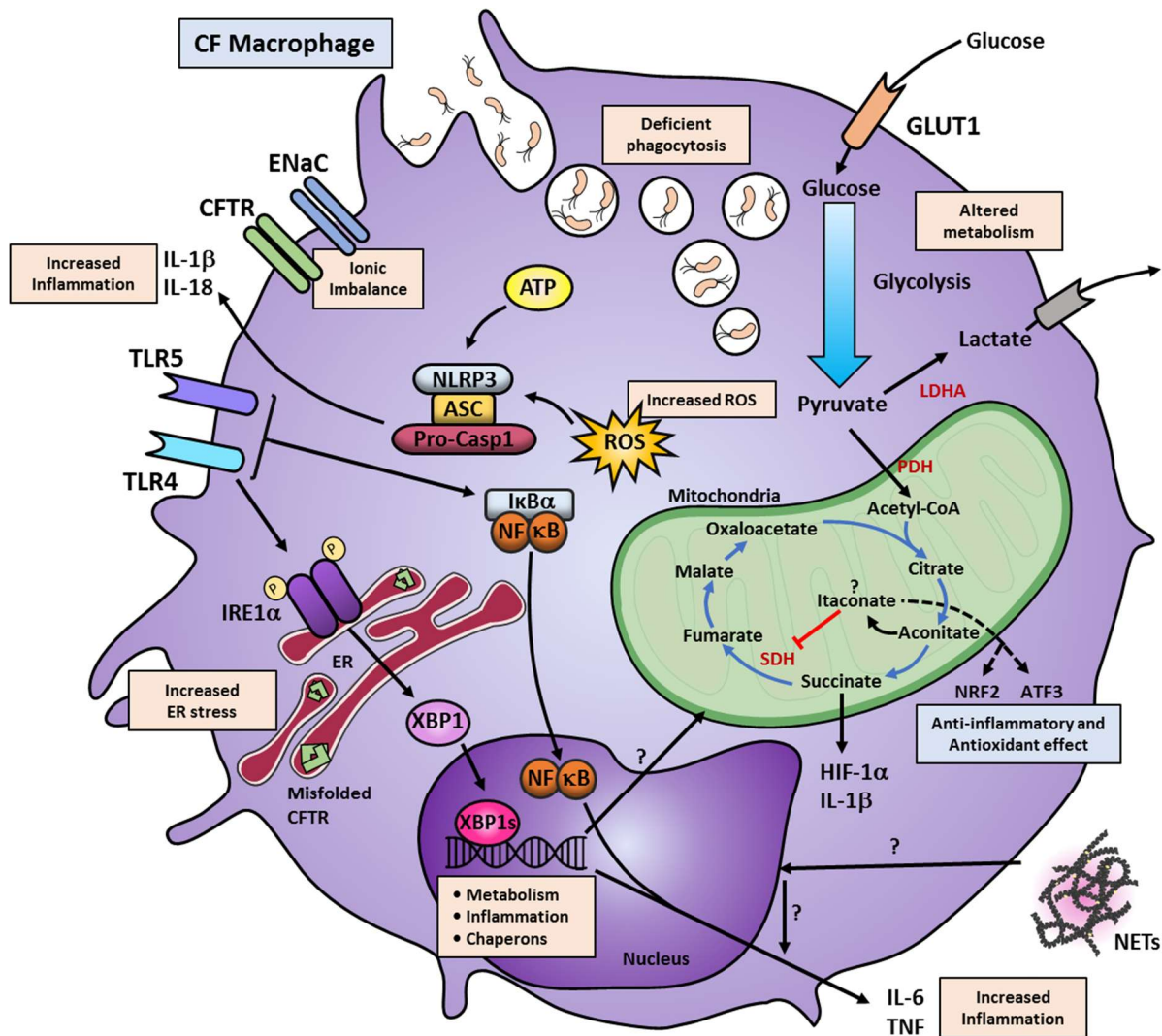


Figure 55 – Altered signalling pathways in CF macrophages

Macrophages with CFTR mutations show alterations in multiple cellular pathways. The mutated CFTR causes ionic imbalance, with accumulation of misfolded protein in the case of the DF508 mutations and primes these myeloid cells towards an altered immune response or chronically activating other signalling pathways. CFTR malfunction primes the overactivation of ENaC, leading to increased Na⁺ influx, which is then compensated by K⁺ efflux. The increased K⁺ efflux, combined with increased ROS and ATP production, activates the NLRP3 inflammasome with further increased IL-1β and IL-18 secretion. CF macrophages have raised levels of TLR4 expression, and the resultant overactivation of NF-κB leads to increased TNF and IL-6 production. Induction TNF and IL-8 may also occur through NETs by an unknown mechanism. Similarly, chronic TLR4 activation, possibly due to the persistent bacterial colonisation in the lungs, leads to overactivation of IRE1a, thereby triggering XBP1s. This production of XBP1s induces transcriptional activation of several UPR responsive genes involving metabolism, inflammation and protein folding. XBP1s overexpression induces a low-grade chronic induction of IL-6 and TNF, which exacerbates the inflammatory response when combined with other signalling pathways. XBP1s also regulate metabolic pathways and, in CF macrophages, the increased metabolic state

can be reduced by IRE1 α inhibition. Macrophages with CFTR mutations also show increased glycolytic flux and mitochondrial respiration. It is known that in M1 macrophages the Krebs cycle favours the accumulation of succinate and citrate. Succinate accumulation leads to stabilisation of HIF-1 α , which can induce IL-1 β production and activation of glycolytic genes. It may be possible that in CF macrophages, this axis is favouring a proinflammatory response and increased glycolytic function. Alternatively, citrate is converted into aconitate, facilitating the synthesis of itaconate, which is a potent anti-inflammatory metabolite; however, the role of itaconate in CF is unknown. CF macrophages also display deficient bacterial killing with intracellular accumulation of phagocytic vesicles. Altogether, these mechanisms influence the altered innate response elicited by macrophages. Abbreviations: LDHA (lactate dehydrogenase A); GLUT (glucose transporter); SDH (Succinate dehydrogenase); PDH (Pyruvate dehydrogenase); ER (endoplasmic reticulum); HIF-1a (Hypoxia Inducible Factor 1 Subunit Alpha); NRF2 (Nuclear factor erythroid-2-related factor 2); ATF3 (Activating transcription factor 3); ROS (reactive oxygen species). This figure is part of a manuscript in press by the author Lara-Reyna et al. CMLS 2020.

6.3 Abnormal metabolic and inflammatory profiles in CF HBECs

In this study, it was reported that cells with CFTR mutations showed increased metabolic and inflammatory profiles. It is interesting to mention that CF HBECs showed increased levels of *TNF* and *IL-6*, which were associated with the increased OCR levels, as similarly shown by the M1 macrophages; however, HBECs did not show any significant differences in the ECAR levels. In the case of the M1 macrophages, it is known that higher glycolytic activity is associated with an inflammatory profile, while the opposite is the case in terms of M2 macrophages. Intriguingly, CF HBECs only showed increased OCR ratios with high basal respiration and ATP production, suggesting that the mitochondria are affected in cells with CFTR mutations, but glycolysis seems not to be affected. High OCR levels indicate a more rapid utilization of oxygen by typically by the ETC, which will be utilised as the final electron acceptor in the production of ATP. Perhaps the higher metabolic profile of CF HBECs is linked to the hyperactive mitochondria which eventually leads to the production of ROS and activation of the UPR. Certainly, cells with CFTR mutations have an abnormal metabolic activity that can be associated with a unique UPR activation and higher production of inflammatory cytokines.

6.4 CF as an autoinflammatory condition

As opposed to autoimmunity, autoinflammation involves the aberrant activation of the innate immune system causing the abnormal production of inflammatory cytokines, whereby the local environmental factors may predispose the cells to an inflammatory phenotype [234]. This concept has been previously shown to be one of the principal causes that induce inflammation in several immune related-disorders including, familial Mediterranean fever (FMF), TRAPS, hyperimmunoglobulinemia D syndrome (HIDS) and cryopyrin-associated periodic syndrome (CAPS) [23, 234, 235]. CF has been described as an autoinflammatory condition before, due to the CFTR dysfunction, which results in a series of pathophysiological complications mainly associated with the innate immune system [23]. Recent studies have shown that the levels of the pro-inflammatory cytokines IL-1 β and IL-18 are increased in patients with CF [209, 217]. These results support the idea that CF should be considered as an autoinflammatory condition due to substantial similarities with other conditions related to the innate immune system. For instance, we have shown that innate immune cells with CFTR mutations, mainly macrophages, have increased activity in the IRE1 α -XBP1 signalling pathway, which leads to an exaggerated secretion of TNF and IL-6. Furthermore, the levels of ROS and mROS were shown to be increased in CF HBECs and macrophages. Altogether, these findings support the idea that CF is mainly an autoinflammatory condition as the adaptive immune system is not required for this exaggerated inflammatory response. It is essential to mention that while T and B cells are crucial players in any bacterial and viral infection, these cells have not been reported to be primarily affected by CFTR mutations to date. The constant interaction between innate and adaptive immune cells is crucial to maintain the equilibrium in

different tissues and to protect the host against different types of infections. It would be interesting to investigate the interaction between the innate and adaptive immune system in CF, and whether any abnormalities exist during these processes.

6.5 Conclusion

We have shown that innate immune cells containing CFTR mutations have dysregulated intracellular mechanism, including increased ER stress, metabolic and inflammatory levels. Monocytes and macrophages are essential cells capable of controlling the inflammatory response, and, in this study, it was demonstrated that mutations in the CFTR gene compromise these functions. To the best of our knowledge, CF is an autoinflammatory condition and treatments that regulate the inflammatory response, such as IL-6, TNF, IL-1 β and IL-18 blockers, should be considered. Furthermore, only innate immune cells from patients with CF showed a chronic low-grade UPR activation, mainly in the IRE1 α -XBP1 signalling pathway. The results in this study support previous findings that have demonstrated that the IRE1 α -XBP1 signalling pathway regulates the metabolic activity of other immune cells. It was observed that the increased UPR signalling pathway controls the metabolic rate of CF M1 macrophages. Furthermore, these metabolic abnormalities were found in several CF innate immune cells, including CF HBECS, monocytes and M1 macrophages. These metabolic dysregulations affected the ECAR and OCR levels of all innate immune cells previously mentioned. Remarkably, the two IRE1 α inhibitors, 4 μ 8c and MKC-3946, reversed the increased inflammatory and metabolic levels in M1 macrophages.

Altogether, chronic activation of the IRE1 α -XBP1 signalling pathway in M1 macrophages from patients with CF, results in increased ECAR and OCR levels. Moreover, these heightened metabolic levels were associated with an exaggerated inflammatory response. CF M1 macrophages undergo metabolic reprogramming, via the IRE1 α -XBP1 signalling pathway, which leads to higher mitochondrial and glycolytic

activity, with increased levels of TNF and IL-6. These findings may help to explain the clinical complications of patients with CF, who suffer from chronic infections and unresolved lung inflammation. Dysregulation of the CFTR conductance alongside with the CFTR protein abnormalities lead to increased levels of ER stress in CF macrophages. These ER stress levels prime CF macrophages to a hyper-inflammatory and metabolic response, which is mainly driven by XBP1s and exacerbated by the activation of TLR4, and possibly other DAMPs and PAMPs (**Figure 54**). The IRE1 α axis of the UPR has been shown to be an important player in the regulation of inflammation and metabolism, suggesting that modulation of ER stress might be an option to recover the cellular equilibrium of immune cells.

6.6 Study limitations

While it was demonstrated that the mitochondrial flux, glycolytic rate, ER stress and inflammatory profile of cells with CFTR mutations are increased, the following limitations are acknowledged in this study. While it was observed an upregulation of several ER stress markers in the IB3-1, CuFi-1 and CuFi-4, when compared to BEAS2-B, these are immortalised cell lines from different individuals. Also, the IB3-1 and BEAS2-B cell lines were cultured in LHC basal medium while the CuFi-1 and CuFi-4 were cultured in LHC-9 medium; nevertheless, we were able to corroborate the high metabolic levels in the CuFi-1 and CuFi-4 cells when compared with the NuLi-1 cell line, which was cultured in the same conditions CuFi-1 and CuFi-4 cells lines. Furthermore, the fact that similar findings were observed in primary human cells from patients with CF supports the hypothesis stated in this study. While it was observed a constant and significant upregulation of TNF and IL-6 in monocytes and macrophages from patients with CF, these differences might be due to a short epigenetic memory of these innate immune cells. Moreover, the fact that macrophages were grown in vitro for the duration of the experiments and the fact that these cells were grown adding MCS-F and GM-CSF limits this study; however, this is a well-established method for culturing macrophages, which has demonstrated to be reliable and comparable to in vivo macrophages.

6.7 Future Directions

Following from the limitations mentioned before, it would be interesting to investigate further the differences observed in this study in other models of airway inflammation, possibly using isogenic corrected induced pluripotent stem cells (iPSc) to create HBECs and macrophages. Furthermore, to fully understand all the transcriptomic differences in macrophages with CFTR mutations, it would be ideal to perform RNAseq in these myeloid cells. For instance, the transcriptomic differences between CF and HC monocytes, M0, M1 and M2 macrophages could be explored. While there are specific cellular abnormalities associated with inflammatory and metabolic pathways in innate immune cells from patients with CF, the underlying mechanisms are still not fully deciphered, and more research is encouraged.

Appendix



Professor Daniel Peckham
Professor of Respiratory Medicine
University of Leeds
Cystic Fibrosis of Unit, J06
St. James's University Hospital
Beckett Street, Leeds
LS9 7TF

Email: hra.approval@nhs.net

24 May 2017

Dear Professor Peckham

Letter of HRA Approval

Study title:	Identifying the biochemical signalling pathways involved in lung inflammation and arthropathy in patients with cystic fibrosis
IRAS project ID:	201570
REC reference:	17/YH/0084
Sponsor	University of Leeds

I am pleased to confirm that HRA Approval has been given for the above referenced study, on the basis described in the application form, protocol, supporting documentation and any clarifications noted in this letter.

Participation of NHS Organisations in England

The sponsor should now provide a copy of this letter to all participating NHS organisations in England.

Appendix B provides important information for sponsors and participating NHS organisations in England for arranging and confirming capacity and capability. **Please read *Appendix B* carefully**, in particular the following sections:

- *Participating NHS organisations in England* – this clarifies the types of participating organisations in the study and whether or not all organisations will be undertaking the same activities
- *Confirmation of capacity and capability* - this confirms whether or not each type of participating NHS organisation in England is expected to give formal confirmation of capacity and capability. Where formal confirmation is not expected, the section also provides details on the time limit given to participating organisations to opt out of the study, or request additional time, before their participation is assumed.
- *Allocation of responsibilities and rights are agreed and documented (4.1 of HRA assessment criteria)* - this provides detail on the form of agreement to be used in the study to confirm capacity and capability, where applicable.

Further information on funding, HR processes, and compliance with HRA criteria and standards is also provided.

It is critical that you involve both the research management function (e.g. R&D office) supporting each organisation and the local research team (where there is one) in setting up your study. Contact details and further information about working with the research management function for each organisation can be accessed from www.hra.nhs.uk/hra-approval.

Appendices

The HRA Approval letter contains the following appendices:

- A – List of documents reviewed during HRA assessment
- B – Summary of HRA assessment

After HRA Approval

The document "*After Ethical Review – guidance for sponsors and investigators*", issued with your REC favourable opinion, gives detailed guidance on reporting expectations for studies, including:

- Registration of research
- Notifying amendments
- Notifying the end of the study

The HRA website also provides guidance on these topics, and is updated in the light of changes in reporting expectations or procedures.

In addition to the guidance in the above, please note the following:

- HRA Approval applies for the duration of your REC favourable opinion, unless otherwise notified in writing by the HRA.
- Substantial amendments should be submitted directly to the Research Ethics Committee, as detailed in the *After Ethical Review* document. Non-substantial amendments should be submitted for review by the HRA using the form provided on the [HRA website](#), and emailed to hra.amendments@nhs.net.
- The HRA will categorise amendments (substantial and non-substantial) and issue confirmation of continued HRA Approval. Further details can be found on the [HRA website](#).

Scope

HRA Approval provides an approval for research involving patients or staff in NHS organisations in England.

If your study involves NHS organisations in other countries in the UK, please contact the relevant national coordinating functions for support and advice. Further information can be found at <http://www.hra.nhs.uk/resources/applying-for-reviews/nhs-hsc-rd-review/>.

If there are participating non-NHS organisations, local agreement should be obtained in accordance with the procedures of the local participating non-NHS organisation.

User Feedback

The Health Research Authority is continually striving to provide a high quality service to all applicants and sponsors. You are invited to give your view of the service you have received and the application procedure. If you wish to make your views known please use the feedback form available on the HRA website: <http://www.hra.nhs.uk/about-the-hra/governance/quality-assurance/>.

HRA Training

We are pleased to welcome researchers and research management staff at our training days – see details at <http://www.hra.nhs.uk/hra-training/>

Your IRAS project ID is **201570**. Please quote this on all correspondence.

Yours sincerely,

Natalie Wilson
Assessor

Email: hra.approval@nhs.net

*Copy to: NHS Research Ethics Officer, University of Leeds, Sponsor contact
Mrs Anne Gowing, Leeds Teaching Hospitals NHS Trust, Lead NHS R&D contact*

References

1. Quinton PM: **Physiological basis of cystic fibrosis: a historical perspective.** *Physiol Rev* 1999, **79**(1 Suppl):S3-s22.
2. ANDERSEN DH: **CYSTIC FIBROSIS OF THE PANCREAS AND ITS RELATION TO CELIAC DISEASE: A CLINICAL AND PATHOLOGIC STUDY.** *American Journal of Diseases of Children* 1938, **56**(2):344-399.
3. Tsui LC, Buchwald M, Barker D, Braman JC, Knowlton R, Schumm JW, Eiberg H, Mohr J, Kennedy D, Plavsic N *et al*: **Cystic fibrosis locus defined by a genetically linked polymorphic DNA marker.** *Science* 1985, **230**(4729):1054-1057.
4. Riordan JR, Rommens JM, Kerem B, Alon N, Rozmahel R, Grzelczak Z, Zielenski J, Lok S, Plavsic N, Chou JL *et al*: **Identification of the cystic fibrosis gene: cloning and characterization of complementary DNA.** *Science* 1989, **245**(4922):1066-1073.
5. Eiberg H, Mohr J, Schmiegelow K, Nielsen LS, Williamson R: **Linkage relationships of paraoxonase (PON) with other markers: indication of PON-cystic fibrosis syntenry.** *Clin Genet* 1985, **28**(4):265-271.
6. Cant N, Pollock N, Ford RC: **CFTR structure and cystic fibrosis.** *Int J Biochem Cell Biol* 2014, **52**:15-25.
7. Mulberg AE, Resta LP, Wiedner EB, Altschuler SM, Jefferson DM, Broussard DL: **Expression and localization of the cystic fibrosis transmembrane conductance regulator mRNA and its protein in rat brain.** *J Clin Invest* 1995, **96**(1):646-652.
8. Guo Y, Su M, McNutt MA, Gu J: **Expression and distribution of cystic fibrosis transmembrane conductance regulator in neurons of the human brain.** *J Histochem Cytochem* 2009, **57**(12):1113-1120.
9. Guo Y, Su M, McNutt MA, Gu J: **Expression and distribution of cystic fibrosis transmembrane conductance regulator in neurons of the spinal cord.** *J Neurosci Res* 2009, **87**(16):3611-3619.
10. Johannesson M, Bogdanovic N, Nordqvist AC, Hjelte L, Schalling M: **Cystic fibrosis mRNA expression in rat brain: cerebral cortex and medial preoptic area.** *Neuroreport* 1997, **8**(2):535-539.
11. Su M, Guo Y, Zhao Y, Korteweg C, Gu J: **Expression of cystic fibrosis transmembrane conductance regulator in paracervical ganglia.** *Biochem Cell Biol* 2010, **88**(4):747-755.
12. Warth JD, Collier ML, Hart P, Geary Y, Gelband CH, Chapman T, Horowitz B, Hume JR: **CFTR chloride channels in human and simian heart.** *Cardiovasc Res* 1996, **31**(4):615-624.

13. Davies WL, Vandenberg JI, Sayeed RA, Trezise AE: **Cardiac expression of the cystic fibrosis transmembrane conductance regulator involves novel exon 1 usage to produce a unique amino-terminal protein.** *J Biol Chem* 2004, **279**(16):15877-15887.
14. Lange T, Jungmann P, Haberle J, Falk S, Duebbers A, Bruns R, Ebner A, Hinterdorfer P, Oberleithner H, Schillers H: **Reduced number of CFTR molecules in erythrocyte plasma membrane of cystic fibrosis patients.** *Mol Membr Biol* 2006, **23**(4):317-323.
15. McDonald TV, Nghiem PT, Gardner P, Martens CL: **Human lymphocytes transcribe the cystic fibrosis transmembrane conductance regulator gene and exhibit CF-defective cAMP-regulated chloride current.** *J Biol Chem* 1992, **267**(5):3242-3248.
16. Dong YJ, Chao AC, Kouyama K, Hsu YP, Bocian RC, Moss RB, Gardner P: **Activation of CFTR chloride current by nitric oxide in human T lymphocytes.** *Embo j* 1995, **14**(12):2700-2707.
17. Sturges NC, Wikstrom ME, Winfield KR, Gard SE, Brennan S, Sly PD, Upham JW: **Monocytes from children with clinically stable cystic fibrosis show enhanced expression of Toll-like receptor 4.** *Pediatr Pulmonol* 2010, **45**(9):883-889.
18. Tarique AA, Sly PD, Cardenas DG, Luo L, Stow JL, Bell SC, Wainwright CE, Fantino E: **Differential expression of genes and receptors in monocytes from patients with cystic fibrosis.** *J Cyst Fibros* 2018.
19. Tarique AA, Sly PD, Holt PG, Bosco A, Ware RS, Logan J, Bell SC, Wainwright CE, Fantino E: **CFTR-dependent defect in alternatively-activated macrophages in cystic fibrosis.** *J Cyst Fibros* 2017, **16**(4):475-482.
20. Saint-Criq V, Gray MA: **Role of CFTR in epithelial physiology.** In: *Cell Mol Life Sci.* vol. 74; 2017: 93-115.
21. Lukacs GL, Verkman A: **CFTR: folding, misfolding and correcting the $\Delta F508$ conformational defect.** *Trends Mol Med* 2012, **18**(2):81-91.
22. Bonfield TL, Panuska JR, Konstan MW, Hilliard KA, Hilliard JB, Ghnaim H, Berger M: **Inflammatory cytokines in cystic fibrosis lungs.** *Am J Respir Crit Care Med* 1995, **152**(6 Pt 1):2111-2118.
23. Peckham D, Scambler T, Savic S, McDermott MF: **The burgeoning field of innate immune-mediated disease and autoinflammation.** *J Pathol* 2017, **241**(2):123-139.
24. Singh VK, Schwarzenberg SJ: **Pancreatic insufficiency in Cystic Fibrosis.** *J Cyst Fibros* 2017, **16** Suppl 2:S70-s78.
25. Wilschanski M, Durie PR: **Pathology of pancreatic and intestinal disorders in cystic fibrosis.** *J R Soc Med* 1998, **91**(Suppl 34):40-49.

26. Wilschanski M, Novak I: **The Cystic Fibrosis of Exocrine Pancreas.** In: *Cold Spring Harb Perspect Med.* vol. 3; 2013.
27. Baldwin C, Zerofsky M, Sathe M, Troendle DM, Perito ER: **Acute Recurrent and Chronic Pancreatitis as Initial Manifestations of Cystic Fibrosis and Cystic Fibrosis Transmembrane Conductance Regulator-Related Disorders.** *Pancreas* 2019, **48**(7):888-893.
28. Kelsey R, Manderson Koivula FN, McClenaghan NH, Kelly C: **Cystic Fibrosis-Related Diabetes: Pathophysiology and Therapeutic Challenges.** *Clin Med Insights Endocrinol Diabetes* 2019, **12**:1179551419851770.
29. Moheet A, Moran A: **CF-related diabetes: Containing the metabolic miscreant of cystic fibrosis.** *Pediatr Pulmonol* 2017, **52**(S48):S37-s43.
30. Lara-Reyna S, Scambler T, Holbrook J, Wong C, Jarosz-Griffiths HH, Martinon F, Savic S, Peckham D, McDermott MF: **Metabolic Reprograming of Cystic Fibrosis Macrophages via the IRE1 α Arm of the Unfolded Protein Response Results in Exacerbated Inflammation.** *Front Immunol* 2019, **10**.
31. Clarke EA, Watson P, Freeston JE, Peckham DG, Jones AM, Horsley A: **Assessing arthritis in the context of cystic fibrosis.** *Pediatr Pulmonol* 2019, **54**(6):770-777.
32. De Boeck K, Zolin A, Cuppens H, Olesen HV, Viviani L: **The relative frequency of CFTR mutation classes in European patients with cystic fibrosis.** *J Cyst Fibros* 2014, **13**(4):403-409.
33. Okiyoneda T, Harada K, Takeya M, Yamahira K, Wada I, Shuto T, Suico MA, Hashimoto Y, Kai H: **Δ F508 CFTR Pool in the Endoplasmic Reticulum Is Increased by Calnexin Overexpression.** *Mol Biol Cell* 2004, **15**(2):563-574.
34. Veit G, Avramescu RG, Chiang AN, Houck SA, Cai Z, Peters KW, Hong JS, Pollard HB, Guggino WB, Balch WE *et al*: **From CFTR biology toward combinatorial pharmacotherapy: expanded classification of cystic fibrosis mutations.** In: *Mol Biol Cell.* vol. 27; 2016: 424-433.
35. Highsmith WE, Jr., Burch LH, Zhou Z, Olsen JC, Strong TV, Smith T, Friedman KJ, Silverman LM, Boucher RC, Collins FS *et al*: **Identification of a splice site mutation (2789 +5 G > A) associated with small amounts of normal CFTR mRNA and mild cystic fibrosis.** *Hum Mutat* 1997, **9**(4):332-338.
36. Silvis MR, Picciano JA, Bertrand C, Weixel K, Bridges RJ, Bradbury NA: **A mutation in the cystic fibrosis transmembrane conductance regulator generates a novel internalization sequence and enhances endocytic rates.** *J Biol Chem* 2003, **278**(13):11554-11560.

37. Marson FAL, Bertuzzo CS, Ribeiro JD: **Classification of CFTR mutation classes.** *Lancet Respir Med* 2016, **4**(8):e37-e38.
38. De Boeck K, Amaral MD: **Progress in therapies for cystic fibrosis.** *Lancet Respir Med* 2016, **4**(8):662-674.
39. Henke MO, Ratjen F: **Mucolytics in cystic fibrosis.** *Paediatr Respir Rev* 2007, **8**(1):24-29.
40. Manzenreiter R, Kienberger F, Marcos V, Schilcher K, Krautgartner WD, Obermayer A, Huml M, Stoiber W, Hector A, Griese M *et al*: **Ultrastructural characterization of cystic fibrosis sputum using atomic force and scanning electron microscopy.** *J Cyst Fibros* 2012, **11**(2):84-92.
41. Brinkmann V, Reichard U, Goosmann C, Fauler B, Uhlemann Y, Weiss DS, Weinrauch Y, Zychlinsky A: **Neutrophil extracellular traps kill bacteria.** *Science* 2004, **303**(5663):1532-1535.
42. Papayannopoulos V: **Neutrophil extracellular traps in immunity and disease.** *Nat Rev Immunol* 2018, **18**(2):134-147.
43. Dwyer M, Shan Q, D'Ortona S, Maurer R, Mitchell R, Olesen H, Thiel S, Huebner J, Gadjeva M: **Cystic fibrosis sputum DNA has NETosis characteristics and neutrophil extracellular trap release is regulated by macrophage migration-inhibitory factor.** *J Innate Immun* 2014, **6**(6):765-779.
44. Papayannopoulos V, Staab D, Zychlinsky A: **Neutrophil elastase enhances sputum solubilization in cystic fibrosis patients receiving DNase therapy.** *PLoS One* 2011, **6**(12):e28526.
45. Martínez-Alemán SR, Campos-García L, Palma-Nicolas JP, Hernández-Bello R, González GM, Sánchez-González A: **Understanding the Entanglement: Neutrophil Extracellular Traps (NETs) in Cystic Fibrosis.** *Front Cell Infect Microbiol* 2017, **7**.
46. Konstan MW, Ratjen F: **Effect of dornase alfa on inflammation and lung function: potential role in the early treatment of cystic fibrosis.** *J Cyst Fibros* 2012, **11**(2):78-83.
47. Edmondson C, Davies JC: **Current and future treatment options for cystic fibrosis lung disease: latest evidence and clinical implications.** In: *Ther Adv Chronic Dis.* vol. 7; 2016: 170-183.
48. Tse HN, Tseng CZS: **Update on the pathological processes, molecular biology, and clinical utility of N-acetylcysteine in chronic obstructive pulmonary disease.** In: *Int J Chron Obstruct Pulmon Dis.* vol. 9; 2014: 825-836.
49. Dauletbaev N, Fischer P, Aulbach B, Gross J, Kusche W, Thyroff-Friesinger U, Wagner TO, Bargon J: **A phase II study on safety and efficacy of high-**

- dose N-acetylcysteine in patients with cystic fibrosis. *Eur J Med Res* 2009, **14**(8):352-358.
50. Conrad C, Lymp J, Thompson V, Dunn C, Davies Z, Chatfield B, Nichols D, Clancy J, Vender R, Egan ME *et al*: **Long-term treatment with oral N-acetylcysteine: affects lung function but not sputum inflammation in cystic fibrosis subjects. A phase II randomized placebo-controlled trial.** *J Cyst Fibros* 2015, **14**(2):219-227.
 51. Elkins MR, Robinson M, Rose BR, Harbour C, Moriarty CP, Marks GB, Belousova EG, Xuan W, Bye PT: **A controlled trial of long-term inhaled hypertonic saline in patients with cystic fibrosis.** *N Engl J Med* 2006, **354**(3):229-240.
 52. Aitken ML, Bellon G, De Boeck K, Flume PA, Fox HG, Geller DE, Haarman EG, Hebestreit HU, Lapey A, Schou IM *et al*: **Long-term inhaled dry powder mannitol in cystic fibrosis: an international randomized study.** *Am J Respir Crit Care Med* 2012, **185**(6):645-652.
 53. Bilton D, Daviskas E, Anderson SD, Kolbe J, King G, Stirling RG, Thompson BR, Milne D, Charlton B: **Phase 3 randomized study of the efficacy and safety of inhaled dry powder mannitol for the symptomatic treatment of non-cystic fibrosis bronchiectasis.** *Chest* 2013, **144**(1):215-225.
 54. Goss CH, Burns JL: **Exacerbations in cystic fibrosis. 1: Epidemiology and pathogenesis.** *Thorax* 2007, **62**(4):360-367.
 55. Harrison F: **Microbial ecology of the cystic fibrosis lung.** *Microbiology* 2007, **153**(Pt 4):917-923.
 56. Foundation. CF: **Patient Registry 2004 Annual Data Report.** In. 1–2. Bethesda, Maryland; 2005.
 57. Kidd TJ, Canton R, Ekkelenkamp M, Johansen HK, Gilligan P, LiPuma JJ, Bell SC, Elborn JS, Flume PA, VanDevanter DR *et al*: **Defining antimicrobial resistance in cystic fibrosis.** *J Cyst Fibros* 2018, **17**(6):696-704.
 58. Roesch EA, Nichols DP, Chmiel JF: **Inflammation in cystic fibrosis: An update.** *Pediatr Pulmonol* 2018, **53**(S3):S30-s50.
 59. Gray RD, Hardisty G, Regan KH, Smith M, Robb CT, Duffin R, Mackellar A, Felton JM, Paemka L, McCullagh BN *et al*: **Delayed neutrophil apoptosis enhances NET formation in cystic fibrosis.** *Thorax* 2018, **73**(2):134-144.
 60. Culic O, Erakovic V, Parnham MJ: **Anti-inflammatory effects of macrolide antibiotics.** *Eur J Pharmacol* 2001, **429**(1-3):209-229.
 61. Jaffe A, Bush A: **Anti-inflammatory effects of macrolides in lung disease.** *Pediatr Pulmonol* 2001, **31**(6):464-473.
 62. Southern KW, Barker PM, Solis-Moya A, Patel L: **Macrolide antibiotics for cystic fibrosis.** *Cochrane Database Syst Rev* 2012, **11**:Cd002203.

63. Mustafa MH, Khandekar S, Tunney MM, Elborn JS, Kahl BC, Denis O, Plesiat P, Traore H, Tulkens PM, Vanderbist F *et al*: **Acquired resistance to macrolides in *Pseudomonas aeruginosa* from cystic fibrosis patients.** *Eur Respir J* 2017, **49**(5).
64. Whiting P, Al M, Burgers L, Westwood M, Ryder S, Hoogendoorn M, Armstrong N, Allen A, Severens H, Kleijnen J: **Ivacaftor for the treatment of patients with cystic fibrosis and the G551D mutation: a systematic review and cost-effectiveness analysis.** *Health Technol Assess* 2014, **18**(18):1-106.
65. Moss RB, Flume PA, Elborn JS, Cooke J, Rowe SM, McColley SA, Rubenstein RC, Higgins M: **Efficacy and safety of ivacaftor in patients with cystic fibrosis who have an Arg117His-CFTR mutation: a double-blind, randomised controlled trial.** *Lancet Respir Med* 2015, **3**(7):524-533.
66. De Boeck K, Munck A, Walker S, Faro A, Hiatt P, Gilmartin G, Higgins M: **Efficacy and safety of ivacaftor in patients with cystic fibrosis and a non-G551D gating mutation.** *J Cyst Fibros* 2014, **13**(6):674-680.
67. Kramer EL, Clancy JP: **CFTR Modulator Therapies in Pediatric Cystic Fibrosis: Focus on Ivacaftor.** *Expert Opin Orphan Drugs* 2016, **4**(10):1033-1042.
68. Molinski SV, Ahmadi S, Ip W, Ouyang H, Vilella A, Miller JP, Lee P, Kulleperuma K, Du K, Di Paola M *et al*: **Orkambi® and amplifier co-therapy improves function from a rare CFTR mutation in gene-edited cells and patient tissue.** *EMBO Mol Med* 2017, **9**(9):1224-1243.
69. Maiuri L, Stefano DD, Raia V, Kroemer G: **The holy grail of cystic fibrosis research: pharmacological repair of the F508del-CFTR mutation.** *3* 2015.
70. Wainwright CE, Elborn JS, Ramsey BW, Marigowda G, Huang X, Cipolli M, Colombo C, Davies JC, De Boeck K, Flume PA *et al*: **Lumacaftor-ivacaftor in Patients with Cystic Fibrosis Homozygous for Phe508del CFTR.** *N Engl J Med* 2015, **373**(3):220-231.
71. Connett G: **Lumacaftor-ivacaftor in the treatment of cystic fibrosis: design, development and place in therapy.** In: *Drug Des Devel Ther.* vol. 13; 2019: 2405-2412.
72. Taylor-Cousar JL, Munck A, McKone EF, van der Ent CK, Moeller A, Simard C, Wang LT, Ingenito EP, McKee C, Lu Y *et al*: **Tezacaftor–Ivacaftor in Patients with Cystic Fibrosis Homozygous for Phe508del.** *N Engl J Med* 2017.
73. Jennings MT, Dezube R, Paranjape S, West NE, Hong G, Braun A, Grant J, Merlo CA, Lechtzin N: **An Observational Study of Outcomes and Tolerances in Patients with Cystic Fibrosis Initiated on Lumacaftor/Ivacaftor.** *Ann Am Thorac Soc* 2017, **14**(11):1662-1666.

74. Hubert D, Chiron R, Camara B, Grenet D, Prevotat A, Bassinet L, Dominique S, Rault G, Macey J, Honore I *et al*: **Real-life initiation of lumacaftor/ivacaftor combination in adults with cystic fibrosis homozygous for the Phe508del CFTR mutation and severe lung disease.** *J Cyst Fibros* 2017, **16**(3):388-391.
75. **Two Phase 3 Studies of the Triple Combination of VX-445, Tezacaftor and Ivacaftor Met Primary Endpoint of Improvement in Lung Function (ppFEV1) in People with Cystic Fibrosis** [<https://investors.vrtx.com/news-releases/news-release-details/correcting-and-replacing-two-phase-3-studies-triple-combination>]
76. Keating D, Marigowda G, Burr L, Daines C, Mall MA, McKone EF, Ramsey BW, Rowe SM, Sass LA, Tullis E *et al*: **VX-445–Tezacaftor–Ivacaftor in Patients with Cystic Fibrosis and One or Two Phe508del Alleles.** *N Engl J Med* 2018.
77. Middleton PG, Mall MA, Drevinek P, Lands LC, McKone EF, Polineni D, Ramsey BW, Taylor-Cousar JL, Tullis E, Vermeulen F *et al*: **Elexacaftor–Tezacaftor–Ivacaftor for Cystic Fibrosis with a Single Phe508del Allele.** *N Engl J Med* 2019, **381**(19):1809-1819.
78. **Drug Development Pipeline** [<https://www.cff.org/Trials/Pipeline>]
79. Donnelley M, Parsons DW: **Gene Therapy for Cystic Fibrosis Lung Disease: Overcoming the Barriers to Translation to the Clinic.** *Front Pharmacol* 2018, **9**:1381.
80. Marangi M, Pistritto G: **Innovative Therapeutic Strategies for Cystic Fibrosis: Moving Forward to CRISPR Technique.** *Front Pharmacol* 2018, **9**.
81. Jacquot J, Tabary O, Le Rouzic P, Clement A: **Airway epithelial cell inflammatory signalling in cystic fibrosis.** *Int J Biochem Cell Biol* 2008, **40**(9):1703-1715.
82. Stecenko AA, King G, Torii K, Breyer RM, Dworski R, Blackwell TS, Christman JW, Brigham KL: **Dysregulated cytokine production in human cystic fibrosis bronchial epithelial cells.** *Inflammation* 2001, **25**(3):145-155.
83. Kube D, Sontich U, Fletcher D, Davis PB: **Proinflammatory cytokine responses to P. aeruginosa infection in human airway epithelial cell lines.** *Am J Physiol Lung Cell Mol Physiol* 2001, **280**(3):L493-502.
84. Muhlebach MS, Reed W, Noah TL: **Quantitative cytokine gene expression in CF airway.** *Pediatr Pulmonol* 2004, **37**(5):393-399.
85. Perez A, Issler AC, Cotton CU, Kelley TJ, Verkman AS, Davis PB: **CFTR inhibition mimics the cystic fibrosis inflammatory profile.** *Am J Physiol Lung Cell Mol Physiol* 2007, **292**(2):L383-395.

86. Mittal M, Siddiqui MR, Tran K, Reddy SP, Malik AB: **Reactive oxygen species in inflammation and tissue injury.** *Antioxid Redox Signal* 2014, **20**(7):1126-1167.
87. Pongnimitprasert N, Hurtado M, Lamari F, El Benna J, Dupuy C, Fay M, Foglietti MJ, Bernard M, Gougerot-Pocidallo MA, Braut-Boucher F: **Implication of NADPH Oxidases in the Early Inflammation Process Generated by Cystic Fibrosis Cells.** *ISRN Inflamm* 2012, **2012**.
88. Ribeiro CM, Paradiso AM, Carew MA, Shears SB, Boucher RC: **Cystic fibrosis airway epithelial Ca²⁺ i signaling: the mechanism for the larger agonist-mediated Ca²⁺ i signals in human cystic fibrosis airway epithelia.** *J Biol Chem* 2005, **280**(11):10202-10209.
89. Ribeiro CM, Paradiso AM, Schwab U, Perez-Vilar J, Jones L, O'Neal W, Boucher RC: **Chronic airway infection/inflammation induces a Ca²⁺i-dependent hyperinflammatory response in human cystic fibrosis airway epithelia.** *J Biol Chem* 2005, **280**(18):17798-17806.
90. Semaniakou A, Croll RP, Chappe V: **Animal Models in the Pathophysiology of Cystic Fibrosis.** *Front Pharmacol* 2018, **9**.
91. Clarke LL, Grubb BR, Yankaskas JR, Cotton CU, McKenzie A, Boucher RC: **Relationship of a non-cystic fibrosis transmembrane conductance regulator-mediated chloride conductance to organ-level disease in Cftr(-/-) mice.** *Proc Natl Acad Sci U S A* 1994, **91**(2):479-483.
92. Kent G, Iles R, Bear CE, Huan LJ, Griesenbach U, McKerlie C, Frndova H, Ackerley C, Gosselin D, Radzioch D *et al*: **Lung disease in mice with cystic fibrosis.** *J Clin Invest* 1997, **100**(12):3060-3069.
93. Guilbault C, Martin P, Houle D, Boghdady ML, Guiot MC, Marion D, Radzioch D: **Cystic fibrosis lung disease following infection with Pseudomonas aeruginosa in Cftr knockout mice using novel non-invasive direct pulmonary infection technique.** *Lab Anim* 2005, **39**(3):336-352.
94. Guilbault C, Novak JP, Martin P, Boghdady ML, Saeed Z, Guiot MC, Hudson TJ, Radzioch D: **Distinct pattern of lung gene expression in the Cftr-KO mice developing spontaneous lung disease compared with their littermate controls.** *Physiol Genomics* 2006, **25**(2):179-193.
95. Durie PR, Kent G, Phillips MJ, Ackerley CA: **Characteristic multiorgan pathology of cystic fibrosis in a long-living cystic fibrosis transmembrane regulator knockout murine model.** *Am J Pathol* 2004, **164**(4):1481-1493.
96. Bruscia EM, Bonfield TL: **Cystic Fibrosis Lung Immunity: The Role of the Macrophage.** *J Innate Immun* 2016, **8**(6):550-563.
97. Zhou Z, Duerr J, Johannesson B, Schubert SC, Treis D, Harm M, Graeber SY, Dalpke A, Schultz C, Mall MA: **The ENaC-overexpressing mouse as a**

- model of cystic fibrosis lung disease. *J Cyst Fibros* 2011, **10** Suppl 2:S172-182.
98. Moore PJ, Tarran R: **The epithelial sodium channel (ENaC) as a therapeutic target for cystic fibrosis lung disease.** *Expert Opin Ther Targets* 2018, **22**(8):687-701.
99. Welsh MJ, Rogers CS, Stoltz DA, Meyerholz DK, Prather RS: **Development of a porcine model of cystic fibrosis.** *Trans Am Clin Climatol Assoc* 2009, **120**:149-162.
100. Stoltz DA, Meyerholz DK, Pezzulo AA, Ramachandran S, Rogan MP, Davis GJ, Hanfland RA, Wohlford-Lenane C, Dohrn CL, Bartlett JA *et al*: **Cystic fibrosis pigs develop lung disease and exhibit defective bacterial eradication at birth.** *Sci Transl Med* 2010, **2**(29):29ra31.
101. Ostedgaard LS, Meyerholz DK, Chen JH, Pezzulo AA, Karp PH, Rokhlina T, Ernst SE, Hanfland RA, Reznikov LR, Ludwig PS *et al*: **The DeltaF508 mutation causes CFTR misprocessing and cystic fibrosis-like disease in pigs.** *Sci Transl Med* 2011, **3**(74):74ra24.
102. Sun X, Sui H, Fisher JT, Yan Z, Liu X, Cho HJ, Joo NS, Zhang Y, Zhou W, Yi Y *et al*: **Disease phenotype of a ferret CFTR-knockout model of cystic fibrosis.** *J Clin Invest* 2010, **120**(9):3149-3160.
103. Sun X, Olivier AK, Liang B, Yi Y, Sui H, Evans TI, Zhang Y, Zhou W, Tyler SR, Fisher JT *et al*: **Lung phenotype of juvenile and adult cystic fibrosis transmembrane conductance regulator-knockout ferrets.** *Am J Respir Cell Mol Biol* 2014, **50**(3):502-512.
104. Keiser NW, Birket SE, Evans IA, Tyler SR, Crooke AK, Sun X, Zhou W, Nellis JR, Stroebelen EK, Chu KK *et al*: **Defective innate immunity and hyperinflammation in newborn cystic fibrosis transmembrane conductance regulator-knockout ferret lungs.** *Am J Respir Cell Mol Biol* 2015, **52**(6):683-694.
105. Sun X, Yi Y, Yan Z, Rosen BH, Liang B, Winter MC, Evans TIA, Rotti PG, Yang Y, Gray JS *et al*: **In utero and postnatal VX-770 administration rescues multiorgan disease in a ferret model of cystic fibrosis.** *Sci Transl Med* 2019, **11**(485).
106. Fan Z, Perisse IV, Cotton CU, Regouski M, Meng Q, Domb C, Van Wettere AJ, Wang Z, Harris A, White KL *et al*: **A sheep model of cystic fibrosis generated by CRISPR/Cas9 disruption of the CFTR gene.** *JCI Insight* 2018, **3**(19).
107. Navis A, Bagnat M: **Loss of cftr function leads to pancreatic destruction in larval zebrafish.** *Dev Biol* 2015, **399**(2):237-248.
108. Mesureur J, Feliciano JR, Wagner N, Gomes MC, Zhang L, Blanco-Gonzalez M, van der Vaart M, O'Callaghan D, Meijer AH, Vergunst AC:

- Macrophages, but not neutrophils, are critical for proliferation of Burkholderia cenocepacia and ensuing host-damaging inflammation.** *PLoS Pathog* 2017, **13**(6):e1006437.
109. Chaplin DD: **Overview of the Immune Response.** *J Allergy Clin Immunol* 2010, **125**(2 Suppl 2):S3-23.
 110. Tan HL, Regamey N, Brown S, Bush A, Lloyd CM, Davies JC: **The Th17 pathway in cystic fibrosis lung disease.** *Am J Respir Crit Care Med* 2011, **184**(2):252-258.
 111. Zhang S, Shrestha CL, Kopp BT: **Cystic fibrosis transmembrane conductance regulator (CFTR) modulators have differential effects on cystic fibrosis macrophage function.** *Sci Rep* 2018, **8**(1):17066.
 112. Porto PD, Cifani N, Guarnieri S, Di Domenico EG, Mariggiò MA, Spadaro F, Guglietta S, Anile M, Venuta F, Quattrucci S *et al*: **Dysfunctional CFTR Alters the Bactericidal Activity of Human Macrophages against Pseudomonas aeruginosa.** In: *PLoS One*. vol. 6; 2011.
 113. Lubamba BA, Jones LC, O'Neal WK, Boucher RC, Ribeiro CM: **X-Box-Binding Protein 1 and Innate Immune Responses of Human Cystic Fibrosis Alveolar Macrophages.** *Am J Respir Crit Care Med* 2015, **192**(12):1449-1461.
 114. Law SM, Gray RD: **Neutrophil extracellular traps and the dysfunctional innate immune response of cystic fibrosis lung disease: a review.** *J Inflamm (Lond)* 2017, **14**:29.
 115. Alexis NE, Muhlebach MS, Peden DB, Noah TL: **ATTENUATION OF HOST DEFENSE FUNCTION OF LUNG PHAGOCYTES IN YOUNG CYSTIC FIBROSIS PATIENTS.** *J Cyst Fibros* 2006, **5**(1):17-25.
 116. Rao S, Wright AK, Montiero W, Ziegler-Heitbrock L, Grigg J: **Monocyte chemoattractant chemokines in cystic fibrosis.** *J Cyst Fibros* 2009, **8**(2):97-103.
 117. Bruscia EM, Zhang PX, Satoh A, Caputo C, Medzhitov R, Shenoy A, Egan ME, Krause DS: **Abnormal trafficking and degradation of TLR4 underlie the elevated inflammatory response in cystic fibrosis.** *J Immunol* 2011, **186**(12):6990-6998.
 118. Zaman MM, Gelrud A, Junaidi O, Regan MM, Warny M, Shea JC, Kelly C, O'Sullivan BP, Freedman SD: **Interleukin 8 secretion from monocytes of subjects heterozygous for the deltaF508 cystic fibrosis transmembrane conductance regulator gene mutation is altered.** *Clin Diagn Lab Immunol* 2004, **11**(5):819-824.
 119. Bonfield TL, Hodges CA, Cotton CU, Drumm ML: **Absence of the cystic fibrosis transmembrane regulator (Cftr) from myeloid-derived cells slows**

- resolution of inflammation and infection. *J Leukoc Biol* 2012, **92**(5):1111-1122.
120. Murray PJ, Allen JE, Biswas SK, Fisher EA, Gilroy DW, Goerdt S, Gordon S, Hamilton JA, Ivashkiv LB, Lawrence T *et al*: **Macrophage activation and polarization: nomenclature and experimental guidelines.** *Immunity* 2014, **41**(1):14-20.
121. Davies LC, Taylor PR: **Tissue-resident macrophages: then and now.** *Immunology* 2015, **144**(4):541-548.
122. Davies LC, Jenkins SJ, Allen JE, Taylor PR: **Tissue-resident macrophages.** *Nature Immunology* 2013, **14**(10):986-995.
123. Biswas SK, Mantovani A: **Macrophage plasticity and interaction with lymphocyte subsets: cancer as a paradigm.** *Nat Immunol* 2010, **11**(10):889-896.
124. Shapouri-Moghaddam A, Mohammadian S, Vazini H, Taghadosi M, Esmaeili SA, Mardani F, Seifi B, Mohammadi A, Afshari JT, Sahebkar A: **Macrophage plasticity, polarization, and function in health and disease.** *J Cell Physiol* 2018, **233**(9):6425-6440.
125. Ulrich M, Worlitzsch D, Viglio S, Siegmann N, Iadarola P, Shute JK, Geiser M, Pier GB, Friedel G, Barr ML *et al*: **Alveolar Inflammation in Cystic Fibrosis.** *J Cyst Fibros* 2010, **9**(3):217-227.
126. Meyer M, Huaux F, Gavilanes X, van den Brule S, Lebecque P, Lo Re S, Lison D, Scholte B, Wallemacq P, Leal T: **Azithromycin reduces exaggerated cytokine production by M1 alveolar macrophages in cystic fibrosis.** *Am J Respir Cell Mol Biol* 2009, **41**(5):590-602.
127. Karpati F, Hjelte FL, Wretling B: **TNF-alpha and IL-8 in consecutive sputum samples from cystic fibrosis patients during antibiotic treatment.** *Scand J Infect Dis* 2000, **32**(1):75-79.
128. Reeves EP, Williamson M, O'Neill SJ, Grealley P, McElvaney NG: **Nebulized hypertonic saline decreases IL-8 in sputum of patients with cystic fibrosis.** *Am J Respir Crit Care Med* 2011, **183**(11):1517-1523.
129. Walter P, Ron D: **The unfolded protein response: from stress pathway to homeostatic regulation.** *Science* 2011, **334**(6059):1081-1086.
130. Li H, Korennykh AV, Behrman SL, Walter P: **Mammalian endoplasmic reticulum stress sensor IRE1 signals by dynamic clustering.** *Proc Natl Acad Sci U S A* 2010, **107**(37):16113-16118.
131. Wouters BG, Koritzinsky M: **Hypoxia signalling through mTOR and the unfolded protein response in cancer.** *Nat Rev Cancer* 2008, **8**(11):851-864.
132. Zeeshan HM, Lee GH, Kim HR, Chae HJ: **Endoplasmic Reticulum Stress and Associated ROS.** *Int J Mol Sci* 2016, **17**(3):327.

133. Savic S, Ouboussad L, Dickie LJ, Geiler J, Wong C, Doody GM, Churchman SM, Ponchel F, Emery P, Cook GP *et al*: **TLR dependent XBP-1 activation induces an autocrine loop in rheumatoid arthritis synoviocytes.** *J Autoimmun* 2014, **50**:59-66.
134. Brewer JW: **Regulatory crosstalk within the mammalian unfolded protein response.** *Cell Mol Life Sci* 2014, **71**(6):1067-1079.
135. Hollien J, Lin JH, Li H, Stevens N, Walter P, Weissman JS: **Regulated Ire1-dependent decay of messenger RNAs in mammalian cells.** *J Cell Biol* 2009, **186**(3):323-331.
136. Calfon M, Zeng H, Urano F, Till JH, Hubbard SR, Harding HP, Clark SG, Ron D: **IRE1 couples endoplasmic reticulum load to secretory capacity by processing the XBP-1 mRNA.** *Nature* 2002, **415**(6867):92-96.
137. Lee K, Tirasophon W, Shen X, Michalak M, Prywes R, Okada T, Yoshida H, Mori K, Kaufman RJ: **IRE1-mediated unconventional mRNA splicing and S2P-mediated ATF6 cleavage merge to regulate XBP1 in signaling the unfolded protein response.** *Genes Dev* 2002, **16**(4):452-466.
138. Lee AH, Iwakoshi NN, Glimcher LH: **XBP-1 regulates a subset of endoplasmic reticulum resident chaperone genes in the unfolded protein response.** *Mol Cell Biol* 2003, **23**(21):7448-7459.
139. Piperi C, Adamopoulos C, Papavassiliou AG: **XBP1: A Pivotal Transcriptional Regulator of Glucose and Lipid Metabolism.** *Trends Endocrinol Metab* 2016, **27**(3):119-122.
140. Song M, Sandoval TA, Chae CS, Chopra S, Tan C, Rutkowski MR, Raundhal M, Chaurio RA, Payne KK, Konrad C *et al*: **IRE1alpha-XBP1 controls T cell function in ovarian cancer by regulating mitochondrial activity.** *Nature* 2018, **562**(7727):423-428.
141. Margariti A, Li H, Chen T, Martin D, Vizcay-Barrena G, Alam S, Karamariti E, Xiao Q, Zampetaki A, Zhang Z *et al*: **XBP1 mRNA splicing triggers an autophagic response in endothelial cells through BECLIN-1 transcriptional activation.** *J Biol Chem* 2013, **288**(2):859-872.
142. Adachi Y, Yamamoto K, Okada T, Yoshida H, Harada A, Mori K: **ATF6 is a transcription factor specializing in the regulation of quality control proteins in the endoplasmic reticulum.** *Cell Struct Funct* 2008, **33**(1):75-89.
143. Harding HP, Zhang Y, Ron D: **Protein translation and folding are coupled by an endoplasmic-reticulum-resident kinase.** *Nature* 1999, **397**(6716):271-274.
144. Wek RC, Jiang HY, Anthony TG: **Coping with stress: eIF2 kinases and translational control.** *Biochem Soc Trans* 2006, **34**(Pt 1):7-11.

145. Li Y, Guo Y, Tang J, Jiang J, Chen Z: **New insights into the roles of CHOP-induced apoptosis in ER stress.** *Acta Biochim Biophys Sin (Shanghai)* 2014, **46**(8):629-640.
146. Nishitoh H: **CHOP is a multifunctional transcription factor in the ER stress response.** *J Biochem* 2012, **151**(3):217-219.
147. Brush MH, Weiser DC, Shenolikar S: **Growth arrest and DNA damage-inducible protein GADD34 targets protein phosphatase 1 alpha to the endoplasmic reticulum and promotes dephosphorylation of the alpha subunit of eukaryotic translation initiation factor 2.** *Mol Cell Biol* 2003, **23**(4):1292-1303.
148. Cullinan SB, Zhang D, Hannink M, Arvisais E, Kaufman RJ, Diehl JA: **Nrf2 is a direct PERK substrate and effector of PERK-dependent cell survival.** *Mol Cell Biol* 2003, **23**(20):7198-7209.
149. Ma Q: **Role of Nrf2 in Oxidative Stress and Toxicity.** *Annu Rev Pharmacol Toxicol* 2013, **53**:401-426.
150. McGonagle D, McDermott MF: **A proposed classification of the immunological diseases.** *PLoS Medicine* 2006, **3**(8):1242-1248.
151. Martinon F, Chen X, Lee AH, Glimcher LH: **TLR activation of the transcription factor XBP1 regulates innate immune responses in macrophages.** *Nat Immunol* 2010, **11**(5):411-418.
152. Dickie LJ, Aziz AM, Savic S, Lucherini OM, Cantarini L, Geiler J, Wong CH, Coughlan R, Lane T, Lachmann HJ *et al*: **Involvement of X-box binding protein 1 and reactive oxygen species pathways in the pathogenesis of tumour necrosis factor receptor-associated periodic syndrome.** *Ann Rheum Dis* 2012, **71**(12):2035-2043.
153. Grootjans J, Kaser A, Kaufman RJ, Blumberg RS: **The unfolded protein response in immunity and inflammation.** *Nat Rev Immunol* 2016, **16**(8):469-484.
154. Talty A, Deegan S, Ljujic M, Mnich K, Naicker SD, Quandt D, Zeng Q, Patterson JB, Gorman AM, Griffin MD *et al*: **Inhibition of IRE1alpha RNase activity reduces NLRP3 inflammasome assembly and processing of pro-IL1beta.** *Cell Death Dis* 2019, **10**(9):622.
155. Iwasaki Y, Suganami T, Hachiya R, Shirakawa I, Kim-Saijo M, Tanaka M, Hamaguchi M, Takai-Igarashi T, Nakai M, Miyamoto Y *et al*: **Activating transcription factor 4 links metabolic stress to interleukin-6 expression in macrophages.** *Diabetes* 2014, **63**(1):152-161.
156. Wang S, Kaufman RJ: **The impact of the unfolded protein response on human disease.** *J Cell Biol* 2012, **197**(7):857-867.
157. Cantarini L, Lucherini OM, Muscari I, Frediani B, Galeazzi M, Brizi MG, Simonini G, Cimaz R: **Tumour necrosis factor receptor-associated periodic**

- syndrome (TRAPS): state of the art and future perspectives. *Autoimmun Rev* 2012, **12**(1):38-43.
158. Dickie LJ, Aziz AM, Savic S, Lucherini OM, Cantarini L, Geiler J, Wong CH, Coughlan R, Lane T, Lachmann HJ: **Involvement of X-box binding protein 1 and reactive oxygen species pathways in the pathogenesis of tumour necrosis factor receptor-associated periodic syndrome.** *Annals of the Rheumatic Diseases* 2012, **71**(12):2035-2043.
159. Harrison S, University of Leeds IoRaMM, Leeds, United Kingdom, um11srh@leeds.ac.uk, Scambler T, University of Leeds IoRaMM, Leeds, United Kingdom, umtes@leeds.ac.uk, Oubussad L, University of Leeds IoRaMM, Leeds, United Kingdom, L.Ouboussad@leeds.ac.uk, Wong C *et al*: **IRE1-mediated downregulation of miR-146a and miR-155 in primary dermal fibroblasts across three TNFRSF1A mutations results in hyperresponsiveness to LPS.** *Frontiers in Immunology* 2018, **9**.
160. Swanson KV, Deng M, Ting JP: **The NLRP3 inflammasome: molecular activation and regulation to therapeutics.** *Nat Rev Immunol* 2019, **19**(8):477-489.
161. Menu P, Mayor A, Zhou R, Tardivel A, Ichijo H, Mori K, Tschopp J: **ER stress activates the NLRP3 inflammasome via an UPR-independent pathway.** *Cell Death Dis* 2012, **3**:e261.
162. Kim S, Joe Y, Jeong SO, Zheng M, Back SH, Park SW, Ryter SW, Chung HT: **Endoplasmic reticulum stress is sufficient for the induction of IL-1beta production via activation of the NF-kappaB and inflammasome pathways.** *Innate Immun* 2014, **20**(8):799-815.
163. Bronner DN, Abuaita BH, Chen X, Fitzgerald KA, Nunez G, He Y, Yin XM, O'Riordan MX: **Endoplasmic Reticulum Stress Activates the Inflammasome via NLRP3- and Caspase-2-Driven Mitochondrial Damage.** *Immunity* 2015, **43**(3):451-462.
164. Lerner AG, Upton JP, Praveen P, Ghosh R, Nakagawa Y, Igbaria A, Shen S, Nguyen V, Backes BJ, Heiman M *et al*: **IRE1 α induces thioredoxin-interacting protein to activate the NLRP3 inflammasome and promote programmed cell death during endoplasmic reticulum stress.** *Cell Metab* 2012, **16**(2):250-264.
165. Qiu Q, Zheng Z, Chang L, Zhao YS, Tan C, Dandekar A, Zhang Z, Lin Z, Gui M, Li X *et al*: **Toll-like receptor-mediated IRE1 α activation as a therapeutic target for inflammatory arthritis.** *EMBO J* 2013, **32**(18):2477-2490.
166. Kim S, Joe Y, Kim HJ, Kim YS, Jeong SO, Pae HO, Ryter SW, Surh YJ, Chung HT: **Endoplasmic reticulum stress-induced IRE1 α activation mediates cross-talk of GSK-3 β and XBP-1 to regulate inflammatory cytokine production.** *J Immunol* 2015, **194**(9):4498-4506.

167. Tagawa Y, Hiramatsu N, Kasai A, Hayakawa K, Okamura M, Yao J, Kitamura M: **Induction of apoptosis by cigarette smoke via ROS-dependent endoplasmic reticulum stress and CCAAT/enhancer-binding protein-homologous protein (CHOP).** *Free Radic Biol Med* 2008, **45**(1):50-59.
168. Kelsen SG, Duan X, Ji R, Perez O, Liu C, Merali S: **Cigarette smoke induces an unfolded protein response in the human lung: a proteomic approach.** *Am J Respir Cell Mol Biol* 2008, **38**(5):541-550.
169. Rao J, Yue S, Fu Y, Zhu J, Wang X, Busuttill RW, Kupiec-Weglinski JW, Lu L, Zhai Y: **ATF6 Mediates a Pro-inflammatory Synergy between ER Stress and TLR Activation in the Pathogenesis of Liver Ischemia Reperfusion Injury.** *Am J Transplant* 2014, **14**(7):1552-1561.
170. Ribeiro CM, Boucher RC: **Role of endoplasmic reticulum stress in cystic fibrosis-related airway inflammatory responses.** *Proc Am Thorac Soc* 2010, **7**(6):387-394.
171. Martino ME, Olsen JC, Fulcher NB, Wolfgang MC, O'Neal WK, Ribeiro CM: **Airway epithelial inflammation-induced endoplasmic reticulum Ca²⁺ store expansion is mediated by X-box binding protein-1.** *J Biol Chem* 2009, **284**(22):14904-14913.
172. Blohmke CJ, Mayer ML, Tang AC, Hirschfeld AF, Fjell CD, Sze MA, Falsafi R, Wang S, Hsu K, Chilvers MA *et al*: **Atypical activation of the unfolded protein response in cystic fibrosis airway cells contributes to p38 MAPK-mediated innate immune responses.** *J Immunol* 2012, **189**(11):5467-5475.
173. Bartoszewski R, Rab A, Jurkuvenaite A, Mazur M, Wakefield J, Collawn JF, Bebők Z: **Activation of the Unfolded Protein Response by Δ F508 CFTR.** *Am J Respir Cell Mol Biol* 2008, **39**(4):448-457.
174. Kerbiriou M, Le Drévo M-A, Férec C, Trouvé P: **Coupling cystic fibrosis to endoplasmic reticulum stress: Differential role of Grp78 and ATF6.** *Biochimica et Biophysica Acta (BBA) - Molecular Basis of Disease* 2007, **1772**(11):1236-1249.
175. Oglesby IK, Agrawal R, Mall MA, McElvaney NG, Greene CM: **miRNA-221 is elevated in cystic fibrosis airway epithelial cells and regulates expression of ATF6.** *Mol Cell Pediatr* 2015, **2**.
176. Lodish H, Berk A, Zipursky SL, Matsudaira P, Baltimore D, Darnell J: **Oxidation of Glucose and Fatty Acids to CO₂:** W. H. Freeman; 2000.
177. Krebs HA: **The citric acid cycle: A reply to the criticisms of F. L. Breusch and of J. Thomas.** *Biochem J* 1940, **34**(3):460-463.
178. Litwack G: **Glycolysis and Gluconeogenesis.** In: *Human Biochemistry.* Los Angeles, CA, United States: Academic Press; 2017: 183-198.

179. Potter M, Newport E, Morten KJ: **The Warburg effect: 80 years on.** In: *Biochem Soc Trans.* vol. 44; 2016: 1499-1505.
180. Ganeshan K, Chawla A: **Metabolic Regulation of Immune Responses.** *Annu Rev Immunol* 2014, **32**:609-634.
181. O'Neill LAJ, Artyomov MN: **Itaconate: the poster child of metabolic reprogramming in macrophage function.** *Nat Rev Immunol* 2019.
182. O'Neill LA, Hardie DG: **Metabolism of inflammation limited by AMPK and pseudo-starvation.** *Nature* 2013, **493**(7432):346-355.
183. O'Neill LA, Kishton RJ, Rathmell J: **A guide to immunometabolism for immunologists.** *Nat Rev Immunol* 2016, **16**(9):553-565.
184. Newsholme P, Curi R, Gordon S, Newsholme EA: **Metabolism of glucose, glutamine, long-chain fatty acids and ketone bodies by murine macrophages.** *Biochem J* 1986, **239**(1):121-125.
185. Fukuzumi M, Shinomiya H, Shimizu Y, Ohishi K, Utsumi S: **Endotoxin-induced enhancement of glucose influx into murine peritoneal macrophages via GLUT1.** *Infect Immun* 1996, **64**(1):108-112.
186. Jha AK, Huang SC, Sergushichev A, Lampropoulou V, Ivanova Y, Loginicheva E, Chmielewski K, Stewart KM, Ashall J, Everts B *et al*: **Network integration of parallel metabolic and transcriptional data reveals metabolic modules that regulate macrophage polarization.** *Immunity* 2015, **42**(3):419-430.
187. Arango Duque G, Descoteaux A: **Macrophage cytokines: involvement in immunity and infectious diseases.** *Front Immunol* 2014, **5**:491.
188. Atri C, Guerfali FZ, Laouini D: **Role of Human Macrophage Polarization in Inflammation during Infectious Diseases.** In: *Int J Mol Sci.* vol. 19; 2018.
189. Tannahill G, Curtis A, Adamik J, Palsson-McDermott E, McGettrick A, Goel G, Frezza C, Bernard N, Kelly B, Foley N *et al*: **Succinate is a danger signal that induces IL-1 β via HIF-1 α .** *Nature* 2013, **496**(7444):238-242.
190. Ogryzko NV, Lewis A, Wilson HL, Meijer AH, Renshaw SA, Elks PM: **Hif-1 α -Induced Expression of Il-1 β Protects against Mycobacterial Infection in Zebrafish.** In: *J Immunol.* vol. 202; 2019: 494-502.
191. Osowski CM, Hara T, O'Sullivan-Murphy B, Kanekura K, Lu S, Hara M, Ishigaki S, Zhu LJ, Hayashi E, Hui ST *et al*: **Thioredoxin-interacting protein mediates ER stress-induced beta cell death through initiation of the inflammasome.** *Cell Metab* 2012, **16**(2):265-273.
192. Michl J, Ohlbaum DJ, Silverstein SC: **2-Deoxyglucose selectively inhibits Fc and complement receptor-mediated phagocytosis in mouse peritoneal macrophages II. Dissociation of the inhibitory effects of 2-deoxyglucose on phagocytosis and ATP generation.** *J Exp Med* 1976, **144**(6):1484-1493.

193. Kelly B, O'Neill LA: **Metabolic reprogramming in macrophages and dendritic cells in innate immunity.** *Cell Res* 2015, **25**(7):771-784.
194. Kellett DN: **2-Deoxyglucose and inflammation.** *J Pharm Pharmacol* 1966, **18**(3):199-200.
195. Zhao Q, Chu Z, Zhu L, Yang T, Wang P, Liu F, Huang Y, Zhang F, Zhang X, Ding W *et al*: **2-Deoxy-d-Glucose Treatment Decreases Anti-inflammatory M2 Macrophage Polarization in Mice with Tumor and Allergic Airway Inflammation.** *Front Immunol* 2017, **8**.
196. Rodriguez-Prados JC, Traves PG, Cuenca J, Rico D, Aragonés J, Martín-Sanz P, Cascante M, Bosca L: **Substrate fate in activated macrophages: a comparison between innate, classic, and alternative activation.** *J Immunol* 2010, **185**(1):605-614.
197. Moon JS, Hisata S, Park MA, DeNicola GM, Ryter SW, Nakahira K, Choi AMK: **mTORC1-Induced HK1-Dependent Glycolysis Regulates NLRP3 Inflammasome Activation.** *Cell Rep* 2015, **12**(1):102-115.
198. O'Sullivan D, van der Windt GJ, Huang SC, Curtis JD, Chang CH, Buck MD, Qiu J, Smith AM, Lam WY, DiPlato LM *et al*: **Memory CD8(+) T cells use cell-intrinsic lipolysis to support the metabolic programming necessary for development.** *Immunity* 2014, **41**(1):75-88.
199. Mills EL, Ryan DG, Prag HA, Dikovskaya D, Menon D, Zaslona Z, Jedrychowski MP, Costa ASH, Higgins M, Hams E *et al*: **Itaconate is an anti-inflammatory metabolite that activates Nrf2 via alkylation of KEAP1.** *Nature* 2018, **556**(7699):113-117.
200. Michelucci A, Cordes T, Ghelfi J, Pailot A, Reiling N, Goldmann O, Binz T, Wegner A, Tallam A, Rausell A *et al*: **Immune-responsive gene 1 protein links metabolism to immunity by catalyzing itaconic acid production.** *Proc Natl Acad Sci U S A* 2013, **110**(19):7820-7825.
201. Lampropoulou V, Sergushichev A, Bambouskova M, Nair S, Vincent EE, Loginicheva E, Cervantes-Barragan L, Ma X, Huang SC, Griss T *et al*: **Itaconate Links Inhibition of Succinate Dehydrogenase with Macrophage Metabolic Remodeling and Regulation of Inflammation.** *Cell Metab* 2016, **24**(1):158-166.
202. Bartoszewski R, Rab A, Fu L, Bartoszewska S, Collawn J, Bebok Z: **CFTR expression regulation by the unfolded protein response.** *Methods Enzymol* 2011, **491**:3-24.
203. Pihlgren M, Silva AB, Madani R, Giriens V, Waeckerle-Men Y, Fettelschoss A, Hickman DT, Lopez-Deber MP, Ndao DM, Vukicevic M *et al*: **TLR4- and TRIF-dependent stimulation of B lymphocytes by peptide liposomes enables T cell-independent isotype switch in mice.** *Blood* 2013, **121**(1):85-94.

204. Cheng S, Wang H, Zhou H: **The Role of TLR4 on B Cell Activation and Anti-beta2GPI Antibody Production in the Antiphospholipid Syndrome.** *J Immunol Res* 2016, **2016**:1719720.
205. Reynolds JM, Martinez GJ, Chung Y, Dong C: **Toll-like receptor 4 signaling in T cells promotes autoimmune inflammation.** *Proc Natl Acad Sci U S A* 2012, **109**(32):13064-13069.
206. Italiani P, Boraschi D: **From Monocytes to M1/M2 Macrophages: Phenotypical vs. Functional Differentiation.** *Front Immunol* 2014, **5**:514.
207. Lacey DC, Achuthan A, Fleetwood AJ, Dinh H, Roiniotis J, Scholz GM, Chang MW, Beckman SK, Cook AD, Hamilton JA: **Defining GM-CSF- and macrophage-CSF-dependent macrophage responses by in vitro models.** *J Immunol* 2012, **188**(11):5752-5765.
208. van 't Wout EF, van Schadewijk A, van Bortel R, Dalton LE, Clarke HJ, Tommassen J, Marciniak SJ, Hiemstra PS: **Virulence Factors of Pseudomonas aeruginosa Induce Both the Unfolded Protein and Integrated Stress Responses in Airway Epithelial Cells.** *PLoS Pathog* 2015, **11**(6):e1004946.
209. Scambler T, Jarosz-Griffiths HH, Lara-Reyna S, Pathak S, Wong C, Holbrook J, Martinon F, Savic S, Peckham D, McDermott MF: **ENaC-mediated sodium influx exacerbates NLRP3-dependent inflammation in cystic fibrosis.** *Elife* 2019, **8**.
210. Shan B, Wang X, Wu Y, Xu C, Xia Z, Dai J, Shao M, Zhao F, He S, Yang L *et al*: **The metabolic ER stress sensor IRE1alpha suppresses alternative activation of macrophages and impairs energy expenditure in obesity.** *Nat Immunol* 2017, **18**(5):519-529.
211. Ron D, Walter P: **Signal integration in the endoplasmic reticulum unfolded protein response.** *Nat Rev Mol Cell Biol* 2007, **8**(7):519-529.
212. Lara-Reyna S, Scambler T, Holbrook J, Jarosz-Griffiths HH, Peckham D, McDermott MF: **Regulation of the Unfolded Protein Response in Disease: Cellular Stress and microRNAs.** 2018.
213. Ray PD, Huang BW, Tsuji Y: **Reactive oxygen species (ROS) homeostasis and redox regulation in cellular signaling.** *Cell Signal* 2012, **24**(5):981-990.
214. Ozgur R, Uzilday B, Iwata Y, Koizumi N, Turkan I: **Interplay between the unfolded protein response and reactive oxygen species: a dynamic duo.** *J Exp Bot* 2018, **69**(14):3333-3345.
215. Kritsiligkou P, Rand JD, Weids AJ, Wang X, Kershaw CJ, Grant CM: **Endoplasmic reticulum (ER) stress-induced reactive oxygen species (ROS) are detrimental for the fitness of a thioredoxin reductase mutant.** *J Biol Chem* 2018, **293**(31):11984-11995.

216. Ramsey BW, Davies J, McElvaney NG, Tullis E, Bell SC, Drevinek P, Griese M, McKone EF, Wainwright CE, Konstan MW *et al*: **A CFTR potentiator in patients with cystic fibrosis and the G551D mutation.** *N Engl J Med* 2011, **365**(18):1663-1672.
217. McElvaney OJ, Zaslona Z, Becker-Flegler K, Palsson-McDermott EM, Boland F, Gunaratnam C, Gulbins E, O'Neill LA, Reeves EP, McElvaney NG: **Specific Inhibition of the NLRP3 Inflammasome as an Anti-Inflammatory Strategy in Cystic Fibrosis.** *Am J Respir Crit Care Med* 2019.
218. Netea MG, Latz E, Mills KH, O'Neill LA: **Innate immune memory: a paradigm shift in understanding host defense.** In: *Nat Immunol.* vol. 16. United States; 2015: 675-679.
219. Boraschi D, Italiani P: **Innate Immune Memory: Time for Adopting a Correct Terminology.** *Front Immunol* 2018, **9**.
220. Van Belleghem JD, Bollyky PL: **Macrophages and innate immune memory against Staphylococcus skin infections.** *Proc Natl Acad Sci U S A* 2018, **115**(47):11865-11867.
221. Scheper W, Hoozemans JJ: **The unfolded protein response in neurodegenerative diseases: a neuropathological perspective.** *Acta Neuropathol* 2015, **130**(3):315-331.
222. Koss DJ, Platt B: **Alzheimer's disease pathology and the unfolded protein response: prospective pathways and therapeutic targets.** *Behav Pharmacol* 2017, **28**(2 and 3-Spec Issue):161-178.
223. Martinez A, Lopez N, Gonzalez C, Hetz C: **Targeting of the unfolded protein response (UPR) as therapy for Parkinson's disease.** *Biol Cell* 2019, **111**(6):161-168.
224. García-González P, Cabral-Miranda F, Hetz C, Osorio F: **Interplay Between the Unfolded Protein Response and Immune Function in the Development of Neurodegenerative Diseases.** *Front Immunol* 2018, **9**.
225. Abisambra JF, Jinwal UK, Blair LJ, O'Leary JC, 3rd, Li Q, Brady S, Wang L, Guidi CE, Zhang B, Nordhues BA *et al*: **Tau accumulation activates the unfolded protein response by impairing endoplasmic reticulum-associated degradation.** *J Neurosci* 2013, **33**(22):9498-9507.
226. Heneka MT, Kummer MP, Latz E: **Innate immune activation in neurodegenerative disease.** *Nat Rev Immunol* 2014, **14**(7):463-477.
227. Becher B, Spath S, Goverman J: **Cytokine networks in neuroinflammation.** *Nat Rev Immunol* 2017, **17**(1):49-59.
228. Carrabino S, Carpani D, Livraghi A, Di Cicco M, Costantini D, Copreni E, Colombo C, Conese M: **Dysregulated interleukin-8 secretion and NF-kappaB activity in human cystic fibrosis nasal epithelial cells.** *J Cyst Fibros* 2006, **5**(2):113-119.

229. van der Harg JM, van Heest JC, Bangel FN, Patiwaël S, van Weering JR, Scheper W: **The UPR reduces glucose metabolism via IRE1 signaling.** *Biochim Biophys Acta Mol Cell Res* 2017, **1864**(4):655-665.
230. Ho N, Xu C, Thibault G: **From the unfolded protein response to metabolic diseases - lipids under the spotlight.** *J Cell Sci* 2018, **131**(3).
231. Mogilenko DA, Haas JT, L'Homme L, Fleury S, Quemener S, Levavasseur M, Becquart C, Wartelle J, Bogomolova A, Pineau L *et al*: **Metabolic and Innate Immune Cues Merge into a Specific Inflammatory Response via the UPR.** *Cell* 2019, **177**(5):1201-1216.e1219.
232. Lin YF, Haynes CM: **Metabolism and the UPR(mt).** *Mol Cell* 2016, **61**(5):677-682.
233. Oh J, Riek AE, Weng S, Petty M, Kim D, Colonna M, Cella M, Bernal-Mizrachi C: **Endoplasmic Reticulum Stress Controls M2 Macrophage Differentiation and Foam Cell Formation***. In: *J Biol Chem.* vol. 287; 2012: 11629-11641.
234. McGonagle D, McDermott MFJpm: **A proposed classification of the immunological diseases.** 2006, **3**(8):e297.
235. Pathak S, McDermott M, Savic S: **Autoinflammatory diseases: update on classificationn diagnosis and management.** *Journal of Clinical Pathology* 2016, IN PRESS.